Trophoblast Models for Tumour Studies: Understanding the similarities of tumour and trophoblast invasion

A Thesis Submitted by

Reham Mohammed Balahmar

Nottingham Trent University, UK

For the partial requirements for the degree of

Doctor of Philosophy

June 2016

Copyright statement

Communications resulting from this study

Conference Abstracts:

Reham Balahmar, and Shiva Sivasubramaniam (2014). Status analysis of tumour associated factors in human placentae and stem-lik cells derived from placental cell lines. Placenta, Vol. 35, Issue 9, P A99. Poster presentation at International Federation of Placenta Association (IFPA), France.

Reham M Balahmar, Vernon Ebegboni, Sankalita Ray and Shiva Sivasubramaniam (2015).Variability in the expressions of Aurora kinases (AURK) in pre-eclamptic placentae. *Placenta*, Vol. 36, Issue 9, A17–A18. Poster presentation at International Federation of Placenta Association (IFPA), Australia

Awards:

Charlie Loke Travel Award for young investigator based on the scientific content of the poster - 18th Annual Meeting of International Federation of Placenta Association (IFPA - Brisbane, Australia) - Placenta: Influence and Impact

Acknowledgements

I would like to express my special appreciation and thanks to my advisor, Dr.Shiva Sivasubramaniam for his support, guidance and continuous monitoring. His office door was always open for me when I ever had a problem or a question about my research or writing. He showed me in the right direction whenever was out of track in this four year period. I am so grateful for his exceptional supervision and help particularly during the thesis evaluation. I want to take this opportunity to express my gratitude to my second supervisor, Dr Selman Ali for helping and advising me all time.

Sincere thanks to my Independent Assessor Prof. Graham Pockley for his valuable constructive criticisms and feedbacks on this work.

I would also like to acknowledge my sponsor scholarship provided by King Abdullah Bin-Abdulaziz Al-saud (May he rest in peace) and Ministry of Higher Education of Saudi Arabia. Thank you for giving me this opportunity to expand my knowledge in science.

Special thanks to who this work which is dedicated to the most important people in my life, my mother and father for providing me with unfailing support, continuous encouragements and prayers all the way. I will never forget their word "you will make it", without their love and wonderful spirit I wouldn't be able to make it to this stage. Special thanks to my sister Norah for her support and my little brother Obaid.

Words cannot express how grateful I am to my second sister Dr. Anushuya for her help with a smile. I remember how we spend time to optimise western blot for tissue. Thanks to my both little sisters Shweta and Sankalita and my brother Vernon. I will miss you guys so much.

Finally, I would also like take this opportunity to thank all my friends Maha and Ibtisam, Shatha, Marwah, Hayat, Alanod, Nada, Najiah, Sukina, Jumanah, Biola, Naqash, Bhugsy, Deepak. Thank you for being part of my life along this way, thank you for sharing my happiness and sadness and being my second family in Nottingham.

Abstract

Cell proliferation, migration and invasion are the important features of tumour metastasis. Interestingly, during embryonic development, trophoblast cells show similar attributes like tumour cells to establish foeto-maternal communications and support normal pregnancy. The invasive nature of tumour as well as trophoblast cells (especially during the first trimester) are believed to be enhanced by a collection of "stem-like cells" (SLCs) called ''spheroid *bodies*''. This sub-population of SLCs within tumour or trophoblast cells can proliferate to form a heterogeneous cell groups with different functional attributes. However, tumour SLCs proliferate during invasion; while trophoblast cells proliferate and then invade. Although several previous studies have produced SLCs from tumour cell lines *in vitro*, limited attempts were made to produce SLCs from trophoblast cells. Therefore, this study firstly aimed to produce and characterise SLCs from transformed first trimester trophoblast cell lines (HTR8sv/neo and TEV-1) and choriocarcinoma (trophoblast tumour cell lines JEG-3 and BeWo) in relation to a non-placental tumour cell line MCF-7. Secondly, to date, the factors that are responsible for there uncontrolled versus controlled invasion are not fully understood. On the other hand, it is worth noting that in pre-eclampsia (PE), the invasion of first trimester trophoblast cells is found to be reduced. Therefore, it was hypothesised that it would be possible to identify the important molecules that may be involved in the controlled trophoblast invasion by comparing the status of different factors that are identified with altered expression in tumour cells between (a) normotensive (NT) and PE placentae, and (b) in the SLCs produced *in vitro* from trophoblast cells.

SLCs from transformed trophoblast and choriocarcinoma cells were produced by growing in non-attachable or ultra-low attachment flasks with or without doxorubicin (DOX) to produce DOX-resistant and non-resistant spheroids. The "stemness" feature of these spheroids was characterised by comparing the expressions of stem cell markers. The migration and invasive capacities of DOX-resistant and non-resistant spheroids were compared with their parental cells by wound-healing and 2-D/3-D invasion assays. The status and expression of novel factors that may be involved in cell proliferation and invasion was checked by quantitative real-time PCR and western blotting. Also a comparative proteomic (SWATH-MS) analysis was carried out to identify and compare the global changes of the peptide expression during SLCs transformation. In addition the RNA and protein expression of factors that are involved in trophoblast invasion were compared in 13 NT and 12 PE placentae.

Both the transformed trophoblastic cell lines (HTR8/Sv-neo and TEV-1,) and gestational choriocarcinoma cell lines (JEG-3 and BeWo) were able to produce non- spheroidal cells (non-resistant and drug resistant) under 3-D conditions. These spheroids showed increased protein expression of stem cells markers, such as OCT4, SOX2 and NANOG. On the other hand, both trophoblast CDX2 and the cell fate determining transcription factor, NOTCH1, were reduced in spheroidal cells confirming the "stem-like" transformation. Moreover, the 2-D invasion assay showed a statistically significant increase in the invasive potential (number invaded cells) of spheroids. This significance was found to be higher in untreated spheroids from transformed trophoblast cells; $P<0.0005$ (for both HTR8svneo and TEV-1) and in one of the choriocarcinoma cells JEG-3; whilst the significance between untreated spheroids of BeWo and their parental cells was slightly less ($P<0.05$).

The 3-D invasion assays have shown a significant time dependent increase in the invasions of non-resistant spheroidal cells in comparison with DOX-resistant counterpart, especially the non-resistant spheroidal cells produced from HTR8/Svneo ($p<0.0005$) at 48 hours. Spheriodal cell invasion of non-resistant TEV-1 and choricarcinoma cells was significantly higher than DOX-resistant cells ($p<0.005$). Therefore this study has produced spheroidal cells from (a) transformed first trimester trophoblast (HTR8/Svneo and TEV-1) and (b) choriocarcinoma (JEG-3 and BeWo) cells. Since these cell lines are of trophoblast origin, it is possible to use these spheroids as comparative models to study the effects of chemotherapeutic agents on (a) physiologically rapidly dividing cells (HTR8/Svneo and TEV-1) and (b) tumour models (JEG-3 and BeWo) of similar origins.

Comparisons of mRNA and protein expression between NT and PE placentae have shown a statistically significant increase in the expressions of ALDH3A1, AURK-A, PDGFRα, and TWIST1 in PE placentae ($p<0.05$); whilst AURK-C and JAG-1 expression was down-regulated. SWATH-MS analysis has also highlighted up-regulation of novel proteins that are associated with proliferation, invasion and cell cycle control in the spheroids produced from these cell lines. These proteins include plasminogen, vitronectin and ALDH1A3. However, the function of most of these factors have not been fully investigated in placenta. In summary the study has generated and characterised "stem-like" spheroids from transformed trophoblast and choriocarcinoma cells. These spheroidal cells may be useful as *in vitro* toxicological models to study the *in vivo* cellular effects on rapidly dividing cells.

List of Figures

List of Tables

Abbreviations

ALDH3	Aldehyde dehydrogenase 3
ALDH3A1	Aldehyde Dehydrogenase 3 Family, Member A1
APM	Antigen Presentation Machinery
AURK	Aurora kinases
AURK-A	Aurora kinase A
AURK-C	Aurora kinase C
BCA	Bicinchoninic acid
bFGF	basic Fibroblast Growth Factor
bHLH	basic Helix-Loop-Helix
BME	Basement Membrane Extract
BSA	Bovine Serum Albumin
cDNA	Complementary DNA
CDS	Coding Sequences
CDX2	Caudal Type Homeobox 2
CRIP2	Cysteine-Rich Protein 2
CSC	Cancer Stem Cell
CSF	Colony Stimulating Factor
CTB	Cytotrophoblasts
CTLs	Cytotoxic T Cells
DAB	3,3'-Diaminobenzidine
DCs	Dendritic Cells
DNA	Deoxyribonucleic acid
DOX	Doxorubicin hydrochloride
DPBS	Dulbecco's Phosphate-Buffered Saline
DTT	Dithiothreitol
ECM	Extra-Cellular Matrix
ECs	Endothelial Cells
egEVT	endoglandular Extravillous Trophoblast, endoglandular trophoblast
EGF	Epidermal Growth Factor
EMT	Epithelial-Mesenchymal Transition
enEVT	endovascular Extravillous Trophoblast, endovascular trophoblast
ES, ESC	Embryonic Stem Cells
EVT	Extravillous Trophoblast

FBS	Foetal Bovine Serum
FGR	Foetal Growth Restriction
FSCs	Foetal Stem Cells
GAPDH	Glyceraldehyde 3-phosphate dehydrogenase
hAEC	Human Amniotic Epithelial Cells
HB-EGF	Heparin-Binding Epidermal Growth Factor
hCG	human Chorionic Gonadotropin
HGF	Hepatocyte Growth Factor
HIAR	Heat Induced Antigen Retrieval
HLA-G	Human Leukocyte Antigen-G
HOX	Homeobox
hPL	human Placental Lactogen
HPRT1	Hypoxanthine-guanine phosphoribosyltransferase
HSCs	Hematopoietic Stem Cells
IAA	Iodoacetamide
ICM	Inner Cell Mass
iEVT	interstitial Extravillous Trophoblast
IFN-γ	Interferon gamma
IGF-1	Insulin like Growth Factor 1
IHC	Immunohistochemistry
IL-10	Interleukin 10
IUGR	Intra-Uterine Growth Restriction
JAG-1	Jagged-1
LDH	Lactate Dehydrogenase
LIF	Leukaemia Inhibitory Factor
MAPK	Mitogen Activated Protein Kinases
MET	Mesenchymal-Epithelial Transition
MHC	Major Histocompatibility Complex
MMP-9	Matrix Metalloproteinase 9
MMPs	Matrix Metalloproteinase
mRNA	messenger RNA
MSCs	Mesenchymal Stem Cells
MTT	3-(4,5-Dimethylthiazol-2-yl)-2,5-Diphenyltetrazolium Bromide
NAD	Nicotinamide adenine dinucleotide
NADH	Reduced form of NAD

NANOG	Homeobox Transcription Factor Nanog
NCBI	National Centre for Biotechnology Information
NK	Natural Killer Cells
NOTCH1	Notch Homolog Translocation-Associated
NT	Normotensive, Normal placenta
OCT4	Octamer-binding transcription factor 4
PBS	Phosphate-buffered saline
PBST	PBS with Tween 20
PCR	polymerase chain reaction
PDGF	Plated-Delivered Endothelial Growth Factor
PDGFRα	Platelet-Derived Growth Factor Receptor Alpha
PE	Pre-Eclamptic, Pre-Eclampsia
PGF	Placental Growth Factor
PI3K	Phosphoinositide 3-Kinase
PIGF	Placenta-Like Growth Factor
POU	Pit-Oct-Unc
qRT-PCR	Quantitative Real-Time PCR
RNA	Ribonucleic acid
RNS	Reactive Nitrogen Species
ROS	Reactive Oxygen Species
SCs	Stem Cells
SEM	Standard Error Mean
SFM	Serum-Free Media
SOX2	Sex-determining region Y (SRY)-Box 2
STB	Syncytiotrophoblasts
Ta	Annealing temperatures
TAEB	Triethyl ammonium bicarbonate buffer
TBS	Tris-buffered saline
TCR	T-Cell Receptor
TGF-β	Transforming Growth Factor beta
TICs	Tumour-Initiating Cells
TIMP-1	Tissue Inhibitors of Metalloproteinase 1
TIMPs	Tissue Inhibitors of Metalloproteinases
TNF-α	Tumour Necrosis Factor alpha
tPA	tissue-type Plasminogen Activator

TSC	Trophoblast Stem Cells
TSP-1	Thrombospondin 1
UCB	Umbilical Cord Blood Stem Cells
uPA	urokinase-type Plasminogen Activator
vCTBs	villous Cytotrophoblast
VEGF	Vascular Endothelial Growth Factor Family
WB	Western Blotting
WHO	World Health Organisation

Table of Contents

Chapter 1
Introduction

1.0 Introduction

The process of embryo development is somewhat similar to tumourigenesis in terms of biological behaviour such as proliferation, migration, invasion, gene expression, and the mechanism of immune escape (Ferretti *et al.*, 2007). This makes the placenta an interesting physiological model to study and compare the process of proliferation and invasion with that seen in tumour development (Ma *et al.*, 2010). This study might help to understand the behavioural similarities and differences between tumour and placenta.

1.1 Human Placenta

The birth of a healthy infant depends on the development of a highly specialised organ called the placenta (Guttmacher *et al.*, 2014). The placenta is a temporary organ which plays a significant role in maintaining pregnancy and supporting the normal growth and development of the foetus. The world placenta comes from two terms, the first from a Latin word "placenta", meaning a flat cake (Enders and Blankenship, 1999), and the second from Greek "*plakoenta*" meaning flat **(www[1])**. During pregnancy the normal growth of the foetus depends on the crosstalk between foetal membranes and amniotic fluid (Gude *et al.*, 2004). Human placenta is categorised as a haemochorial villous organ. Despite the fact the maternal and foetal circulation do not directly mix, an intimate contact is established between maternal blood circulation and placental trophoblast cells in order to support an adequate supply of nutrients to the foetus (Gude *et al.*, 2004). Figure 1.1 shows the materno-foetal interface with a detailed of the placenta.

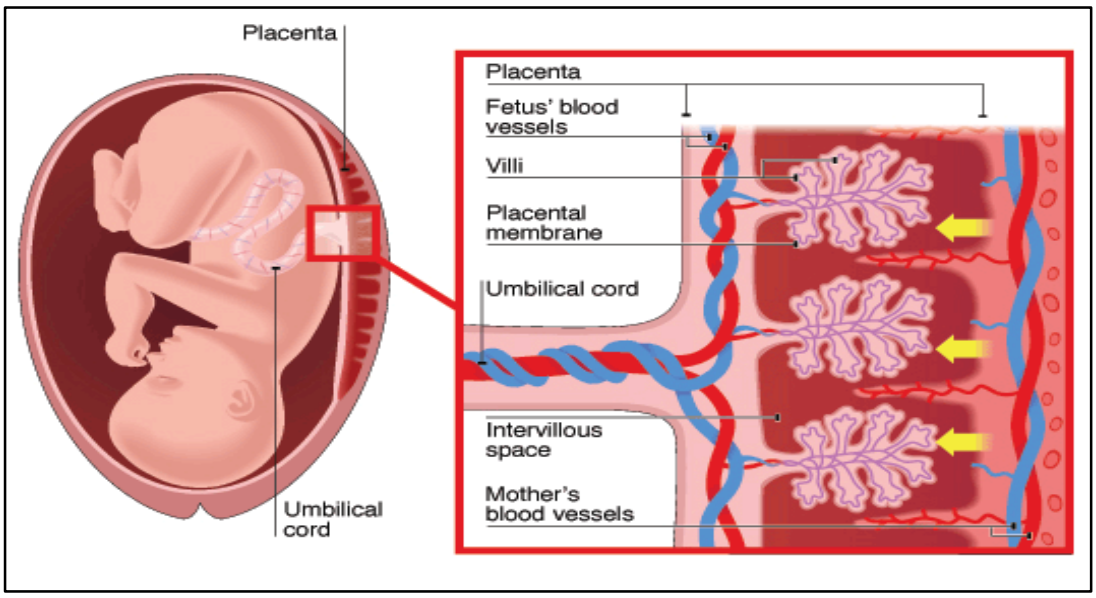

Figure1.1: The interface between mother and foetus in placenta.

This figure shows the localisation of the placenta in the uterus and the cross-section of placenta displaying circulation of the blood. *Figure adapted from (**www[2]**)*

1.1.1 Structure of mature human placenta

In humans, the placenta is discoidal in shape. A mature full-term placenta is around 22 cm in diameter with a central thickness of 2.5 cm. The placenta weighs around 470 g (Huppertz, 2008) . These measurements differ from one placenta to other and also depends on the mode of delivery (since measurements are made on the post-delivery placenta). However, the weight of the placenta is related to that of the foetus. There are two surfaces of a placenta: (a) foetal surface and (b) maternal surface (Huppertz, 2008) (**www**[3]).

- **Foetal surface**

The foetal surface is known as the chorionic plate and has the umbilical cord associated to its centre (See Figure 1.2 **A**). It is covered by the amnion and a single layered epithelium (Huppertz, 2008). The umbilical cord is a continuation of the chorionic vessels that arise from the chorionic mesenchyme. The chorionic arteries arise from two umbilical arteries which supply the villous trees. Furthermore, the villous trees continue to the chorionic veins and finally forms a single umbilical vein (Huppertz 2008).

- **Maternal surface**

The attachment site of the placenta onto the uterus is called the maternal surface (or decidua basalis or basal plate) (Huppertz, 2008). The surface is covered with grooves and clefts as seen in Figure 1.2 **B**. Furthermore, it consists of a mixture of trophoblast and maternal cells from uterine decidua, including decidual stroma cells, natural killer cells (NK) and macrophages (Gude *et al.,* 2004)

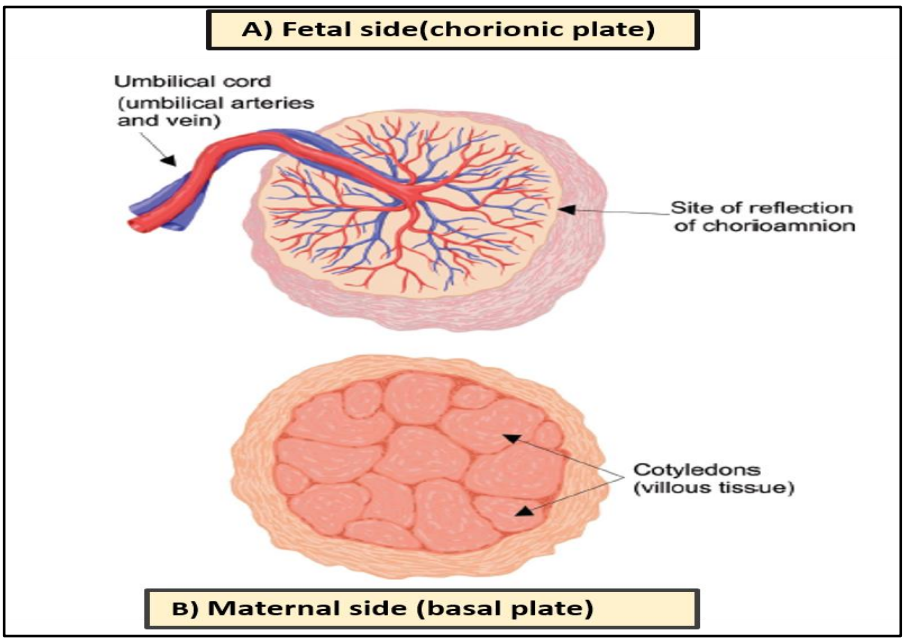

Figure1.1: Illustration of both human placental sides**. A) Represents the foetal side; B) Represents the maternal side.** ***[Figure adapted from Kay et al., 2011]***

1.1.2 Functions of the placenta

The placenta provides a suitable environment which enables the foetus to exchange gases, such as oxygen from maternal blood to foetus and carbon dioxide from foetus to maternal blood (Gude *et al.*, 2004). Moreover, it also facilitates the exchange of nutrients and electrolytes from mother to foetus, such as carbohydrates (glucose) which is considered to be the source of energy for the foetus (Gude *et al.,* 2004). Other examples include lipids (fatty acid, glycolipids, vitamins, and cholesterol) and amino acids which are essential for the synthesis of proteins in the foetus (Ji *et al.,* 2013). Likewise, the placenta also serves as an endocrine and metabolic organ by producing hormones, growth factors, antibodies, and other nutrients required to support the growth of the foetus; while also removing waste products. It acts as a barrier which separates the foetal and maternal blood, which plays an essential role in protecting the foetus from the maternal immune attack during pregnancy (Ji *et al.,* 2013). It also helps to protect the foetus from diseases and infection of maternal origin and from xenobiotic molecules (Donnelly and Campling, 2014).

1.1.3 Early development of the placenta

The early development of the placenta starts with interactions between the invading blastocyst and the uterine wall (Forbes and Westwood, 2010). This process is dependent on several factors, such as receptivity of the uterus, blastocyst apposition/adhesion to the endometrial epithelium, and invasion into endometrial stroma. The type of implantation which occurs in humans is termed as interstitial implantation, where the embryo is completely embedded within endometrium (Forbes and Westwood, 2010). The steps after fertilisation are discussed below (see sections 1.1.3.1. to 1.1.3.4).

1.1.3.1 Pre-implantation

Fertilisation usually occurs in the fallopian tube at 24 to 48 hours after ovulation when the mature oocytes are fertilised by a sperm to form a diploid zygote and this is counted as (Day 0) of placental development (Hamilton and Boyd, 1960). Pre-implantation events in relation to their appropriate position in the female reproductive tract are summarised in Figure 1.3.

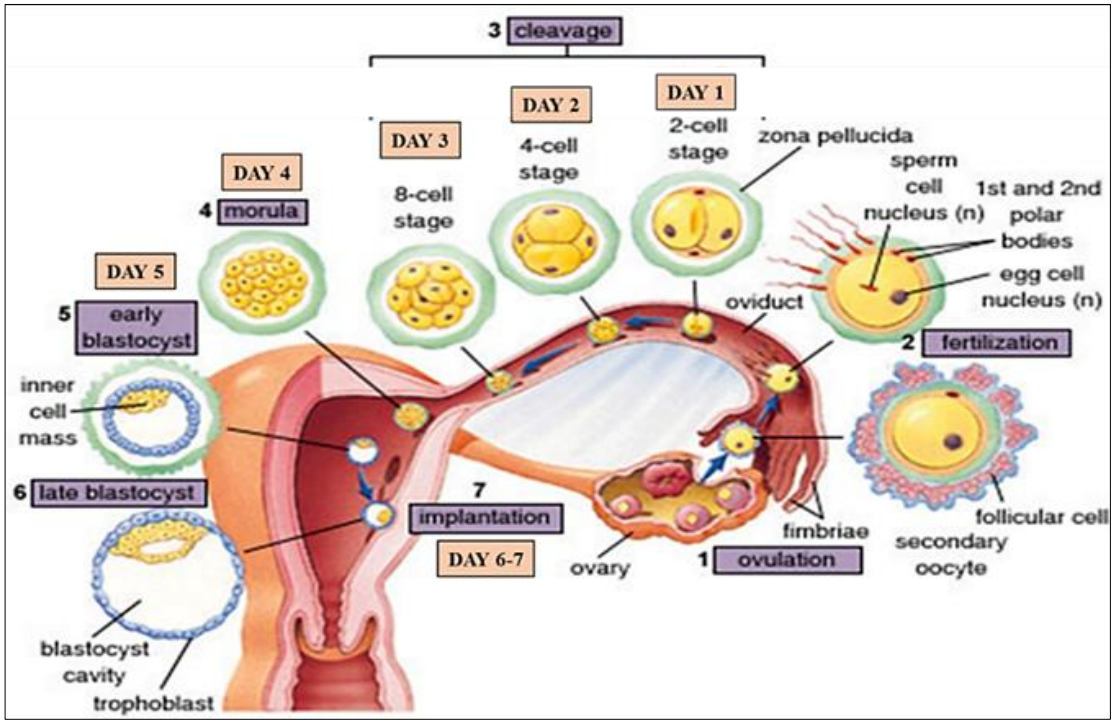

Figure1.3: Illustration of the early stages of human placental development. ***Figure revised from*** **(www[4])**

The fertilised egg (zygote) moves along the fallopian tube into the uterus and undergoes several stages of cleavage and differentiation. During the first mitotic division, the zygote divides to become the two cell stage (Day 1). This is followed by the four cells stage (Day 2), and eight cell stage (Day 3), Divisions continue until the zygote reaches a round mass of cells (blastomere or morula) which is formed with 12-16 cells (Day 4) (Norwitz, 2001). The morula then enters the uterine cavity; during which a fluid-filled cavity appears in the inner side of the morula and further cell divisions occur, resulting in development of the morula to a blastocyst (Norwitz, 2001). The cells on the outer side of the morula thicken and flatten out while the cells inside become more compact and adhere to one another forming a cavity. This gives rise to an outer layer of trophoblast cells and an inner cell mass of embryo proper. The blastocyst "hatches" from the zona pellucida by constant contraction and expansion. The free blastocyst then aligns along the uterine wall. The inner cell mass give rise to the foetus while the outer trophoblast layer gives rise to extra embryonic structures, and leads to the implantation of the blastocyst into the uterus to form the placenta (Red-horse *et al.*, 2004; Foulk, 2012).

1.1.3.2 Implantation

Implantation is a complex process and can only take place in a limited period of time, named the "*window of receptivity"* (Lunghi *et al.*, 2007). During days 6-7, the blastocyst implants into the endometrium of the uterus and around Day 10 the blastocyst is fully embedded in

the stromal tissue of the uterine wall (Lunghi *et al.*, 2007). The implantation process includes three stages: **apposition**, **adhesion** and **invasion** – see below (James *et al.*, 2012). To support implantation, and receive the blastocyst, the endometrium is changed extensively in its morphology, biochemical composition and the ability to secrete hormones such as oestrogen and progesterone. This step is known as decidualisation, an essential step to establish the pregnancy resulting in modification of endometrial stromal cells, vessels, and uterine glands (Lunghi *et al.*, 2007; van Mourik *et al.*, 2009).

- **Apposition of blastocyst on the uterine mucosa:**

As mentioned in section 1.1.3.1, at the end of the pre-implantation stage the free blastocyst aligns along the uterine wall. Meanwhile, the outer layer of blastocyst starts the cellular differentiation process which results in formation of trophectoderm and the remaining part is the embryoblast which later becomes the embryo body **(www[5])**. Establishment of cytotrophoblasts (CTBs) at the embryonic pole is the result of mitotic division of a diploid layer of trophoectoderm. Later the cytotrophoblast cells produce a non-mitotic layer of syncytial cells called syncytiotrophoblasts (STBs) **(www[5])**.

Soon after the embryo is released from the zona pellucida, STBs place in proximity to the uterine wall where the outer compact zone of the endometrium interacts with these trophoblast cells **(www[5])**. The elevation of progesterone and oestrogen during this period plays a major role in flattening the uterine cavity in order to minimise the chance of the blastocyst being flushed out and also being pressed against the uterine epithelium **(www[5])**. The apposition process is summarised in Figure 1.4.

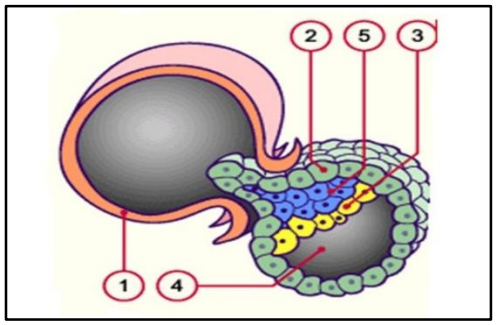

Figure1.4: Schematic representation of different layers of developing trophoblast

The blastocyst hatches out of the partially dissolved zona pellucida. (**1)** Zona pellucuida, (**2)** Trophoblast (outer cell layer), **(3)** Hypoblast (part of the inner cell mass), (**4)** Blastocyst cavity, (**5)** Epiblast (part of inner cell mass or embryo proper). ***Figure revised from*** **(www[5])**.

- **Adhesion of the blastocyst to the endometrium**

Soon after the apposition of the blastocyst, its adhesion onto the maternal endometrium begins. During this time the cytoskeleton of endometrial epithelial lining undergoes

structural modulation to facilitate the formation of pinopodes (Carlson and Mosby, 1994). This structural change can enhance the adhesion of STBs with endometrial epithelial lining (See Figure 1.5). At this stage, the microvilli present on the outer surface of STBs interact with the epithelial cell membrane of the endometrium which reduces the chance of being flushed out of the blastocyst (Carlson and Mosby, 1994). The presence of cytokines, such as leukaemia inhibitory factor (LIF) in uterine fluid, is believed to support successful implantation of the blastocyst. Up-regulated LIF along with heparin-binding epidermal growth factor (HB-EGF) stimulates the hatching of the blastocyst and trophoblast growth (Carlson and Mosby, 1994).

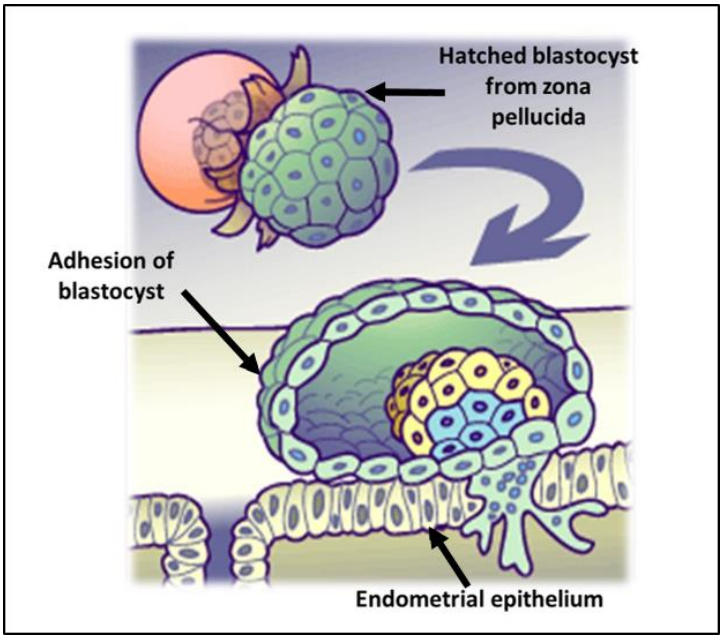

Figure1.5: Schematic representation of adhesion of blastocyst. ***Figure revised from*** **(www[5])**.

- **Invasion**

After adhesion of the blastocyst to the maternal endometrium, intra/inter-cellular signalling mechanisms initiate changes in polarisation of the endometrial epithelial cells. These cells are involved in redistribution of apical cells, basolateral membrane domains, and remodelling of tight and adhering junctions of endometrium tissues (Gude *et al.*, 2004). The invasion of the blastocyst is accomplished by the inter-link between STBs and the lateral border of the endometrial epithelial cells. The invasion is facilitated by decidual cells, which contribute to the breakdown of basal lamina as well as other materials of basement membrane including laminin, collagen IV etc. In order to facilitate this implantation process maternal endometrium undergoes several physiological preparations supported by many hormones. These hormones in turn regulate other growth factors, cytokines and adhesion

molecules to enhance implantation (Gude *et al.*, 2004). The rapid proliferation of mononuclear trophoblast cells followed by invasion is not very different from that seen in aggressive tumours.

1.1.3.3 Detailed structure and functions of trophoblast

Trophoblast, the specialized cell type in a placenta, plays an important role in implantation and formation of the materno-foetal interface (Huppertz, 2008). In the invasion process, trophoblast cells undergo differentiation to form a multinucleated syncytiotrophoblast (STB) (Huppertz, 2008). This STB penetrates the uterine epithelium crossing the basal lamina and embeds the embryo into the stroma. The mononucleated cytotrophoblast cells (CTBs) form the second layer and do not come into contact with the maternal interface. They act as stem cells for the STB, which upon rapid division and fusion finally lead to the expansion of the placenta (Aplin, 1991). The main event during placental development is trophoblast invasion into maternal spiral arteries to remodel the arterial walls to enhance blood supply, which is an important process for successful development of the placenta and pregnancy (Aplin, 1991). Trophoblast invasion begins early in pregnancy and continues until the 20th week of gestation. This invasion (and migration) of trophoblast is controlled by several factors secreted by endometrial glands, such as epidermal growth factor (EGF), vascular endothelial growth factor (VEGF), cytokines, transcription factors, extracellular matrix degradation enzymes, and human leukocyte antigen-G (HLA-G). The molecular steps involved in trophoblast differentiation are poorly understood (Goldman-Wohl and Yagel, 2002; Knöfler and Pollheimer, 2012). However, trophoblast invasion has been found to be increased or decreased under different oxygen concentrations (Anin *et al.*, 2004). Shallow or poor trophoblast invasion is associated with pregnancy complications such as miscarriage, pre-eclampsia (PE) and intrauterine growth restriction (IUGR). Likewise, the excessive invasion of trophoblast leads to placenta accreta (Harris, 2010).

1.1.3.4 Pathways of human trophoblast cell differentiation

The human trophoblast cells have a heterogeneous group of immature cell populations which include stem cells (trophoblast stem cells, TSC) and progenitor cells (Gude *et al.*, 2004). The differentiation of these mononuclear cytotrophoblast progenitor cells is categorised into two main pathways: **1)** the invasive extra-villous trophoblast pathway which is found to be active during first trimester, and **2)** the non-invasive villous trophoblast pathway which appears later in pregnancy. This suggests that the differentiation process of trophoblast cells is a dynamic procedure that continues until the end of pregnancy (Gude *et al.*, 2004; Ji *et al.*, 2013). The two pathways are summarised in Figure 1.6.

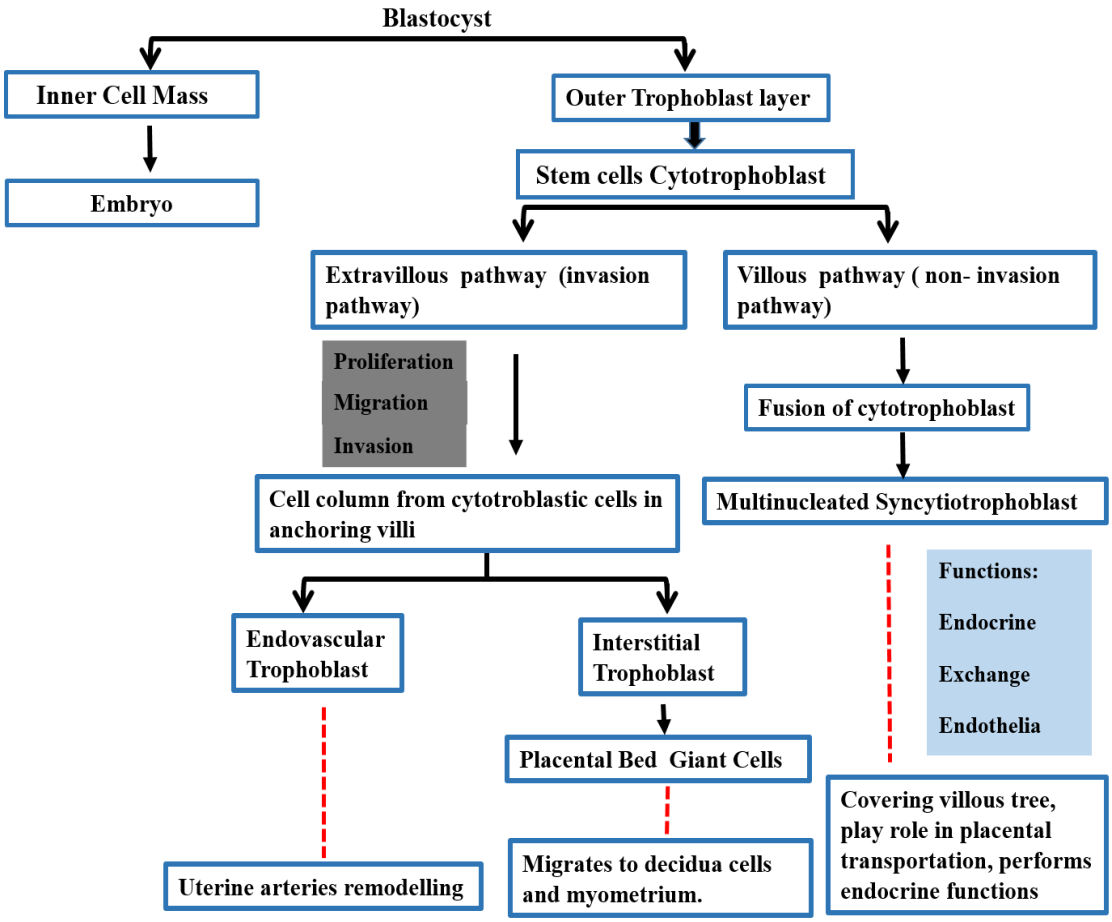

Figure1.6:**Trophoblast differentiation via different cell lineages.**

[Figure adapted from Gude et al., 2004]

(1) **Invasive Pathway**

During the invasive extravillous pathway, CTB stem cells, at the basement membrane of the anchoring villi, invade into the uterine tissue, where they first proliferate and then migrate into the decidua and the myometrium (Guibourdenche *et al.,* 2009). EVT are primarily mononuclear cells that are found in the smooth chorion, chorionic plate and basal plate. The functions of EVT include transformation of the maternal spiral arteries, toleration to hypoxia, adhesion to ECM, stimulating the CTB proliferation/differentiation, interaction with the maternal immune system and enhancing apoptosis (Guibourdenche *et al.,* 2009). The EVT cells divide into three subtypes, namely **(a)** interstitial trophoblast (iEVT), **(b)** the endovascular trophoblast (enEVT) and **(c)** endoglandular trophoblast (egEVT) (Hammer, 2011). Several studies have confirmed that the reduction in numbers of both interstitial and endovascular trophoblast and failure in re-modelling are associated with PE and IUGR (Guibourdenche *et al.,* 2009).

- **Interstitial extravillous trophoblast (iEVT)**

These non-proliferative cells are dispersed in the decidua and express three different phenotypes: (**1**) the large polygonal iEVTs (not invasive) (**2**) small spindle-shapes iEVTs (invasive) and (**3**) placental bed giant cells (Ferreti *et al.,* 2007). The large polygonal iEVTs stay in the transition phase between placenta and decidua, maintaining firm attachment to the uterus throughout the pregnancy (Ferreti *et al.,* 2007). They also secrete trophoblastic glue to enhance adhesion. On the other hand, the small spindle shaped iEVT cells invade to the inner layer of myometrium during the second trimester of the pregnancy (Ji *et al.,* 2013). They move deeper into the decidua and start to differentiate into multinucleated round cells called placental bed giant cells. These cells restrict the EVT invasion outside myometrium and therefore limit the invasion (Ji *et al.,* 2013). They have the ability to secrete human chorionic gonadotropin (hCG) and human placental lactogen (hPL) which supplies energy to the embryo (Ferreti *et al.,* 2007). It has been suggested, that these cells play a role in the maintenance of pregnancy and secretion of protease inhibitors which are responsible for controlling the EVTs invasion past myometrium (Hammer, 2011).

Placental invasion can extend beyond the uterus and establish a long-term presence in the mother (Kinder *et al.,* 2015). Physiologically, invasion of the endometrium by the trophoblast is limited to the decidua basalis. Placenta accreta is present when there is excessive invasion during placentation extending beyond the decidua basalis. While placenta increta presents if there is extended invasion into the uterine myometrium. Moreover, if the placental villa penetrate the myometrium and reach the uterine serosa or even invade neighbouring organs such as the bladder and intestines this is known as placenta percreta (Findeklee and Costa, 2015).

- **Endovascular trophoblast (enEVT)**

The enEVT cells play a significant role in the re-modelling of the uterine spiral arteries (Lyall, 2006). After 11-14 weeks of pregnancy EVTs start to invade the uterine spiral arteries, and by replacing the maternal endothelial lining they induce: (**a**) the loss of elastic tissue and (**b**) reduction of the number of the smooth muscle cells (Ashton *et al.,* 2005). This mechanism is known as "*pseudo-vasculogenesis*" or vascular mimicry (Ashton *et al.,* 2005). The permeation process of enEVT to the spiral arteries causes the blockage of the vessels by forming plugs which aids vascular remodelling of spiral arteries at the end of first trimester. As mentioned above, this leads to changes in the structure of arteries, extends the vessels, and creates a low resistance against blood flow resulting in high flow utero-placental circulation (Ji *et al.,* 2013) (See Section 1.1.3.5 for a detailed explanation).

The five stages that occur during remodelling include:

i. Decidual activity associated with early vascular remodelling,
ii. iEVT involved in vascular remodelling,
iii. enEVT migration,
iv. The insertion of enEVTs into the vessel wall, and
v. The re-endothelisation and sub-intimal thickening (Staff *et al.*, 2010) (See Figure 1.7).

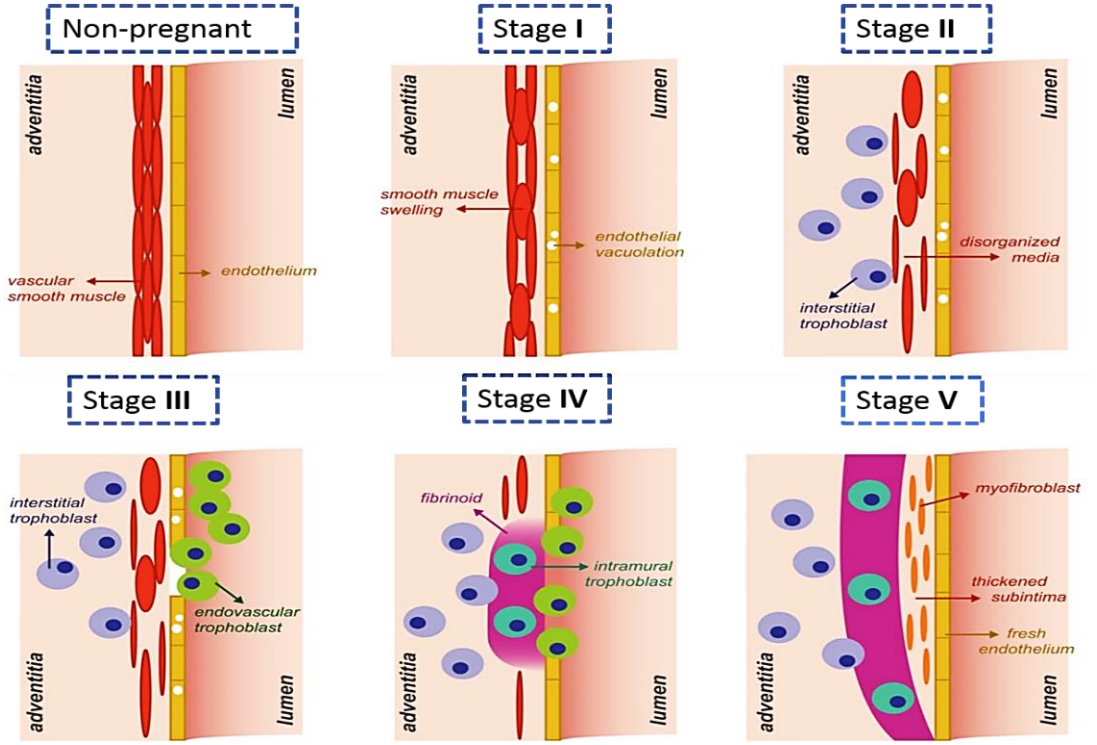

Figure1.7: The different stages involved in spiral artery remodelling.

Starting with non-pregnancy conditions, **Stage I** shows the earliest stage in vascular remodelling which consists of compact endothelia. **Stage II** is associated with disorganisation of the vascular smooth muscles. **Stage III** is initiated by the start of plug formation by enEVT. In **Stage IV** enEVT is embedded and replaces the original smooth muscle cells. The re-endothelialisation occurs at last **stage V**. *[Figure adapted from Pijneborg et al., 2006]*

As the maternal blood circulates through the intervillous space, this helps the developing foetus to establish its haemotrophic nutrition (Moser *et al.*, 2010). As stated above, the invasion of trophoblast cells is important for establishing foeto-maternal circulation.

- **Endoglandular trophoblast (egEVT)**

A study by Huppertz *et al.* (2008) have suggested the presence of an additional sub-population of EVTs named as endoglandular extravillous trophoblast cells (egEVT) (see Figure 1.8). The first evidence of egEVTs existence was produced in an *in vitro* study in the

first trimester decidua and placenta explant co-culture, where indication of glandular remodelling was observed with a similar mechanism to enEVT spiral artery remodelling (Moser *et al.*, 2010). The glandular cell replacement by the egEVT may provide a mechanism which supports both (**a**) opening of the uterine glands to the intervillous space and (**b**) provides histiotrophic nutrition to the embryo ahead of the development of good perfusion of the placenta (Ji *et al.,* 2013).

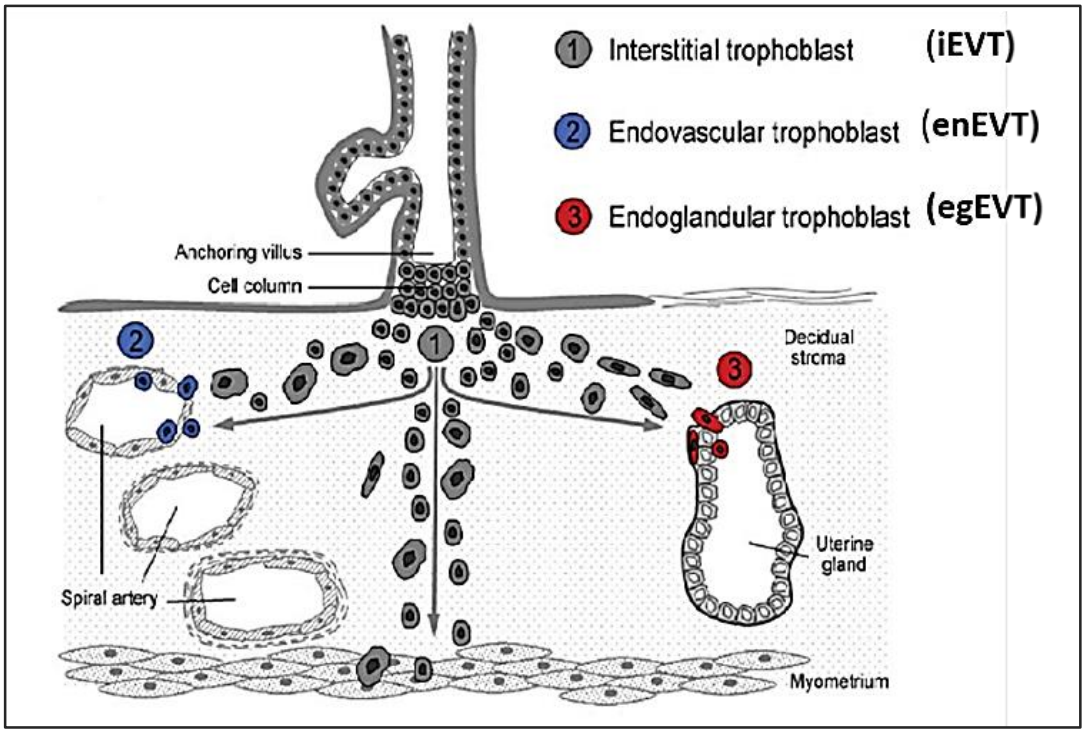

Figure1.8: Different types of trophoblast cells during invasion.

iEVT invade and embed into myometrial smooth muscle to make a firm attachment. enEVT invades the spiral arteries to remodel them. enEVT are involved in the remodelling of uterine endometrial glands. *[Figure adopted from Moser et al., 2010]*

(2) Non-invasive Villous pathway

The non-invasive villous pathway is also known as the syncytial pathway and includes the CTB cells which differentiate by fusion to form the multinucleated STBs that covers the entire surface of the villi (Guibourdenche *et al.*, 2009). Therefore, the villous cytotrophoblast (vCTBs - the inner layer) consists of both the STBs and CTBs (Hammer, 2011). These villi are in direct contact with maternal blood within the intervillous space and are involved in gas, nutrient and waste exchange (Ferretti *et al.,* 2007). Moreover, the syncytial layer plays a major role in the maintenance of the pregnancy by releasing important hormones into the maternal circulation such as hCG and hPL (Ferretti *et al.,* 2007). As explained in section 1.1.3.2, STBs protect the foetus by inhibiting the maternal immune response. The STB layer

is maintained by the continual proliferation, differentiation, and fusion of CTBs (Forbes and Westwood, 2010; Ji *et al.*, 2013).

1.1.3.5 Spiral artery remodelling in detail

As explained in Section 1.1.3.4, uterine spiral arteries in non-pregnant women have a compact vascular smooth muscle cells which helps them to maintain a steady blood flow (See Figure 1.7). However, during pregnancy this blood supply must be increased to match the demands of the developing foetus and is usually carried out by invasive endovascular (enEVT) trophoblast cells (Chandan *et al.*, 2002). The first step starts with the vacuolation of endothelial cells within the spiral arteries, followed by the migration of iEVTs which will invade the uterine tissue. They have the ability to penetrate one-third of the adjacent myometrium (Chandan *et al.*, 2002). The enEVTs migrate towards uterine arteries and replace all the endothelial cell lining in the arteries. They also degrade the muscular layer which is essentially required to maintain blood vessel integrity (Chandan *et al.*, 2002). This is called re-endothelisation which helps in the lowering of vascular resistance to allow increased flow during pregnancy (Aplin, 2006). This remodelling of spiral arteries transforms the endometrial blood flow from "high resistant, low flow" to "low resistant, high flow" circulation (See Figure1.9). This is essential for the maintenance of pregnancy as it prevent any hypoxia induced oxidative stress (Knöfler and Pollheimer, 2012).

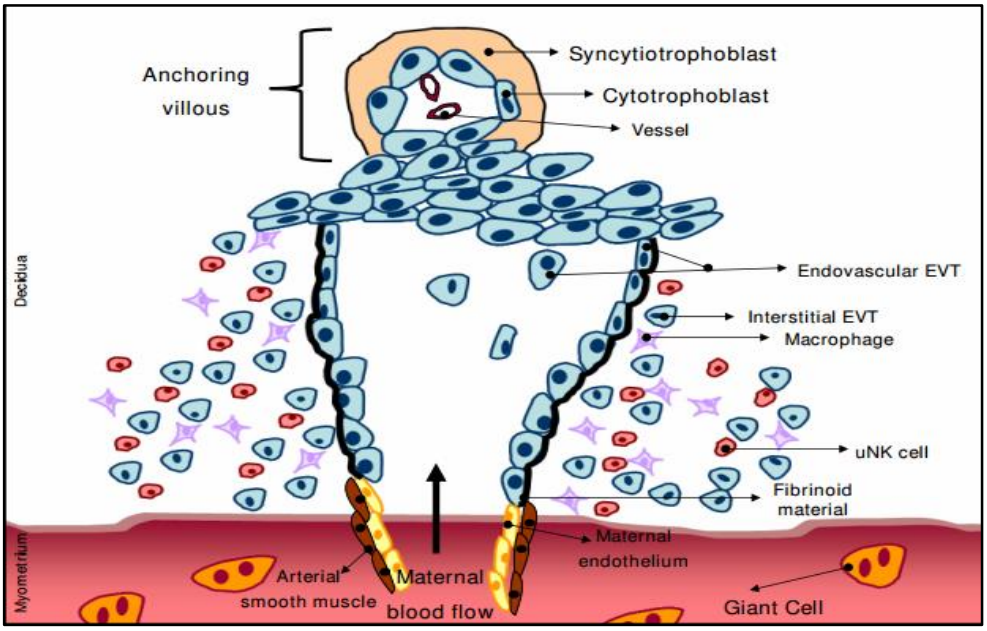

Figure1.9: Schematic representation of normal spiral artery remodelling.

The remodelling process involves replacement of endothelial cells by enEVTs and destruction of smooth muscles by iEVTs. ***Figure Adapted from*** **(www[6])**

1.1.3.6 Regulation of trophoblast differentiation and invasion

The trophoblast invasion is tightly controlled by several factors including hormones, cytokines, proteases like matrix metalloproteinase (MMPs) and their inhibitors [tissue inhibitors of metalloproteases (TIMP)], major histocompatibility complex (MHC) and surface integrins (Ferretti *et al.*, 2007). Differentiation and development of trophoblast cells is influenced by many other factors which exert their effects in a paracrine or autocrine manner (Staun-Ram and Shalev, 2005). The vascular endothelial growth factor family includes five members namely VEGF-A, -B, -C, -D and placenta-like growth factor (PIGF) which are considered essential for differentiation (Ferretti *et al.*, 2007). Furthermore, the Placental Growth Factor (PGF) is found in spiral artery remodelling. Trophoblast cells also express several other factors such as human leukocyte antigens (HLA), including HLA-E, polymorphic HLA-C, and HLA-G, which interact with decidual NK cells (Holtan *et al.*, 2009). All these factors are secreted not only by the trophoblast cells and villous mesenchymal cells, but also secreted from the uterine stromal, glandular, endothelial cells, and many other immune cells present at the maternal-foetal interface. Some of these factors and their functions are summarised in Table 1.1

Table 1.1: Summary of factors involved in trophoblast invasion *[Table adapted from Staun-Ram and Shalev, 2005].*

Factors	Source	Differentiation	Proliferation	Migration	Invasion	Functions
VEGF family	CTBs, STBs, EVTs, and decidua cells.	↑	↑	↓	↑	Regulate trophoblast invasion by activating different signalling cascades as PI3K/Akt pathway. Vasodilation, syncytialisation, angiogenesis
EGF	Decidua, CTBs, EVTs,	↑	↑	↑	↑	STBs differentiation, placental endocrine function modulation, embryo implantation
PIGF	Trophoblast cells	↑	↑	↓	↓	Angiogenesis
IGF-1	Trophoblast cells	↑	↑	↑	↑	Both foetal and placental development
TGF-β	Decidua, trophoblast, uNK cells	↓	↓	↓	↓	Inhibit early trophoblast differentiation and induces syncytialisation, down regulate invading of CBTs
HGF	CTBs, decidua, trophoblast villous STBs	↑	↑	↑	↑	Rapid trophoblast cell proliferation
CSF	Placenta, decidua	↑	↑	N/A	↑	Stimulate growth invasive trophoblast cells
Angiopoietin	Decidua, endothelial cells, STBs, CTBs	↑	N/A	N/A	N/A	Angiogenesis
Adhesion molecules	Tips of anchoring villi, CTBs	N/A	N/A	↑	↑	Placental anchorage
hCG	Produced by trophoblast	↑	N/A	↑	↑	Control regulation of invasion process
Progesterone	Produced by placenta	N/A	N/A	N/A	↑	Maintain placenta, and control CTBs invasion

EGF = Epidermal growth factor; IGF-1 = Insulin like growth factor; TGF-β = Transforming growth factor beta; HGF = Hepatocyte growth factor; CSF = Colony stimulating factor; hCG = human chorionic gonadotrophin. ↑ = Increased; ↓ = decreased; N/A = data not available

1.1.4 Placental complications

There are diverse clinical conditions and complications associated with pregnancy (**www**[7]). Complications resulting from abnormal placentation of embryo at second-trimester may lead to foetal death, and at the early stage may lead to severe diseases such as: pre-eclampsia (PE), intra-uterine growth restriction (IUGR) and abruption of placenta (Chaddha *et al.*, 2004). PE is most common disease that occurs in near-term pregnancies and causes death or early delivery of the foetus (**www**[7]). A detailed description of this syndrome is given below.

1.1.4.1 Pre-eclampsia (PE)

PE affects around 3-8% of pregnancies in the world and is one of the leading causes of perinatal maternal morbidity and mortality. Pre-eclampsia is derived from the Greek word 'eklampsis', meaning sudden flash or growth (Red-Horse *et al.*, 2004). It is a pregnancy-specific condition which develops after 20 weeks of pregnancy and is characterized by hypertension (≥140/90 mm Hg), proteinuria (concentration ≥30 mg/24 hours) and other systemic disorders such as organ damage and convulsions (Redman and Sargent, 2005). For mothers, it may cause other cardiovascular diseases such as chronic hypertension, ischemic stroke and heart disease (Goldman-Wohl and Yagel, 2002). Also, the babies who are born from pre-eclamptic pregnancies, are at risk of coronary heart disease, metabolic syndromes (such as diabetes) or stroke in their adult life (Roberts and Cooper, 2001; Uzan *et al.*, 2011). The risk factors for PE include pre-natal obesity, a family history of PE, multiple pregnancies, and chronic medical disorders such as long-term hypertension or diabetes (Redman and Sargent, 2005). Moreover, Immune and paternal factors may also affect women's risk for preeclampsia. It has been suggested that the risk for preeclampsia is increase with a change in paternity, limited sperm exposure with the same partner, or increased duration of time between pregnancies. These findings has noted that an immune tolerance mechanism contributes to the pathogenesis of preeclampsia (Saftlas *et al.*, 2003). Shallow trophoblast invasion during spiral artery remodelling can lead to PE, and IUGR (Kaufman and Disis, 2004; Pijenborg *et al.*, 2006).

1.1.4.2 Pathophysiology of Pre-eclampsia

Maternal PE is a condition that occurs in the last stage of pregnancy. This conditions starts with maternal responses like hypertension. In most of the cases, it is influenced either by environmental factors or maternal nutritional factors (Redman and Sargent, 2005). The maternal disease (or symptoms) occurs after 20 weeks and shows as full blown PE before 34 weeks of pregnancy. In contrast, placental PE is a condition where the placenta is becoming defective under hypoxia and oxidative stress (See Figure 1.10). Although the mechanism which leads to PE remains unclear, the pathophysiology may have two distinct stages: two distinct stages depending on the placental interaction: (**1**) placental PE and (**2**) maternal PE (Redman and Sargent, 2005).

Stage 1:This is called "poor placentation" and is characterized by shallow trophoblast invasion that results in placental ischemia (Sankaralingam *et al.,* 2006). The failure of trophoblasts to convert the spiral arteries results in poor remodelling, therefore restricting the utero-placental flow before 20 weeks of pregnancy, i.e. well before any clinical signs of PE (Goldman-Wohl and Yagel, 2002; Redman and Sargent, 2005).

Stage 2: This is characterized by a maternal inflammatory responses to defective placental circulation and a resultant hypoxia, by releasing factors which activate (or cause) the maternal endothelial dysfunction (Sankaralingam *et al.*, 2006). The recruitment of dendritic cells, macrophages and NK cells towards decidua is coupled with maternal symptoms such as hypertension and proteinuria, blood clotting and liver dysfunction (Redman and Sargent, 2005). In rare cases, the foetus may suffer from respiratory insufficiency, decreased nutritional supply and asphyxia leading to death (Redman and Sargent, 2005).

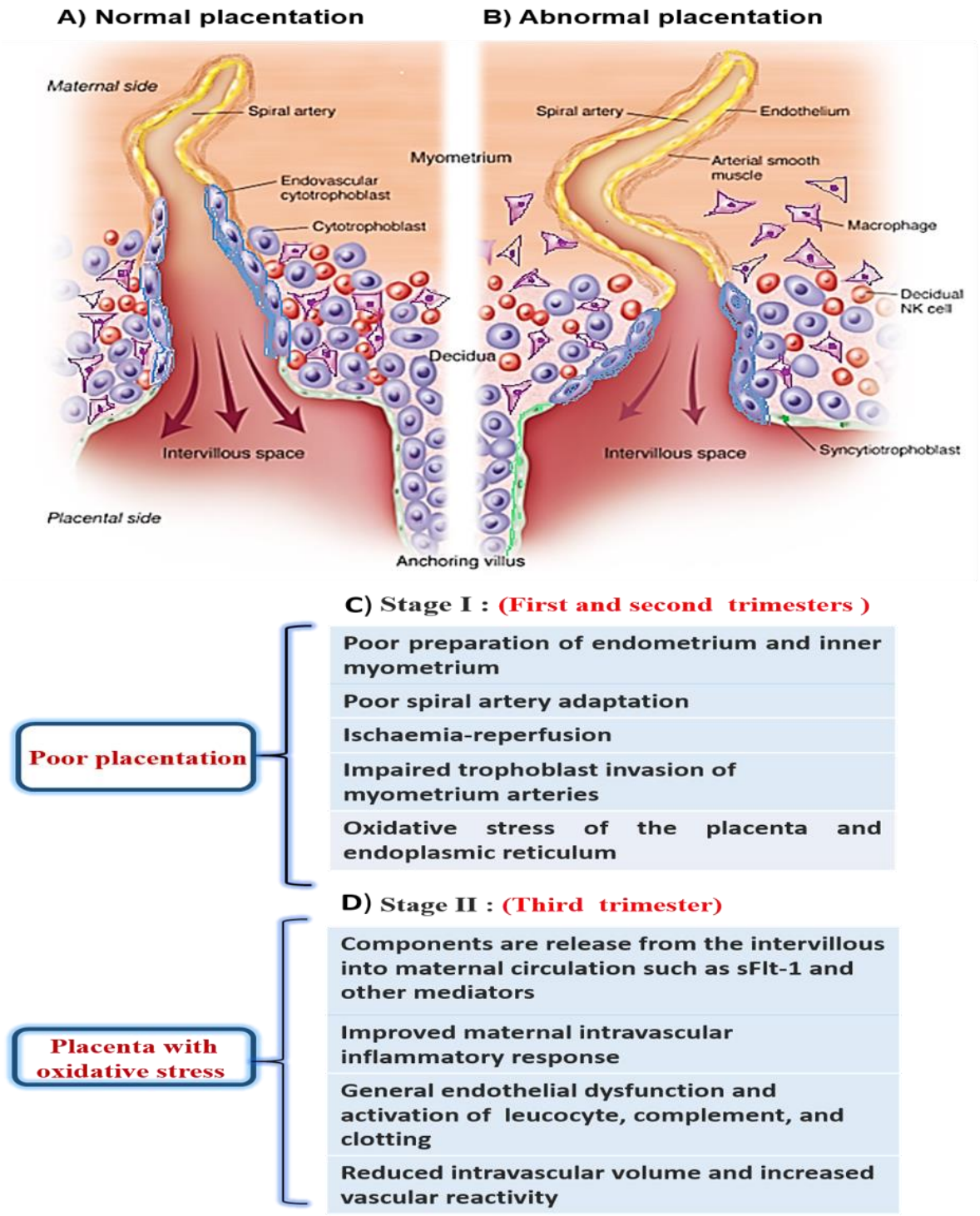

Figure1.10: Spiral artery remodelling between NT and PE placentation.

[**A**] Normal placentation associated with maternal decidua by anchoring villi. The cytotrophoblasts (**blue**) cross the placental maternal bridges and invade the maternal decidua next to the spiral arteries. The maternal endothelium (**yellow**) is encouraging remodelling of the arterial wall that results in smooth muscle replacement and arterial dilatation. In a normal pregnancy the activity of immune cells such as NK cells (**red**) and macrophages (**purple**) are down regulated to help the cytotrophoblasts invasion into the myometrial segments. [**B**] Pre-eclampsia is characterised by an impaired arterial remodelling and shallow cytotrophoblast invasion. [**C**] and [**D**] illustrate the two stages of PE. *[Figure adopted from Redman and Sargent, 2005]*

1.2 Tumour

Cancer is one of the major health problems which leads to a large number of deaths worldwide (**www[8]**). According to the World Health Organisation (WHO) it is second among deadly diseases, following cardiovascular diseases (**www[8]**). It is a highly heterogeneous disease that includes more than 100 different types of human cancer (Grizzi *et al.,* 2006). Tumourigenesis is a complex multi-development process consisting of transformation, proliferation, growth, invasion and metastasis which leads to cancer (Grizzi *et al.,* 2006). There are several contributing factors to the development of cancer, these include bacterial/viral infection, carcinogenic chemicals, organic and inorganic fibers and physical aberrations including ionising radiation and ultraviolet rays, somatic mutations etc. About 50% of all cancers are linked to lifestyle, such as diet, exposure to industrial toxins, tobacco and alcohol consumption (Devi, 2004; Abel and Di Giovanni, 2008). The tumour can be benign, if its growth is local (i.e. without invasion). It can also be malignant, if growth is uncontrolled, invades the neighbouring tissues and results in metastasis

1.2.1 Hallmarks of cancer

Hanahan and Weinberg (2000), initially identified six fundamental hallmarks of tumour growth and metastasis, which are shared by most of the tumour cells: (**1**) Sustaining proliferative signalling, (**2**) evading growth suppression, (**3**) resistance to cell death program, (**4**) enabling replicative immortality, (**5**) inducing angiogenesis, (**6**) activation of invasion and the metastasis process. In 2011, they added four more additional hallmarks namely (**7**) deregulating cellular energetics, (**8**) avoiding immune destruction, (**9**) genomic instability and mutation, and (**10**) tumour promoting inflammation (See Figure 1.11). All these hallmarks are described below.

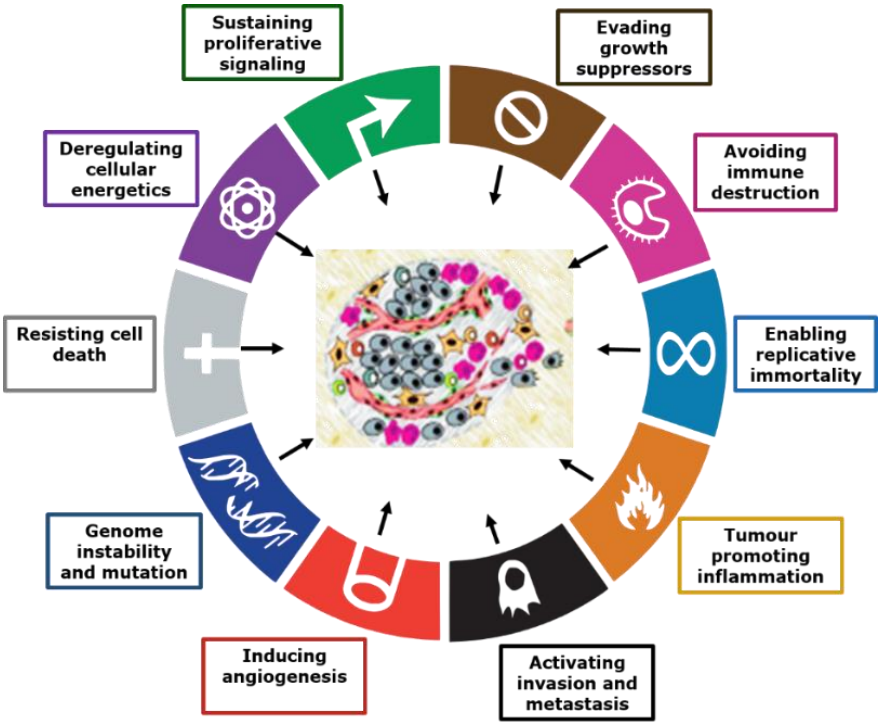

Figure1.11: Hallmarks of Cancer.

The figure represents the 10 characteristic changes taking place in cancer cells for tumour growth and transformation. *[Adapted from Hanahan and Weinberg, 2011]*

(1) Sustaining proliferative signalling

In normal tissues, cells are controlled by the production and release of growth-promoting signals (Hanahan and Weinberg, 2011). These signals enhance cell growth and division cycle, and lead to normal tissue functions. In order for normal cells to convert from inactive to a proliferative state, they need mitogenic growth signals (or growth factors) and in the absence of these growth signals, normal cells die (Hanahan and Weinberg, 2011). On the other hand, cancer cells may produce growth factors themselves (Lemmon and Schlessinger, 2010). Moreover, they gain the ability to enhance these mitogenic signals and alter growth receptors (Kroll *et al.*, 2010).

(2) Evading growth suppressors

In normal cells, the proliferation process is regulated by growth suppressors which drive the healthy cells into quiescent stage (G_0). According to Hanahan and Weinberg (2011), the developing tumour cells must evade anti-proliferative signals in order to drive them to malignant growth. Moreover, inactivation of tumour suppressor genes (that stop cell growth and proliferation) has been reported in many human cancers (Hanahan and Weinberg, 2011)

(3) Resisting cell death

A stable ratio between cell proliferation and cell death helps to maintain the growth of normal tissues (Elmore, 2007). Apoptosis (or programmed cell death) is an important cellular process which occurs in both physiological and pathological conditions. However, cancer cells lose the balance between cell division and cell death (Elmore, 2007). Almost all tumour cells develop an ability to evade apoptosis by down regulating pro-apoptotic factors (such as Bax, Bim, and Puma), and increasing the expression of anti-apoptotic regulators (Bcl-2, Bcl-x_L) or that of survival signals (Igf1/2) (Hanahan and Weinberg, 2011; Wong 2011).

(4) Enabling replicative immortality

One of the interesting features of normal cells is their potential to lose the ability of replication at some point leading to senescence (Hanahan and Weinberg, 2011). It has been reported that the tumour cells evade senescence by the inactivation of the tumour suppressor genes (e.g. p53 and pRb) resulting in uncontrolled proliferation and growth of the tumour (Herzig and Christofori, 2002). Cell death is mainly caused due to progressive shortening of the telomeres which occurs after each cell cycle. Yet this phenomenon is also surmounted by the over-expression of telomerase activity which ultimately results in indefinite cell proliferation (Kim *et al.,* 1994).

(5) Inducing angiogenesis

Tumour cells require oxygen, nutrients and the removal of waste products during rapid growth and invasion (Folkman, 1971). In order to do this they need to vascularize which is achieved by a complex process called angiogenesis and in its absence a tumour may become necrotic or apoptotic (Holmgren *et al.,* 1995). Therefore, angiogenesis is an important step for successful invasion, metastasis and growth of the tumour. Physiological angiogenesis is a complex process that normally occurs during embryonic development and in wound healing (Oklu *et al.,* 2010). However, pathological angiogenesis is critical for cancer cells.

Angiogenesis is regulated by a balance between angiogenic activators and angiogenic inhibitors. The expression levels of angiogenic factors reflect the aggressiveness of the tumour cells (Nishida *et al.,* 2006). Tumour endothelial, stromal, and circulating host cells (endothelial progenitor cells, platelets, and macrophages) are capable of stimulating angiogenesis by producing several angiogenic factors, such as VEGF, EGF, bFGF, TGF-β and TNF-α (Nishida *et al.,* 2006) (See Table 1.2). VEGF has two primary roles: Firstly it induce a proliferative effect on the endothelial cells thereby enhances their growth by increasing their survival and lowering the rate of the apoptosis in them, and secondly, it is

known to increase vascular permeability (Nishida *et al.,* 2006). These aid the invasion by creating a way for extravasation and migration for the tumour from/into the circulation (Dimova *et al.,* 2014). Apart from this, there are a number of cellular stress factors important to stimulate angiogenesis signalling such as hypoxia, low pH, and lack of nutrients. In fact, angiogenesis in tumour tissue is a multistep development, mediated by endothelial cells (ECs) (Dimova *et al.,* 2014).

Table 1. 1: Activators and inhibitors of angiogenesis [Table adapted from Nishida *et al.,* 2006]

Angiogenesis Activators	Angiogenesis Inhibitors
Vascular endothelial growth factor family (VEGF)	Interleukin IL4
basic fibroblast growth factor (bFGF)	Interleukin IL10
Acidic fibroblast growth factor (aFGF)	Interleukin IL12
Transforming growth factor (TGF-β)	Endostatin
Tumour necrosis factor (TNF-α)	Interferon IFN- α
Platelet-derived growth factor (PDGF)	Tissue inhibitors of metalloproteinase (TIMPs)
Hepatocyte growth factor (HGF)	Angiopoietin-2
Epidermal growth factor (EGF)	Angiotensin
Placental growth factor (PGF)	Thrombospondin 1 (TSP-1)
Colony stimulating factor (CSF)	p53
Matrix metalloproteinase (MMPs)	

To summarise a small tumour is formed when a cell has acquired genetic modifications that allow unlimited growth and escape from apoptosis. Once a tumour has reached the size of about 1 to 2 mm^3, the oxygen and nutrient supply become insufficient (Thijssen *et al.,* 2009). This results in production and release of different growth factors into the nearby tissue. The secreted growth factors bind to receptors on ECs in nearby vessels. The ECs are then activated and start producing proteases and other digestive enzymes, such as MMPs, to degrade the basal membrane and the extracellular matrix (Oklu *et al.,* 2010). This extracellular matrix dissolution allows the release of pro-angiogenic factors. Finally, the ECs start to divide, and migrate into the surrounding tissues to form new vascular structures. This helps tumour cells to grow, and undergo metastasis (see below) (Thijssen *et al.,* 2009 ; Oklu *et al.,* 2010).

(6) Activating invasion and metastasis

Metastasis is a complex multistep process, responsible for around 90% of all cancer mortalities (Djamgoz *et al.*, 2014). During metastasis cell separation from the primary tumour occurs first when cells gain the ability to survive without adherence (Weinberg, 2008). They then detach from the primary tumour mass and invade the neighbouring tissues and basement membranes ((Nguyen, 2008). Following this, they enter the blood vessels and lymphatic circulation (intravasation), being transported by these circulations to new organ or tissue sites in the body (extravasation) (Nguyen, 2008; Weinberg, 2008; Bravo-Cordero *et al.*, 2012). These steps for metastasis are summarized in Figure 1.12.

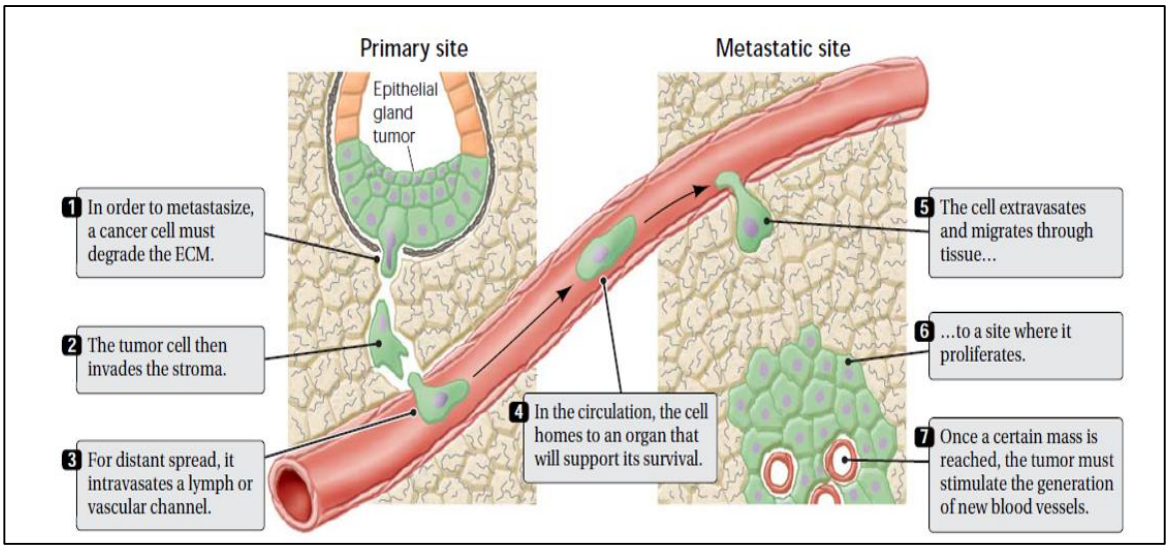

Figure1.12: The metastasis process during tumour invasion.

[Adapted from Geho et al., 2005]

During cancer development, tumour cells change their plasticity by morphological and phenotypical conversions from epithelial to mesenchymal transition (EMT) (Kong *et al.*, 2011). However, it is worth noting EMT is also shown in normal cells. It is a normal physiological process recognized as a feature of embryogenesis, especially during morphogenesis and is characterized by the epithelial cells losing adhesion and detachment from tight junctions. They change cell shape, and become more migrant and invasive (Kong *et al.*, 2011). Apart from embryogenesis, EMT plays an important role during wound healing, chronic inflammation and fibrosis. EMT has a critical role in tumour metastasis, which is induced by factors associated with tumour aggressiveness, such as FGF, VEGF, PDGF and integrins (Kong *et al.*, 2011; Van Zijl *et al.*, 2011). Cells with EMT phenotype are rich sources for cancer stem-like cells. In the case EMT is associated with a loss of

epithelial factors such as E-cadherin (Das *et al.,* 2014). In most tumour types, down-regulation in the expression of E-cadherin has been illustrated and correlated with the increased invasion and metastatic process (Devi, 2004). Another important transformation during metastasis is the opposite of EMT that is from mesenchymal-epithelial transition cells (MET), especially at secondary sites (Kong *et al.,* 2011). This reverse mesenchymal-epithelial transition generates secondary epithelia (Samatov *et al.,* 2013). This process allows mesenchymal cells to regain the epithelial cell-to-cell junctions for colonisation at secondary sites (Van Zijl *et al.,* 2011). Thus, EMT and MET play essential roles in both normal development and cancer metastasis (Heerboth *et al.,* 2015).

(7) Deregulating cellular energetics

During normal cellular respiration, glucose through glycolysis gets converted to pyruvate, which is further converted to carbon dioxide in mitochondria resulting in ATP production. However, during anaerobic metabolism, only the glycolysis takes place, to reduce the usage of oxygen and leads to the accumulation of lactic acid (Warburg mechanism). This latter mechanism is also observed in tumour cells even during the presence of oxygen. This results in an 18-fold reduction in ATP production. This deficit in synthesis of ATP is compensated by the up-regulation of glucose transporter proteins in the cell membrane, leading to increased transport of glucose molecules inside the cells (DeBerardinis *et al.,* 2008; Hsu and Sabatini, 2008; Jones and Thompson, 2009). Therefore, cancer cells can conserve energy to entrap glucose which is needed for rapid proliferation by artificially producing an anaerobic metabolism.

(8) Avoiding immune destruction

Tumour cells create a microenvironment to escape from the immune response. Immune surveillance is essential to prevent the development and progression of tumour cells (Kaufman and Disis, 2004). In this process, the innate and the adaptive immune systems cooperate in functioning, and T cells play an essential role in detecting and eliminating the tumour cells. T cells are activated by the T-cell receptor (TCR) that binds with antigen peptides presented on major histocompatibility complex molecules (MHCs). The recognition of peptides presented by MHC class I molecules results in the activation of CD8+ cytotoxic T cells (CTLs). Additionally, another subset of T cells, the CD4+ T cells, recognises peptides presented by MHC class II molecules and improve the ability of dendritic cell (DCs) to induce CTLs (Bennaceur *et al.,* 2009). CD4+ T cell activation significantly increases innate immunity, such as activation of macrophages and NK cells, by enhanced IFN-γ secretion (Töpfer *et al.,* 2011)). IFN-γ levels improve the recognition

capacity of T cells through induction of higher expression levels of MHC class I molecules on the target cell (Töpfer *et al.*, 2011). Apart from them, neutrophils are also involved in innate immunity. They bring about rejection of tumours by directly killing the tumour cells through various mechanisms such as destruction of tumour vessels and inhibition of angiogenesis (Igney and Krammer, 2002). Moreover, tumours can display tumour antigens and can stimulate other immune cells.

Interestingly, tumour cells escape CTL recognition by producing abnormalities in the antigen presentation machinery (APM). This includes down regulation or complete loss of MHC class I molecules as observed in many types of carcinoma. (Töpfer *et al.*, 2011). There are several mechanisms by which the tumour can escape from the immune cells. For example, the down-regulation of adhesion molecules present in malignant tissue may inhibit the immune system. The tumour stroma also plays a critical role in inhibiting immunity, which serves as a physical barrier between the tumour and immune cells. The down-regulated expression of the tumour antigen results in enhanced tumour incidence and metastasis. Furthermore, the downregulation expression of HLA-A and-B on the cell surface of tumour cells will normally prevent recognition CD8+ cytotoxic T cells, class II HLA downregulation expression prevents recognition by CD4+ T cells but expression of HLA-C and HLA-G non-classical MHC class I leads to inhibtions of NK cell cytotoxicity function (Töpfer et al., 2011). Tumour stroma also expresses immunosuppressive factors and these factors may be expressed by the malignant cells themselves or by non-cancerous (such as epithelial or stromal) cells that are present at the tumour site (Ochsenbein *et al.*, 2001). There are several immunosuppressive factors, such as TGF-β, that play an essential role in proliferation, activation, and differentiation of cells of innate and adaptive immunity (Gabrilovich *et al.*, 1996). Other immunosuppressive factors expressed by malignant cells are prostaglandins, interleukin (IL-10), macrophage and CSF (Igney and Krammer, 2002; Kroll *et al.*,2010).

(9) **Genomic instability and mutation**

Tumour progression is a multistep process and is believed to be acquired by successive clonal expansions resulting in a mutant genotype (Hanahan and Weinberg, 2011). In each cell, there exists a DNA repair mechanism that detects and resolves various defects in the DNA after every replication, ensuring a minimal rate of spontaneous mutations. In cancers, there is an increase in this rate of mutation due to its sensitivity to mutagenic agents or failure of DNA repair mechanism which ultimately results in tumour formation (Negrini *et al.*, 2010; Salk *et al.*, 2010).

(10) Tumour promoting inflammation

Inflammation is a helpful response that is activated to repair tissue injury. However, if inflammation is unregulated, it can become chronic, inducing malignant cell transformation in the surrounding tissue (Landskron *et al.*, 2014). The inflammatory response shares several molecular targets and signalling pathways with the tumourigenic process (Landskron *et al.*, 2014). The inflammatory system can act as activator or inhibitor in tumour growth (Welch, 2008). The hypoxic environment and severe metabolic stress activates inflammatory infiltrates, such as cytokines (Whiteside, 2008). Depending on the tumour microenvironment, cytokines can modulate an anti-tumoural response but during chronic inflammation they can also induce cell transformation and malignancy. Inflammation also induces generation of reactive oxygen species (ROS) and reactive nitrogen species (RNS) at the site of inflammation. These species trigger DNA damage and mutations on the genes of differentiating and proliferating cells (Landskron *et al.*, 2014). In fact, most cells responsible for inflammation may contribute to some of the hallmarks of cancer by supplying growth factors, matrix-metalloproteinases, pro-angiogenic factors and survival factors (Karnoub and Weinberg, 2007; DeNardo *et al*, 2010).

1.3 Similarities between placentation and tumourigenesis

In both placentation and tumourigenesis the invasion phenotype is acquired by up/down regulation of many cell specific adhesion molecules, extended activity of matrix-digested enzymes (along with other expressed enzymes such as telomerase) and/or expression of proto-oncogenes (Soundararajan and Rao, 2004). Trophoblast and tumour cells both have the capability of escaping the host's immune system and can also establish an abundant blood supply (Soundararajan and Rao, 2004) (See Figure 1.13). The regulatory components for tumour cell migration and invasion are also shared by the human trophoblast cells. In fact, due to the migratory and invasive capacities, the trophoblast cells are often considered as '*pseudo-malignant tissue*' which show 'physiological metastasis' (Soundararajan and Rao, 2004). As seen in Figure 1.13, different adhesion molecules, proteases MMPs and plasminogen are involved in both the processes. Apart from these molecules, EGF can up regulate the enzymatic signal transduction in order to activate mitogen activated protein kinases (MAPK) (Ferretti *et al.*, 2007). Also, PDGFR which is expressed by EVT as well as tumour cells can trigger c-Myc function to stimulate cell proliferation (Soundararajan and Rao, 2004). Both processes are compared in detail as follows.

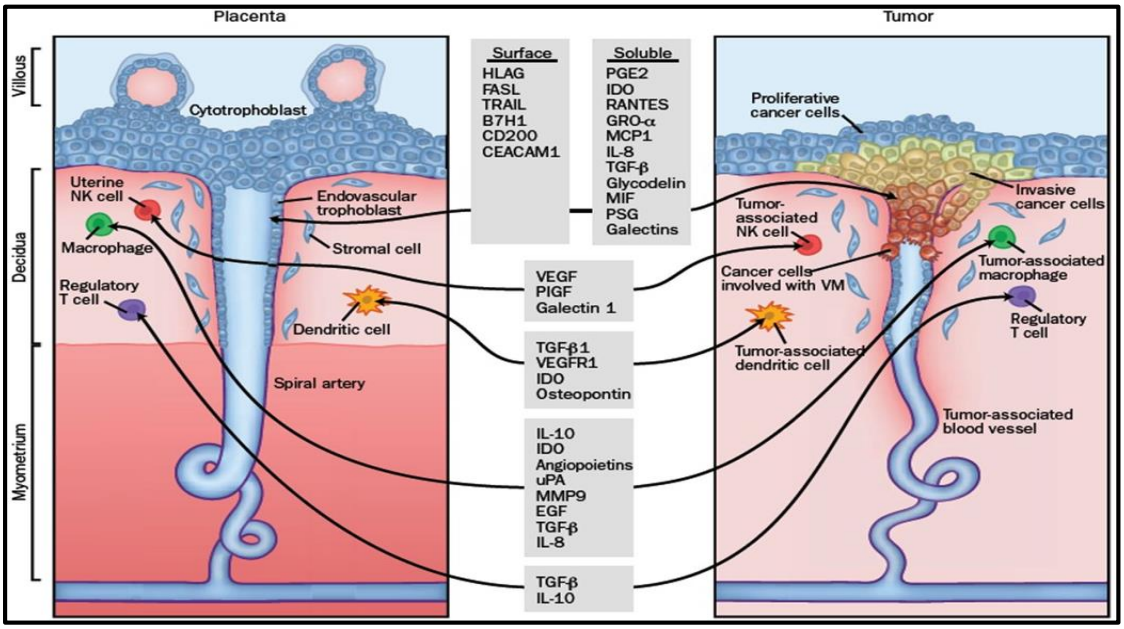

Figure 1.13: Micro-environments of placental and tumour invasion.

Both placenta and tumour interfaces are supported by similar molecules as shown in the figure. *[Adapted and modified from Holtan et al., 2009]*

1.3.1 Invasion

Both establishment of a successful pregnancy and tumourigenesis are dependent on maintaining adequate blood and nutrient supply (Holtan *et al.*, 2009). However, the cellular events of trophoblast cells are much more organised as they follow a specific pattern of "*differentiation during proliferating*" followed by "*invasion without distance metastasis*" (Holtan *et al.*, 2009). As explained in Section 1.1.3.2, EVT cells differentiate into an invasive phenotype. These cells then migrate into the maternal decidua through the CTB cell columns (Holtan *et al.*, 2009). Several molecular factors are involved during the '*physiological metastisation*' (Ferretti *et al.*, 2006). In contrast, the cancer cells show "*proliferation during invasion*" followed by "*distant metastasis*". Tumour cells follow a three-step process (known as the three-step hypothesis) to complete the invasion process within host tissue (Liotta, 1984). The first step is the attachment or adhesion of tumour cells with host tissue and is similar to blastocyst adhesion after hatching from the zona-pellucida. The second step is degradation of the extra cellular matrix (ECM) by aggressive cancerous cells with the help of secreted hydrolysis enzymes (Liotta, 1984). This is also seen in EVT cell migration in placental development. The third step is motility or locomotion of the invading tumour cells within modified ECM (similar to the events in spiral artery remodelling). However, the aggressive invasion of tumour cells is brought about by the cyclic repetition of these steps (Plantefaber and Hynes, 1989; Albelda *et al.*, 1990; Behrens *et al.*, 1993; Oka *et al.*, 1993).

1.3.2 Proliferation

The capacity for extensive proliferation is identical in trophoblast and tumour cells. At the early stage of adhesion, cytotrophoblast stem cells trigger rapid proliferation (Ferretti *et al.*, 2006). Studies have shown that there is a close resemblance between the behaviour of highly proliferative vCTBs and evCTBs which show a tumorigenic phenotype after neoplastic transformation (Ferretti *et al.*, 2006). However, CTB proliferation is highly controlled (Pollheimer and Knofler, 2005). In both cases, the ability to oscillate cell expansion is not only determined by proliferation rate, but also by the rate of evasion of apoptosis. Activation of many cell surface receptors can induce the escape mechanism for apoptosis in non-malignant trophoblast and malignant cells (Ferretti *et al.*, 2006). For example, trophoblast and cancer cells both express common ligand/receptor pairs including insulin growth factor1/2 (IGF1/2) ligand for the receptor IGF-1R to achieve survival signal stimuli (Butt *et al.*, 1999). Phosphorylation of these receptors can activate the phosphoinositide 3-kinase (PI3K) pathway to minimize apoptosis rates in both tumour and trophoblast cells (Butt *et al.*, 1999).

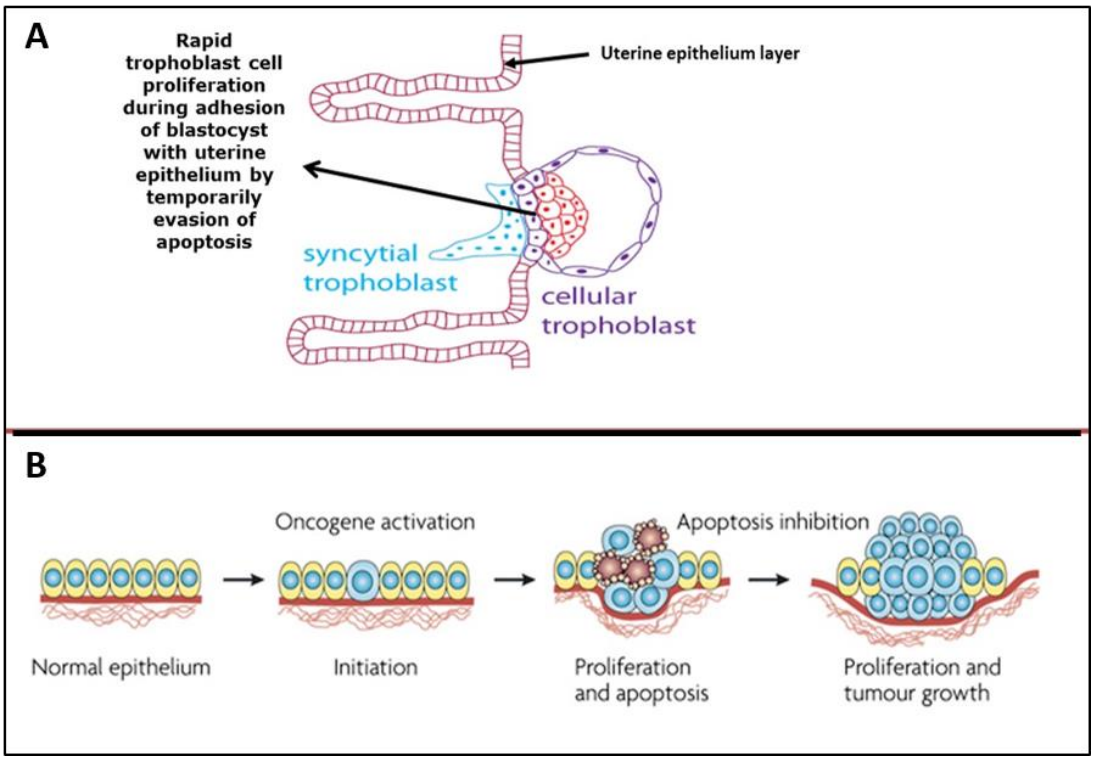

Figure1.14: Similarities in cell proliferation between trophoblast and tumour cell.

During trophoblast cell proliferation, rapid cell expansion leads to formation of STBs (A) and a similar attribute in tumour cells also helps in cell multiplication (B). *[Adapted and modified from Mathew et al., 2007]*

1.3.3 Vasculogenic mimicry and immune escape

During vasculogenic mimicry, invading trophoblast cells within maternal spiral arteries further differentiate into a vascular phenotype and similar attributes are also present in tumour cells (Zhou *et al.,* 1997). Elementary key genes and cell signalling pathways for vasculogenic mimicry are shared by both malignant and non-malignant trophoblast cells (Zhou *et al.,* 1997). Angiopoietins, the chief controllers of vascular remodelling are up-regulated during early placentation and also in tumour angiogenesis. Also, PGF which is a member of the VEGF family is highly expressed by trophoblast cells and tumour cells (Cao and Leu, 2007). Despite the fact that trophoblasts express paternal antigens, the maternal immune monitoring system is unable to reject the embryo (Ferretti *et al.,* 2006). This is mainly due to the down-regulation of major histocompatibility complex (MHC) class I or class II molecules. Due to this, invading trophoblast cells still manage to evade the maternal immune system (Weetman, 1999). This down-regulation is also shown in tumour cells enabling them to elude T-cell-mediated immune responses (Bubenik, 2003). In addition, evCTBs highly express the non-classic MHC gene which encodes HLA-G in order to inactivate NK cell function. By sharing similar cellular mechanism, the tumour cells also inactive NK cells (Sinkovics and Horvath, 2005).

1.4 Differences between trophoblast and tumour invasion

Although there are several similarities between early embryo and tumour development, there are also differences between them (See Figure 1.15). As mentioned (in Section 1.3), the main difference between trophoblast and tumour invasion is that during trophoblast development, the molecular mechanisms such as proliferation, invasion and migration are well regulated (Ferretti *et al.,* 2007). The invasion of trophoblastic cells is spatial, in that the invasion mechanism is stopped after the development of placenta (Ferretti *et al.,* 2007). Instead of continuing invasion, trophoblast cells start apoptosis after establishing a definitive placenta (Kliman *et al.,* 1990). Specifically, trophoblast invasion declines rapidly 20 weeks after establishing materno-foetal communication, this demonstrates that trophoblast differentiation occurs under tightly controlled circumstances (Fitzgerald *et al.,* 2005). Thus, the regulated migration and invasion of trophoblast cells is also known as a "*controlled programme of terminal differentiation*" (Soundararajan and Rao, 2004).

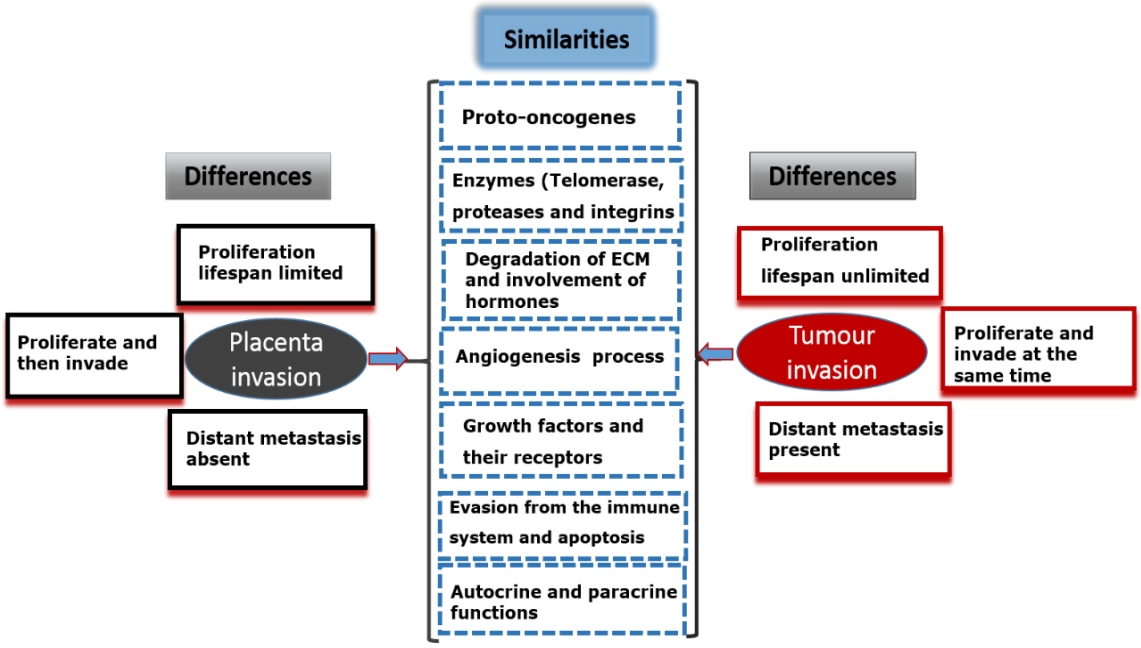

Figure1.15: Similarities and differences between trophoblast and tumour invasions.

In contrast, tumour invasion happens randomly, without any control in the cells transferring to distant organs. In tumour cells, there is a loss of regulation of cell cycle proteins which causes abnormal proliferation of cells and uncontrolled cell division (Cross *et al.*, 2003). However, trophoblast cells do not show any deviation from the normal cell cycle, which is achieved by placenta-specific genes, cytokines and endocrine factors through either inhibition or promotion of the invasion processes (Cross *et al.*, 2003). As trophoblast cells divide, differentiate and then invade, the lifespan of a single trophoblast cell (and also the invasive depth) is limited (Richard, 2011). In contrast, tumour cells divide and invade at the same time. As mentioned before, trophoblast invasion is controlled during implantation in both space (endometrium) and time in the first trimester (12 weeks post conception) (Cohen and Bischof, 2007).

1.5 Potential factors of interest common to tumours and placenta

Interestingly, several different factors are believed to play important roles in placental and tumour invasion. However, the functional status of many of these factors has not been fully established. Some of these factors are listed below.

1.5.1 Human aldehyde dehydrogenase 3 family, member A1 (ALDH3A1)

Aldehyde dehydrogenase 3 (ALDH3) belongs to the mammalian aldehyde dehydrogenase family that is involved in the metabolism of endogenous/exogenous aldehydes, and neurotransmitters (Vasiliou and Nebert, 2005). Depending on their physiochemical

properties, 12 ALDH genes are present in humans which are located on different chromosomes, and distributed in various tissues including brain, liver, stomach, kidney and testis. Although, each member of the ALDH family have a different function, collectively their activities include enhancing cell proliferation, differentiation, drug resistance, and cell response to oxidative stress. Interestingly, ALDH also activates other compounds that are beneficial to the cells (Canuto *et al.,* 2001). For example, ALDH3A1 converts an aldehyde precursor to an acid thereby preventing DNA damage (Ho *et al.*, 2008). This indicates that ALDH3 is capable of providing cellular protection. The activity of ALDH has been used to identify, and select stem-like cell lineage amongst endothelial progenitor, mesenchymal, epithelial and hematopoietic stem cells. For example, van den Hoogen *et al*. (2010) used ALDH3A1 to compare and isolate populations of primary human prostate cancer cells. Likewise, the expression and activity of ALDH3A1 was found to be a marker for cancer stem cells in many solid tumours, such as breast, ovarian and colon cancer (Ma and Allan, 2011). It has an important effect in tumour progression during metastatic initiation but the mechanism that controls the constitutive expression of ALDH3A1 remains unclear (Reisdorph and Lindahl, 2001). Most importantly the mechanism of ALDH3A1 at the trophoblast invasion stage is yet to be clearly understood (Jelski and Szmitkowski, 2008).

1.5.2 Aurora kinases (AURK)

Aurora kinase (AURK) genes are a group of serine-threonine kinases which are commonly known as mitotic kinases which were first isolated from *Drosophila* (Bhat et *al.,* 1996). They play an important role in regulation of cell division in G2 to M phase, and the deregulation of AURK activity leads to defects in the functions of centrosome, maturation, and spindle formation (Dar *et al.,* 2010). Moreover, the signalling of Aurora kinase associated with mitotic errors is closely connected to chromosomal aneuploidy in cancer cells (Dar *et al.,* 2010; Banno, 2013). The two subtypes of AURK which are of interest in this study are explained below.

- **Aurora kinase A (AURK-A)**

Aurora kinase A (AURK-A) is also named as STK15/BTAK, BTAK (Breast Tumour Activated Kinase) (Berdnik and Knoblich, 2002). It plays a major role in cell cycle regulation of meiosis, mitosis cytokinesis, chromosome maturation and centrosome separation (Ma *et al.,* 2003). Interestingly, centrosome maturation happens in the G2 phase where many proteins that accumulate at the centrosomes lead to tumourigenesis. AURK-A is over-expressed in several human cancers including gastric cancer, breast cancer and neuroblastoma (Ma *et al.,* 2003). Furthermore, many oncogenic functions including the activation of growth signalling pathways, reduction in the functions of p53, p73, and

phosphatidylinositide 3-kinase/AKT are caused due to the abnormal expression of AURK-A. P53 is a tumour suppressor protein that plays an important role in preventing the development of cancer cells at several regulatory points during the cell cycle (Ryan *et al.*, 2001). P73 regulates the cell cycle and induces apoptosis in cells under stress (Zawacka-Pankau *et al.*, 2010). A strong correlation between AURK-A over-expression, p53 function and tumourigenesis has been reported (Vader and Lens, 2008). By phosphorylating p53, AURK-A decreases the transcriptional activity of p53 mRNA (Vader and Lens, 2008). However, p53 inhibits AURK-A activity by binding to the catalytic domain of AURK-A. In addition, p53 induces a protein called DNA-damage-inducible protein (GADD45a) that also participates in inhibiting AURK-A function (Vader and Lens, 2008). This indicates that the effect of AURK-A over-expression on centrosome regulation is dependent on p53 status (See Figure 1.16).

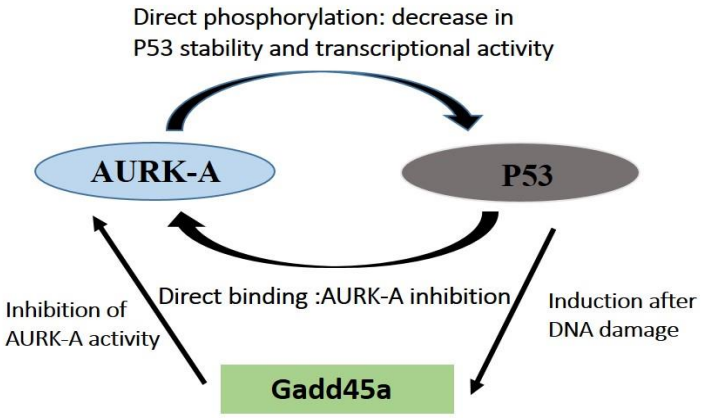

Figure1.16: Summary of the interaction between AURK-A and p53.

The function of P53 is related to the over-expression of AURK-A in tumourigenesis, where p53 stability is decreased by phosphorylation of AURK-A. In contrast, p53 inhibits AURK-A function by inducing GADD45a. [*Figure adopted from Vader and Lens, 2008*]

The role of AURK-A in tumour and trophoblast cells is still not fully understood. It is suggested that over-expression of AURK-A potentially affects cell proliferation and VEGF-mediated angiogenesis. Moreover, on the placental side, it has been suggested that spindle and chromatin dynamics is regulated by AURK-A during early and late stages of mammalian oocyte maturation (Shuda *et al.*, 2009).

- **Aurora kinase C (AURK-C)**

AURK-C is another member of the AURK protein family that is over expressed in many types of cancer, such as breast, liver and prostate, which suggests that AURK-C may have the potential to induce proliferative capacity in tumour cells (Dieterich *et al.,* 2007). Remarkably, it has been found that the mRNA and protein of AURK-C is also over expressed in normal rapidly dividing tissues such as testis. The exact role and function of AURK C in carcinogenesis and placental development is not clearly known (Dar *et al.,* 2010; Kollareddy *et al.,* 2008; Banno, 2013). It has been found that AURK-C plays an important role during pre-implantation of embryo (Zeng *et al.,* 2004; Macaulay *et al.,* 2011).

1.5.3 Platelet-derived growth factor receptor alpha (PDGFRα)

PDGF is a family of growth factors that play a major role in several physiological functions, including embryogenesis and angiogenesis. PDGF also plays an important role in cellular differentiation and development, regulation of growth such as proliferation (Looman *et al.*, 2007). It was characterised as a mitogen for fibroblasts and cells of mesenchymal-origins, such as smooth muscle cells (Looman *et al.,* 2007). PDGF exists in three isoforms PDGF-α, PDGF-β and PDGF-αβ which can function as hetero- or homodimers (Majumdar *et al.*, 2009). Expression of PDGF and its receptors became an area of interest because they are thought to promote human cancer development and progression. PDGF encodes a protein responsible for cell transformation, indicating an autocrine mechanism in tumourigenesis (Raica and Cimpean, 2010). Furthermore, the co-expression of PDGF-α and PDGF-β, and their receptors have been identified in the cellular signalling seen in malignant gliomas (Alvarez *et al.,* 2006). The status and functions of PDGFRα in trophoblast cells are not fully understood.

1.5.4 Basic helix loop helix protein (TWIST1)

TWIST1 is a member of the basic helix-loop-helix (bHLH) family of proteins (Murre *et al.* 1989). The bHLH structure was recognised in the DNA binding proteins E12 and E47, and was first identified in *Drosophila* (O'Rourke and Tam, 2002). It plays an essential role in promoting tumour metastasis from epithelial to mesenchymal transition by promoting the formation of invadopodia, specialized membrane protrusions for ECM degradation (Eckert *et al.,* 2011). It is over-expressed in a variety of tumours, e.g. prostate, lung, breast, uterus, and liver cancer. TWIST1 also plays a vital role during embryonic growth of tissues such as muscle and bone (Cabrera Je, 2013). In mouse and rat, the mRNA expression of TWIST-1 was present in the mesoderm of the gastrulating embryo and was also found in the limb bud mesenchyme during the organogenesis phase (Maestro *et al.,* 1999). Both TWIST-1 and TWIST-2, can inhibit the p53 that is essential for cell death. Interestingly, they can interfere

with the p53 tumour suppressor pathway by modification of the action of ARF/MDM2/p53 action (Maestro *et al.,* 1999; O'Rourke and Tam, 2002).

1.5.5 JAG1 (Jagged-1)

Jag-1 (or Jagged-1) is a protein encoded by the JAG1 gene, also known as CD339 (**www[9]**). It is considered as a ligand for multiple NOTCH receptors and acts as a mediator for NOTCH signalling. It interacts with NOTCH 2 and 3 receptors, but in the presence of calcium it can interact with NOTCH 1 receptors as well (Purrow *et al.,* 2005). The NOTCH signalling may act either positively or negatively to influence cell processes such as proliferation, differentiation and apoptosis, depending on the cell type (Purrow *et al.,* 2005). Therefore, JAG-1 can play a crucial role in tissue formation during the development of an embryo (Karanu *et al.,* 2000). Moreover, NOTCH was found to be present in the cytoplasm of the CTB, EVT and placental stroma in the first trimester of the pregnancy. It was also present in the STB, endothelial cells and stroma of placental villi (De Falco *et al.,* 2007). Studies have shown that JAG1 is a potent pro-angiogenic factor in mice embryos (Benedito *et al.,* 2009). It has been proposed as a promoter of metastasis in both breast and bone cancer by engaging NOTCH signalling, however, the mechanism behind this remains unknown (Sethi *et al.,* 2011).

1.6 Importance of "stem-like" cells in invasion

Another distinctive character shown by both tumour and trophoblast cells is presence of stem cell populations. In the case of tumours, the cancer stem cells (CSCs) show a high tumourigenic capacity of replenish self-renewal and differentiate into other cell types (Yoo *et al.,* 2013). On the other hand, trophoblast stem cells are involved in promoting self-renewal only (Red-Horse *et al.,* 2015). Surprisingly some interesting data has demonstrated that during the development of tumour, ''*sphere forming cells*'' or ''*spheroids*'' can enhance tumourigenesis and increase the metastatic ability of malignant cells *in vivo* (Burleson *et al.,* 2006). Likewise, spheroid like structure formation has also been reported in the case of non-malignant trophoblast cells (Sivasubramaniam, Unpublished data). A detailed discussion of spheroidal attributes of these two cellular types is given in (Chapter 4). A general description of different types of stem cells is given below.

1.6.1 Stem Cells

Cells with the ability to renew themselves and to generate mature cells through the process of differentiation within a particular tissue are known as stem cells (Reya *et al.*, 2001; Gao, 2007). Three significant properties differentiate these cells from normal cells, which are: (a) an ability to renew independently which maintains the stem cell pool within the host; (b) an ability to regulate the number of cells produced, and (c) an ability to differentiate to develop all the functional elements of the tissue (Al -Hajj *et al.*, 2004). Even though stem cells differ in their developmental potential, they must maintain a balance between self-renewal and differentiation. Consequently, the concept of regulation of self-renewal is important in cancer since it is considered to be a disease of unregulated self-renewal (Reya *et al.*, 2001; Tuch, 2006).

1.6.2 Classification of Stem Cells

Depending on their ability to differentiate, stem cells are classified as totipotent, pluripotent, or multipotent. Totipotent stem cells have the ability to become any kind of cell in the body and usually develop from the fertilized egg. Pluripotent stem cells develop from the three embryonic tissue layers, i.e. ectoderm, endoderm and mesoderm (Gao *et al.*, 2008: Kaur *et al.*, 2009). They can be obtained from the inner cell mass (ICM) of the blastocyst. Multipotent stem cells can differentiate into more than one type of specialised cell in tissue or organ, and are isolated from many tissues of the body (Mousa, *et al.*, 2006). These cells can self-renew to repair any damaged tissue like the haematopoetic stem cells in bone marrow, blood, neuronal stem cells of brain and hepatic stem cells of liver (See Figure1.16). Multipotent stem cells are further differentiated into three types depending on their ability to renew; Long term self-renewing cells, Short term self-renewing and Progenitor multi-potent cells incapable of self-renewal (Gao *et al.*, 2008: Kaur *et al.*, 2009). Division of stem cells generates daughter cells possessing the properties of their parent cells. Different types of stem cells that are produced from trophoblast are summarised in Figure1.17.

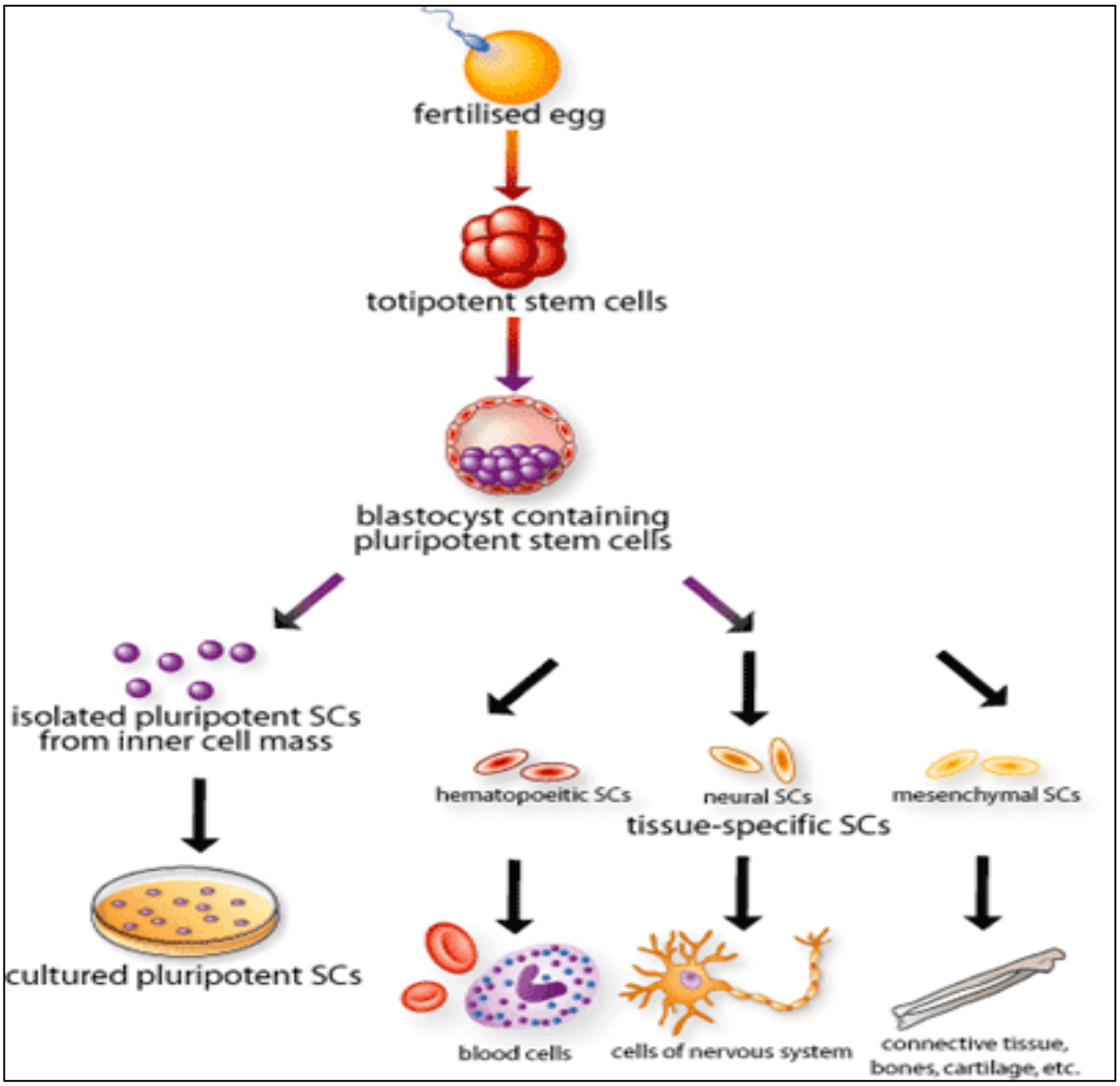

Figure1.17: The origins of specialisation of stem cells.

The single cell begins to divide and multiply at a rate much faster than somatic cells after a sperm fertilizes an egg. The totipotent stem cells (SCs) rising in the inner mass of the blastocyst are known as embryonic stem cells (ES). ES can differentiate into various tissue types of the human body. [*Figure adopted from Chaudry, 2004]*

1.6.3 Stem cell markers

There are many molecular markers used to isolate and characterize various stem cell populations, some of which include OCT4, SOX2, NANOG, NOTCH1 and CDX2. Although the marker profiles of stem cell populations often change depending on their site of origin or species, these molecular markers provide a systematic approach to characterize a healthy stem cell population (**www**[10]).

- **OCT4**

OCT4 is a transcription factor belonging to the POU (Pit-Oct-Unc) transcription factor family and is also known as OCT-3, OCT3/4 and POU5F1 (Schöler *et al.*, 1990). It plays a crucial role in the embryonic development, acts as a regulator of self-renewal and

differentiation, maintains and re-establishes pluripotency of embryonic stem (ES) cells in both human and mouse (Shi and Jin, 2010). It is usually expressed in the early cleavage stage of the inner cell mass. Studies indicate that mRNA and protein expression of OCT4 are found in several human tissue specific adult stem cells and different types of cancer stem cells (Atlasi *et al.,* 2007).

- **SOX2**

SOX2 (Sex-determining region Y (SRY)-Box 2) is a member of the SOX family of transcription factors (**www[11]**). It plays a vital role in maintenance and differentiation of stem cells. It is required for trophoblast formation and progression of several human malignancies Laga *et al.* (2010) findings suggest that SOX2 is a novel biomarker used for subpopulations of stem cell niches related to melanocyte ontogeny and tumorigenesis and a growing number of studies illustrate the relationship between SOX2 and cancer. In breast cancer cells, SOX2 promotes cell proliferation and tumourigenesis (Xiang *et al.,* 2011). Both SOX2 and OCT4 have essential roles during embryogenesis. They generate pluripotent stem cells from human cord blood cells and work together to regulate genes necessary for the self-renewal (Herreros-Villanueva *et al.,* 2013; Rizzino, 2013).

- **NANOG**

NANOG is a homeodomain-containing transcription factor which is expressed in the inner cell mass and embryonic stem cells (ES). It has important roles in maintaining self-renewal amongst undifferentiated pluripotent stem cells during early embryonic development. NANOG and OCT4 work together to support stem cell potency and self-renewal in several germ cell and tumours (Siu *et al.,* 2012; Wang *et al.,* 2013)). It is associated with tumour aggressiveness, metastasis and chemo-sensitivity. The knockdown of NANOG has been reported to inhibit ovarian cancer cell proliferation and invasion. Therefore, several studies suggest that NANOG can be used as a target for molecular therapeutics and as a potential marker to target ovarian cancer (Siu *et al.,* 2012; Wang *et al.,* 2013). OCT4, NANOG and SOX2 are all identified to be co-up-regulated in many human tumours, including prostate and breast cancer and tumours may be controlled by restricting the expression of these three genes. Likewise, they can be used as tumourigenesis markers, which can act as molecular switches that control the CSC cell fate during cancer development (Liu *et al.,* 2013).

- **NOTCH1**

NOTCH1 is a transmembrane receptor which was first identified in *Drosophila.* There are two pathways involved in NOTCH signalling: canonical signalling and non-canonical signalling. Canonical NOTCH signalling is achieved by cell–cell interaction, but non-

canonical signalling is not completely understood (De Falco *et al.,* 2007; Cuman *et al.,* 2014). Studies in the past, demonstrated that the NOTCH signalling pathway was necessary for the development of the placenta (Zhao and Lin, 2012). It is believed NOTCH1 signalling controls uterine decidualisation and plays an essential role in implantation. Moreover, members of the NOTCH signalling pathway have been identified in placental growth and reported to play an important role during placentation (Zhao and Lin, 2012). This involves endometrial trophoectoderm interactions during the initiation of attachment, and regulation of EVT invasion (Zhao and Lin, 2012). It is also essential for spiral artery remodelling in the decidua, angiogenesis progression and vascular homeostasis in the adults. On the other hand, the irregular signalling of NOTCH is found in PE and IUGR (Cuman *et al.,* 2014). Interestingly, NOTCH also plays an essential role in tumour development and can act as an oncogene (Bolós *et al.,* 2007).

- **CDX2**

CDX2 is a nuclear homeobox transcription factor that belongs to the caudal-related family of CDX homeobox (HOX) genes (**www[13]**). The gene encodes CDX2 plays an essential role during embryonic development. It is expressed in the embryonic trophoectoderm and in the spongiotrophoblast component of the placenta at later stages of development (Murthi *et al.,* 2011). HOX genes can be used as markers and targets for some diseases, such as cancer, diabetic wound healing, and Alzheimer's disease. It is also expressed in the intestinal epithelium, where it plays roles in establishment and maintenance of intestinal epithelial cells (Saad *et al.,* 2011). Previous studies have suggested that the expression of CDX2 is down-regulated during colorectal carcinogenesis (Bai *et al.,* 2003). They proposed that CDX2 acts as a tumour suppressor by promoting cellular differentiation and inhibiting proliferation. The absence of CDX2 results in an aggressive tumour with enhanced metastasis of colorectal cancer (Bai *et al.,* 2003).

1.6.4 The ability for trophoblasts to produce stem-like cells

As mentioned before in Section 1.1.3.4, the placenta is a pseudo-malignant organ which shows '*physiological metastasis'* (Ferretti *et al.,* 2007). Both the process of tumorigenesis and placentation begin with a highly invasive form of cells (See Figure 1.18). One of the unique characteristics of the trophoblast cells is the ability to produce stem cell populations that are involved in the promotion of self-renewal (Red-Horse *et al.,* 2014). Trophoblast cells also demonstrated the ability to produce stem-like cells during invasion (John *et al.,* 1993). Likewise, spheroid like structure formation has also been reported in malignant cancers including ovarian cancer (Burleson *et al.,* 2004). Also, *in vitro* studies have shown that the embryonic stem cells (ESCs) can grow into three-dimensional spheres called embryonic

bodies (EBs) in culture media (Sivasubramaiyan *et al.,* 2009). Comparative photoelectron micrographs of tumour spheroidal cells and blastocyst are given in Figure 1.18.

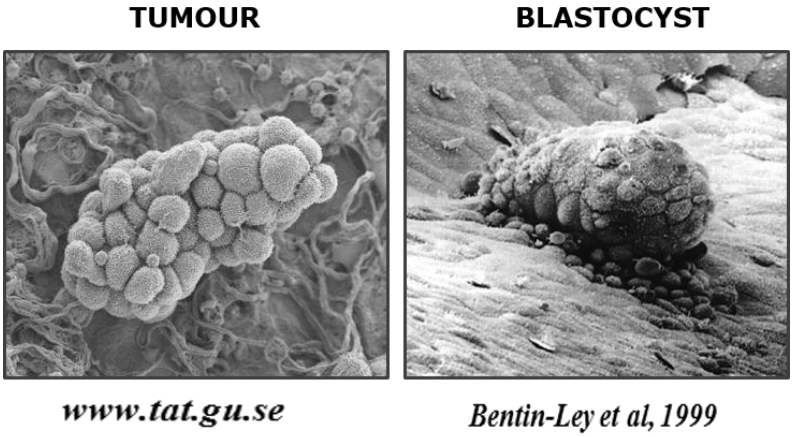

Figure1.18: The similarity of the spheroid like structure in tumour and blastocyst.

1.7 Spheroid (3-D) cell culture

Three-dimensional (3-D) cell culture *in vitro* models have been used in research as an intermediate between *in vitro* cultures and *in vivo* tumour (Fennema *et al.,* 2013). Cells that are cultured in 3-D grow as aggregates have many different names such as mammosphere, micro-mass and spheroid (Fennema *et al.,* 2013). This system mimics various properties of solid tumours such as cell heterogeneity and production of similar proliferating, quiescent regions with a necrotic core (Weiswald *et al.,* 2015). Moreover, tumour cells cultured as spheroids exhibit more resistance to therapy than those cultured as a monolayer. In fact 3-D culture provides "multicellular resistance," enhanced by cell-cell contacts, cell-matrix contacts, and the 3-D shape (similar to the *in vivo* situation) (Phung *et al.,* 2011). Thus, it provides a microenvironment similar to a solid tumour (See Figure 1.19). These features limit the delivery of anti-cancer drugs to core cancer cells that are located far from blood vessels (Phung *et al.,* 2011).

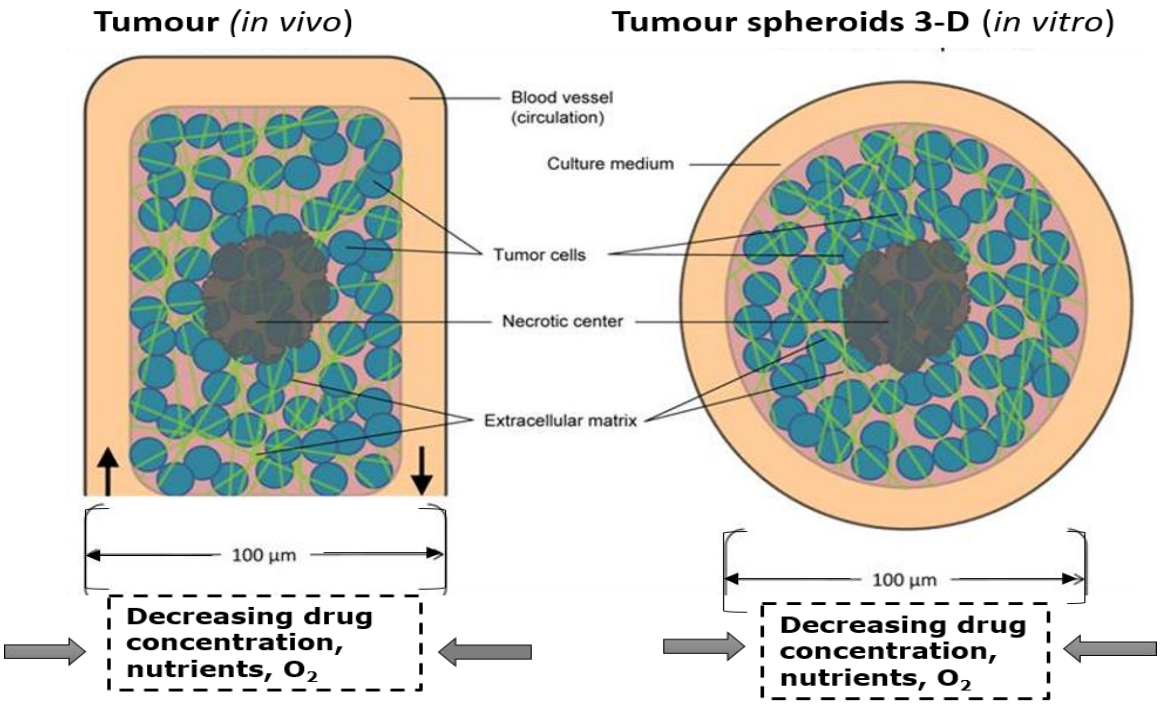

Figure1.19: Comparison between *in vivo* solid tumour and spheroid model.

The 3-D culture creates an oxygen gradient similar to *in vivo* solid tumours. This feature limits the delivery of anticancer drugs to the core of the spheroids. *[Adopted from Phung et al., 2011]*

As explained in in several parts of the introduction, there are similarities and differences between tumour and trophoblast cells. The pseudo-tumourigenic properties of trophoblast cells can be used not only to compare the status of common factors between these two processes; but also can be exploited to study the toxicological effects of chemotherapeutic agents in physiologically rapid dividing cells. In order to achieve the former; trophoblasts of placental disorders with low trophoblast invasion (such as PE) can be compared. Likewise, it is also essential to establish *in vitro* 3-D spheroid cultures of "stem-like cells" from trophoblast derived cells to study the latter.

1.8 Aims and hypothesis

A literature review indicated differential gene expression patterns in normotensive and PE placentae. The factors of interest (ALDH3A1, AURK-A and C, PDGFRα, TWIST1, and JAG1) have also been demonstrated to be involved in proliferation, migration and invasion of various cells. Furthermore it has been shown that due to resemblance of trophoblast cells to tumour cells, it may be possible to produce spheroids from both the cell types. Therefore, it was hypothesised:

- The expression of factors that are involved in trophoblast invasion would be altered in pre-eclamptic placentae.
- These expression patterns may also be different in non-resistant and drug-resistant spheroids from those of the original parental cells.
- The invasive capacities of non-resistant and drug-resistant spheroids would be different from the original parental cells.
- Compared to parental cells, the global protein expression profiles would be altered in non-resistant and drug-resistant spheroidal cells.

Aims:

- To compare the expression patterns of common factors related to invasion, such as ALDH3A1, AURK-A and C, PDGFRα, TWIST1, and JAG1 involved in normotensive (NT) and pre-eclamptic (PE) placentae.
- To generate spheroids from transformed trophoblast (HTR8/SVneo, TEV-1) and choriocarcinoma (JEG-3, BeWo) cell lines and to check the effects of the chemotherapeutic agent Doxorubicin in producing drug resistant spheroids from trophoblast cell lines.
- To characterise the "stemness" feature by studying the expressions of stem cell markers such as OCT4, SOX-2, NANOG, CDX2 and NOTCH1.
- To compare the migration and invasion potentials amongst non-resistant, drug-resistant spheroids and their parental cells.
- To investigate the expression patterns of common factors such as ALDH3A1, AURK- (A and C), PDGFRα, TWIST1, and JAG1 in parental cells and spheroidal cells (untreated and DOX-treated) originated from four trophoblast cell lines.
- To investigate the changes in the global protein (peptide) expression profiles in parental and spheroidal cells (untreated and DOX-treated) which are produced from transformed trophoblast cell lines (HTR8/SVneo and TEV-1) by using SWATH-MS technique.

Chapter 2
Materials and Methods

2.1 Buffers and solutions

All buffers and solutions were prepared in sterile glass bottles and maintained at recommended temperature when not in use with some solutions prepared fresh immediately before to use.

Table 2.1: Buffers and solutions

Reagent	Recipe
TAE Buffer 50X	242 g Tris Base, 57.1 ml Acetic Acid, 100 ml 0.5M EDTA, 1 litre ddH_2O, pH 8.5
1X TAE buffer (pH 8.0)	50X TAE buffer 20ml, ddH_2O 980ml
1% Agarose used for RNA	Agarose 0.4, 1X TAE 40ml, Ethidium bromide (Sigma) 2µl
1.5% Agarose used for DNA	Agarose 0.6, 1X TAE 40ml, Ethidium bromide (Sigma) 2µl
PBS-Tween20 (PBS-T)	1 litre 1X PBS, 5ml Tween 20
TBS-Tween20 (TBS-T)	1 litre 1X TBS, 5ml Tween20
TBS 10X	24.23g Trizma HCl, 80.06g NaCl, 1 litre ddH_2O, pH 7.6
PBS 1X	10 Phosphate Buffered-Saline tablets (Fisher Scientific) in 1 litre ddH_2O
Running Buffer 5X	15 g Tris Base, 72 g Glycine, 5.0 g SDS, 1 litre ddH_2O, pH 8.3.
Transfer Buffer 10X	60.4 g Tris Base, 288 g Glycine, 1.8 litres ddH_2O. Methanol added to 1X transfer buffer before use.
Laemmli Buffer 4X	200mM Tris-HCl pH 6.8, 400mM DTT, 0.8% w/v SDS, 0.4% w/v Bromophenol blue, 40% v/v glycerol, 5% v/v β-mercaptoethanol
Antibody Buffer	3% BSA, TBS-T, 0.02% Sodium Azide
50mM (Triethyl ammonium bicarbonate) TEAB buffer	Diluting 1M stock solution 20 times (i.e. 500 µl of 1M stock solution +9.5 ml of nanopure grade water)
0.5 M dithiothreitol (DTT; MW 154.25)	Dissolve 0.077 g of DTT in 1ml of nanopure water
0.55 M iodoacetamide (IAA; MW 184.96)	Dissolve 0.0407 g of IAA in 400 µl of 50mM TEAB buffer
0.1% formic acid	50 ml of nanopure water in and remove 50 µl of nanopure water and add 50 µl of neat formic acid
5% Acetonitrile in 0.1% formic acid	10 ml of 0.1% formic acid in 15 ml red-top tube remove 500 µl of 1% formic acid and add 500 µl of 100% acetone acetonitrile.

2.2 Antibodies

All antibodies were prepared and stored according to manufacturer's guidelines and used before the expiry date. The concentration of each antibody (primary or secondary) for Immunohistochemistry (IHC), Immunofluorescence (IF) and Western blotting (WB), are summarised in Tables 2.2 and 2.3.

Table 2.2: Details of primary antibodies with concentrations for IHC, WB and IF.

Primary antibodies	**Supplier**	**Antibody dilutions**
Rabbit Anti-ALDH3A1	Abcam	IHC (1:200); WB (1:500)
Rabbit Anti-Aurora A	Abcam	IHC (1:20); WB (1:500)
Rabbit Anti- Aurora C	Abcam	IHC (1:200); WB (1:500)
Rabbit Anti- Jagged1	Abcam	IHC(1:500); WB (1:10000)
Rabbit Anti-PDGFR	Abcam	IHC (1:500); WB (1:500)
Rabbit Anti-TWIST1	Abcam	IHC (1:200); WB (1:500)
Mouse Anti-OCT4	Abcam	IF (1:200); WB (1:500)
Rabbit Anti-SOX2	Abcam	IF (1:500); WB (1:500)
Rabbit Anti-NANOG	Abcam	IF (1:50); WB (1:1000)
Rabbit Anti-CDX2	Abcam	WB (1:500)
Mouse Anti-CDX2	Abcam	IF (1:50)
Rabbit Anti-NOTCH1	Abcam	IF (1:150); WB (1:1000)
Controls		
Mouse Anti-Vimentin (positive control for IHC)	NCL-L-VIM- Leica	IHC (1:400)
Active PDGF protein	Abcam	WB (1:500)

Table 2.3: Details of secondary antibodies with concentrations for IHC, WB and IF.

Secondary Antibodies	Supplier	Antibody dilutions
Donkey Anti-Rabbit Human IgG H+L (HRP) conjugated	Abcam	WB (1:3000)
FluoresceinAnti-Rabbit IgG (H+L)	Vector Laboratories, Inc	WB (1:1000)
Biotinylated Anti-Mouse/Rabbit IgG provided with VECTASTAIN Elite ABC Kit	PK-6200 Vector Laboratories, Inc	IHC (1:1000)
Goat anti-Mouse IgG (H+L), Alexa Fluor®	life technologies	IF (1:1000)
Goat anti-Rabbit IgG (H+L), Alexa Fluor®	life technologies	IF (1:1000)

2.3 Placental tissue collection

Human placental tissue samples were obtained from the Nottingham City Hospital following informed consent from donors under NHS ethical approval [NREC Ref: 12/NE/0112]. This ethical approval was extended to suit this study by the Health Research Authority-NRES Committee North East. The demographic details of the placentae are given in Section 3.2.1. These samples were collected and stored appropriately at -80°C until further use. Some of the samples were further preserved by paraformaldehyde fixation and embedded in paraffin for immunostaining protocol.

2.4 Total RNA extraction

RNeasy® Plus Mini-kit (Qiagen) was used to perform the total RNA isolation and purification from placental tissues according to the manufacturers (Qiagen, Inc) instructions. Homogenisation of placental samples was carried out by crushing the samples with liquid nitrogen and transferred into pre-cooled centrifuge tubes after which 600µl of RLT buffer with 6µl β-mercaptoethanol (Sigma Aldrich) was added to the samples. This homogenized lysate was transferred into a QIAshredder® (Qiagen) and centrifuged at 15,000 x *g* for 2 minutes in a microcentrifuge (Microcentaur Sanyo). The supernatant was transferred into a gDNA eliminator spin column. The column was centrifuged again at 10,000 x *g* for 30 seconds to remove any genomic DNA. The supernatant was mixed with 600µl 70% ethanol (Fisher Scientific). This mixture was transferred to an RNeasy spin column placed in a collection tube. Centrifugation was repeated at 10,000 x *g* for 15 seconds. The RNeasy spin column was retained and 700µl Buffer RW1 was added and centrifuged again at 10,000 x *g* for 15 seconds. This was followed by 2x 500µl RPE Buffer washes. Lastly the column was treated with 30-50µl RNase-free Millipore water and centrifuged at 10,000 x *g* for 1 minute.

The supernatant was transferred to a new eppendorf tube and stored at -80°C. The purity and quantity of RNA were measured by using Nanodrop® spectrophotometer. The extracted RNA samples were electrophoresed in 1% agarose gel (BIOzym group) to fractionate the two RNA subunits, 28S and 18S. 1kb ladder (New England, BioLabs® Inc) was used to identify the two subunits.

2.5 cDNA template preparation by Reverse Transcription

SuperScript™ II Reverse Transcriptase kit (Invitrogen™) was used to convert RNA into cDNA. Depending on the total RNA concentration of 10pg-5µg, a 20µl reaction volume was prepared. The reaction mixture was created in an eppendorf tube with 15 µl of nuclease free water, with 1µl of extracted RNA samples,1 µl Oligo (dT) 15 Primer (Promega), 1µl dNTP mix (10mM each) (Promega) and 1µl RNAsin (Promega). This mixture was gently vortexed then heated to 65°C for 5 minutes followed by chilling quickly on ice. 4µl of 5X First-Strand Buffer and 2µl of 0.1M DTT was added to the reaction and mixed well. The sample was incubated at 42°C for 2 minutes. After this incubation, 1µl of SuperScript™ II was added and allowed to incubate at 42°C for 50 minutes. The sample of cDNA was stored at -20°C.

2.6 Gene expression study

2.6.1 Primer designing and optimising

PCR primers were designed by using Coding DNA sequences (CDS) for the factors of interest from National Centre for Biotechnology Information (NCBI) website **(www[14])**. CDS was used to design the primers using Primer 3 Input version 4 **(www[15])** and Integrated DNA Tool **(www[16])** was used to check the properties of primers such as annealing temperature, hairpin loops, GC content etc. ClustalW2 software was used to find the common nucleotide regions between all the variants (if the factors has more than one variant) **(www[17])**. BLAST software **(www[18])** was used to check specificity of the primer sequences and the specific primers were finalised. The criteria used for primer design are given below:

1) Sequence:
   a) The following were avoided (i) 3 or more runs of G or C at 3´ end, (ii) a T at the 3´ end, (iii) mismatches at the 3´ end and complementary sequences.
   b) 3´ end should end in G or C or CG or GC. This will increase efficiency of priming.
2) The length of primer was kept between 18-22 nucleotides.
3) The GC content was between 40-60%.
4) Melting temperature (T_m) was kept between 55-80 °C.
5) Product size was less than 200 bps.

6) Primer Concentration: 0.1-0.5µM.

The primer sequences with their annealing temperatures are given in Table3.2. The annealing temperatures for the primers were first calculated using the following equations:

$$\boldsymbol{T_m} = 4\,(G + C) + 2\,(A + T)$$

$$\boldsymbol{T_a} = \frac{T_m\ Forward + T_m\ Reverse}{2} - 5℃$$

Where $\mathbf{T_m}$ is melting temperature for the primers, $\mathbf{T_a}$ is the annealing temperature for the gene of interest.

2.6.2 Gene amplification using conventional PCR and gradient PCR

Factors of interest were amplified using the primers designed in Section 2.6.1 by conventional TECHNE® Thermocycler TC3000 (Bibby Scientific Ltd.). The PCR Master Mix (Promega) was used for the reaction mixture. The reaction mixture was prepared according to the company guidelines.

- **Reaction Mixture for 25µl:**

Components	Volume	Final concentration
PCR Master Mix, 2X	12.5µl	1X
upstream primer, 10µM	0.5µl	0.1–1.0µM
downstream primer, 10µM	0. 5µl	0.1–1.0µM
DNA template	1µl	<250ng
Nuclease-Free water	10.5µl	N.A.

- **General program setting for PCR amplification was as follows:**
  - Initial denaturation at 95°C for 2 minutes
    - Denaturation at 95°C for 30 seconds
    - Annealing at X°C for 30 seconds x 40 cycles
    - Extension at 72°C for 30 seconds
  - Final Extension at 72°C for 2 minutes

Note: Where X°C is the Ta calculated in Section 2.6.1

TECHNE® 3Prime temperature gradient PCR (Geneflow Ltd.) was also used to amplify genes for which calculated T_a showed low/no dimer products. The PCR product size was analysed by using 1.5% agarose gel using a 100bp ladder (New England Biolabs® Inc).

2.6.3 Agarose gel electrophoresis

Agarose gel electrophoresis was carried out to check the size and integrity of the product whether from a DNA or RNA sample. The desired percentage of agarose gel was prepared in fresh 1X TAE buffer; 1.5% agarose gel was used to analyse PCR products and 1% agarose gel to detect the integrity of the RNA samples. Ethidium bromide (Sigma) was used as a detection dye in the gel. The gel was electrophoresed at 50 Volts for 15 minutes followed by 80 volts for 30 minutes. The gels were then imaged on Gel Doc (InGenius, Syngene) under UV light.

2.6.4 PCR product confirmation by DNA sequencing

The PCR products were cleaned by using a Wizard® Genomic DNA purification kit (Promega) according to the manufacturer's guidelines. An equal volume of membrane binding solution was mixed with the PCR products. The mixture was transferred to a Minicolumn assembly and incubated at room temperature for 1 minute. The Minicolumn was then centrifuged at 16,000 x *g* for 1 minute. Following this the column was washed twice with membrane wash solution and centrifuged at 16,000 x *g* for 1 minute. Purified DNA was eluted out from the column using nuclease-free water. The purified samples were sent for sequencing at the Functional Genomics, Proteomics and Metabolomics Facility, University of Birmingham, for DNA sequencing. The sequences were analysed using Chromas lite 2.1.1 software for accuracy.

2.6.5 Relative expression of factors of interest by quantitative Real-Time PCR (qRT-PCR)

Factors of interest were amplified by using a Corbett® quantitative PCR (qRT-PCR) thermo cycler (Corbett Lifesciences). The reaction mixture of qRT-PCR was prepared at a final volume of 12.5µl. Millipore water 4.25µl; SYBR Green 6.75µl (Biorad Laboratories, Inc.); forward and reverse primers 0.5µl 10 pM/µL; and cDNA samples 0.5µl were used. Nuclease-free water was used as negative control. The program started with an initial denaturation for 5 minutes at 95°C. The number of cycles for amplification was 40 with a denaturation at 95°C for 30 seconds. Depending on the primer of interest, the annealing temperature was set for 30 seconds and the extension at 72°C for 10 seconds. The annealing temperatures for each gene are given in Table 3.2. The melting curve for the factors was analysed after the reaction using Rotor Gene-6000 Series 1.7 software and the delta Ct values ($2^{-\Delta\Delta Ct}$) were calculated. $2^{-\Delta\Delta Ct}$ is a method to calculate relative quantitative expression by comparing Ct values (Livak and Schmittgen, 2001). The mRNA expression of target factors are normalised to an endogenous reference gene (house-keeping gene) and relative to calibrator (positive control). The house-keeping genes used in this study are GAPDH,

HPRT1and TBP1. The calibrator for factors expression was MCF-7 a tumour cell line of non-placental origin.

2.7 *In vitro* cell culture

2.7.1 Cell revival and subculture

The cells were revived from liquid nitrogen storage by thawing the vials quickly in warm water. Thawed cells were added with 10 ml of growth media to remove the cytotoxic effects of freeze media and centrifuged at 1,000 x *g* for 5 minutes. The supernatant was discarded and 1ml of growth media was added to the pellet. Cells were then transferred into T25 flasks (Sarstedt). All cell lines specifications and culture media are summarized in Table 2.4. The growth media were supplemented by 10% FBS (foetal bovine serum) (Lonza), 2mM L-Glutamine (Lonza) and 25U/ml penicillin/streptomycin (Lonza). Cells were grown in T25 flasks incubating at 37˚C in a humidified atmosphere of 95% (v/v) air/5% (v/v) carbon dioxide. A daily check was performed and the cell lines were sub-cultured when they reached 70-95% confluence.

Table 2.1: Details of the cell lines used in this study.

Cell line	Cell type	Medium	Provider
HTR-8/SVneo	Human First-trimester extravillous trophoblast	RPMI-1640	Dr Charles Graham University of Kingston, Canada
TEV-1	Human First-trimester extravillous trophoblast	RPMI-1640	Dr Mei Choi Choey University of Hong Kong, China
JEG-3	Human placenta choriocarcinoma	EMEM	ECACC*
BeWo	Human placenta choriocarcinoma	Ham's F12	ECACC*
MCF-7	Human breast adenocarcinoma cell line	DMEM	ATCC#

*European Collection of Cell Cultures; #American Type Culture Collection

After the cells attained 70-95% confluency sub-culture was carried out by discarding the media and washing the flasks three times with 1X PBS (Lonza). Trypsin 1X (Sigma) was added to the flask to detach the cells and incubated for 2 minutes at 37°C. The duration of trypsinisation differed according to the cell types. An inverted light microscope (Motic AE2000, Scientific Laboratory Supplies Ltd.) was used to check detachment of the cells.

Afterwards, respective growth media for each cell line was added to stop the action of trypsin. The cells were collected into Sterilin® tubes (Sarstedt) and were centrifuged for 5 minutes at 1,000 x *g* in Harrier 15/80 centrifuge (Sanyo).

The supernatant was discarded and 1ml of growth media was added to the pellet and mixed well to achieve a suspension of single cells. Viable cells were counted by using 0.4% (v/v) trypan blue (Sigma Aldrich). 100µl of cell suspension was mixed with 300µl trypan blue. A small volume (10µl) of this mix was used to count in a haemocytometer. The cell numbers in four large grids were counted to estimate the total cell count using following calculation.

$$\textbf{Cell Numbers/ml} = \text{Average cell number} \times 10^4 \times 4 \text{ (dilution factor)}$$

These cells were both bulked up and transferred into T75/T175 flasks (Sarstedt) and used for further experiments or frozen down as below.

2.7.2 Cryopreservation of cells

For a continuous supply of cell lines, cells were cryopreserved in liquid nitrogen. The cell pellet after centrifugation was re-suspended in freeze media (Media 6.4ml, Penicillin/Streptomycin 0.1ml, FBS 2.5ml, and DMSO 1.0ml). The cells with freeze media were then transferred to cryovials placed on ice and immediately transferred to a -80˚C freezer. The following day the cells were moved into liquid nitrogen for long storage.

2.8 *In vitro* cytotoxicity assays

2.8.1 MTT (3-(4,5-Dimethylthiazol-2-yl)-2,5-Diphenyltetrazolium Bromide) assay

Doxorubicin hydrochloride (10 mg) was obtained from Sigma Aldrich. This was reconstituted by diluting in 10ml of filtered distilled water to achieve the final concentration of 1mg/ml. and stored as aliquots at 4 °C covered with foil. The MTT assay was carried out with an appropriate number of cells (5 x10^4) which were transferred into 96 well plates grown along with different concentration of Doxorubicin hydrochloride (250, 500, 1000, 2000 and 4000 ng/ml) being incubated for 24 and 48 hours at 37°C. After incubation the media were removed from the wells and 50µl of 5mg/ml MTT solution (Sigma Aldrich) was added to each well. The plates were wrapped in aluminium foil and incubated for an hour at 37°C. After incubation 500µl DMSO (Sigma Aldrich) was added to each well and thoroughly mixed. The plates were gently agitated in a plate shaker to dissolve the crystals. A small volume of this solution 200 µl was transferred into a 96 well plate and the absorbance read at 570 nm. MTT (3-[4,5-dimethylthiazol-2-yl]-2,5-diphenyltetrazolium

bromide) is a yellow soluble tetrazolium salt. The MTT assay is a colorimetric assay based on reduction of MTT to insoluble purple formazan crystals by both mitochondrial and extra-mitochondrial dehydrogenases (Fotakis and Timbrell, 2006). The viable and proliferating cells contain higher NADH or NADPH ratios which act as mediators in the reduction of MTT. Likewise, succinate and NADH-linked mitochondrial substrates such as malate, pyruvate or glutamate support MTT reduction (Liu *et al.,* 1997). Therefore, the viability is directly proportional to the amount of crystals formed. All five cell lines which were used in this study are adherent cells. Therefore, a trypsinisation step is required before the cells are prepared for seeding. This causes stress to the cells and reduces their metabolic activity. Most of the cells require 24 hours of recovery from trypsin stress and function again as viable cells. Therefore, the effect of DOX on viable cells with different concentrations was investigated after 24 hours of the cells seeding.

2.8.2 CytoTox 96® Non-Radioactive Cytotoxicity/ Lactate dehydrogenase assay (LDH assay)

An appropriate number of cells (5 x10^4) was plated and treated exactly as in Section 2.8.1. An additional set of wells was plated for maximum lactate dehydrogenase (LDH) release and used as positive Control. The assay was carried out according to the manufacturers' guidelines. After DOX treatment, Lysis Solution (10X) was added to the maximum LDH release control wells. After 45 minutes, the plates were centrifuged at 250 x *g* for 5 minutes. After centrifugation 50µl of the supernatant from each well was mixed with 50µl of Substrate Mix and incubated for 30 minutes on a shaker protected from light. After 30 minutes of incubation the reaction was stopped by adding 50 µl of Stop solution. The absorbance was read at 490 nm. The CytoTox 96® non-radioactive cytotoxicity assay measures the release of LDH from the damaged cell membrane of non-viable cells into the cell culture media. LDH converts lactate to pyruvate with reduction of NAD^+ to $NADH/H^+$. The H^+ from $NADH/H^+$ is transferred to the tetrazolium salt INT (2-(4-iodophenyl)-3-(4-nitrophenyl)-5-phenyltetrazolium chloride) which reduces it to a red formazan dye (Cobb, 2013). The amount of red formazan dye is proportional to the amount of LDH released into the media. Hence, CytoTox 96® non-radioactive cytotoxicity assays indirectly measure cell death.

2.9 Generation of non-resistant (normal) and drug resistant spheroids

Previous studies within this laboratory by Dr Selman Ali have shown that spheroids can be generated from tumour cell lines by two different methods either by (**1**) growing the cells in ultra-low attachment flasks to produce normal spheroid, and (**2**) treating the cells with a chemotherapeutic agent (Doxorubicin) to select drug resistant spheroids. The same protocol

was used in this study to generate respective spheroids from trophoblast cell lines.

2.9.1 Generation of non-resistant (normal) spheroids

This assay was carried out to check the ability of trophoblast cells to produce spheroids. The procedure involves four stages as explained below.

- **Stage 1 (Bulking up of parental cells)**

Cell lines (usually 5 x10^6 cells/ml) were grown in a T75 flask under normal conditions in their respective media for 72 hours. Once the cells reached to 80-90% confluence, they were harvested and sub-cultured for stage 2.

- **Stage 2 (Spheroid formation)**

The cells harvested from stage 1 were trypsinised and counted to determine 5 x10^6 cells/ml. They were then sub-cultured in non-adherent (Ultra-Low Attachment) (Sigma-Aldrich) T75 flasks in 20ml of serum-free media. This media contained (1% w/v L-glutamine and 1% v/v penicillin/streptomycin) supplemented with growth factors: 5µg/ml each of bFGF (Sigma-Aldrich), EGF (Sigma-Aldrich) plus 5µg/ml of insulin (Sigma-Aldrich), and 0.4% BSA (Sigma-Aldrich). Cells were incubated for 3-5 days. Spheroid formation was monitored under the microscope every 24 hours.

- **Stage 3 (Cell sorting by gravity separation)**

The spheroids were separated from single cells by gravity separation. The cell mixture containing both spheroids and single cells was transferred into Sterilin® tubes (Sarstedt) and kept at room temperature for 10 minutes to separate the spheroids from the single cells. The spheroid cells settled at the bottom of the tube. The single cells from the upper layer of the media were carefully removed without disturbing the pellet of spheroids. Afterwards, the spheroids were then centrifuged for 5 minutes at 1,000 x *g*.

- **Stage 4 (The ability of normal spheroid cells to grow under normal conditions)**

Spheroids were grown in normal adherent flasks for 72 hours under normal growth media conditions to observe their growth rate (See Figure 2.1).

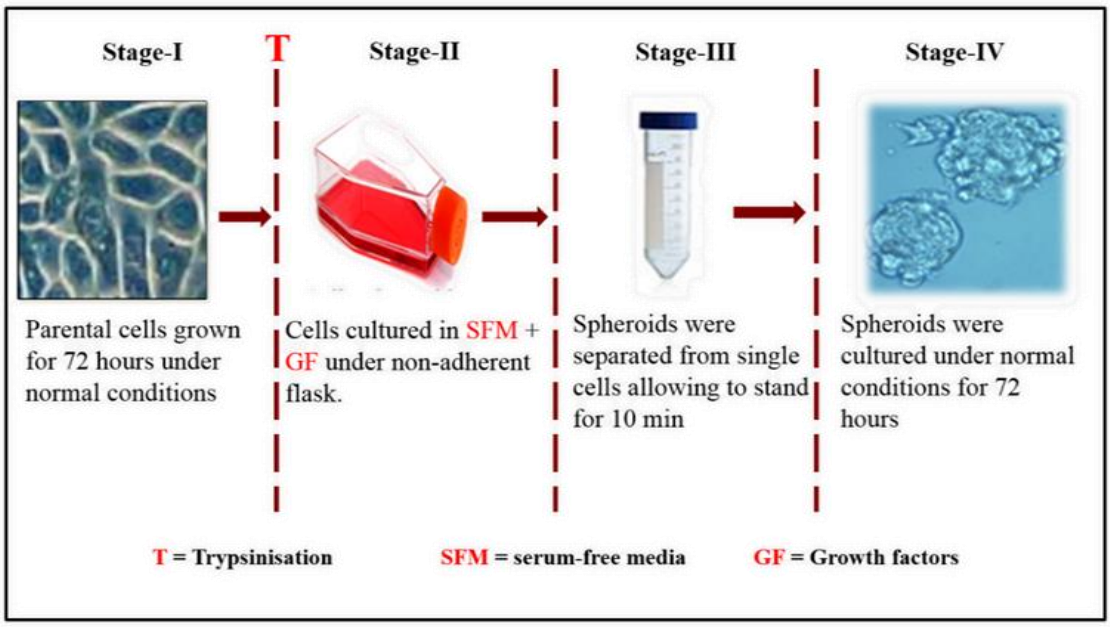

Figure 2.1: Schematic representation of protocol used to generate non-resistant (normal) spheroids.

2.9.2 Generation of Doxorubicin (DOX) resistant spheroids

This assay was carried out to select the spheroids that are resistant to doxorubicin. The procedure involves four stages as shown in Figure 2.2. The protocol was exactly the same as generating non-resistant (normal) spheroids except for the additional drug treatment with different concentrations of doxorubicin for 48 hours at stage one.

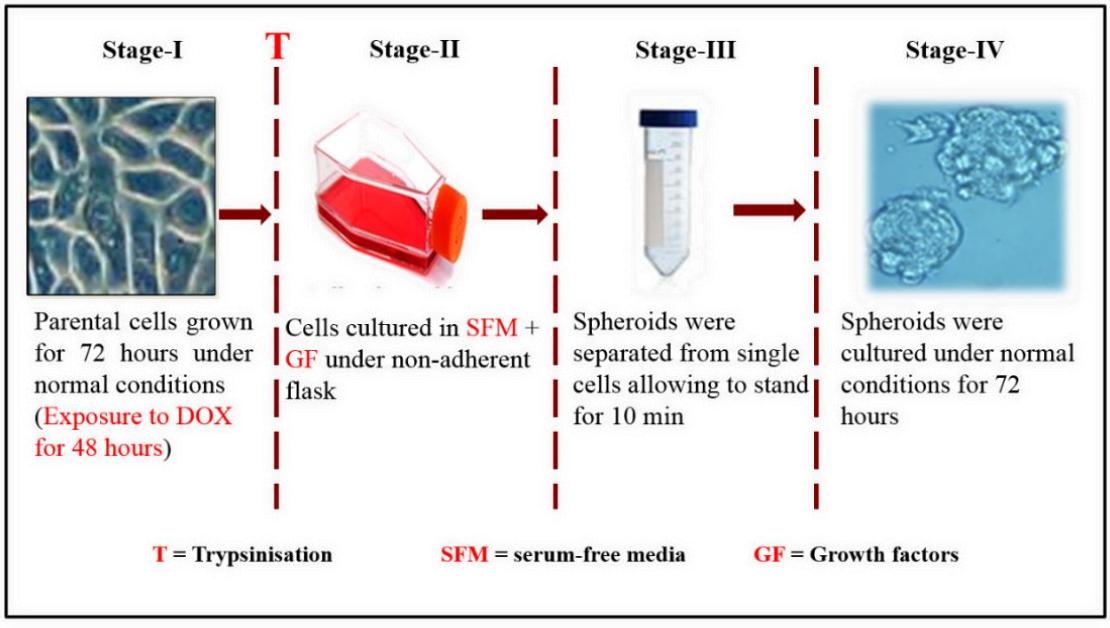

Figure 2.2: Schematic representation of protocol used to generate resistant spheroids.

2.9.3 RNA extraction from normal cells and spheroidal cells

RNA extraction and cDNA template preparation were carried out as explained in sections 2.4 and 2.5 for parental and spheroids cells (untreated and DOX-treated).

2.10 Protein expression studies

2.10.1 Tissue lysate preparation for protein analysis

The placental samples NT and PE were homogenized in liquid nitrogen to avoid protease degradation of proteins and transferred to centrifuge tubes. RIPA (Radio-Immunoprecipitation Assay) buffer 10ml (Sigma Aldrich) and protease inhibitor cocktail (Roche) 0.2 % (v/v) and 1 mM Na3VO4 (Sigma Aldrich) were added to the samples. Then samples were vortexed for 30 minutes followed by 5 minutes incubation on ice. The tubes were incubated on ice for 1 hour then were centrifuged at 27,000 x g for 15 minutes at 4°C (Harrier 15/80 refrigerated centrifuge, Sanyo). The supernatant (i.e. the native form of the tissue lysate) was collected and stored at -80°C.

2.10.2 Cell lysate preparation for protein analysis

Cells were lysed directly in lysis buffer to collect whole cell extracts. Cells were washed twice with 1X PBS then transferred into 20 ml universal tubes and centrifuged at 27,000 x *g* for 15 minutes at 4°C. The supernatant was discarded and the pellet re-suspended in 1X PBS to remove the remaining growth media and centrifuged once again. The supernatant was removed and RIPA buffer 300µl (Sigma Aldrich) with protease inhibitor cocktail (Roche) 0.2 %(v/v) and 1 mM Na3VO4 (Sigma Aldrich) were added to the cell pellet. Cells were then incubated on ice for 1 hour. The samples were centrifuged at 27,000 x *g* for 10 minutes at 4°C (Harrier 15/80 refrigerated centrifuge, Sanyo). Finally the cell lysate supernatant was collected and stored at -80°C.

2.10.3 Estimation of protein concentration by Bicinchoninic acid (BCA) assay

All protein concentrations were determined using BCA (Sigma Aldrich) according to the manufacturer's instructions to estimate the protein concentrations in the tissue and cells lysates prepared as mentioned earlier in Sections 2.10.1 and 2.10.2. The BCA working reagent was prepared by mixing 50 parts of reagent A (BCA) with 1 part of reagent B (4% w/v Copper (II) sulphate solution, Sigma Aldrich). The different concentrations of BSA (Bovine Serum Albumin) (Fisher Scientific) at 0.2, 0.4, 0.6, 0.8 and 1mg/ml were used to establish a standard curve. The placental tissue or cell lysates, together with BSA standards and blank (RIPA buffer) were added to a 96 well plate and mixed with 8 parts of BCA working reagent. The plate was incubated for 30 minutes at 37°C. The absorbance was measured at a wavelength of 570 nm by using a microplate reader (Biochrom Asys

UVM340). The protein concentrations of samples were derived from calculations based on the standard curve.

2.10.4 Protein separation by SDS-PAGE

Protein lysate samples were denatured for SDS-PAGE separation by using Laemmli buffer 4X at 70-80˚C for 10 minutes on a heating block. Equal concentrations of the protein samples were loaded into 10% or 12.5% w/v SDS-PAGE along with molecular weight markers (Bio-rad Laboratories, Inc.). ProtoGel® 30% w/v, ProtoGel® 4X Resolving and ProtoGel® stacking buffers were used to prepare SDS-PAGE gels according to the manufacturers' guidelines (National Diagnostics). The SDS-PAGE was run at 50 volts for 30 minutes followed by 90 volts for 1 hour. Finally the results were visualised by staining with Coomassie Brilliant Blue (Bio-Rad Laboratories, Inc.).

2.10.5 Protein analysis by Immunoblotting

Immunoblotting was carried out after protein separation from SDS-PAGE on to 0.2µm nitrocellulose membrane (Sigma Aldrich) by wet-transfer over-night in a cold room. The nitrocellulose membrane was incubated in blocking solution (3% w/v BSA in 1X TBS-Tween20) for 1 hour. After incubation, the membrane was washed three times with Millipore water followed by a 1X TBS-Tween20 wash. The membrane was then incubated in primary antibody overnight on a shaker at 4^{o}C. Following incubation the membrane was washed and incubated in secondary antibody for 1-2 hours. After this the membrane was washed by 1X TBS-Tween20, three times for 5 minutes each to remove excess secondary antibody, and developed by using UV light (US Chemiluminescent Substrate Interchim). Image capture was carried out by using a Gel Doc, InGenius (Syngene). New GeneSys Image analyser software was used for blots captured by InGenius and AIDA Image analyser software version 5.2 was used to quantify the bands. The expression levels of the proteins of interest were normalised against the house keeping proteins (β-actin).

2.11 Staining protocol

2.11.1 Immunohistochemistry (IHC)

IHC was performed to investigate the cellular localisation of the proteins of interest in the tissue sections. The placental samples were embedded in paraffin, sectioned at 5µm thickness and placed onto poly-L-lysine coated slides (Thermo Scientific) for 1 hour at 60^{o}C. The protocol was divided into the following steps:

a. **Pre-staining:**

   Paraffin wax was removed from the slides using xylene (Fisher Scientific) twice for 5 minutes.

b. **Hydration:**

Slides were hydrated through an alcohol gradient as follows:

- 2x in Absolute alcohol for 2 minutes
- 2x in 95% v/v ethanol for 2 minutes
- 1x in 75% v/v ethanol for 2 minutes
- 1x ddH_2O for 2 minutes

c. **Heat induced antigen retrieval (HIAR):**

HIAR was used to break the methylene bridge formed during PF-fixation. The slides were heated for 20 minutes in a microwave at high temperature with retrieval buffer (10mM Tris-1mM EDTA buffer, pH 9 or 10mM Citrate buffer, pH 6). This was followed by washing with 1XPBS.

d. **Blocking endogenous peroxide :**

To block the slides from the endogenous peroxidase activity 3% v/v hydrogen peroxide (H_2O_2) (Fisher Scientific) in methanol was used for 30 minutes. This was followed by washing with distilled water.

e. **Primary antibody and Secondary antibody:**

The sections were blocked for unspecific binding with horse serum for 30 minutes or longer. The slides were then incubated with 100µl primary antibodies over-night at 4ºC at appropriate dilutions for each antibody. Then the slides were carefully rinsed with 1X PBS 3 times for 5 minutes to remove weakly bound to non-specific sites and to allow a proper binding between primary and secondary antibodies. For the negative controls, no primary antibodies were used in the incubation. After this, the slides were incubated with the biotinylated-conjugated secondary antibody in an ABC kit for 1 hour at room temperature.

f. **DAB (3,3'-diaminobenzidine) DAB:**

After several 1X PBS washes, DAB substrate (Vectastain®) was prepared according to the manufacturers' guidelines and was used to develop the detection of the chromogenic product. In the presence of antibody conjugated to peroxidase enzyme and peroxide, the DAB is oxidised to give a brown colour.

g. **Morphological histochemical staining:**

The slides were dipped for 20 seconds in Gills Haematoxylin. This stained the cell nucleus with blue. This stain is used to demonstrate general tissue structures. Therefore, NT and PE placentae were counter-stained with haematoxylin for morphology comparison as well as for the demonstration of tissue antigens.

h. **Dehydration and Mounting**

The slides were dehydrated in an alcohol gradient as follows:

- 1x in 75% v/v ethanol for 2 minutes. .
- 2x in 95% v/v ethanol for 2 minutes
- 2x in Absolute alcohol for 2 minutes

Absolute alcohol treatment was followed by soaking in xylene for 10 minutes. Then the slides were mounted using Entellen® and covered with coverslips. Finally the slides were viewed and photographed at 20X magnification by using an Olympus camera DP73. The steps of the IHC protocol are summarised in Figure 2.3.

i. **Visualisation and semi-quantification of IHC**

A semi-quantitative scoring system was used to evaluate the status and expression of each factor. The images captured were taken approximately at the same locations in comparative slides. The staining in the images was then semi-quantified using a point scale immuno-reactivity scoring (IRS) system (as shown in Table 2.5). These scorings were carried out compared to the positive staining for vimentin IRS (scored as 3) and negative stain (secondary antibody only; 0) in the same sample. Multiple images of the slides were scored independently by three observers. Their individual scores were then compared and tallied for final scores. The most frequently repeated score between the three scorers (the mode) was taken as the final score for the factors of interest in an overall pool of samples (NT and PE). A weighted kappa statistical analysis was also performed with the scores provided individually by the three scorers to analyse the inter-observer error. The values for the kappa were interpreted as mentioned by Viera and Garrett (2005). If the values were: < 0, there was less chances of agreement; 0.01–0.20, indicated slight agreement; 0.21– 0.40, fair agreement; 0.41–0.60, moderate agreement; 0.61–0.80, substantial agreement and 0.81–0.99, practically perfect agreement

Table 2.2: IRS system for Visualisation and semi-quantification.

Immunoreactivity score system (IRS)	Staining Intensity
0	No staining or very low staining
1	Low staining
2	Medium staining
3	High staining

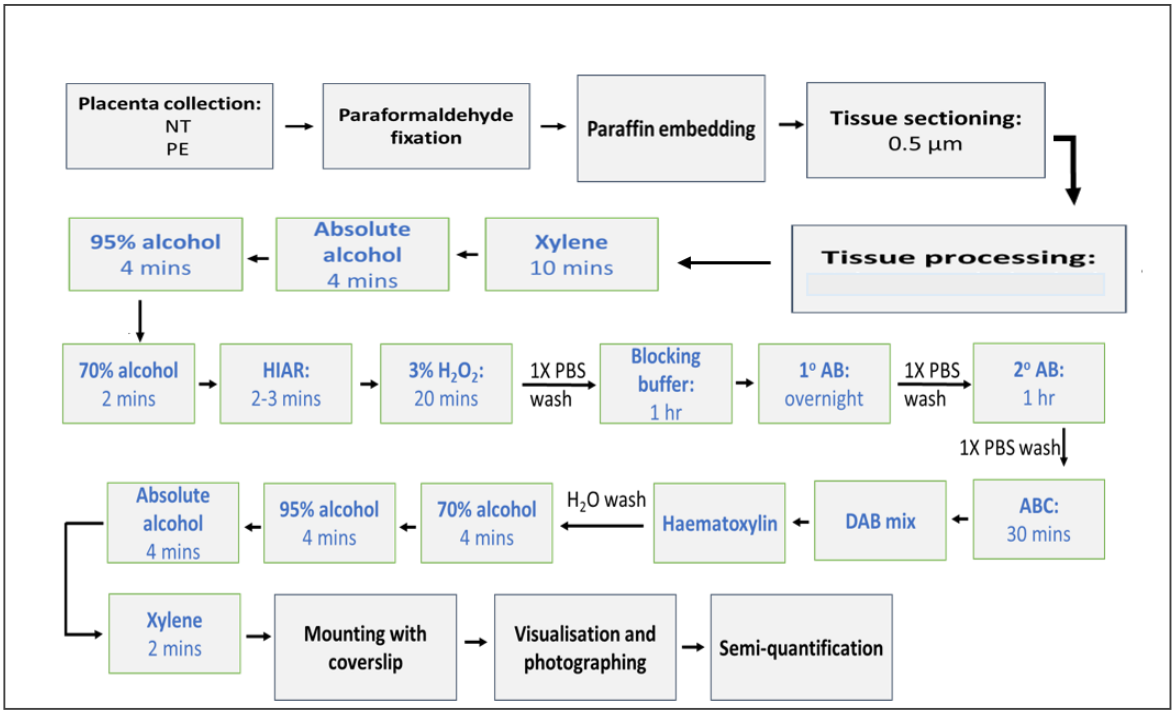

Figure 2.3: Summary flow chart of IHC protocol.

2.11.2 Immunofluorescence staining

The general protocol followed for immunofluorescence staining is given below:

- **Cell culture:** The different types of cells were grown on sterile glass cover slips GG-18-PLL (neuVitro), poly-l-lysine coated coverslips under the respective growth conditions. The coverslips were then rinsed with 1X DPBS
- **Cell fixing:** The media was removed from the culture plate and the coverslips were rinsed with 1X PBS. Cells were then fixed with 4% w/v formaldehyde in 1X PBS for 30 minutes. Next, the cover slip was washed gently by 1X PBS 3 times for 5 minutes.
- **Permeabilisation:** For staining intracellular proteins the cells fixed with paraformaldehyde and methanol were permeabilised in 0.25% v/v Triton X-100 in PBS for 15 minutes. This was followed by three washes in 1X PBS for 5 mintues. The permeabilisation step was not required for acetone fixed cells and for detection of membrane proteins.
- **Blocking:** The cover slips were then incubated in (1% w/v BSA in PBST) for 1 hour at room temperature. For paraformaldehyde-fixed coverslips, 0.3M Glycine was added to the blocking buffer.
- **Primary and secondary antibody incubation:** The coverslips were then incubated in primary antibody diluted in 1% w/v BSA in 1X PBST for 1 hour at room

temperature or overnight at 4ºC in a humidified dark chamber. After incubation the coverslips were washed again in 1X PBS 3 times for 5 mintues. The coverslips were then incubated in secondary antibody diluted in 1% w/v BSA in 1X PBST for 1 hour at room temperature in the dark followed by five minutes washes with 1XPBS.

- **Counter staining:** The coverslips, if required, were counter-stained with VECTASHIELD® HardSet™ mounting medium with DAPI. Once dried, the edges of the coverslips were sealed with colourless nail varnish to prevent them from moving while taking images. The images were captured using an Olympus camera with suitable filters at different magnifications (Objective magnification: 20X and 40X). This assay was carried out to stain the spheroidal cells. The protocol is exactly the same except for the first step when spheroidal cells (untreated and DOX-treated) were collected from a non-adherent flask and transferred into 15 ml universal tubes for centrifugation at 500 x *g* for 10 minutes. Finally spheroids were washed 3 times for 5 minutes and mounted on the slides with two drops of VECTASHIELD® HardSet™ mounting medium after securing the area boundaries by means of a hydrophobic image barrier pen (Vector Laboratories, Inc).

2.12 Scratch /Wound healing assay

A wound healing assay was carried out to evaluate cell migration. Cells were plated at optimum densities ($5x10^4$) into 24 well plates (Falcon) until 90-95% confluence. In the case of spheroids they were trypsinised after harvestinig to break them down to single cells and re-suspended in the respective growth media. Cells were then transferred to 24 well plates (Falcon) until 90-95% confluence. A straight scratch was made on the cell monolayer by using a 2 µl pipette tip at an angle of about 90 degrees. The cells were washed gently with 1X PBS (Lonza) to remove the debris after the scratch. 1ml of serum free media (media with 1% w/v L-glutamine and 1% v/v penicillin/streptomycin) with DOX and without DOX 250 ng/ml (Sigma) was added to the cells according to the set experiments to check the effect of DOX on the migration property of normal and spheroidal cells at 24 and 48 hours. The scratches were continuously imaged in real time using a Leica microscope at 30 minute intervals for 48 hours The images were analysed using Wimscratch® automated analysis by Wimasis® quantitative image analysis **(www[19])**. This software identifies the edge of the scratch and measures the gap area.

2.13 Invasion assay

The invasion assay was carried out using the BD Falcon™ BioCoat tumour invasion systems (BD Falcon) with fluoroBlock™ 96 well insert plate (8µm pore size) coated with BD matrigel matrix. This was compared with migration of cells through uncoated BD Falcon™ FluoroBlok™ 96 well insert plates. The assay used was as follows:

- **Rehydration:** A BD falcon BioCoat™ tumour invasion plate was removed from -20°C and kept for half an hour at room temperature. The apical chambers were filled with 75 µl of warm media and allowed to rehydrate for 2 hours at 37˚C at 5% v/v CO_2. The uncoated BD falcon fluoroBlock™ 96 well insert plate that was used as a cell migration control does not required rehydration.
- **Pre-staining the cells:** The cells were grown to 70% confluency and collected after trypsinisation. Collected cells were incubated with 10µM CellTrace™ CFSE red dye (Molecular Probes®) for 45 minutes. After incubation the cells were centrifuged and re-suspended in warm media.
- **Cell suspension:** Cell densities of $1.25x10^4$ cells were prepared in SFM (media with1% w/v L-glutamine and 1% v/v penicillin/streptomycin).
- **Setting up assay:** The media was removed from apical chambers after rehydration of BD falcon Bio Coat™ tumour invasion plate and replaced with 50µl of cell suspension. The 50µl of cell suspension was also added to the apical chambers of the BD falcon fluoroBlock™ 96 well insert migration plate. The bottom of the chambers was filled with growth media containing 5% v/v FBC, which acts as a chemoattractant. In addition, the apical as well as the bottom chambers were treated with 250 ng of DOX in treatment condition.
- **Taking images:** After incubating the plates for 24 hours at 37°C and 5% CO_2 the membranes were removed from the inserts with a special knife and mounted on slides. The fluorescence of invaded cells was then read at a wavelength of 494/517 nm (Ex/ Em) followed by image capture at the end of the assay using a fluorescent microscope (Olympus BX51) with an Olympus camera. The invasion assay steps are summarised in Figure 2.4
- **Calculation of cell invasion percentage:** The number of cells invaded from the tumour invasion plate together with percentage invasion (see below for equation) was analysed using ImageJ software.

$$Invasion\ \% = \frac{Number\ of\ cells\ invaded}{Number\ of\ cells\ migrated} \times 100$$

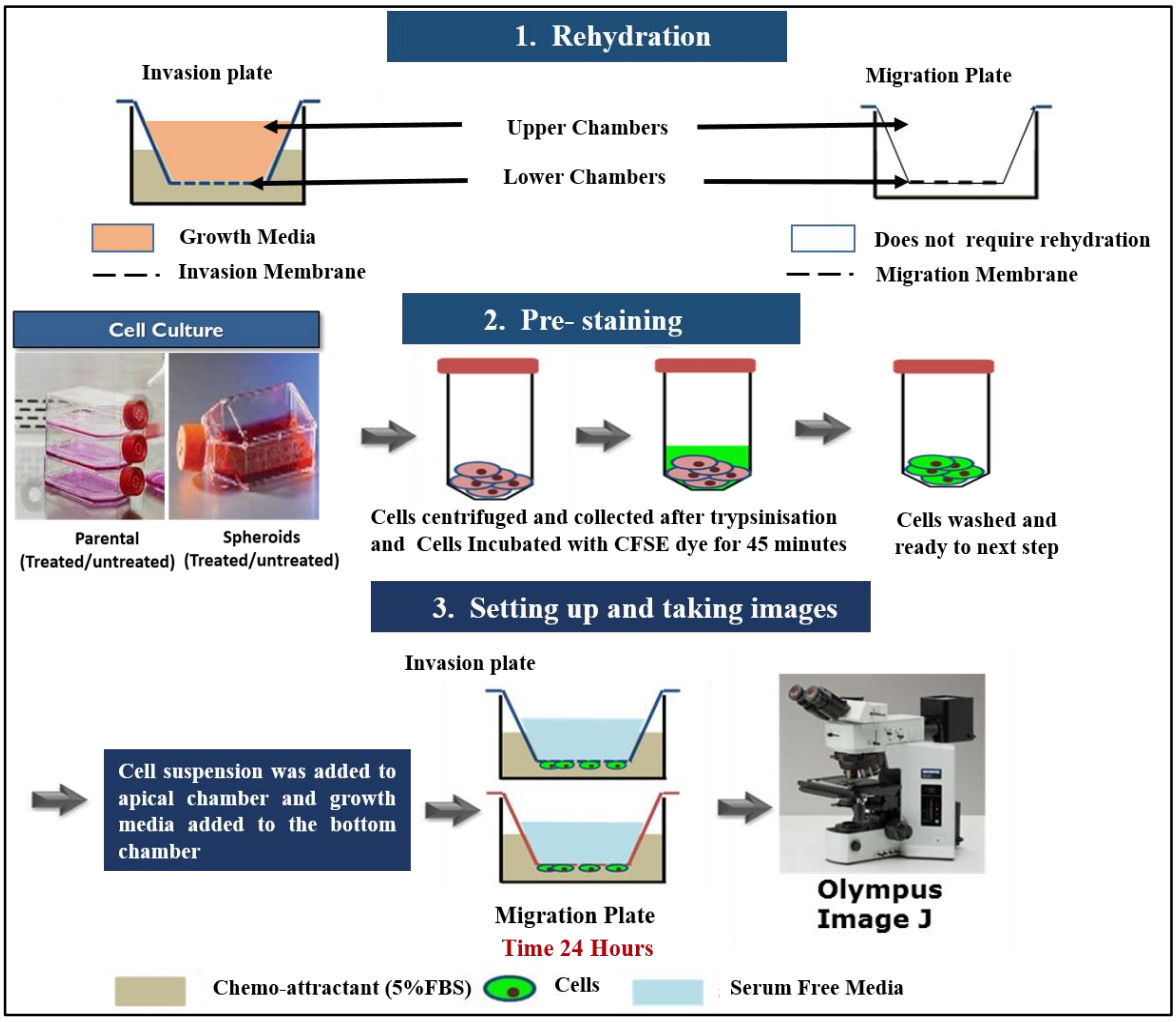

Figure 2.2: Summary of the Invasion assay steps.

2.14 Cultrex® 96 well 3-D spheroid Basement Membrane Extract (BME) cell invasion assay

This assay is standardized for a three-dimensional cell structure, where invasive cells can penetrate a barrier consisting of components resembling basement membranes *in vitro* in response to chemoattractant/invasion modulation compounds. The assay duration was 3 days. At day1, 10X Spheroid Formation ECM was thawed on ice overnight at 4°C in a refrigerator. At day 2, cells were harvested (without and with DOX) and the optimal seeding density for each cell line was added usually $2x10^3$ cells/ml per well for trophoblast cells; whereas MCF-7 was seeded with a density of $1.5x10^3$ cells/ml. A single cell suspension was prepared in 1X spheroid formation ECM and 50µl of single suspension in 1X ECM was dispensed to each well. The plate was centrifuged at 300 x *g* for 5 mins to make all the cells acentric in position then incubated for 72 hours at 37°C with 5% CO_2 supply. After 72 hours the plate was taken out and left on ice for 5 minuts to cool down. Invasion Matrix 50µl was added per well and centrifuged at 200 x *g* for 5mins to remove bubbles. The plate was incubated again for 1 hour at 37 °C with 5% CO_2 supply to promote gel formation. After this

100µl of warm culture media was added to each well. The plate was then placed under a confocal microscope for imaging at 4 hour intervals for 48 hours. Later, images were analysed using Image-J software and data were quantified using GraphPad Prism software.

2.15 Cell lysate preparation for mass spectrometry

A stepwise explanation of this protocol is given below.

Initial Steps:

a. **Sample preparation:** Cell lines ($5x10^6$ cells/ml) were harvested by trypsinisation in the case of parental (adherent) cells, while spheroids (suspension) cells were centrifuged at 300 x *g* for 10 min, washed twice with 1X PBS and then centrifuged at 300 x *g* for 10 min. The residual PBS was discarded. Then 15 µl of 8M urea and 1.5 µl of Protease MAX ™ (Sigma) was added to the cell suspension. Afterwards, the cell lysates were mixed by vortexing. To the lysed solution 58.5µl of 50 mM TEAB (Sigma) was added and incubated on ice for 15 min. To enhance cell lysis a sonicator was used, incubated in a water bath for 5 min and repeated three times. After final sonication the solution was centrifuged at 14,000 x *g* for 15 min at 4ºC. The samples were transferred into a fresh labelled tube for the alkylation and reduction step.
b. **Reduction and Alkylation:** In this step, 1.0µl of 0.5 M DTT (Sigma) was added to samples incubated at 56°C for 20 minutes in a water bath. Following this 2.7µl of 0.55M IAA (Sigma) was added and the sample mixed well and incubated at room temperature in the dark for 15 minutes.
c. **Trypsinisation:** This step was carried out using freshly made trypsin by adding 20µl of 1 mM HCL (Sigma) to re-suspend all trypsin completely. From the cell lysate 50µg of protein together with 100µl of 50 mM TEAB (Sigma) solution was mixed with 2µg of trypsin, vortexed and incubated at 37°C overnight with gentle shaking.

Final step:

After trypsinisation, the samples were concentrated using a SpeedVac concentrator for 30-40 minutes. Finally, 20µl of 5% Acetonitrile/0.1% (Sigma) formic acid solution (Sigma) was added to the samples and transferred into a new tube. The samples were then analysed using a TripleTOF® 6600 System SCIEX. A spectral library was constructed using the output from ProteinPilot 5 (SCIEX) combining 4 IDA runs per comparison and filtered and aligned to spiked in iRT peptides (Biognosys, Switzerland) using PeakView 2.0 (SCIEX). SWATH data extraction, quantitation and fold change analysis were carried out using SCIEX OneOmics cloud processing software.

Chapter 3
Comparative expression analysis of tumour associated factors in Normotensive (NT) and Pre-eclamptic (PE) placentae

3.1 Introduction

Tumour and placenta show several similarities as mentioned in previous chapter 1 in Section 1.3). They both have capacity for proliferation, differentiation, and invasion through the surrounding tissues by degrading the extra-cellular matrix (ECM) (Ferretti *et al.*, 2007). In addition, tumour and placenta also possess other novel characteristics, such as interacting with endothelial cells, evading the immune response, escaping apoptosis, and establishing nutrient supply by angiogenesis (Ferretti *et al.*, 2007). However, the invasion of placental trophoblast cells into the uterine wall, is a unique and controlled process, which is essential for foetal development. If the invasion is shallow, it results in a multisystem disease called pre-eclampsia (PE) which affects 5-7% of pregnant women (Louwen *et al.*, 2012). It is considered as a major cause of maternal and foetal mortality worldwide. The complete pathophysiology of this syndrome is not well understood. However, many factors have been identified for pre-eclampsia which include: genetic predisposition, reduced/abnormal trophoblast invasion with impaired spiral artery remodelling (during placental development), immunologic intolerance, ethnicity and variations in inflammation (Sankaralingam *et al.*, 2006). Most of the research is focused on various gene expression and epidemiological factors that have been modified during pre-eclampsia (Sankaralingam *et al.*, 2006). Microarray techniques and proteomic studies, have identified potential genes and proteins that are altered in PE when compared to normal placenta (Sankaralingam *et al.*, 2006; Enquobahrie *et al.*, 2008). Therefore, these genes and proteins might be used to understand the pathogenesis of PE and also for the development of new therapeutic targets (Yang and Kong, 2015).

Interestingly, most of these altered genes and proteins have been reported to be closely involved in tumour development as well (Louwen *et al.*, 2012). In fact, the NT, PE and tumour, can be considered as three scenarios; (a) normotensive pregnancy where there is a controlled but normal trophoblast invasion, (b) pre-eclampsia, the invasion is low, and (c) tumour where there is uncontrolled invasion. By comparing the status of factors between NT and PE placentae, it will be easy to understand their importance in the invasive process and can further be used to target tumours invasion. Therefore, the primary aim of this chapter is to compare the status of the tumour associated factors, such as ALDH3A1, AURK- (A and C), PDGFRα, TWIST1, and JAG1, in NT and PE placentae. Interestingly, these factors are believed to play important roles in tumour invasion as mentioned in Section (1.5). These factors may also be expressed in human placenta invasion. However, the functional status of many of these factors has not been fully established.

3.2 Results

The mRNA expressions of the above mentioned factors (See Section 3.1) were compared between 13 NT and 12 PE human placental tissue samples. To confirm that changes in mRNA expressions were also faithfully translated into protein changes, the identified proteins were qualitatively and semi-quantitatively compared by immunohistochemistry (IHC) and western blotting. The MCF-7 human breast adenocarcinoma cell line was used as a tumour cell line of non-placental origin for all of the experiments in this study.

3.2.1 Human placental samples

The demographic details of NT and PE samples are given in Table 3.1 (Ethical approval was obtained from NHS REC: 12/NE/0112). Individual patient data can be found in Appendix A.1

Table 3.1: Demographic details of the normotensive and pre-eclamptic subjects.

Parameter	Normotensive (*n=13*)	Pre-eclamptic (*n=12*)	P value [§]
Maternal age (years)	34.2 ± 1.4 (28-41)	28.5 ± 2.2 (19-39)	0.075
Gestational age (weeks)	38.9 ± 0.1 (38.4-39.3)	37.5 ± 0.7 (33-39.4)	0.036
Systolic blood pressure (mmHg)	122.2 ± 3.5 (109-140)	153.8 ± 3.4 (140-168)	**<0.0001**
Diastolic blood pressure (mmHg)	70.6 ± 3.4 (60-90)	98.5 ± 1.9 (91.5-108)	**<0.0001**
Protein in urine (g / lt)	N/D	1.149 ± 0.328	
(g / 24 hour)	N/D	2.687 ± 0.852	
Placental weight (g)	657.4 ± 37.3 (527-855)	506.3 ± 35.8 (360-620)	**0.015**
Mode of delivery			
Parity	1.9 ± 0.3 (1-4)	0.3 ± 0.3 (0-2)	**0.005**
Gestational Weight (Kg)	3.4 ± 0.1 (3.03-4.24)	2.6 ± 0.2 (1.66-3.59)	0.015

The details are expressed as mean ± SD, N/D= none detected, n=number of women in each group. [§] *Mann – Whitney U test.*

3.2.2 Gene expression studies

According to the protocol in Section 2.9.3, total RNA was extracted and reverse transcribed from 13 NT and 12 PE placental samples. The ratio of absorbance at 260/280 nm ranged from 1.9-2.3, showing that the RNA was pure and the integrity was well maintained. The extracted RNA was found to be pure from genomic DNA, when the RNA samples were subjected to electrophoresis in a 1% w/v agarose gel and two bright clear bands were separated (28S and 18S) (See Appendix A.2). Primers for all factors of interest were designed as mentioned in Section 2.6.1. The primer sequences for the factors and the house keeping genes, along with their optimised annealing temperatures (T_a) are summarised in Table 3.2. Single bands were obtained for all the PCR products at regions of approximately 200 bp in a 1.5% agarose gel, without any presence of primer and/or product dimers (See Appendi A.3). The accession numbers for target factors are listed in Appendix A.4. All PCR products were confirmed by DNA sequencing carried out by Source Bioscience (Birmingham, UK). Examples of DNA product confirmation gel and sequencing data can be found in Appendix A.5.

Table 3.2: The primers for the specific gene and their annealing temperatures (Ta)

Factors of interest		Primer sequence (5' to 3')	Primer Length (nucleotides)	Annealing Temperature (T_a) °C
ALDH3A1	Forward	GATCCAGCAGGAGCA	15	**58.2**
	Reverse	GTCTTCACGGGCTCA	15	
AURK- A	Forward	GAATTGGCAAATGCCCTG	18	**53.7**
	Reverse	AGGGGGCAGGTAGTCCAG	18	
AURK-C	Forward	TTGGAGAGACTGCCCCTG	18	**58.2**
	Reverse	GCAGACAGGGCTCAGGAA	18	
PDGFR-α	Forward	CGACAGCAGACAGGGCTTTA	20	**59.5**
	Reverse	AACAGCACAGGTGACCACAA	20	
TWIST1	Forward	CAGTGATTCCCAGACGGA	18	**58.2**
	Reverse	TTCAGTGGCTGATTGGCA	18	
JAG1	Forward	TCAACGGGGGAACTTGTAGC	20	**53.2**
	Reverse	TGACAGGGATCAGAGAGGCA	20	
Housekeeping genes				
GAPDH	Forward	ACCACCAACTGCTTAGCACC	20	**58**
	Reverse	CCATCCACAGTCTTCTGGGT	20	
HPRT1	Forward	TGACACTGGCAAAACAATGCA	21	**55**
	Reverse	GGTCCTTTTCACCAGCAAGCT	21	
TBP1	Forward	TGCACAGGAGCCAAGAGTGAA	21	**56**
	Reverse	CACATCACAGCTCCCCACCA	20	

3.2.2.1 Relative mRNA expression of factors of interest in NT and PE

Quantitative real–time PCR (qRT-PCR) was carried out to determine the mRNA expression level of the different factors of interest in NT and PE placental samples. The $2^{-\Delta\Delta Ct}$ values were calculated as mention in Section 2.6.5. Figure 3.1 shows a Scatter-plot displaying the different mRNA expression level for each factors in NT and PE samples as shown in Figure 3.1. The expression patterns of individual factors are reported below:

- **The human aldehyde dehydrogenase 3A1 (ALDH3A1)**

Relative expression of ALDH3A1 is shown in Figure 3.1, Panel A. There was a significant up-regulation in the levels of ALDH3A1 mRNA expression in PE samples when compared to NT placentae samples ($p<0.05$).

- **Aurora kinase A (AURK-A)**

Interestingly, there was a statistically significant difference in the relative mRNA expressions of AURK-A in PE when compared to NT. The expression of AURK-A mRNA was up regulated in PE placentae ($p<0.001$; See Figure 3.1, Panel B).

- **Aurora kinase C (AURK-C)**

The relative mRNA expression level of AURK-C was significantly reduced in PE samples when compared to NT samples ($p<0.05$; See Figure 3.1, Panel C).

- **Platelet-derived growth factor (PDGFRα)**

The relative mRNA expression level of PDGFα was significantly reduced in NT when compared to PE ($p<0.01$; See Figure 3.1, Panel D).

- **Basic helix loop helix protein (TWIST1)**

As seen in Figure 3.1, Panel E, there was a significant up-regulation in mRNA expression level of TWIST1 in PE placentae when compared to NT ($p<0.01$).

- **JAG1 (Jagged 1)**

In Figure 3.1, Panel F, there was a statistically significant down regulation in mRNA expression level in PE when compared to NT ($p<0.01$).

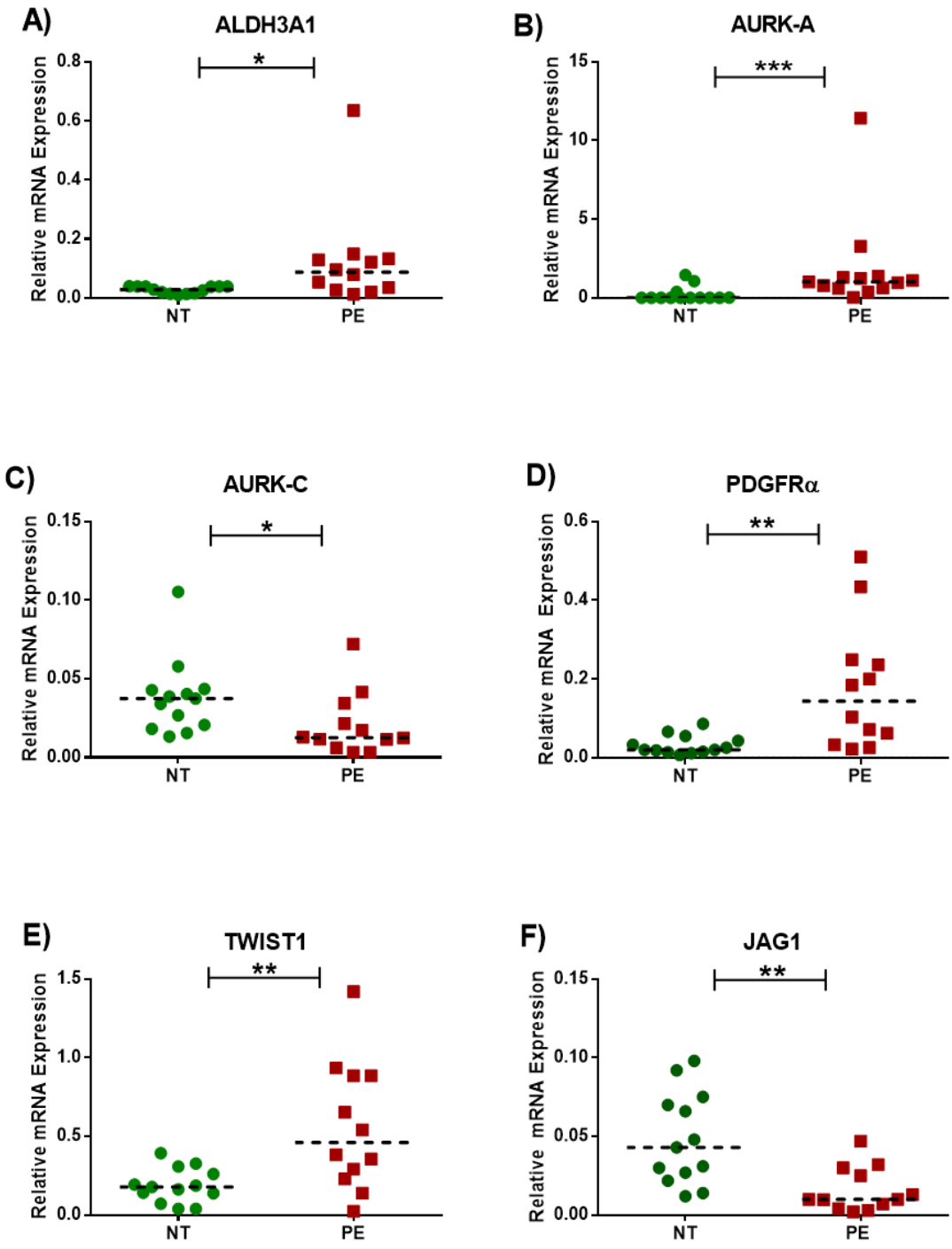

Figure 3. 1: Relative mRNA expression analysis of tumour associated factors between NT and PE placentae.

The relative mRNA expressions of the following factors were found to be significantly up-regulated in PE placenta; ALDH3A1 (panel **A**), AURK-A (panel **B**); PDGFα (panel **D**) and TWIST1 (panel **E**). In contrast, the mRNA expressions of AURK-C (panel **C**), and JAG1 (panel **F**) are significantly down-regulated in PE placentae. Statistical significance was determined using Mann-Whitney U test (n=13 NT and 12 PE respectively;*p<0.05;**p<0.01; ***p<0.001). Data represent the median of three individual experiments, each performed in triplicate.

3.2.3 Protein expression and cellular localisation of factors of interest in NT and PE

The expression of all factors of interest were investigated in both NT and PE samples using western blot analysis, to check the alterations between mRNA and protein expressions; for methods see Section 2.10. Equal amount of placental samples (50µg) were loaded, as confirmed by β-actin on the same blots. Only (20µg) of the positive control were loaded to avoid over-saturation of the blot. The positive controls were suggested by the supplier (Abcam) and was different for each factor. The scatter-plots for protein expression of each factors of interest is shown in the following Figures: 3.2, 3.4, 3.6, 3.8, 3.10, and 3.12. The last lane in both NT and PE blots are the positive controls which are separated by dotted lines in the blot. The protein expression levels were normalised by using housekeeping β-actin protein levels as internal control.

The status and cellular localisation of factors was studied by using Immunohistochemistry (IHC) methods. For IHC the positive and negative controls are required for validity of staining. The brown staining with 3,3′-Diaminobenzidine (DAB) substrate were used as a positive staining and scored according to the intensity of staining. The negative controls were treated only with secondary antibody, therefore no immuno-reactivity (brown staining) was observed. The scoring was carried out by three different individuals (at least one of them was a histologist) and the semi-quantified immune-reactivity scores (IRS) between NT and PE samples are shown in Tables 3.3. The Fleiss Kappa statistics was performed on this IRS data which provided a kappa value of 0.47, suggesting a moderate level of agreement between the scorers.

Table 3. 3: Immuno-reactivity score (IRS) of all factors of interesting

Factors	NT (n=5)	PE (n=5)	P Value	Significance
ALDH3A1	2±0.4	2±0.3	> 0.9999	**Ns**
AURK-A	1±0.2	3±0.2	0.0085	****
AURK-C	2±02	1±0.3	0.0133	*
PDGFRα	2±0.2	2±0.3	> 0.9999	**Ns**
TWIST1	1±0.2	2±0.3	0.0004	***
JAG1	1±0.3	1±0.2	> 0.9999	**Ns**

The intensity of staining was represented by the mode ±SEM of the IRS from 5 individual samples in each group. Unpaired t-test was then performed on the IRS modes of NT and PE (**ns**= no significance) (*p<0.05;**p<0.01; ***p<0.001).

- **Protein expression of ALDH3A1**

The predicated molecular weight of ALDH3A1 protein declared by the supplier (Abcam) was 50 kDa. The single band at 49kDa was observed in most of the placental (NT and PE) samples, as well as in MCF-7 cells, which was used as a positive control for ALDH3A1. ALDH3A1 expression could be observed in almost all PE samples. However, only 10/13 samples of NT showed expression of ALDH3A1. Interestingly, the protein expression patterns agreed with quantitative mRNA analysis data showing a statistically significant increase of ALDH3A1 expression in PE samples ($p<0.05$) (Figure 3.2).

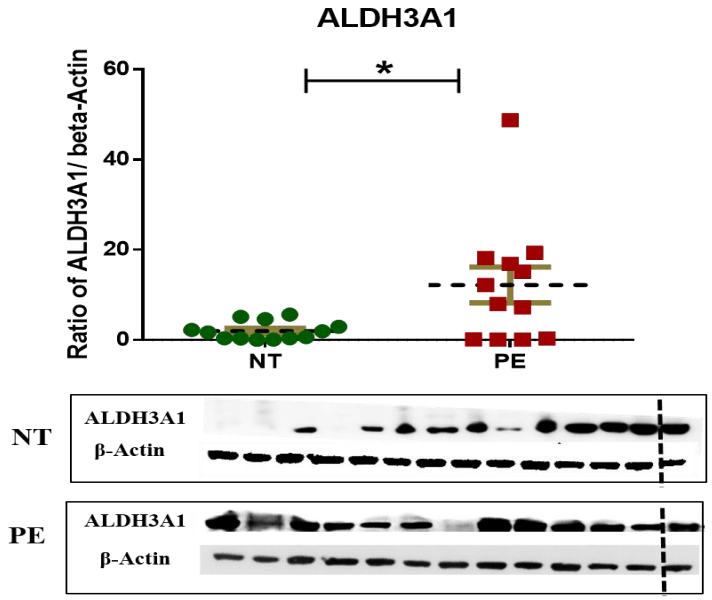

Figure 3. 2: The expression of ALDH3A1 protein in NT and PE placentae.

Scatter-plots are derived from 13 NT and 12 PE samples and relative expression was determined from three independent blots. Mann Whitney U test was performed (*$p<0.05$). Quantified data are expressed as the ratio of the ALDH3A1/ β-actin. The error bars (±SEM) are represented with brown lines. A representative western blots showing the single bands detected by both anti-ALDH3A1 and β-actin antibodies are also shown.

- **Cellular localisation of the ALDH3A1**

Moderate immuno-staining of ALDH3A1 was observed in both NT and PE samples (Figure 3.3). The staining in the STB layers (red arrows) of the placental villi in PE tissues were slightly higher when compared with the STB layer in NT tissues. No staining differences were detected between NT and PE in both the mesenchymal cells (red star) and foetal blood vessels (black arrows). Therefore, the overall staining intensities for NT and PE showed no significant difference (Table 3.3).

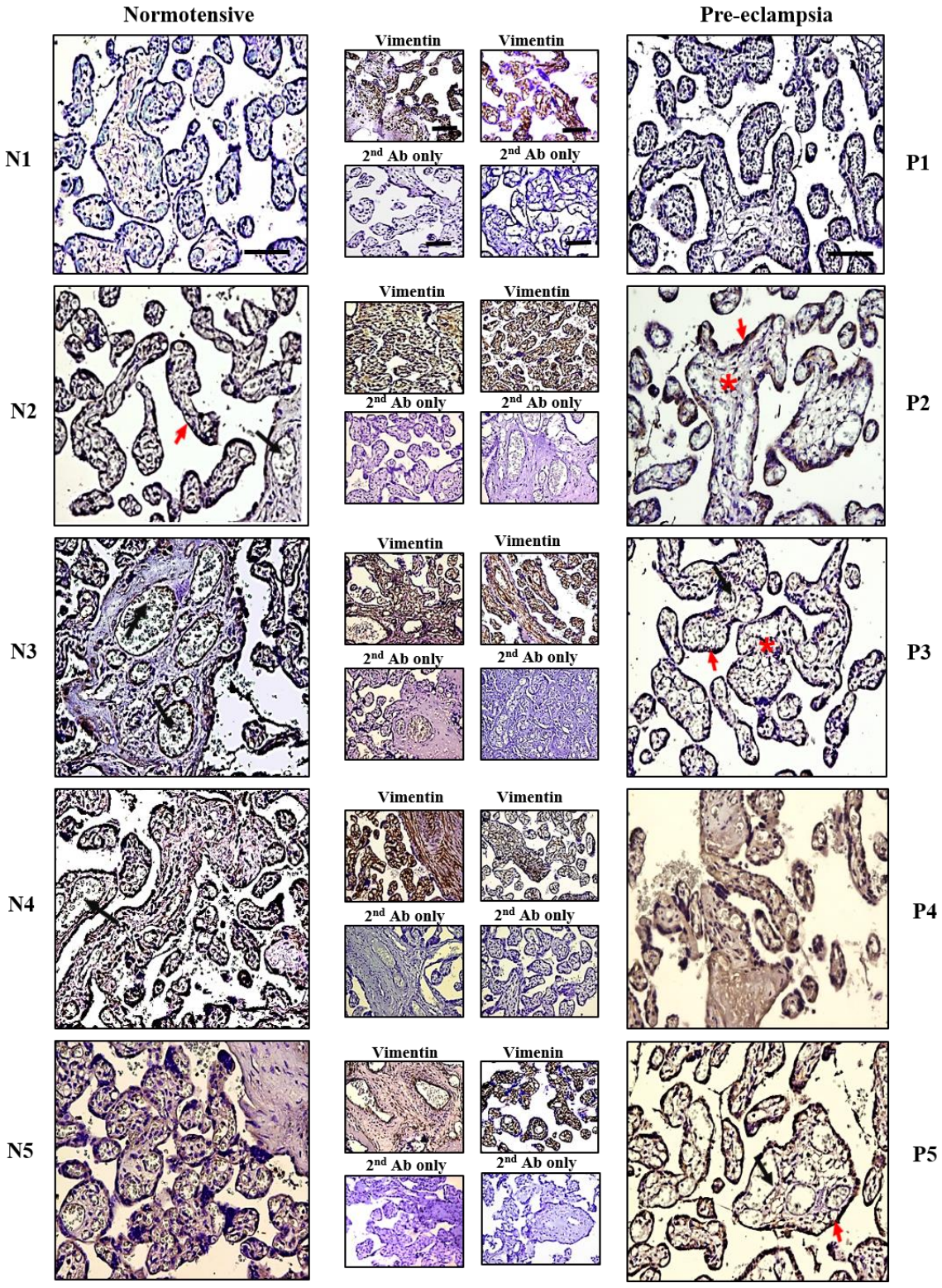

Figure 3.3: ALDH3A1 localisation determined by immunohistochemistry.

Five placental samples for each group (NT and PE) are represented here. The IRS for ALDH3A1 for each sample was scored in comparison to the IRS of positive (Vimentin) and negative controls (2nd Ab only) of the same sample. Magnification 20X; scale bar=100µm. STB layer (red arrows), the mesenchymal stromal cells (red star) and foetal blood vessels (black arrows).

- **Protein expression of AURK-A**

Almost all of the PE samples showed expression of AURK-A protein (Figure 3.4). The single bands for AURK-A were detected at 48kDa for all (NT and PE) placental samples and the positive control (Hela cells) which was within the predicted range (between 46-48 kDa). The expression levels were significantly higher in PE samples ($p<0.001$) when compared to NT samples.

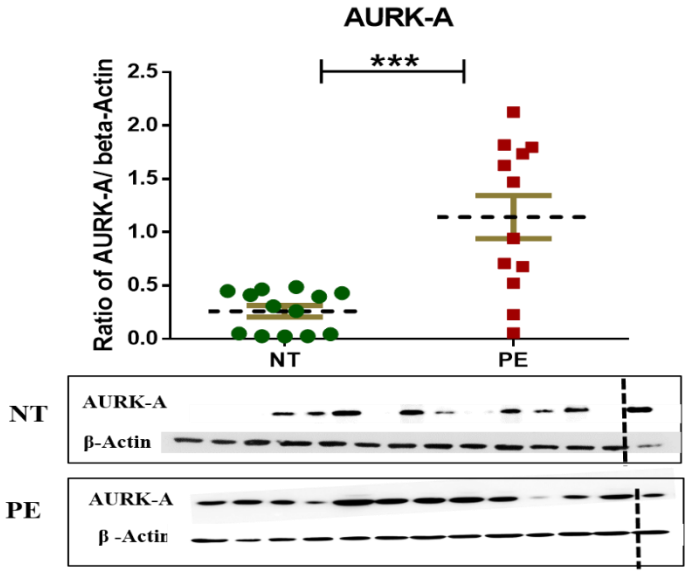

Figure 3.4: AURK-A protein expression in NT and PE placentae.

Scatter-plots are derived from 13 NT and 12 PE samples and relative expression was determined from three independent blots. Mann Whitney U test was performed (***$p<0.001$). Quantified data are expressed as the ratio of the AURK-A / β-actin. The error bars (±SEM) are represented with brown lines. Representative western blots showing the single bands detected by both anti-AURK-A and β-actin antibodies are also shown.

- **Cellular localisation of the AURK-A**

The IRS data of AURK-A suggested that the intensity of staining was more pronounced in PE samples, when compared with NT samples (See Table 3.3). The entire PE sections were completely stained; with higher staining intensities around the STB layer (red arrows). However, the weak staining intensity was found in the mesenchymal stromal cells (red star) and foetal blood vessels (black arrows). Overall, the staining intensity in PE tissues was higher when compared to low staining levels in NT tissues (Figure 3.5).

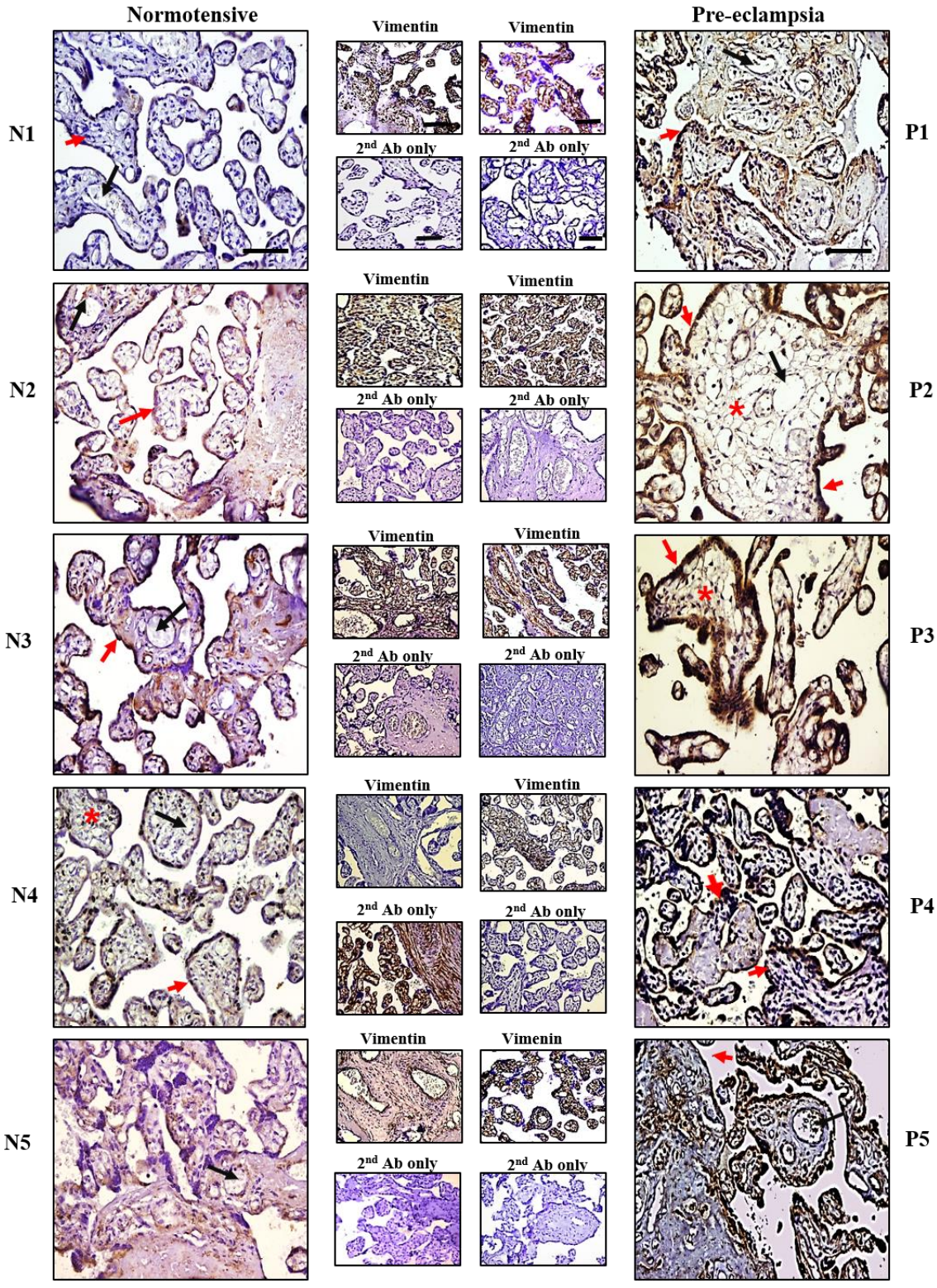

Figure 3.5: AURK-A localisation determined by immunohistochemistry.

Five placental samples for each group (NT and PE) are represented here. The IRS for AURK-A for each sample was scored in comparison to IRS of positive (Vimentin) and negative controls (2^{nd} Ab only) of the same sample. Magnification 20X; scale bar=100µm. STB layer (red arrows), the mesenchymal stromal cells (red star) and foetal blood vessels (black arrows).

- **Protein expression of AURK-C**

The anti-AURK-C antibody produced single bands in almost all of the NT samples and positive control (Hela cells). However, only some of the PE samples showed expression of AURK-C (Figure 3.6). The detected bands were at 36 kDa which is within the predicted range (20-36). The expression levels of AURK-C in NT samples were significantly higher than in PE samples.

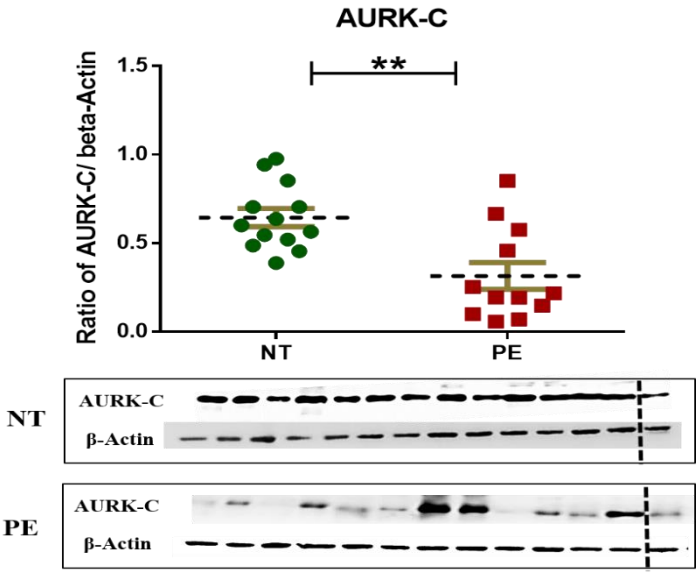

Figure 3.6: AURK-C protein expression in NT and PE placentae.

Scatter-plots are derived from 13 NT and 12 PE samples and relative expression was determined from three independent blots. Mann Whitney U test was performed (**$p<0.01$). Quantified data are expressed as the ratio of the AURK-C / β-actin. The error bars (±SEM) are represented with brown lines. Representative western blot showing the single bands detected by both anti-AURK-C and β-actin antibodies are also shown.

- **Cellular localisation of the AURK-C**

The staining intensity of AURK-C was less in PE samples when compared with NT samples, as seen in Figure 3.7. In NT, IRS for AURK-C was observed in the STB layers (red arrows). No staining difference was observed between NT and PE samples, in both the mesenchymal stromal cells (red star) and foetal blood vessels (black arrows). The IRS data, which showed statistically lower expression of AURK-C staining in PE compared to NT samples ($p<0.05$) (Table 3.3).

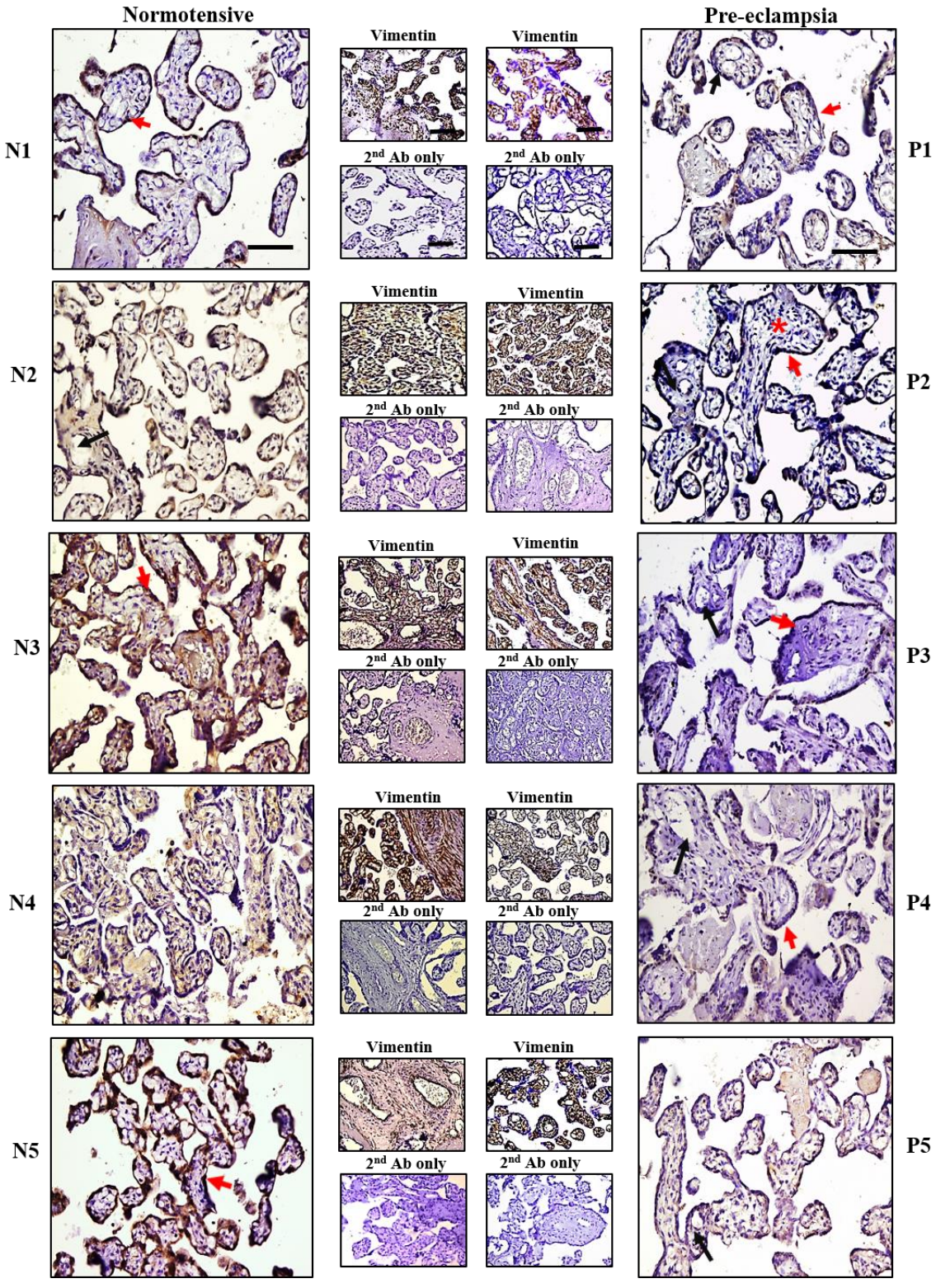

Figure 3.7: AURK-C localisation determined by immunohistochemistry.

Five placental samples for each group (NT and PE) are represented here. The IRS for AURK-C for each sample was scored in comparison to the IRS of positive (Vimentin) and negative controls (2^{nd} Ab only) of the same sample. Magnification 20X; scale bar=100µm. STB layer (red arrows), the mesenchymal stromal cells (red star) and foetal blood vessels (black arrows).

- **Protein expression of PDGFRα:**

The expression of PDGFRα protein showed a single band in both placental samples and positive control (PDGF protein). These bands were detected at 36 kDa whilst the expected molecular weight of the band was in the range of 14-20 kDa. Only a few NT samples showed expression of PDGFRα, when compared to the expression in all the PE samples and positive control (Figure 3.8). Thus, there was a significant difference in the expression levels between NT and PE placentae ($p<0.01$).

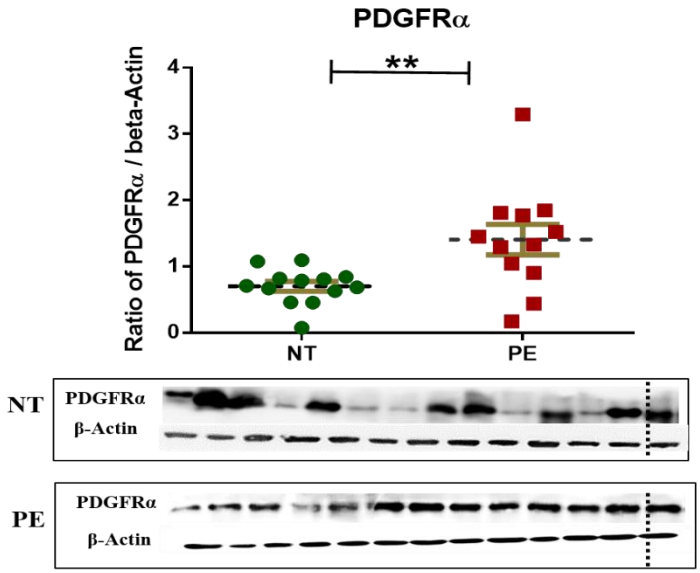

Figure 3.3: PDGFRα protein expression in NT and PE placentae.

Scatter-plots are derived from 13 NT and 12 PE samples and relative expression was determined from three independent blots. Mann Whitney U test was performed (**$p<0.01$). Quantified data are expressed as the ratio of the PDGFRα / β-actin. The error bars (±SEM) are represented with brown lines. Representative western blots showing the single bands detected by both anti- PDGFRα and β-actin antibodies are also shown.

- **Cellular localisation of the PDGFRα**

Both NT and PE tissues showed moderate immuno-reactivity for PDGFRα (See Figure 3.9). In general, the STB layer (red arrow) was clearly stained in both NT and PE tissues. Although, the STB layer in PE showed deeper staining than STB layer in NT. The IRS data showed equal intensities of staining in NT and PE tissues, without any significant difference (Table 3.3).

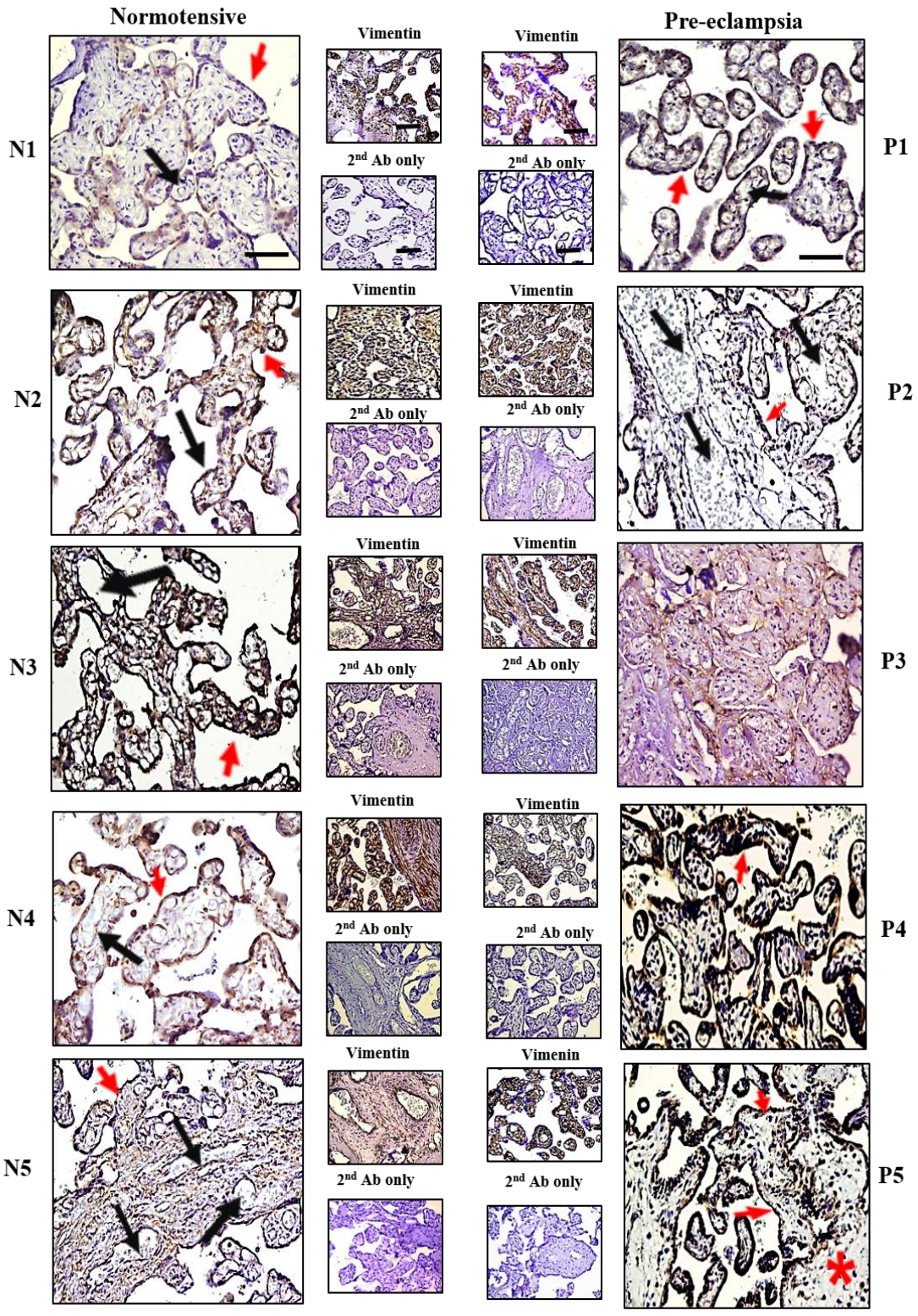

Figure 3.9: PDGFRα localisation determined by immunohistochemistry.

Five placental samples for each group (NT and PE) are represented here. The IRS for PDGFRα for each sample was scored in comparison to IRS of positive (Vimentin) and negative control (2nd Ab only) of the same sample. Magnification 20X; scale bar=100µm. STB layer (red arrows), the mesenchymal stromal cells (red star) and foetal blood vessels (black arrows).

- **Protein expression of TWIST1**

The predicated molecular weight of TWIST1 protein as declared by the antibody supplier (Abcam) was between 21- 36 kDa. However, a single band was observed for TWIST1 in both positive control (Hela cells) and placental samples at 49 kDa (Figure 3.10). The protein expression level of TWIST1 was significantly increased in PE samples when compared to NT placentae ($p<0.05$).

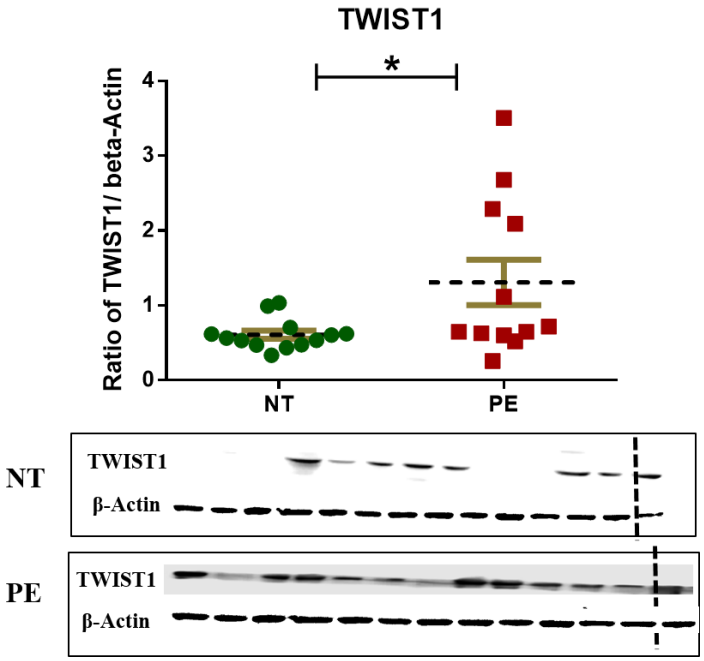

4Figure 3.10: TWIST1 protein expression in NT and PE placentae.

Scatter-plots are derived from 13 NT and 12 PE samples and relative expression was determined from three independent blots. Mann Whitney U test was performed (*$p<0.05$). Quantified data are expressed as the ratio of the TWIST1 / β-actin. The error bars (±SEM) are represented with brown lines. Representative western blots showing the single bands detected by both anti- TWIST1 and β-actin antibodies are also shown.

- **Cellular localisation of the TWIST1**

As seen in Figure 3.11, the staining intensity of TWIST1 expression was more intense in PE when compared with the NT tissues, especially in the STB layer. Interestingly, these are also confirmed by the IRS data which showed statistical significance for differences in TWIST1 expression in PE and NT samples ($p<0.001$) (Table 3.3). The staining was clearly observed in the STB layer in both NT and PE.

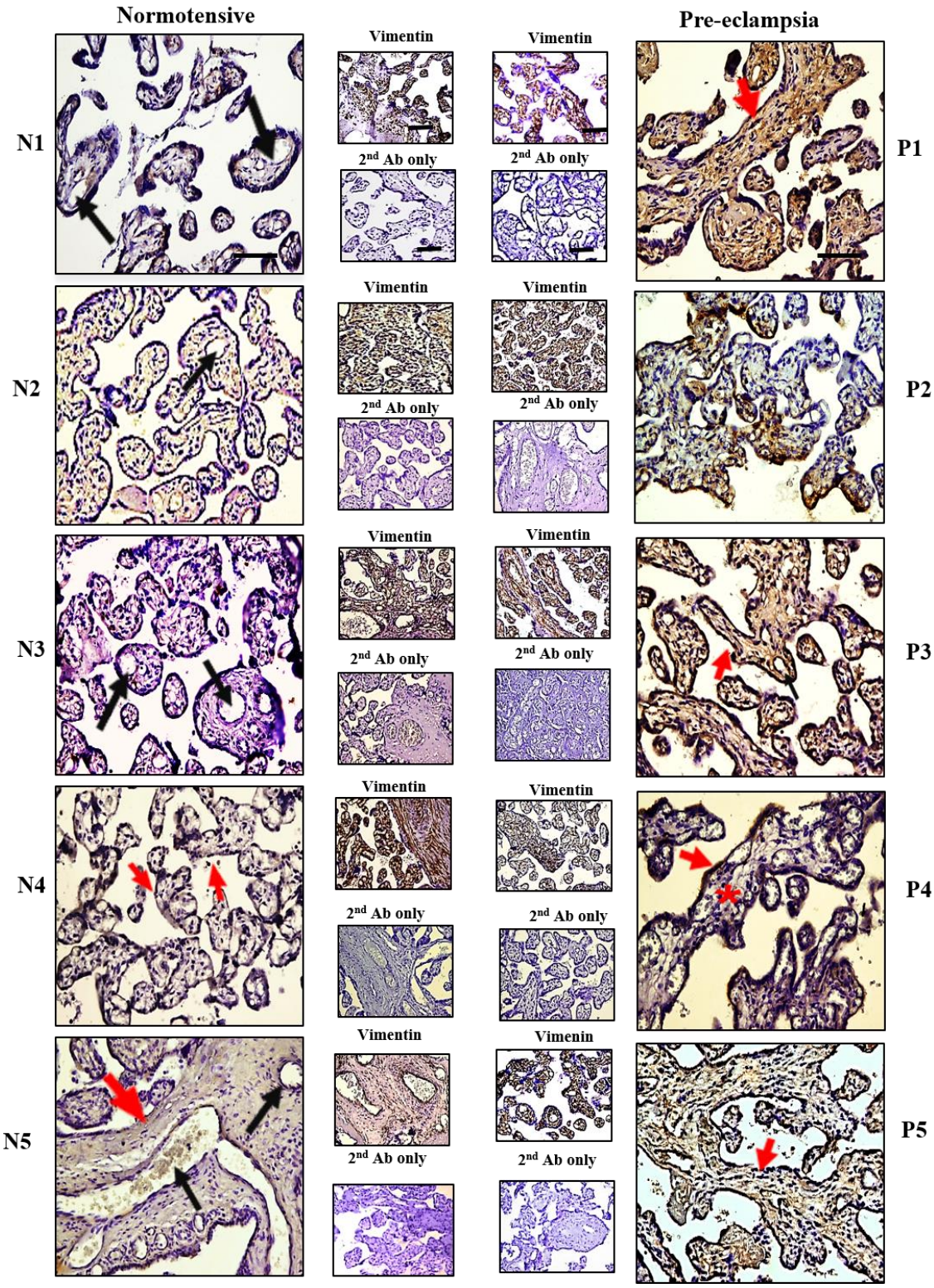

Figure 3.11: TWIST1 localisation determined by immunohistochemistry.

Five placental samples for each group (NT and PE) are represented here. The IRS for TWIST1 for each sample was scored in comparison to IRS of positive (Vimentin) and negative control (2nd Ab only) of the same sample. Magnification 20X; scale bar=100µm. STB layer (red arrows), the mesenchymal stromal cells (red star) and foetal blood vessels (black arrows).

- **Protein expression of JAG1**

The molecular weight of the JAG1 protein was predicted between 75-137 kDa according to the antibody supplier (Abcam). A single band of JAG1 expression were observed at 75 kDa in the positive control (Hela cells) and in placental samples. A significant reduction in the expression was observed in PE samples when compared to NT samples ($p<0.01$) (See Figure 3.12).

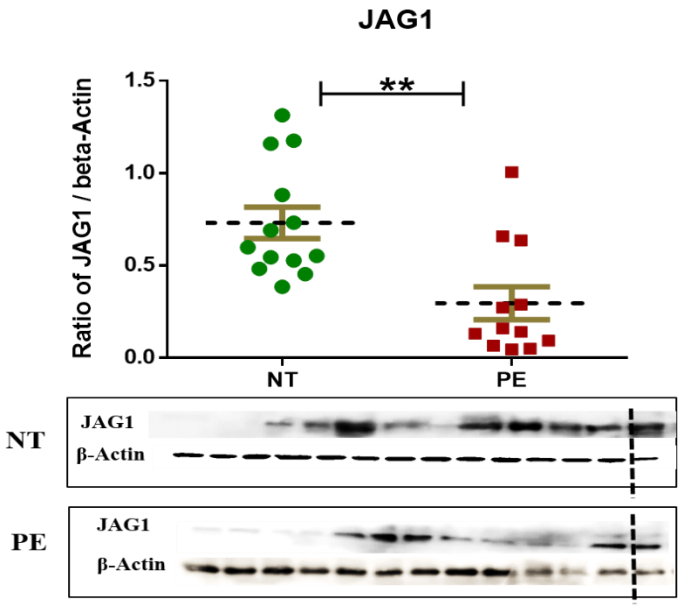

Figure 3.12: JAG1 protein expression in NT and PE placentae.

Scatter-plots are derived from 13 NT and 12 PE samples and relative expression was determined from three independent blots. Mann Whitney U test was performed (**$p<0.01$). Quantified data are expressed as the ratio of the JAG1/ β-actin. The error bars (±SEM) are represented with brown lines. Representative western blots showing the single bands detected by both anti-JAG1 and β-actin antibodies are also shown.

- **Cellular localisation of the JAG1**

Both NT and PE samples showed lower immuno-reactivity to JAG1 (Figure 3.13). The STB located at the surface of placental villi (red arrow) layer showed intense staining in NT samples when compared with PE samples. On the other hand, the IRS data analysis did not show any statistically significant difference in staining between the two groups (See Table 3.3). Some staining was also observed in the mesenchymal stromal cells (red star) in NT tissues.

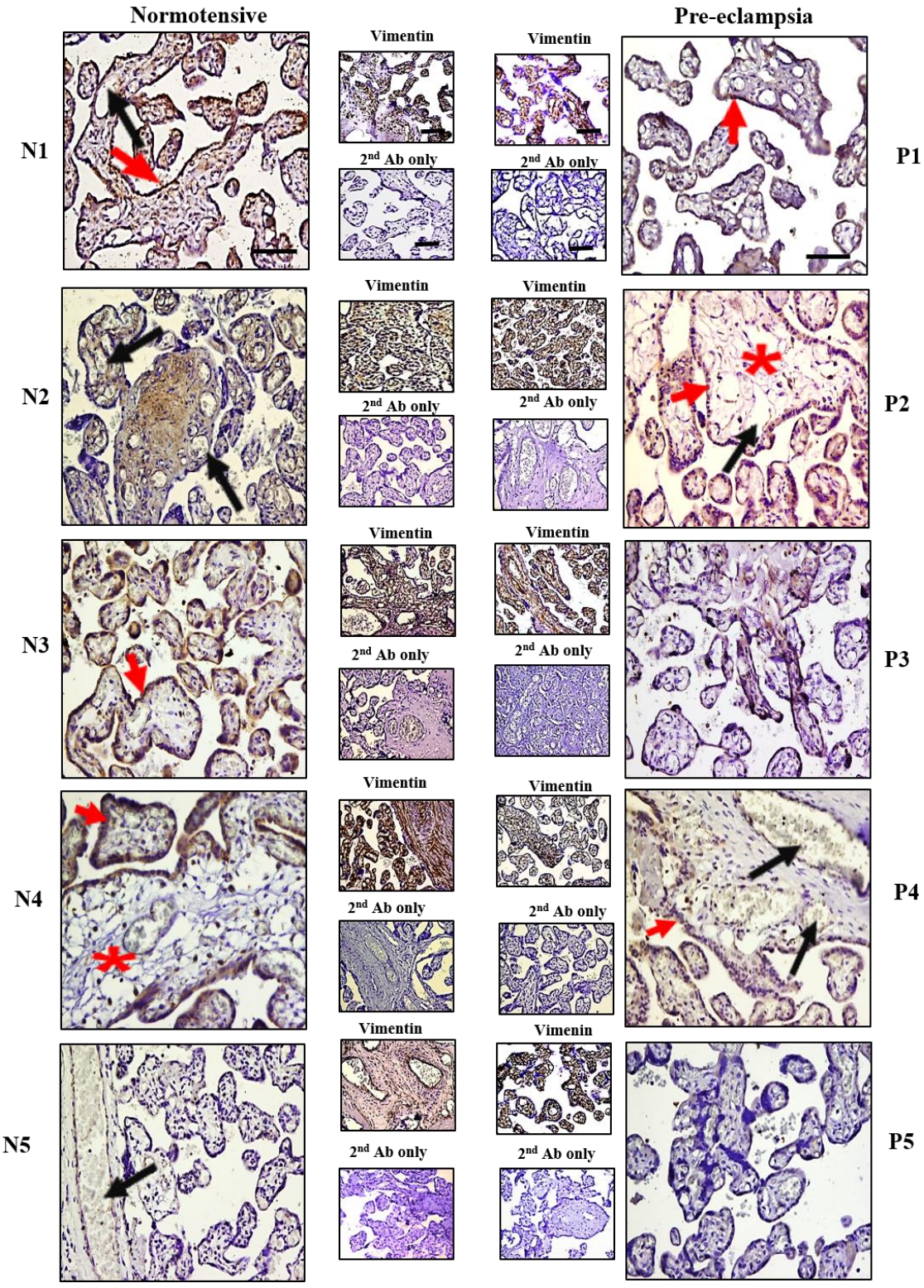

Figure 3.13: JAG1 localisation determined by immunohistochemistry.

Five placental samples for each group (NT and PE) are represented here. The IRS for JAG1 for each sample was scored in comparison to IRS of positive (Vimentin) and negative control (2^{nd} Ab only) of the same sample. Magnification 20X; scale bar=100µm. STB layer (red arrows), the mesenchymal stromal cells (red star) and foetal blood vessels (black arrows).

3.3 Discussion

The Placenta has a central role in foetal and maternal physiology and development (Sood *et al.*, 2006). The variation of placental gene expression patterns can be associated with several maternal or foetal abnormalities including PE (Kleinrouweler *et al.,* 2013). Several studies, using RNA or DNA microarray techniques, have shown that some genes are common in placental and tumour development, therefore, it was essential to understand their molecular mechanisms during placental development (Sood *et al.,* 2006; Louwen *et al.,* 2012; Kleinrouweler *et al.,* 2013). The expression of these genes can be used as novel biomarkers in diagnostics, especially for early detection of PE (Kleinrouweler *et al.,*2013). The prime aim of this chapter was to compare the level of mRNA and protein expression (in NT and PE placentae) of some factors of interest that were identified from microarray technology (Ali, 2011). Although, there were several investigations about PE in past few years, the mechanisms of PE development still remains unknown (Vanwijk *et al.,* 2000). However, it is generally accepted that the pathogenesis of PE begins during the first and early second trimester of pregnancy, where there is impaired trophoblast invasion and remodelling of the spiral arteries (Goldman-Wohl and Yagel, 2009). Moreover, several factors that have been suggested to be involved in PE, but several others still remain to be investigated or discovered.

The factors which are considered in this chapter include ALDH3A1, AURK-A, AURK-C, PDGFRα, TWIST1 and JAG1, which were identified by microarray as common molecules involved in tumour invasion (Ali, 2011) and could be involved in trophoblast invasion due to the resemblance of placental invasion to tumour. They mostly fall under the categories of enzymes (ALDH3A1, AURK-A, AURK-C), transcription factor (TWIST1), growth factor receptors (PDGFRα) and signalling proteins (JAG1) The status of these factors in PE placentae have not been investigated earlier. Furthermore, since these factors have been suggested to play roles in tumour invasion (Ali, 2011), studying the status of these factors in PE (where the invasion is low) would help it to better understand their functions.

ALDH3A1 is an enzyme which plays a role in normal and cancer stem cell biology, and hence used as a marker for the identification and isolation of cancer cells (Januchowski *et al.*,2013). Aurora kinases (AURK-A and C) both are overexpressed in several human cancers and normal tissues. Their overexpression could help to provide a new target for the treatment and understanding of cancer mechanisms (Xu *et al.,* 2014). PDGFRα is a growth factor that plays a major role in several physiologic functions, including embryogenesis and angiogenesis (Majumdar *et al.,* 2009). The transcription factor, such as TWIST1, which

plays a vital role during embryonic growth, is also associated with cancer development and overexpressed in a variety of tumours e.g., prostate, lung, and breast (Cabrera Je, 2013). JAG1 or Jagged-1 is a protein encoded by JAG1 gene and plays a crucial role in tissue formation during the development of embryo (Karanu *et al.*, 2000). The mRNA and protein expression level of JAG1 are used as biomarkers for breast cancer (Dickson *et al.*, 2007). Therefore, understanding these factors that may be affected in reduced trophoblast invasion (as in PE) could shed some light on their importance in tumour invasion as well. The results of this chapter are summarised in Table 3.4.

Table 3.4: Overall correlation between mRNA, protein expression and IRS in PE in comparison to NT placentae.

	PE			
Factors interesting	**mRNA by qRT-PCR (compared to NT)**	**Protein by WB (compared to NT)**	**IHC**	
			IRS	**Cell type**
ALDH3A1	**(+)***	**(+)***	**ns**	STB
AURK-A	**(+)*****	**(+)*****	**(+)****	STB, mesenchymal stromal cells and foetal blood vessels
AURK-C	**(-)***	**(-)****	**(-)***	STB
PDGFRα	**(+)****	**(+)****	**ns**	STB
TWIST1	**(+)****	**(+)***	**(+)*****	STB
JAG1	**(-)****	**(-)****	**ns**	STB, mesenchymal stromal cells

The results of AURK-A, AURK-C and TWIST1, showed correlation between mRNA, protein expression and IRS. (-) down regulated; (+) up regulated; **ns**= no significance; *p<0.05;**p<0.01; ***p<0.001.

3.3.1 Comparative expression analysis between NT and PE placentae

- **ALDH3A1**

ALDH3A1 is a member of the ALDH3 family; others include ALDH3A2, ALDH3B1, and ALDH3B2). The ALDH3 family plays important role in cell proliferation, differentiation and survival, especially during the cellular responses to oxidative stress (Marchitti *et al.*, 2010). Its expression has also been reported in mouse embryonic cells. Although ALDH3A1 proteins are believed to play a role in tumourigenesis, their exact functions are not completely understood, apart from the fact that they are up-regulated in tumour cells (Muzio

et al., 2012). It has been suggested to play a role in maintaining tumour cell growth, motility, and gene expression and are therefore used as a functional markers for cancer (Muzio *et al.*, 2012).

Over the last few years, ALDH3A1 has been studied in placental tissues, but then its role in placenta remains unclear (Marchitti *et al.,* 2010). The data from this study suggest that both mRNA and protein levels of ALDH3A1 are significantly increased in PE placentae when compared to NT ($p<0.05$). However, no significant difference could be observed from the IHC data, apart from visible strong staining in the STB layers of PE tissues compared to NT tissues. IHC is a qualitative tool to confirm the presence or absence, and localization of a protein in or on cells/tissue by using antibody (Torlakovic *et al.,* 2015). However, it has some limitations for quantitation, for example, the brown colour of DAB reaction product is not a true absorber of light, but rather it scatters light (Rudbeck, 2015). The more protein there is in the tissue, the more DAB will precipitate, but the colour does not follow a linear relationship between the amounts of DAB and how dark it shows (Rudbeck, 2015). Moreover, thick sections of tissue tend to give stronger staining intensity than thin sections because there is more tissue with more antigen into which the DAB product may precipitate (van der Loos, 2008). Although, the sections used in this study were all 5 μm in thickness to minimise these limitations there were still no correlation to mRNA and protein by western blotting. Furthermore, Western blotting was carried out in this study which is a relatively accurate method for protein quantitation. Machitti *et al.* in 2010, used western blot analyses to show that ALDH3A1 was expressed in different mouse tissues including placentae. In placental tissues, its expression plays a helpful and physiological role against oxidative stress, i.e. it protects the trophoblasts from damage, prevents pregnancy loss at early stages and placental toxicity, and can be considered as a foetal antioxidant (Marchitti *et al.,* 2010). Therefore, the overall high expression of ALDH3A1 in PE tissues could act to overcome the oxidative stress caused by the abnormal re-modelling of the spiral arteries.

- **AURK-A**

The involvement of Aurora-A during cell division makes it a potential drug target for cancer therapy (Staff *et al.,* 2009). To the best of the author's knowledge, this is the first study on the expression of AURK-A in NT and PE placentae, and there were no previous data to be found on AURK-A expression in placenta. Interestingly, the data from this study showed that AURK-A was overexpressed in PE placental samples.

Yoon *et al.* in 2012 have indicated that Aurora A is essential for post-implantation embryo growth and survival. Moreover, their data show that the effects of ablation of Aurora A at post-implantation stages can impact the embryo differently depending on the tissues affected by the mutation, such as in epiblast. Interestingly, in this present study, results showed an overall positive correlation between mRNA and protein expression levels, and were up-regulated in PE samples. This present study thus provides evidence for the expression of AURK-A in both NT and PE placentae.

Results from IHC illustrated that AURK-A also showed higher staining for PE than NT placentae. Thus, there was a high significant correlation between, mRNA, WB and IHC for AURK-A. Its over-expression in PE tissues shows that it might play a role in placental abnormalities and other pathological characteristics of PE. Moreover, the overexpression of AURK-A in both PE and cancerous tissues suggest that it could be a potential therapeutic target for these diseases.

- **AURK-C**

AURK-C is overexpressed in many cancer cell lines and it is believed to increase the cellular proliferation and migration of tumours (Dieterich *et al.*, 2007). Khan *et al.* (2012), found that AURK-C can stimulate formation of multinuclear cells from mononuclear cells condition by amplifying the centrosome. Furthermore, AURK-C is also linked to male infertility (Fellmeth *et al.,* 2015). Schindler *et al.* (2012) reported the involvement of AURK-C in the cytokinesis process during normal oocyte maturation and in pre-implantation of embryos. Although, it is highly expressed in normal tissues (e.g. testis), its function is not yet clear (Harrington *et al.,* 2004). Interestingly, there was a correlation between the intensity of IHC staining, mRNA and protein expression levels of AURK-C. Both mRNA and protein expression levels of AURK-C were decreased in PE. AURK-C expression was localised in the STB layers of both NT and PE samples. According to semi-quantitative analysis of IHC for AURK-C, it is evident that AURK-C IRS is significantly higher in NT placentae in comparison with PE placentae. Thus, from this study it can be predicted that AURK-C might be expressed during first trimester trophoblast cells to enhance, proliferation and invasion of EVT cells, which are important for successful pregnancy. Additionally, there may be possible involvement of AURK-C during the formation of STB from mononuclear CTB. During formation of STB from CTB in normal placenta, some of the trophoblast cells undergo apoptosis in order to maintain the cell numbers (Crocker *at al.,* 2003). However, in PE placenta this cell death number is dramatically increased resulting in placental dysfunction (Ishihara *et al.*, 2002). The down-regulation of AURK-C in PE placenta when compared with NT placentae reported in this

study, could be due to disturbed trophoblast fusion during syncytial layer formation during this condition.

- **PDGFRα**

PDGFRα belongs to the tyrosine kinase receptor family which has 2 subtypes: PDGFRα and PDGFRβ. Although the underlying mechanisms remain largely unknown, PDGFRα are predicted to be involved in cellular proliferation, differentiation, growth development and pro-angiogenesis (Andrae *et al.,* 2008). During embryonic development, PDGFRα regulates cell growth and differentiation (Majumdar *et al.,* 2009). PDGFR signalling has important functions during embryogenesis, and its overexpression is associated with several pathological conditions such as cancer (Betsholtz *et al.,* 2001). It has been found to be expressed in mouse pre-embryos and in human placental cells (Osterlund *et al.,*1996). PDGFR α signalling is essential for the normal blood vessel formation and for the proper cellular organization of several organs such as brain, kidney and placenta (Looman *et al.,* 2007). Hence, they are one of the important mediators of mammalian development. While the importance of the β-isoform of PDGFR in trophoblast proliferation during pregnancy have been demonstrated (Holmgren *et al.,* 1995). Conversely the function of α-isoform has not been fully established in placental development.

In addition, a study by Kita *et al.* (2003) has shown that both PDGFRα and β in human placenta are expressed in the syncytiotrophoblast and the villous cytotrophoblast. The present finding of this study also supports these previous studies, where STB layers express PDGFRα in both NT and PE. However, the STB layer in PE showed deeper staining than in NT. Although, the overall IRS data showed equal intensities of staining in NT and PE tissues without any significant differences. Interestingly, there was a correlation between the mRNA and protein expression levels of PDGFRα, which were increased significantly ($p<0.01$) in PE compared to NT. This confirms the findings of Jurcovicova *et al.* (1998) who presented that PDGF mRNA expression values for NT placenta are considerably lower when compared to PE placentae. In contrast a study by (Jarvenpaa *et al.,* 2007), showed that PDGFRα was down-regulated in patients with PE associated with intrauterine growth restriction (IUGR), using microarray analysis. It is worth noting that the PE placentae samples used in current study did not have IUGR complications.

In this present study, 13 NT and 12 PE placentae were used, whereas only 3 NT and 2 PE with (IUGR) were used by (Jarvenpaa *et al.,* 2007). Furthermore, the PE placentae used in this study were only mild pre-eclamptic, not severe unlike the one used by (Jarvenpaa *et al.,* 2007). According to Morey *et al* (2006), qRT-PCR is the most common validation tool used

for confirming gene expression results obtained from microarray analysis and confirmed their results usually are in agreement. Yet, there is still a debate on which of the two techniques is most reliable. Therefore, in this study western blot was used to check the validity of the mRNA and IHC results.

- **TWIST1**

TWIST1, is a transcription factor that belongs to the basic helix-loop-helix (bHLH) family. It plays a major role in regulatory functions during embryogenesis. It regulates cell proliferation, migration and differentiation in embryonic development (Ansieau *et al.*, 2008). Moreover, it also plays multiple role in cancer initiation, progression and metastasis process (Qin *et al.*, 2012). It can override oncogene-induced cell senescence and apoptosis (Maestro *et al.*, 1999). In addition, TWIST1 increases cancer cell resistance to chemotherapy and enhances cancer stem cell (CSC) population (Mani *et al.*, 2008). It plays a role in inducing epithelial–mesenchymal transition (EMT) and it allows the acquisition of a mesenchymal phenotype that permit the invasion and release of cells from the primary tumour (Ansieau *et al.*, 2010). In addition, it regulates many proteins associated with EMT such as E-cadherin, which is essential for epithelial cell-cell adhesion (Ansieau *et al.*, 2010). Therefore, TWIST1, can be considered as an important tumour biomarker. The expression of TWIST1 during embryonic development of mouse has been studied previously (Qin *et al.*, 2012) However, information relating to the TWIST1 expression profile during human embryogenesis is lacking. A strong mRNA expression of TWIST1 was observed in placenta, especially in the foetal side of the placenta during a study conducted by Wang *et al.* (1997) using human tissues and cells originating from different human tissues to observe TWIST1 expression. Furthermore, it is highly expressed in the mesoderm-derived embryonic mesenchyme and the adult stem cells of the mesenchyme (Qin *et al.*, 2012).

In the present study, a statistically significant increase was observed in both mRNA ($p<0.01$) and protein expression levels ($p<0.05$) of TWIST1 in PE. Interestingly, when these results were also validated with IHC, intense staining for TWIST1 was detected in the STB layer of PE placentae rather than NT placentae. A study by Sitras *et al.* (2009) also reported up-regulation of the second member of the bHLH family (BHLHB2) in PE placentae. Therefore, it could be suggested that TWIST1 over-expression in placental tissues might play a role in placental abnormalities and the pathological characteristics of PE.

- **JAG1**

JAG1 belongs to the group of NOTCH signalling proteins which are responsible for vasculogenesis and angiogenesis in embryonic development during gestation (Funahashi *et al.,* 2011). Therefore, most researchers investigated previously the expression pattern of NOTCH receptors and their ligands during pregnancy in order to study the vasculogenesis and angiogenesis process in human placenta. NOTCH signalling might represent a key regulatory pathway that controls trophoblast proliferation, motility, and differentiation (Haider *et al.,* 2014). Furthermore, the published studies demonstrate that NOTCH signalling and their ligands pathway have a crucial role in the development of the placenta. The normal function of JAG1 is to stimulate vasculogenesis and angiogenesis, but its mechanism in metastasis remains to be elucidated (Purow *et al.,* 2013: Sethi *et al.,* 2011).

In this study, both mRNA and protein expression levels of JAG1 were decreased ($p<0.01$) in PE compared to NT placentae. The STB layer along with some mesenchymal stromal cells showed intense staining in NT when compared to PE. These results agreed with the investigations of Herr and colleagues (2011), Jarvenpaa *et al.* (2007) and De Falco *et al.* (2007), where down-regulation of JAG1 were also reported in PE placentae followed by up-regulation in STB and placental stromal layer of NT placenta.

The functional details of these factors will be discussed in chapter 7.

3.4 Conclusions

The collective data from mRNA, protein expression and IHC studies, suggest that the expression patterns of ALDH3A1, AURK-A, PDGFRα, and TWIST1 are increased in PE placentae. Since placental invasion resembles tumorigenesis, and the fact that expression of the presumed tumour markers is altered in PE (that has low invasiveness), they may be an interesting avenue to explore. In contrast, the data from this chapter suggest the expression patterns of AURK-C and JAG1 are down-regulated in PE samples. This could be associated with the signaling pathways in development of placenta and in various invasion mechanisms. The investigation of the protein expression of these factors (ALDH3A1, AURK-A and-C, PDGFRα, TWIST1 and JAG1) may provide valuable insights into placental function and help to identify molecular mechanism of both NT and PE. To further investigate the molecular mechanisms of these factors, *in vitro* study by using different placental origin cell lines to investigate the protein expression of these factors were conducted (See Chapter 6). Therefore, it is important to study and investigate the functions of these factors during placental development by using primary cultures (See Section 7.8: Future Studies).

Chapter 4
Establishment and characterisation of stem like cells from trophoblast and tumour cell lines

4.1 Introduction

As previously mentioned in Chapter 1, placenta is an extra-embryonic temporary organ and yet it encompasses innumerable functions for development and survival of the foetus (Sood *et al.,* 2006). Due to ethical constraints, it is impossible to carry out *in vivo* studies; equally development of *ex vivo* models remains to be challenging. The human placenta is made up of a heterogeneous groups of cells which include trophoblast, mesenchymal and stromal fibroblasts with neighbouring connective tissues (Novakovic *et al.,* 2011). These cell types exhibit differences in morphology, function and gene expression. Therefore, *in vitro* research using cell lines remains the important model systems in which to study placental development. Previous *in vitro* studies have used all these different cell types to understand the physiological and pathological functions of placenta (Ji *et al.,* 2013).

There are two ways for *in vitro* studies; (1) primary cells developed from term and /or first trimester aborted pregnancies, such as CTBs, ST and EVTs and (2) placental derived cell lines from placental extravillous trophoblast and tumour cells (such as choriocarcinoma) (Novakovic *et al.,* 2011). Bilban and colleagues (2009 and 2010) by using microarray and bioinformatics analysis compared the gene expression profile of three choriocarcinoma cell lines (JEG-3, BeWo and ACH-3P), two EVT-derived cell lines (HTR8/SVneo and SGHPL-5) and primary trophoblasts (EVTs and CTBs). They reported that the three types of cells were found to be significantly different with respect to their gene expression profiles. Although, primary trophoblast cultures are highly useful in studying the differentiation and functions of trophoblasts, these cells remain suitable only for short term studies, but not for longer culture to study early development phases (Ji *et al.,* 2013).

On the other hand, a number of trophoblast cell lines are available for *in vitro* analysis of placental function (King *et al.,* 2000). These cell lines are important research tools used as a replacement for primary trophoblast cells (Burleigh *et al.,* 2007). Placental derived cell lines have similar characteristics and behave similarly to cells they were isolated from (Novakovic *et al.,* 2011). An example of a placental derived cell line is BeWo, which was established in 1968 by Patillo and Gey. Following this, several other placenta derived cell lines were established (Fogh *et al.,* 1977; Graham *et al.,* 1993; Feng *et al.,* 2005). These cell lines are immortalised by several techniques and they are regarded as powerful tools for long term examination. However, during immortalization the physiological function of these cells may be altered. Therefore, it is strongly suggested to use more than one cell line during any *in vitro* investigation to determine the functional compatibility of these cell lines and to obtain meaningful data.

In this study, four different placental cell lines were used. Two of which were transformed (non-tumour) placental cell lines (HTR8/SVneo and TEV-1), produced by individual immortalisation of first trimester EVT using SV-40 large T antigen (Novakovic *et al.,* 2011) and retroviral vector respectively (Feng *et al.,* 2005). The other two cell lines (JEG-3 and BeWo), were derived from gestational choriocarcinoma. Both the EVT and choriocarcinoma cells show capacity to invade, however, the EVT cells invade only after proliferation while choriocarcinoma cells can proliferate and invade at the same time (Farnk *et al.,* 1999). Therefore, it was evident that there are differences in mechanisms, gene expressions and functions between the two groups. Thus, two different groups of cell lines were used in this study. MCF-7, breast adenocarcinoma cell line has unique biological properties (Osborne *et al.*, 1987). In this study MCF-7 was used as a tumour cell line of non-placental origin. The information relating to all cell lines used are summarized in Table 4.1.

Table 4.1: The origins and features of the different cell lines used in this study *(*Table *adapted from Novakovic et al., 2011).*

	HTR8/SVneo	TEV-1	JEG-3	BeWo	MCF-7
Origin	HTR8 First trimester villous explants	First trimester placental explants	Choriocarcinoma	Choriocarcinoma	Breast adenocarcinoma
Cell morphology	Epithelial	Epithelial	Epithelial	Epithelial	Epithelial
Tissue	Placenta	Placenta	Placenta	Placenta	Breast
Immortalization method	Electroporation with (pSV3neo) containing early region of SV40encoding the (SV40 Tag)	Retroviral vectors with Human papillomavirus type 16 (HPV16) E6/E7 genes	Naturally occurring	Naturally occurring	Naturally occurring
Migration	+	+	+	+	+
Invasion	+	+	+	+	(non-invasive type).
References	Graham et al 1993	Feng et al 2005	Kohler and Bridson 1971	Patillo and Gey 1968	Herbert Soule and other 1973

4.1.1 Establishing stem like cells from human trophoblast and tumour cell lines

Stem cell research has offered solutions for several clinical problems and opened new windows in drug testing, placental development studies, cancer and gene therapy (Mousa *et al.,* 2006). They are the undifferentiated primary cells of all multicellular organisms, that have the capacity for self-renewal, proliferation and differentiation into specialized cell types (Mousa *et al.,* 2006). Stem cells can be isolated from various types of tissues and/or organs. For example, adult stem cells can be obtained from bone marrow, skeletal muscle and skin; while embryonic stem cells are derived from embryos **(www[20])**. The placenta can be used as a main source to isolate different types of stem cells such as hematopoietic stem cells (HSCs), human amniotic epithelial cells (hAEC), embryonic stem cells (ES), mesenchymal stem cells (MSCs), trophoblast stem cells (also known as trophoendodermal stem cells), umbilical cord blood stem cells (UCB) and foetal stem cells (FSCs) (Mousa *et al.,* 2006 ; Avasthi *et al.,* 2008). These stem cells can form aggregated clusters called spheroids with stem cell features able to grow in suspension culture (Manuel Iglesias *et al.,* 2013). There are many molecular markers have been used to characterize various stem cell populations such as surface marker (CD133, CD90, CD29 and CD44) and transcription factors (OCT4, SOX2, and NANOG) (Zhao *et al.,* 2012). These spheroids were selected from 3-D culture. In cancer research, 3-D cell culture is used as a tool to produce spheroids to investigate the growth formation and behaviour of tumours as they behave like solid tumour (Mehta *et al.,* 2013). Besides spheroids culture is a useful method *in vitro* to understand the physiological and biological processes involved in organogenesis in the embryo (Oudar 2000). This study focused on embryonic stem cell markers such as transcription factors (OCT4, SOX2, and NANOG), trophoblast transcription factor (CDX2) and a receptor involved in cell fate determination (NOTCH1). Most of these factors are expressed not only in embryonic stem cells but also in a number of tumour cells (James *et al.,* 2012). The transcription factors (OCT4, SOX2, and NANOG) play crucial roles in embryonic development, acting as a regulator of self-renewal/differentiation, maintaining and re-establishing pluripotency of embryonic stem cells (ESCs) (Miyazawa *et al.,* 2014). CDX2 has an essential role in the differentiation process of the trophectoderm (the outer epithelial layer of the blastocysts) (James *et al.,* 2012). Likewise, the over-expression of NOTCH1 protein was associated with several aggressive tumours (Hendrix *et al.,* 2003). Moreover, this chapter deals with the generation of spheroids from four trophoblast cell lines (HTR8/SVneo, TEV-1, JEG-3 and BeWo) and MCF-7 cell line.

As explained in chapter 1, human trophoblast cells exhibits some similarities with malignant cells, including rapid proliferation and the ability to invade the surrounding tissue; whereas

they do not have the ability to metastasise or exhibit unlimited growth (Fennema *et al.*, 2013). Hence, the aim of this chapter was to generate and select non-resistant (normal) and drug resistant spheroids from transformed trophoblast (HTR8/SVneo, TEV-1) and choriocarcinoma (JEG-3, BeWo) cell lines and to check for "stemness" feature by studying the expressions of stem cell markers such as OCT4, SOX2, NANOG, CDX2 and NOTCH1.

4.1.2 Using DOX to select drug resistant spheroids

Doxorubicin (DOX)/Adriamycin, is an anthracycline antibiotic isolated from *Streptomyces peucetius* var. *caesius* and has been widely used as a chemotherapeutic agent for the treatment cancers (Suzuki *et al.*, 2005). The chemical name of DOX is (8S-cis)-10-[(3-amino-2,3,6-trideoxy-α-L-lyxohexopyranosyl)-oxy]-7,8,9,10-tetrahydro-6,8,11-trihydroxy-8-(hydroxyacetyl)-1-methoxy-5,12-naphthacenedione) (Suzuki *et al.*, 2005). Its structure is given in (Figure 4.1)

There are two mechanisms by which DOX acts on the cancer cells: (**1**) it has an ability to interact with plasma membranes, intercalate with DNA, and disrupt topoisomerase-II, (**2**) generation of the free radicals and their damage to cellular membranes, DNA and proteins (Gewirtz, 1999). DOX is oxidized to semi-quinone, an unstable metabolite, which is converted back to doxorubicin .This process releases reactive oxygen species (ROS) that can lead to lipid peroxidation and membrane/DNA damage, oxidative stress, and activates apoptotic pathways (Doroshow, 1986).

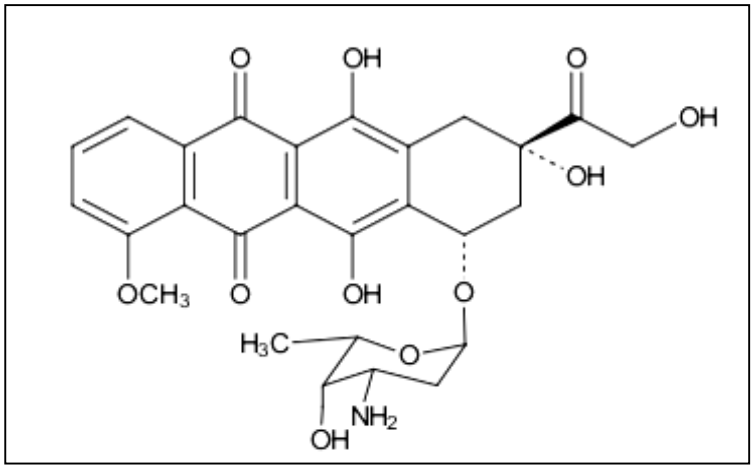

Figure 4.1: Chemical structure of Doxorubicin. (Adopted from Suzuki *et al.*, 2005)

4.2 Results

4.2.1 Determination of cell seeding density for different cell lines

It was essential to determine the appropriate cell seeding densities for each cell line before performing any of the assays. A previous study within this laboratory (by Dr Anushuya Tamang) has determined the accurate cell density by using an MTT assay. Based on these findings, (5x 10^4/ml) cells were selected as optimal seeding density for all placental cell lines.

4.2.2 Use of Doxorubicin to select resistant spheroids

To determine the optimal concentration of DOX to select resistant spheroids, the cells were treated with different concentration of Doxorubicin (250, 500, 1000, 2000 and 4000 ng/ml) coupled with MTT and LDH assays.

4.2.2.1 Effect of Doxorubicin on cell viability and toxicity

In HTR8/SVneo, there were no significant changes in the mitochondrial activity (cell viability) when they were treated with 250 ng/ml of DOX compared to control (no treatment). There was a slight reduction in the mitochondrial activity (cell viability) when cells were treated with 500 ng/ml treatment but was not significant when compared with the untreated control. With the concentrations of 1000 ng/ml and above, a significant reductions in the mitochondrial activity (cell viability) were observed (See Figure 4.2, Panel **A**). Figure 4.2 Panel **B** shows the status of LDH released into the media by HTR8/SVneo cell line. A significant reduction in the level of LDH release was observed with the cells treated with both 250 ng/ml and 500ng/ml of DOX at 24 and 48 hours compared to control (100% lysis buffer). The reduction was significant only at 48 hours for 1000ng/ml treatment but not at 24 hours for the same treatment. Interestingly, a significant increase in the level of LDH release was observed with 4000ng/ml of DOX only at 48 hours of treatment ($p<0.01$) when compared to control (100% lysis buffer).

In the MTT assay, the TEV-1 cell line showed no significant change of viability when they were treated with 250 ng/ml of DOX at 24 hours; but a significant increase in the mitochondrial activity (cell viability) was observed for the same treatment at 48 hours. There was a significant reduction of mitochondrial activity (cell viability) with 500 ng/ml treatment ($p < 0.001$). Concentrations of 1000 ng/ml and above, showed a significant reduction in the mitochondrial activity (cell viability) ($p< 0.0001$) (See Figure 4.2, Panel **C**). In the case of LDH assay, the status of LDH released into the media by TEV-1 cell line is shown in Figure. 4.2, Panel **D**. A significant reduction in the level of LDH release was observed with cells treated with 250 ng/ml, 500 ng/ml and 1000 ng/ml of DOX at both 24 and 48 hours,

compared to control (100% lysis buffer). No significant change in the level of LDH release was observed with 2000 ng/ml and 4000 ng/ml treatment.

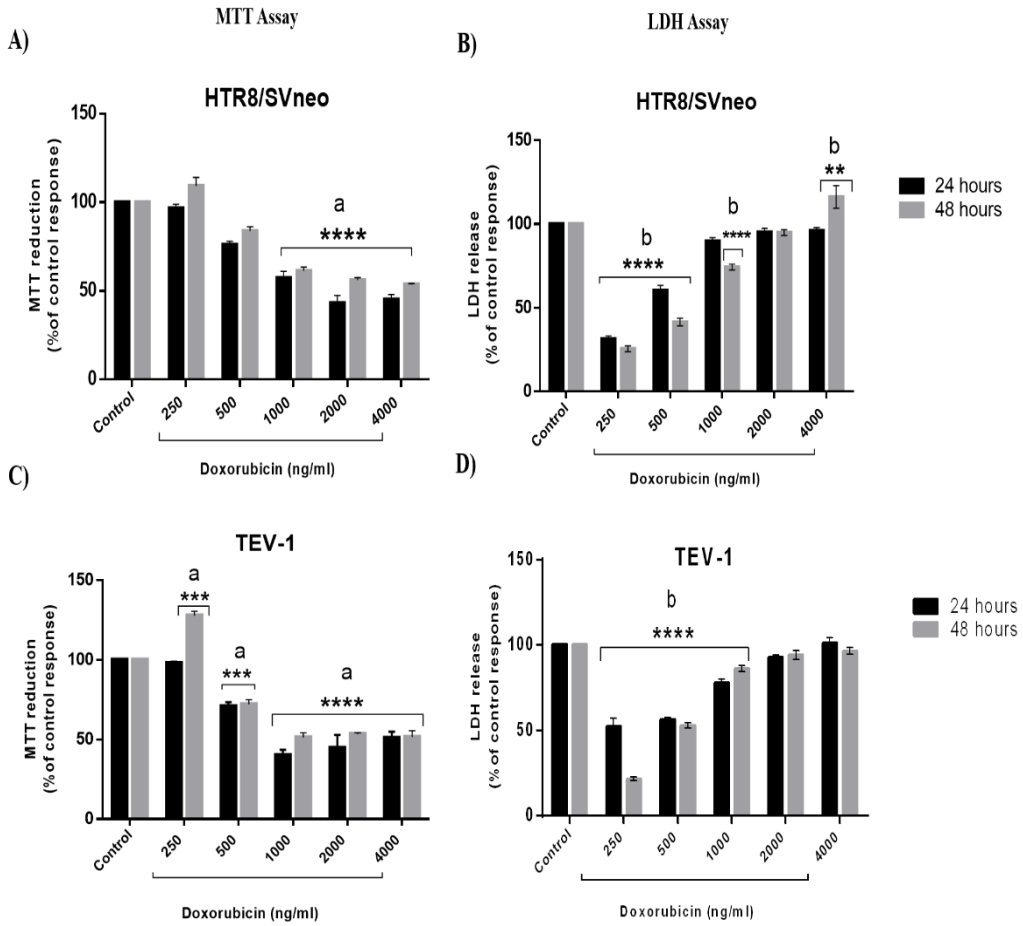

Figure 4.2: The effect of doxorubicin on mitochondrial activity (MTT) and toxicity (LDH) of transformed trophoblast cell lines.

Statistical analysis was carried out using two-way ANOVA (Dunnett's multiple comparison test against control). The data are a representation as the percentage of control cells (= 100%) and represent the mean ± SEM of three independent experiments each performed in triplicate. (**$p < 0.01$, ***$p < 0.001$, and ****$p < 0.0001$); MTT assay was carried out in comparison with no treatment as control (depicted as "a" in the figures), while LDH assay was in comparison with 100% lysis control (depicted as "b" in the figures).

The effect of DOX on placental choriocarcinoma cell lines showed slightly different results when compared with the transformed cell lines. In the MTT assay, there was a significant increase in the mitochondrial activity (cell viability) in both the JEG-3 ($p<0.001$) and the BeWo ($p<0.01$) cell lines with 48 hours of 250 ng/ml DOX treatment when compared to control. In addition, a significant reduction in mitochondrial activity was noted at 24 hours of treatment for the BeWo cell line alone ($p<0.01$). However, when cells were treated with concentration at 500 ng/ml and above, there was a significant reduction in mitochondrial activity ($p<0.0001$) (See Figure 4.3, Panel **A** and **C**). There was a significant reduction

(p<0.0001) in levels of LDH release from these cells lines treated with 250 mg/ml and 500 ng/ml DOX when compared to control (100% lysis buffer) (See Figure 4.3, Panel **B** and **D**). Significant reduction of LDH levels were also noted at 1000 ng/ml in JEG-3 (p<0.0001) and BeWo (p<0.01) cell lines. There was no significant change in the levels of LDH at 2000 ng/ml and 4000 ng/ml DOX treatment in both the cell lines.

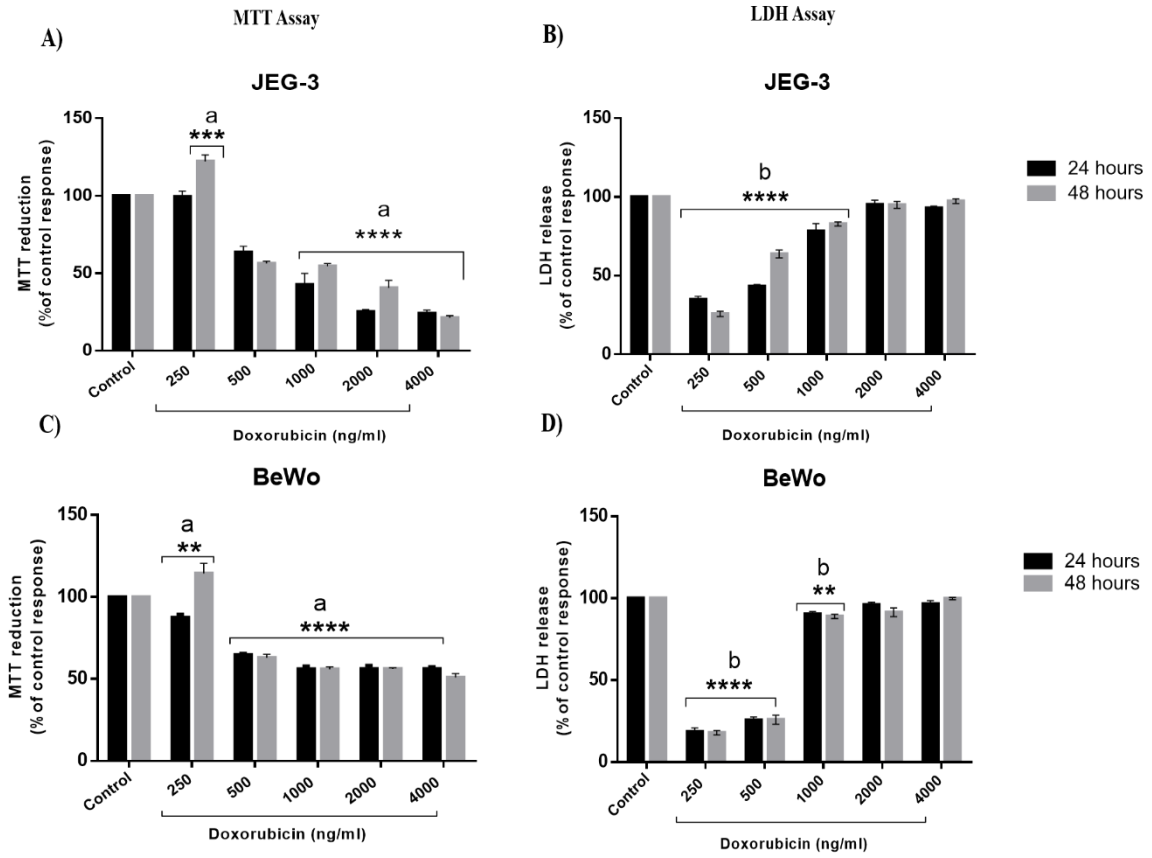

Figure 4.3: The effect of doxorubicin on mitochondrial activity (MTT) and toxicity (LDH) of placental choriocarcinoma cells.

Statistical analysis was carried out using two-way ANOVA (Dunnett's multiple comparison test against control). The data are a representation as the percentage of control cells (= 100%) and represent the mean ± SEM of three independent experiments each performed in triplicate. (**p < 0.01, ***p < 0.001, and ****p < 0.0001); MTT assay was carried out in comparison with no treatment as control (depicted as "a" in the figures), while LDH assay was in comparison with 100% lysis control (depicted as "b" in the figures).

In the case of MCF-7, as seen in Figure 4.4, Panel **A**, treatment with 250ng/ml of DOX resulted in increase in mitochondrial activity (p<0.01) at 48 hours, whereas no significant change was observed at 24 hours of treatment. There was a significant reduction in the mitochondrial activity at the concentration of 500 ng/ml (p<0.001) and above (p<0.0001) compared to the control. Panel **B** in Figure 4.4 shows the levels of LDH release with a

significant reduction in the LDH release at 250 ng/ml, 500 ng/ml and 1000 ng/ml DOX treatment; while no significant change was observed at 2000 ng/ml and 4000 ng/ml treatment compared to control (100% lysis buffer).

Overall, all concentrations of DOX above 1000 ng/ml were found to be toxic to placental as well as tumour cells. In summary, the 250 ng/ml and 500 ng/ml treatments were optimal concentrations of DOX for further investigations.

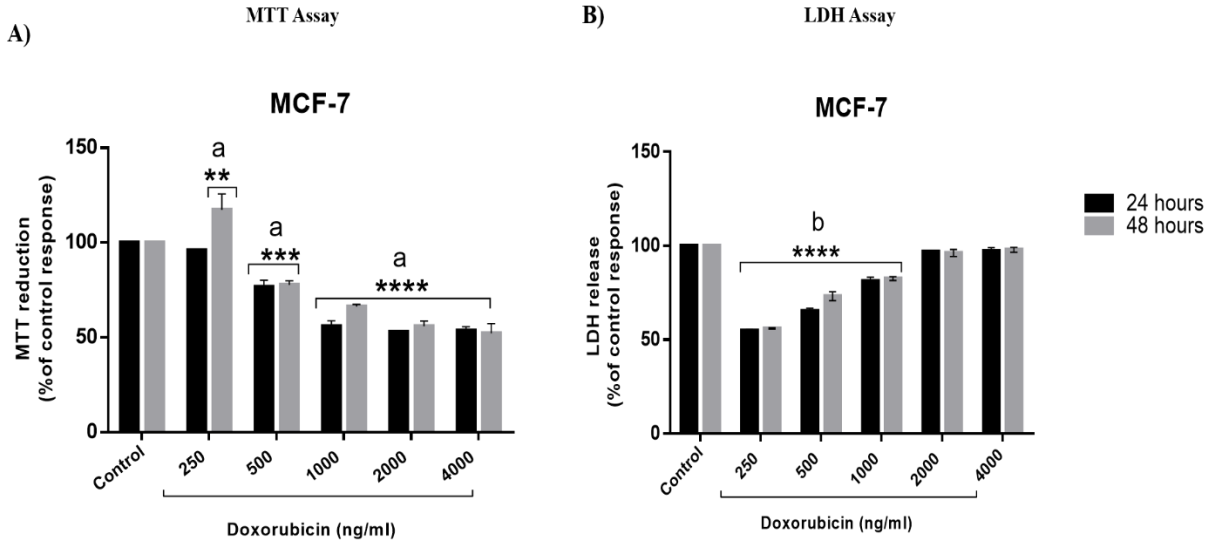

Figure 4.4: The effect of doxorubicin on mitochondrial activity (MTT) and toxicity (LDH) of MCF-7 cells.

Statistical analysis was carried out using two-way ANOVA (Dunnett's multiple comparison test against control). The data are a representation as the percentage of control cells (= 100%) and represent the mean ± SEM of three independent experiments each performed in triplicate. (**$p < 0.01$, ***$p < 0.001$, and ****$p < 0.0001$); MTT assay was carried out in comparison with no treatment as control (depicted as "a" in the figures), while LDH assay was in comparison with 100% lysis control (depicted as "b" in the figures).

4.2.3 Generation of spheroids from trophoblast and tumour cells

As mentioned in Section (2.9), two methods were carried out to generate spheroids, namely: (a) non-resistant (normal) spheroid generation and (b) drug resistant spheroid generation.

4.2.3.1 Generation of non-resistant (normal) spheroids

The placental derived cell lines were checked for ability to form 3-D spheroids on non-adherent flask without treating them with DOX. All the cell lines showed the ability to produce spheroids. As seen in Figure 4.5, Panel **A** and **B** (row 2), both the transformed trophoblast cell lines (HTR8/SVneo and TEV-1) were capable of producing spheroid bodies in non-adherent flasks. Also, they were able to revert back to normal grow (after detachment and in growth media) in the adherent flask [See Figure 4.5, Panel **A** and Panel **B** (row 3)].

The two choriocarcinoma cells (JEG-3 and BeWo) also showed a similar trend in forming spheroid bodies [See Figure 4.5, Panel **C** and Panel **D** (row 2 and 3)]. A larger sized spheroid was observed for MCF-7 cells when compared to the spheroids produced from other trophoblast cell lines. MCF-7 spheroids also had the ability to grow under normal adherent conditions [See Figure 4.5, Panel **E** (row 2 and 3)].

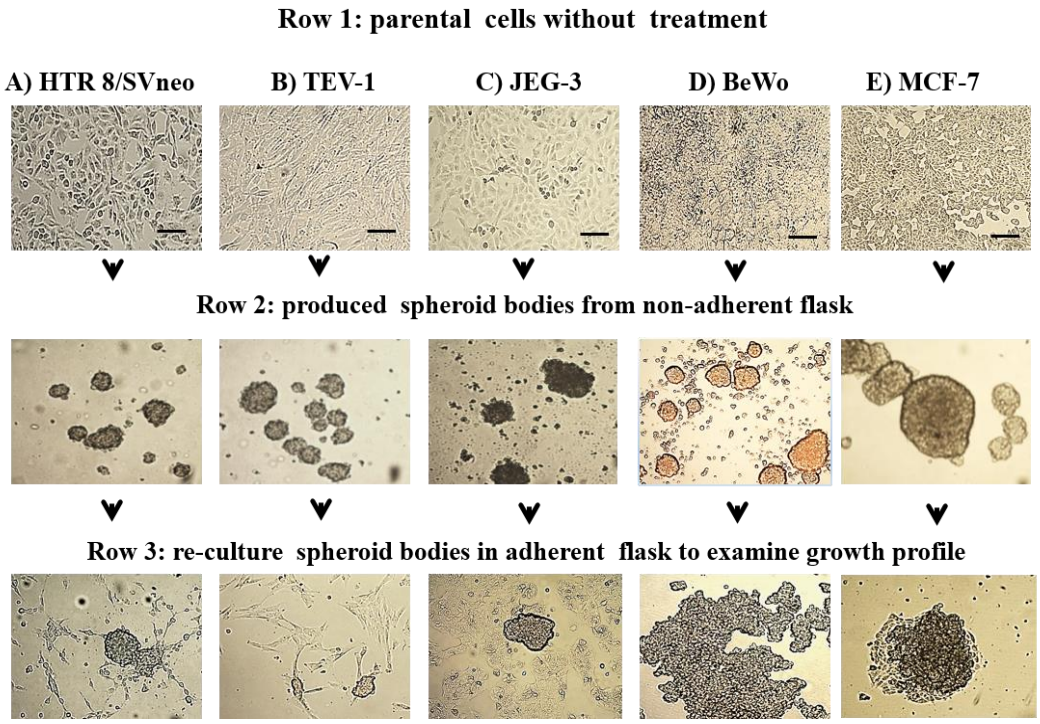

Figure 4.5: Generation of normal spheroids.

The ability of transformed trophoblast (HTR8/SVneo and TEV-1) and choriocarcinoma (BeWo and JEG-3) cell lines to generate non-resistant spheroids are shown in Panels **A** to **D**. Likewise, the MCF-7 is shown in Panel **E**. Row 1 = Parental cells without treatment; Row 2 = Spheroidal cells produced from non-adherent 3-D culture; Row 3 = the ability of spheroidal cells to re-grow onto normal adherent 2-D culture. Scale bar= 100µm.

4.2.3.2 Generation of drug resistant spheroids

DOX was used to produce an environment for physiological stress, which can develop drug-resistant spheroids. This was achieved by treating cells with chemotherapeutic drugs such as DOX. HTR8/SVneo and TEV-1 cell lines, which were exposed to all concentrations above 1000 ng/ml of DOX in normal condition for 48 hours, were found to be dead and appeared floating rather than clustering together to form spheroids in the non-adherent flask [See Figure 4.6 and 4.7, Panels **A** and **B**]. However, cells with both 250 ng/ml and 500 ng/ml DOX treatments, cultured in non-adherent flasks with serum free media, supplemented with growth factors produced viable spheroids. The cells which were treated with 500ng/ml, found to form spheroids of smaller sizes when compared to spheroids produced from cells treated with 250 ng/ml. Interestingly, for most of the spheroids produced by treating with

250 ng/ml, the cells retained the ability to attach and re-grow in the adherent flask under normal conditions after they were manually disseminated. Also, some of these cells had similar morphology to the parental cells, which indicates these cells have the ability to self-renew and differentiate to form cells that are similar to that of the parental cells [See Figure 4.6 and 4.7, Panel **D**]. Therefore, 250 ng/ml was used as the optimal concentration of DOX for selecting spheroids from both transformed trophoblast cell lines. Similar results were obtained from both choriocarcinoma cell lines (JEG-3 and BeWo) treated with 250 ng/ml of DOX [See Figure 4.8 and 4.9, Panels **B**, **C** and **D**]. MCF-7 showed similar results to the placental derived cell lines with both DOX concentrations (250 and 500 ng/ml); however, the spheroids formed by MCF-7 were bigger in size compared to placental cell lines [See Figure 4.10, Panels **B**, **C** and **D**]. In addition, MCF-7 cells treated with 1000 ng/ml of DOX were able to produce small spheroids compared to trophoblast cells lines (which did not form any spheroids at 1000 ng/ml).

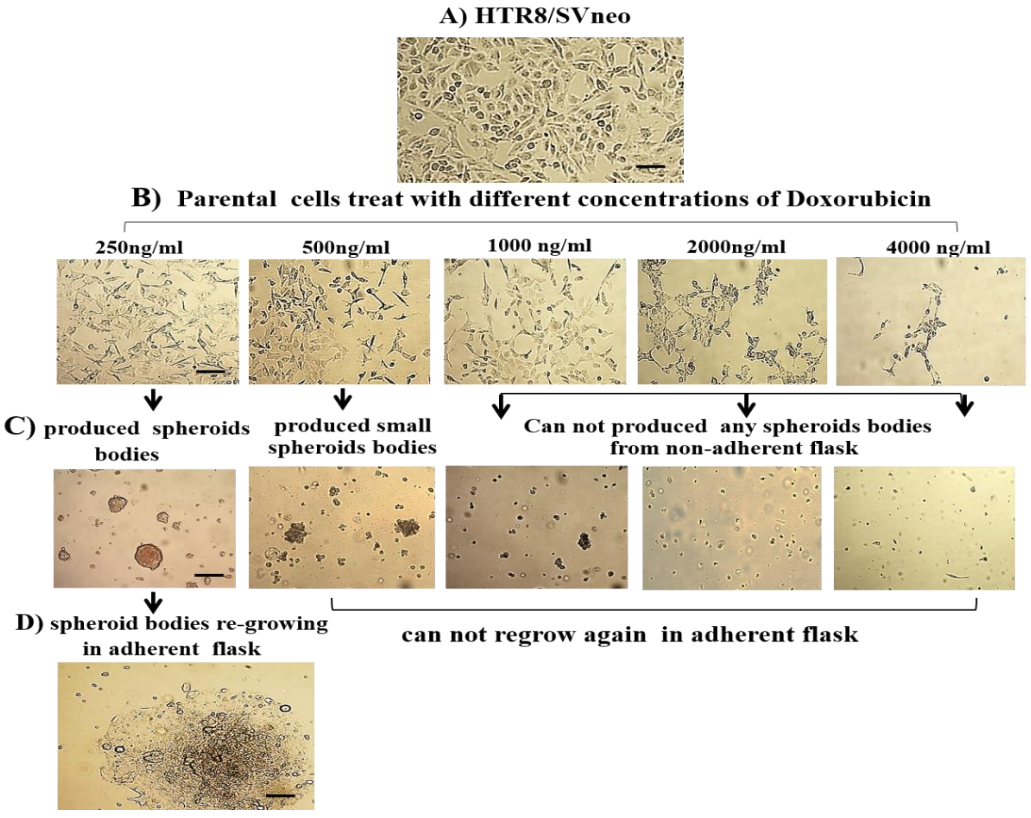

Figure 4.6: Generation of resistant spheroids from transformed trophoblast cell line (HTR8/SVneo).

Panel **A** shows HTR8/SVneo normal parental cells; Panel **B** shows parental cells after treatment with different concentrations of DOX. Panel **C** shows the ability of the cells to produce spheroid bodies from each concentration of DOX; Panel **D** shows the re-growth of the cells dispersed from spheroids onto adherent flasks under normal conditions. This was only observed in 250 ng/ml concentration of DOX. Scale bar= 100µm.

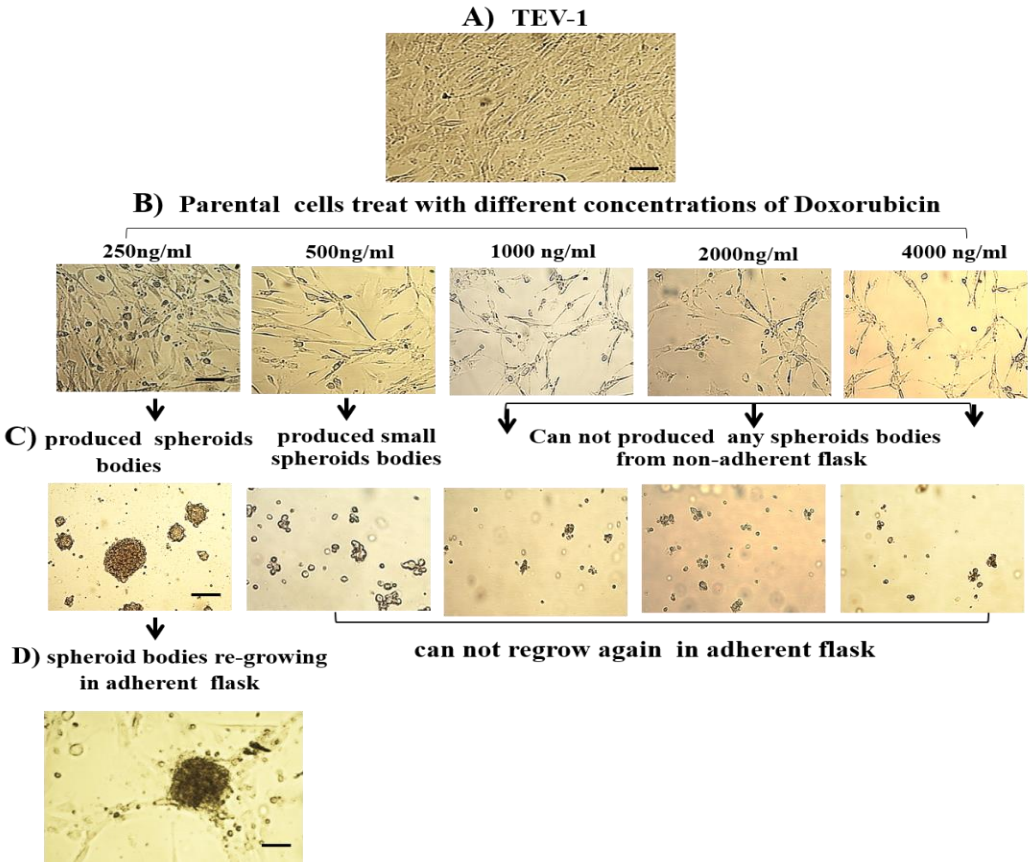

Figure 4. 2: Generation of resistant spheroids from transformed trophoblast cell line (TEV-1).

Panel **A** shows TEV-1 normal (parental cells); Panel **B** shows parental cells after treatment with different concentration of DOX. Panel **C** shows the ability of the cells to produce spheroid bodies from each concentration of DOX; Panel **D** shows the re-growth of the cells dispersed from spheroids onto adherent flasks under normal conditions. This was only observed in 250 ng/ml concentration of DOX. Scale bar= 100µm.

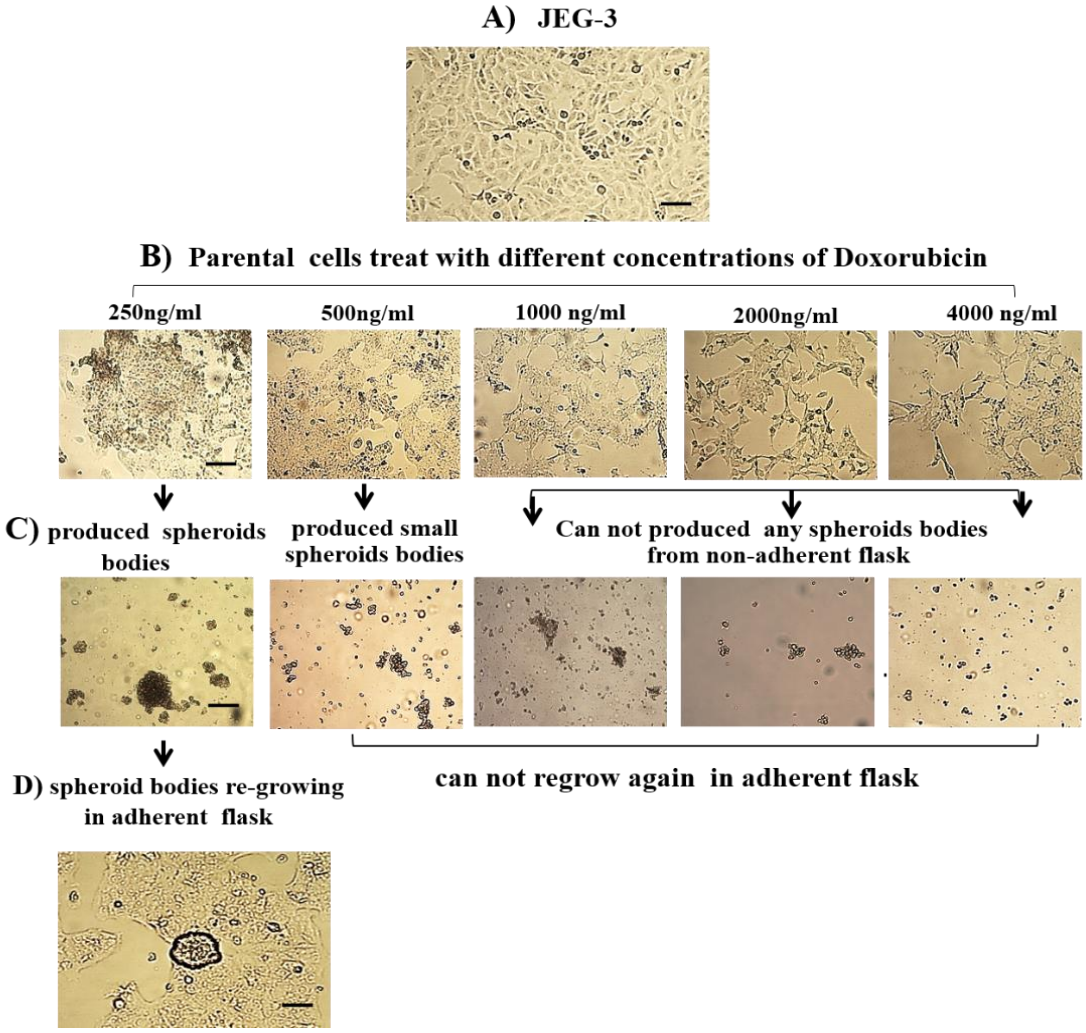

Figure 4. 3: Generation of resistant spheroids from choriocarcinoma cell line (JEG-3).

Panel **A** shows JEG-3 normal (parental cells); Panel **B** shows parental cells after treatment with different concentration of DOX. Panel **C** shows the ability of the cells to produce spheroid bodies from each concentration of DOX; Panel **D** shows the re-growth of the cells dispersed from spheroids onto adherent flasks under normal conditions. This was only observed in 250 ng/ml concentration of DOX. Scale bar= 100µm.

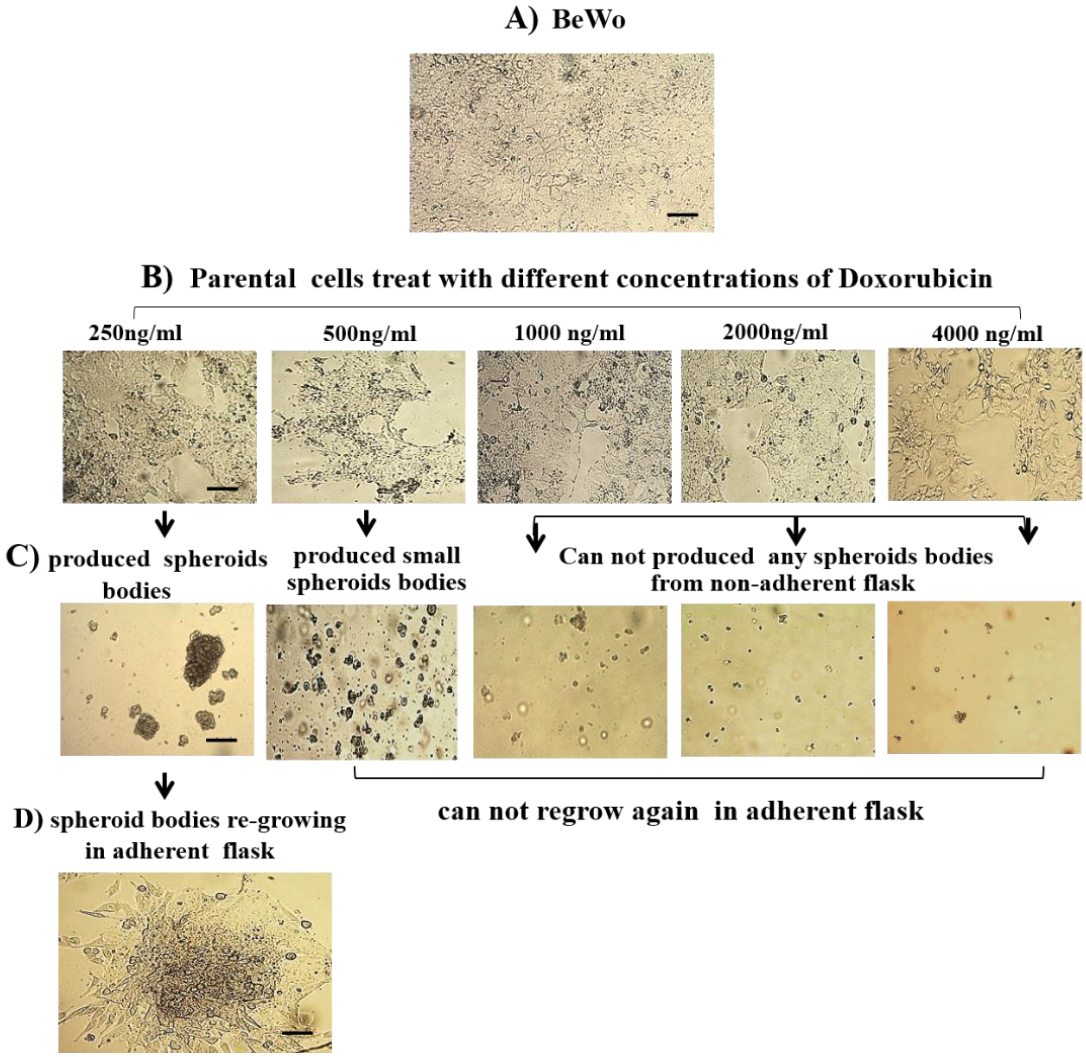

Figure 4. 4: Generation of resistant spheroids from choriocarcinoma cell line (BeWo).

Panel **A** shows BeWo normal (parental cells); Panel **B** shows parental cells after treatment with different concentration of DOX. Panel **C** shows the ability of the cells to produce spheroid bodies from each concentration of DOX; Panel **D** shows the re-growth of the cells dispersed from spheroids onto adherent flasks under normal conditions. This was only observed in 250 ng/ml concentration of DOX. Scale bar= 100µm.

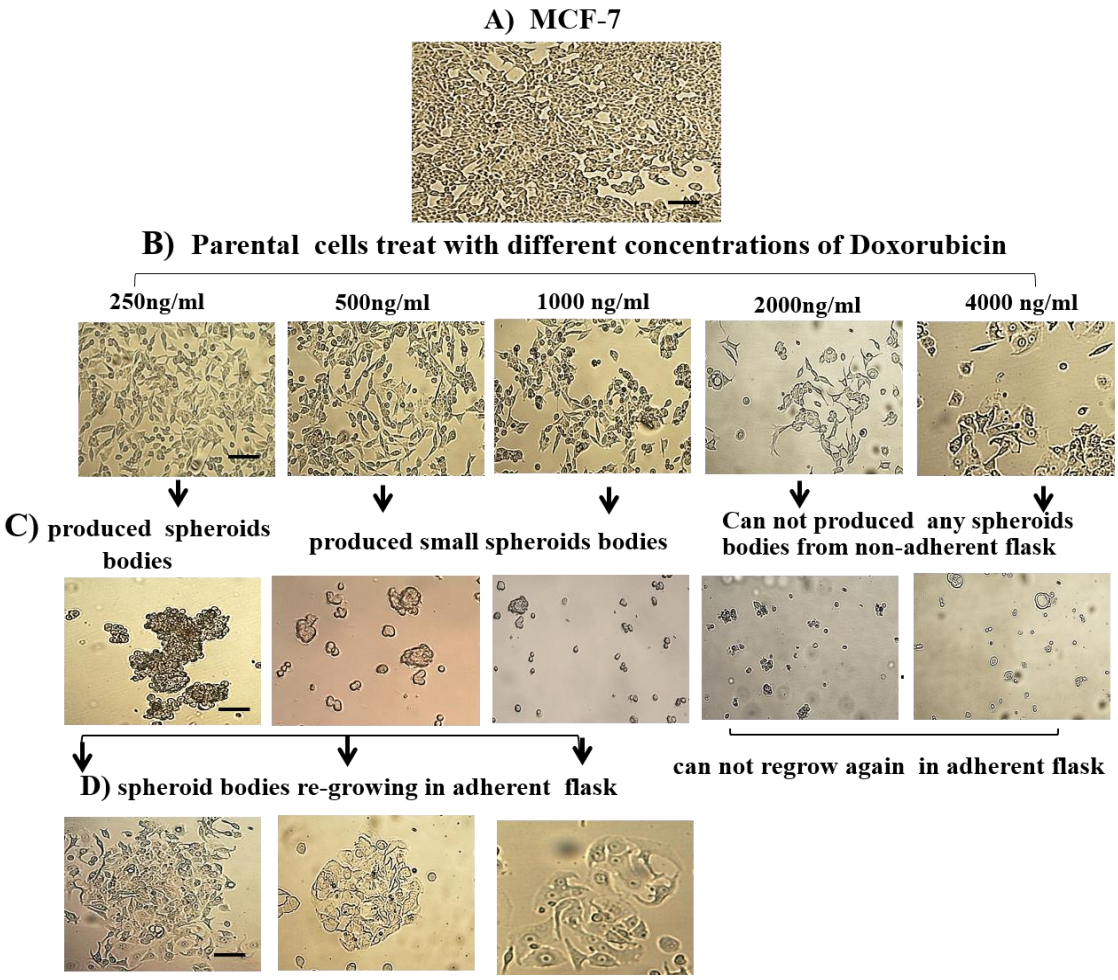

Figure 4.10: Generation of resistant spheroids from human breast adenocarcinoma cell line (MCF-7).

Panel **A** shows MCF-7 normal (parental cells); Panel **B** shows parental cells after treatment with different concentration of DOX. Panel **C** shows the ability of the cells to produce spheroid bodies from each concentration of DOX; Panel **D** shows spheroid bodies produced by treating with 250, 500 and 1000 ng/ml of DOX re-growing in an adherent flask under normal conditions while others cannot. Scale bar= 100µm.

4.2.4 Immunofluorescence staining of stem cell markers

As mentioned in Section 2.11.2, co-immunofluorescence staining was carried out in parental cells (with and without DOX treatment) and spheroids (non-resistant and DOX-resistant). The stem cell markers which were studied include: transcription factors (OCT4, SOX2 and NANOG), trophoblast transcription factor (CDX2), and NOTCH1 which is a receptor involved in regulating cell fate determination associated with both cancer stem cells and human embryonic stem cells.

4.2.4.1 Expression of OCT4 and SOX2 markers

As shown in Figure 4.11, Panel **I (**row **A),** HTR8/SVneo parental cells (both untreated and DOX-treated) showed positive green staining of OCT4. The perinuclear and cytoplasmic localization was clear on closer observation. Since spheroidal cells (untreated and DOX-treated) appear as aggregated cells, intracellular localisation was not distinctly visible. Figure 4.11, Panel **II (**row **A),** there was no staining of OCT4 in TEV-1 parental cells compared to spheroid (untreated and DOX-treated). However, TEV-1 parental and spheroidal cells showed positive red staining of SOX2 (Panel **II**; row **B**).

As for choriocarcinoma cells, there was no staining of OCT4 observed in parental cells in JEG-3 cell line [See Figure 4.12, Panel **I** (row **A**)], while BeWo parental cells showed a positive staining [See Figure 4.12, Panel **II** (row **A**)]. On the other hand, the staining for SOX2 was consistent in parental cells (both DOX-treated and un-treated) of JEG-3 and BeWo. The spheroids of both cell lines were positive to OCT4 and SOX2. However, the intracellular localization of these factors in spheroidal cells is not clear.

MCF-7 cells showed a similar results to the TEV-1 cell, there was no staining of OCT4 observed in the parental cells (untreated and DOX-treated). However, spheroidal (untreated and DOX-treated) cells of the same cell line showed clear staining of OCT4 [See Figure 4.13, Panel **I (**row **A)**]. Panel **II** (row **B**) from the same figure showed positive red staining for SOX2 of perinuclear and cytoplasm regions, which was clearly visible in parental cells compared to spheroidal cells.

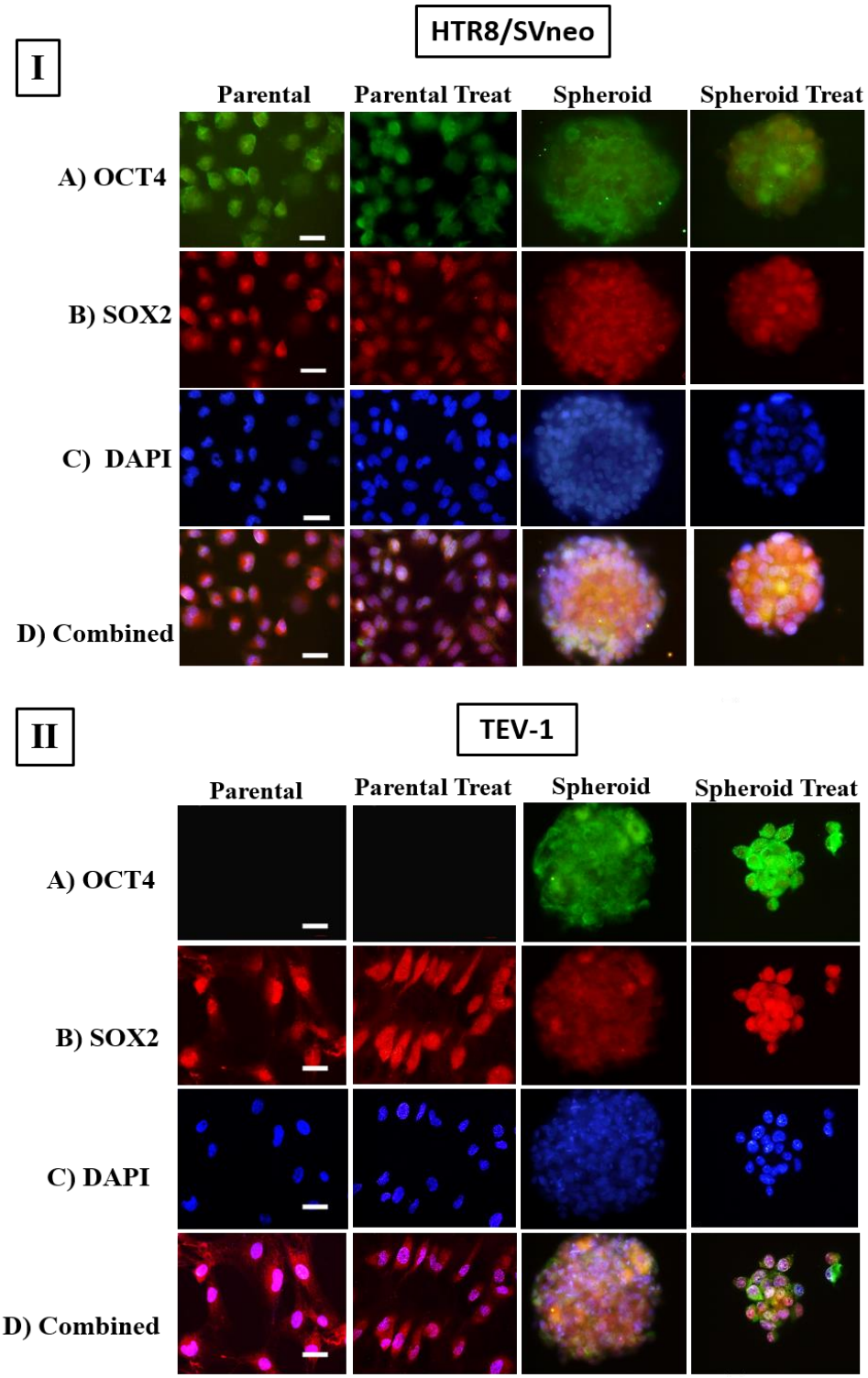

Figure 4.11: Immunofluorescence staining of OCT4 and SOX2 in transformed trophoblast cells.

Panel **I** and **II** shows immunofluorescence staining images for HTR8/SVneo and TEV-1 cells. Rows **A**, **B** and **C** show staining for OCT4, SOX2 and nuclear staining with DAPI respectively, in parental and spheroidal cells. Rows **D** show the three combined staining (OCT4+SOX2+DAPI) in parental cells and spheroidal cells. [Objective magnification=40X; Scale bar =50 µm].

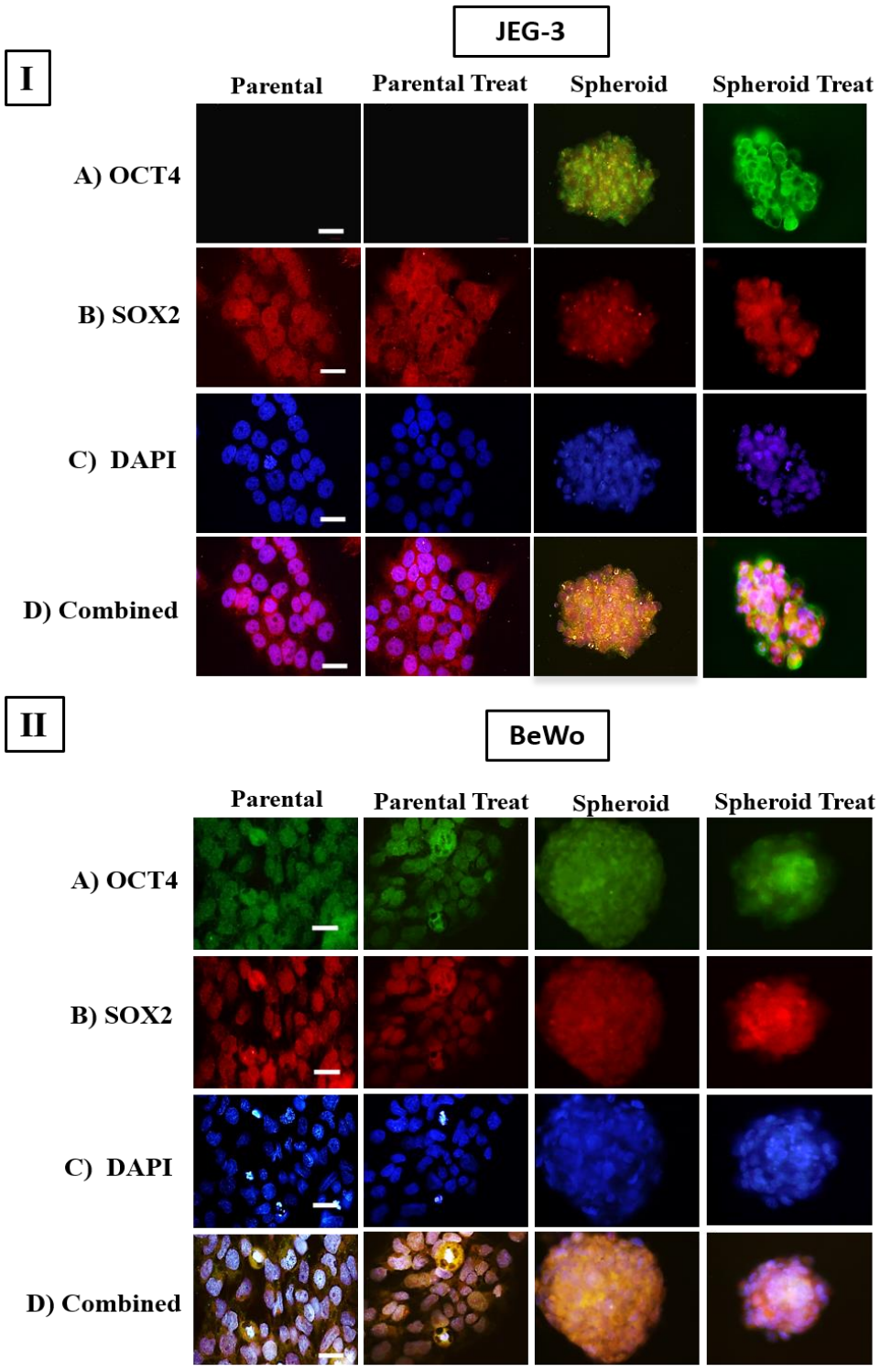

Figure 4.12: Immunofluorescence staining of OCT4 and SOX2 in choriocarcinoma cells.

Panel **I** and **II** shows immunofluorescence staining images for JEG-3 and BeWo cells. Rows **A**, **B** and **C** show staining for OCT4, SOX2 and nuclear staining with DAPI respectively, in parental and spheroidal cells. Rows **D** show the three combined staining (OCT4+SOX2+DAPI) in parental cells and spheroidal cells. [Objective magnification=40X; Scale bar =50 µm].

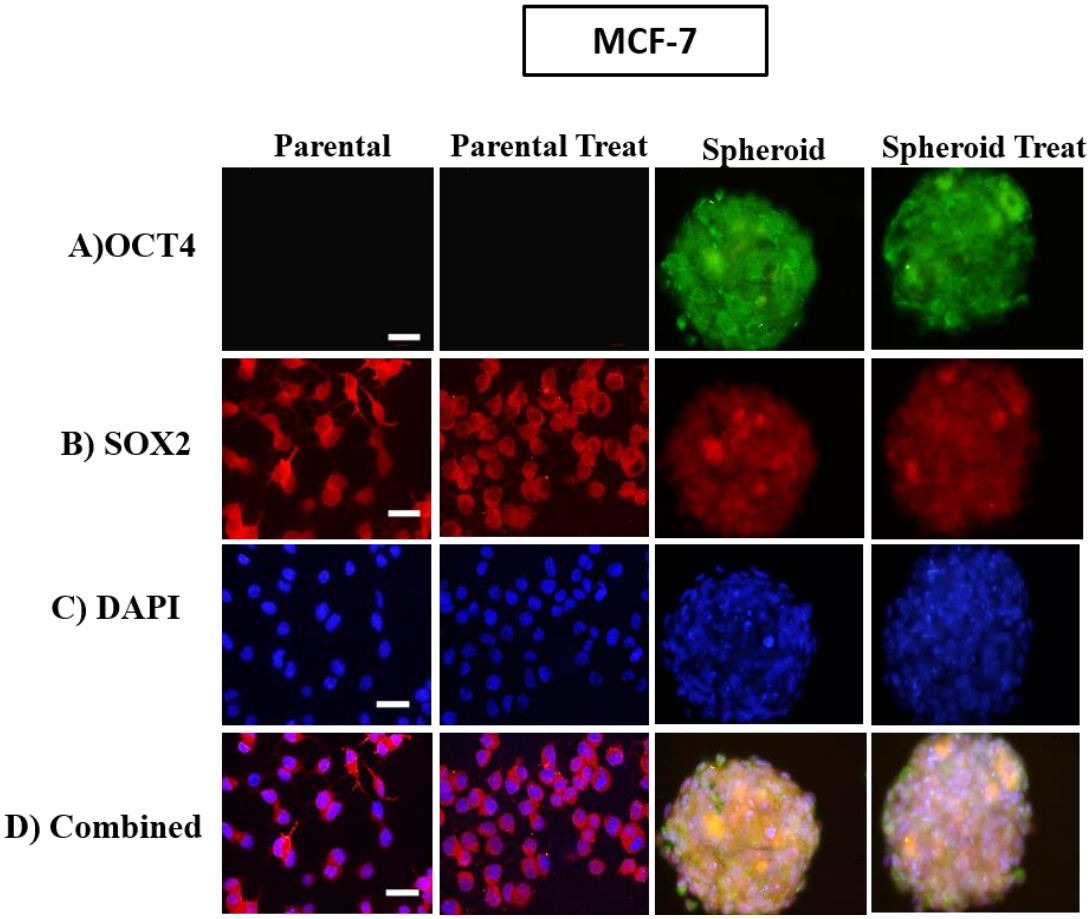

Figure 4.13: Immunofluorescence staining of OCT4 and SOX2 in MCF-7 cells.

Row **A** shows immunofluorescence staining images of OCT4 in MCF-7 cell. Row **B** shows immunofluorescence staining images of SOX2. Row **C** shows nuclear staining with DAPI and Row **D** shows two combined staining (SOX2+DAPI) in parental cells and three combined staining (OCT4+SOX2+DAPI) in spheroidal cells. [Objective magnification=40X; Scale bar =50 µm].

4.2.4.2 Expression of OCT4 and NANOG1 markers

The HTR8/SVneo parental cells (both untreated and DOX-treated) showed positive green staining of OCT4 in the perinuclear and cytoplasmic region. This intracellular localization was more distinct in parental cells when compared to spheroid cells due to cell aggregates [See Figure 4.14, Panel **I** (row **A**)]. On the other hand, Figure 4.14, Panel **II** (row **A**), showed that there was no staining of OCT4 observed in TEV-1 parental cells (untreated and DOX-treated), while clear staining of OCT4 was observed in the spheroid cells (untreated and DOX-treated). Moreover, Figure 4.14, Rows **B** in Panels **I** and **II**, showed positive red staining of NANOG in the perinuclear and cytoplasmic regions. This localization was clear in parental cells compared to spheroid cells from both HTR8/SVneo and TEV-1 cell lines.

There was no staining of OCT4 observed in JEG-3 parental cells (untreated and DOX-treated). However, spheroid cells (untreated and DOX-treated) of the same cell line showed clear staining of OCT4 [See Figure 4.15, Panel **I** (row **A)**]. In the case of BeWo cells, parental (both untreated and DOX-treated) cells showed positive green staining of OCT4 in the perinuclear and cytoplasmic regions. This intracellular localization was distinct in parental cells than in spheroidal cells. Figure 4.15, Panels **I** and **II** (row **B)** showed positive red staining of NANOG in the perinuclear and cytoplasmic regions which was clearly apparent in parental cells compared to spheroid cells from both JEG-3 and BeWo cell lines.

From Figure 4.16, Panel I (row **A)**, there was no staining of OCT4 observed in MCF-7 parental cells (untreated and DOX-treated). However, spheroid (untreated and DOX-treated) of the same cell line showed clear staining of OCT4. Row **B** from the same figure showed positive red staining of NANOG in perinuclear and cytoplasmic regions which was clearly apparent in parental cells compared to spheroid (untreated and DOX-treated) cells.

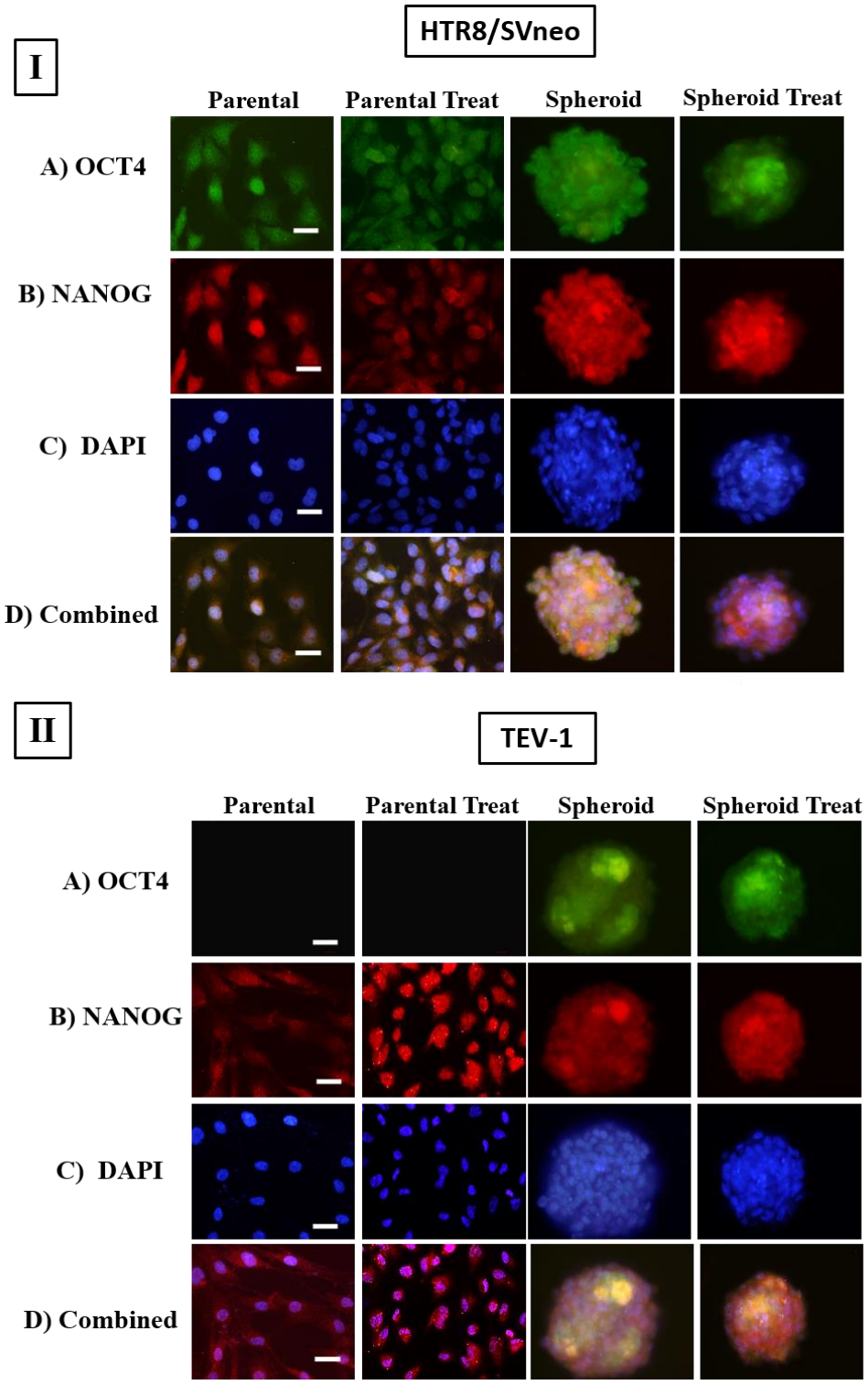

Figure 4.14: Immunofluorescence staining of OCT4 and NANOG in transformed trophoblast cells.

Panel **I** and **II** shows immunofluorescence staining images for HTR8/SVneo and TEV-1 cells. Rows **A**, **B** and **C** show staining for OCT4, NANOG and nuclear staining with DAPI respectively, in parental and spheroidal cells. Rows **D** show the three combined staining (OCT4+NANOG+DAPI) in parental cells and spheroidal cells. [Objective magnification=40X; Scale bar =50 µm].

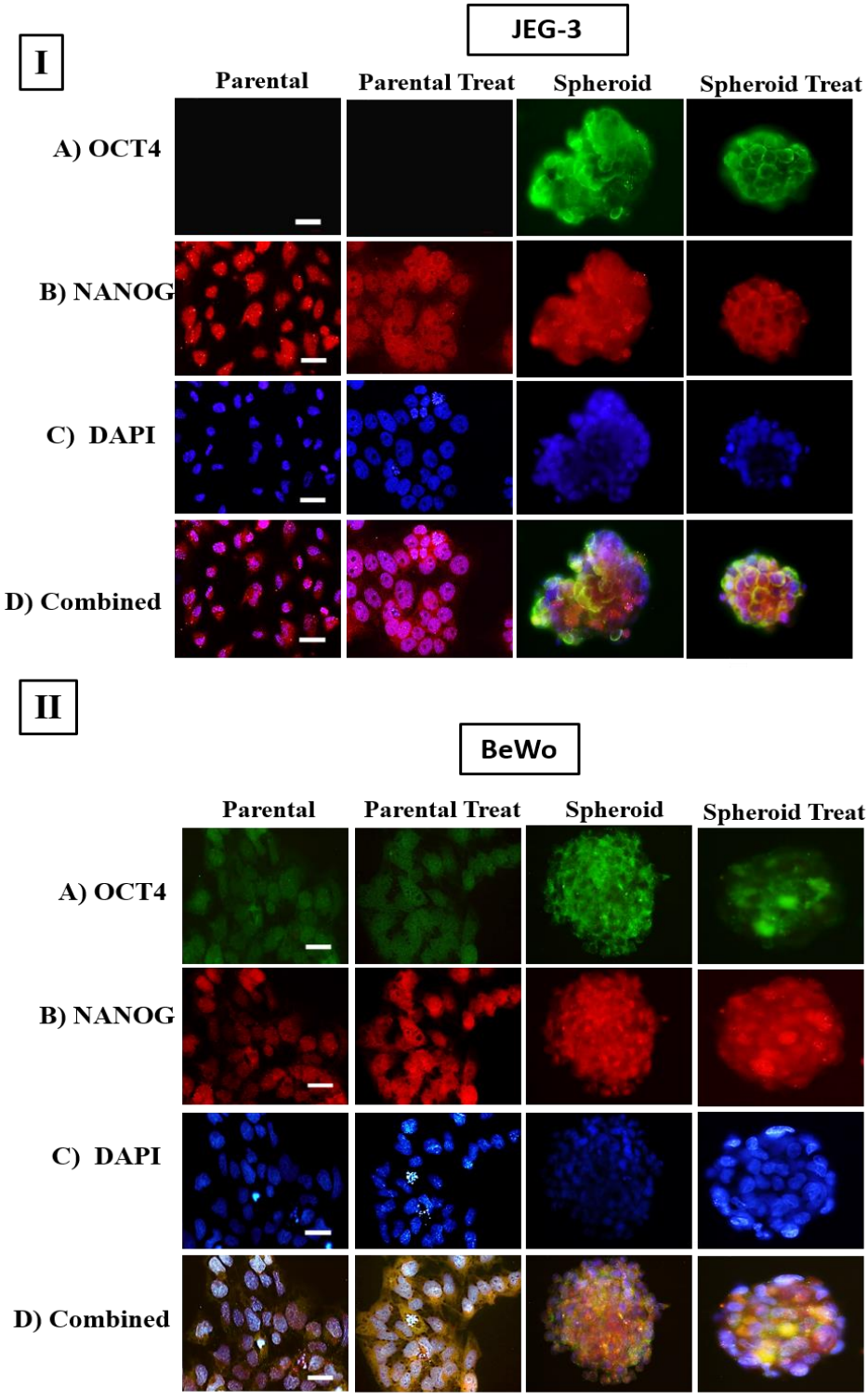

Figure 4.15: Immunofluorescence staining of OCT4 and NANOG in choriocarcinoma cell lines.

Panel **I** and **II** shows immunofluorescence staining images for JEG-3 and BeWo cells. Rows **A**, **B** and **C** show staining for OCT4, NANOG and nuclear staining with DAPI respectively, in parental and spheroidal cells. Rows **D** show the three combined staining (OCT4+NANOG+DAPI) in parental cells and spheroidal cells. [Objective magnification=40X; Scale bar =50 µm].

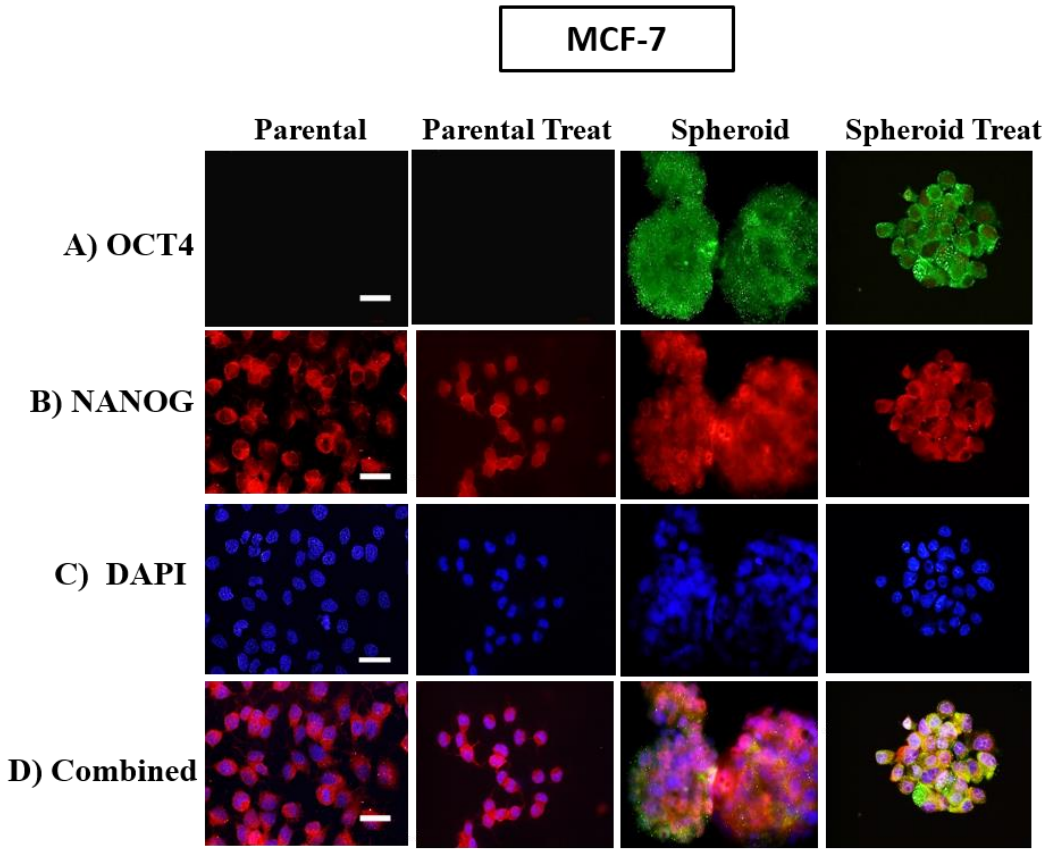

Figure 4.16: Immunofluorescence staining of OCT4 and NANOG in MCF-7 cells.

Row **A** shows immunofluorescence staining images of OCT4 in MCF-7 cell. Row **B** shows immunofluorescence staining images of NANOG. Row **C** shows nuclear staining with DAPI and Row **D** shows two combined staining (NANOG+DAPI) in parental cells and three combined staining (OCT4+NANOG+DAPI) in spheroidal cells. [Objective magnification= 40X; Scale bar =50 µm].

4.2.4.3 Expression of CDX2 and NOTCH1 markers

The transformed trophoblast parental cells, HTR8/SVneo and TEV-1, untreated and DOX-treated showed positive green staining of CDX2 within perinuclear and cytoplasmic regions. This intracellular localisation was distinct only in parental cells. On the other hand, there was no staining of CDX2 observed in spheroid untreated and DOX-treated from both HTR8/SVneo and TEV-1 cell lines [See Figure 4.17, Panels **I** and **II** (row **A**)]. From Panels **I** and **II** (row **B**) of Figure 4.17, clear red staining of NOTCH1 in perinuclear and cytoplasmic regions in parental cells than in spheroidal cells.

Both parental cells (untreated and DOX-treated) and spheroid (untreated and DOX-treated), from both placental choriocarcinoma cell lines (JEG-3 and BeWo) showed negative staining for CDX2 [See Figure 4.18, Panels **I** and **II** (row **A**)]. In contrast, Panels **I** and **II** (row **B**) in

Figure 4.18, showed there was a clear red staining of NOTCH1 in perinuclear and cytoplasmic regions. This was more apparent in parental cells than in spheroidal cells.

Both parental cells (untreated and DOX-treated) and spheroid (untreated and DOX-treated) derived from MCF-7, showed similar results as both trophoblast choriocarcinoma cells (JEG-3 and BeWo). There was no significant staining of CDX2 in all cell conditions [See Figure 4.19, Panel **I** (row **A**)]. On the other hand, (row **B**) from the same figure showed a clear red staining of NOTCH1 in perinuclear and cytoplasmic regions in parental cells. However, the localisation of NOTCH1 in spheroidal cells was not distinguishable.

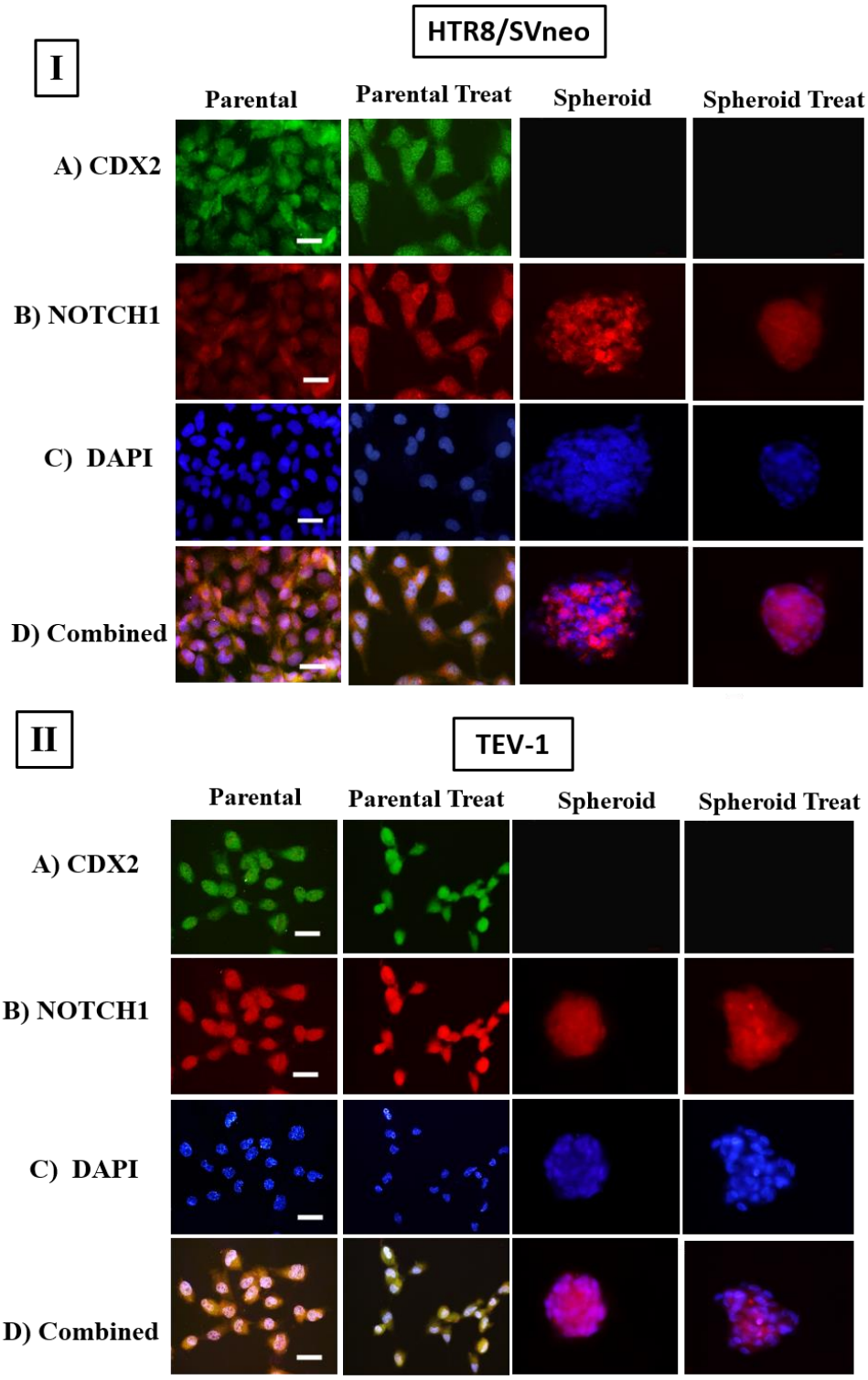

Figure 4.17: Immunofluorescence staining of CDX2 and NOTCH1 in transformed trophoblast cells.

Panel **I** and **II** shows immunofluorescence staining images for HTR8/SVneo and TEV-1 cells. Rows **A**, **B** and **C** show staining for CDX2, NOTCH1 and nuclear staining with DAPI respectively, in parental and spheroidal cells. Rows **D** show the three combined staining (CDX2+NOTCH1+DAPI) in parental cells and spheroidal cells. [Objective magnification=40X; Scale bar =50 µm].

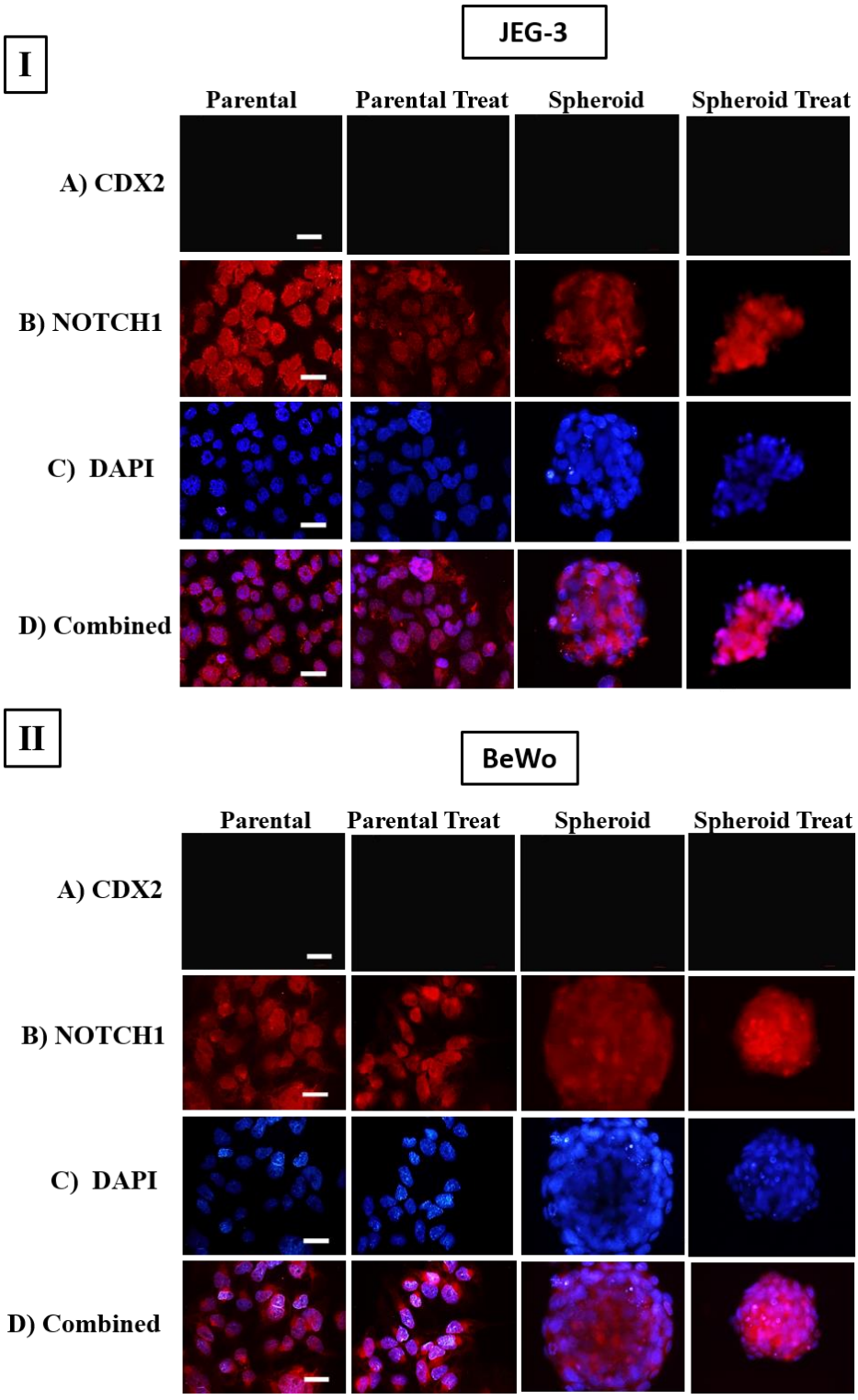

Figure 4.18: Immunofluorescence staining of CDX2 and NOTCH1 in choriocarcinoma cell lines.

Panel **I** and **II** shows immunofluorescence staining images for JEG-3 and BeWo cells. Rows **A**, **B** and **C** show staining for CDX2, NOTCH1 and nuclear staining with DAPI respectively, in parental and spheroidal cells. Rows **D** show the three combined staining (CDX2+NOTCH1+DAPI) in parental cells and spheroidal cells. [Objective magnification=40X; Scale bar =50 µm].

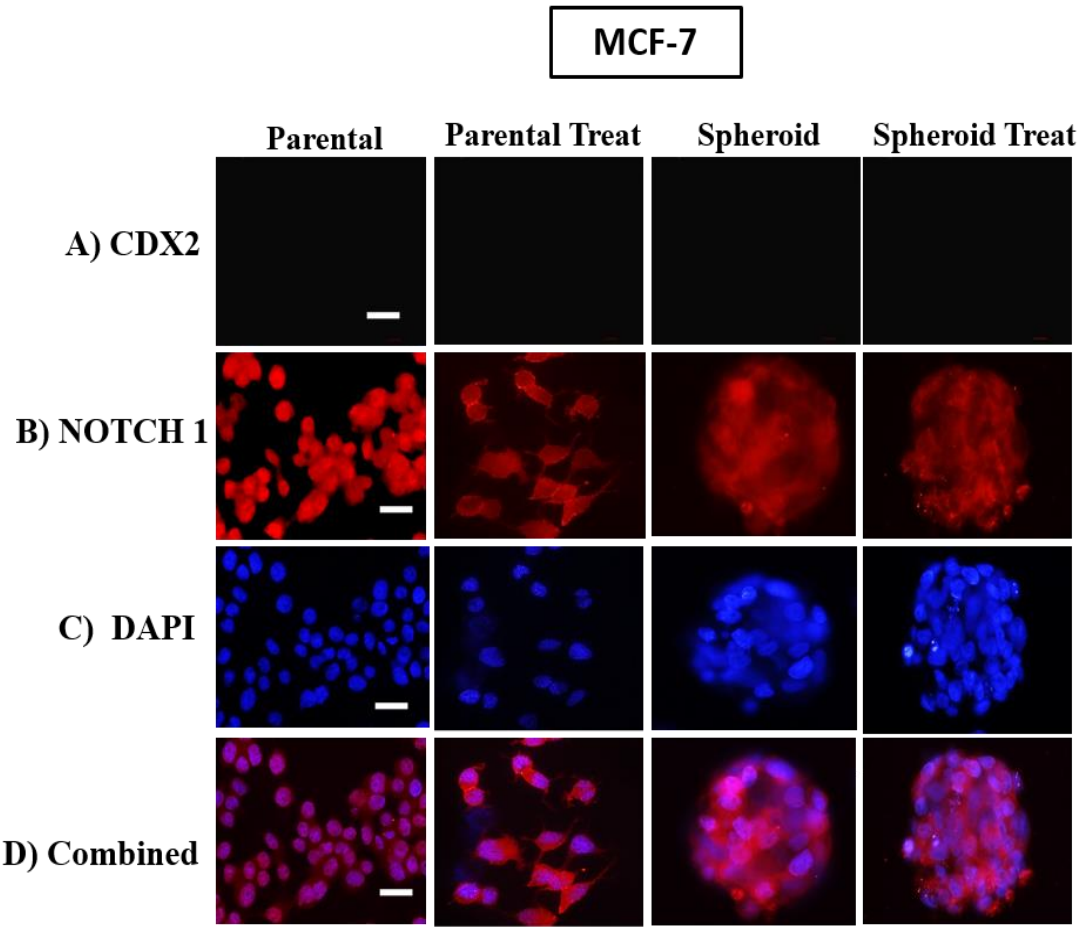

Figure 4.19: Immunofluorescence staining of CDX2 and NOTCH1 in MCF-7 cells.

Row **A** shows immunofluorescence staining images of CDX2 in MCF-7 cell. Row **B** shows immunofluorescence staining images of NOTCH1. Row **C** shows nuclear staining with DAPI and Row **D** shows two combined staining (NOTCH1+DAPI) in parental cells and spheroidal cells. [Objective magnification: 40X (scale bar =50 µm)].

4.2.5 Gene expression studies of stem cell markers

As explained in Section 2.9.3, the total RNA was extracted from HTR8/SVneo, TEV-1, JEG-3, BeWo and MCF-7 cell lines, and reverse transcribed to produce cDNA templates. The purity and integrity of RNA samples was high without any genomic DNA contamination, as indicated by the ratio of 260/280 nm which ranged in between 1.9-2.3. When the total RNA samples were subjected to electrophoresis in a 1% agarose gel two bright and clear bands were observed corresponding to 28S and 18S as shown in Appendix A.6.

Primers for all markers of interest were designed as mentioned in Section 2.6.1. The sequence details of each primer and the optimised annealing temperatures (T_a) are summarised in Table 4.2. The purity and the final product sizes of all PCR products were checked by agarose gel electrophoresis Appendix A.7. The accession numbers of stem cell markers used to design the primers are listed in Appendix A.8.

Table 4.1: The primers for specific markers and their annealing temperature (T_a).

Markers of Interest		Primers sequence (5' to 3')	Primer Length (nucleotides)	Annealing Temperature T_a (°C)
OCT4	Forward	AATTTGTTCCTGCAGTGCCC	20	**55**
	Reverse	CTCTCGTTGTGCATAGTCGC	20	
SOX2	Forward	CGGAAAACCAAGACGCTCAT	20	**55**
	Reverse	TTCATGTGCGCGTAACTGTC	20	
NANOG	Forward	CCATCCTGCAAATGTCTTCTG	21	**60.9**
	Reverse	CTTTGGGACTGGTGGAAGAAT	21	
CDX2	Forward	GGGAGGACTGGAATGGCTAC	20	**59.9**
	Reverse	CCCAGAAGCGCAGGAAGG	18	
NOTCH1	Forward	GGCGGTGCACACCTATTCTG	19	**58.2**
	Reverse	CAGGCGAGGAGTAGCTGTG	19	
Housekeeping genes				
GAPDH	Forward	ACCACCAACTGCTTAGCACC	20	**58**
	Reverse	CCATCCACAGTCTTCTGGGT	20	
HPRT1	Forward	TGACACTGGCAAAACAATGCA	21	**55**
	Reverse	GGTCCTTTTCACCAGCAAGCT	21	
TBP1	Forward	TGCACAGGAGCCAAGAGTGAA	21	**56**
	Reverse	CACATCACAGCTCCCCACCA	20	

4.2.5.1 Relative mRNA expression of stem cells markers in trophoblast and tumour cell lines

Following the qualitative immunofluorescence study, the relative expressions of stemness and trophoblast markers were checked by comparing the mRNA (qRT-PCR) and protein (western blotting) expression in different conditions. The mRNA expression was compared between: (a) untreated parental versus DOX-treated parental, (b) untreated parental versus untreated spheroid, (c) untreated spheroids versus DOX-treated spheroids and (d) DOX-treated parental versus DOX-treated spheroids. Statistical significant was determined by a one-way ANOVA followed by Tukey's test for multiple comparisons between these different conditions.

- **OCT4**

HTR8/SVneo showed a significant up-regulation of OCT4 mRNA expression level in both sets of comparison (a) untreated parental versus DOX-treated parental, and (b) untreated parental versus untreated spheroids. TEV-1 cells lines showed similar results to HTR8/SVneo (See Figure 4.20, Panels **A** and **B**). On the other hand, the mRNA expression of OCT4 in the first choriocarcinoma cells (JEG-3) was significantly down-regulated in untreated parental cells in comparison with spheroidal cell ($p<0.001$). Likewise, DOX-treated parental showed down-regulation in OCT4 expression in comparison with respective spheroidal cells ($p<0.01$) (See Figure 4.20, Panel **C**). In the second choriocarcinoma cell line (BeWo), the mRNA expression of OCT4 was significantly up-regulated in DOX-treated spheroidal cells compared to both untreated spheroids ($p<0.05$) and DOX- treated parental cells ($p<0.01$) (See Figure 4.20, Panel **D**). The untreated spheroids of MCF-7 have shown a significant up-regulation relative to all other cell populations ($p<0.0001$) (See Figure 4.20, Panels **E**).

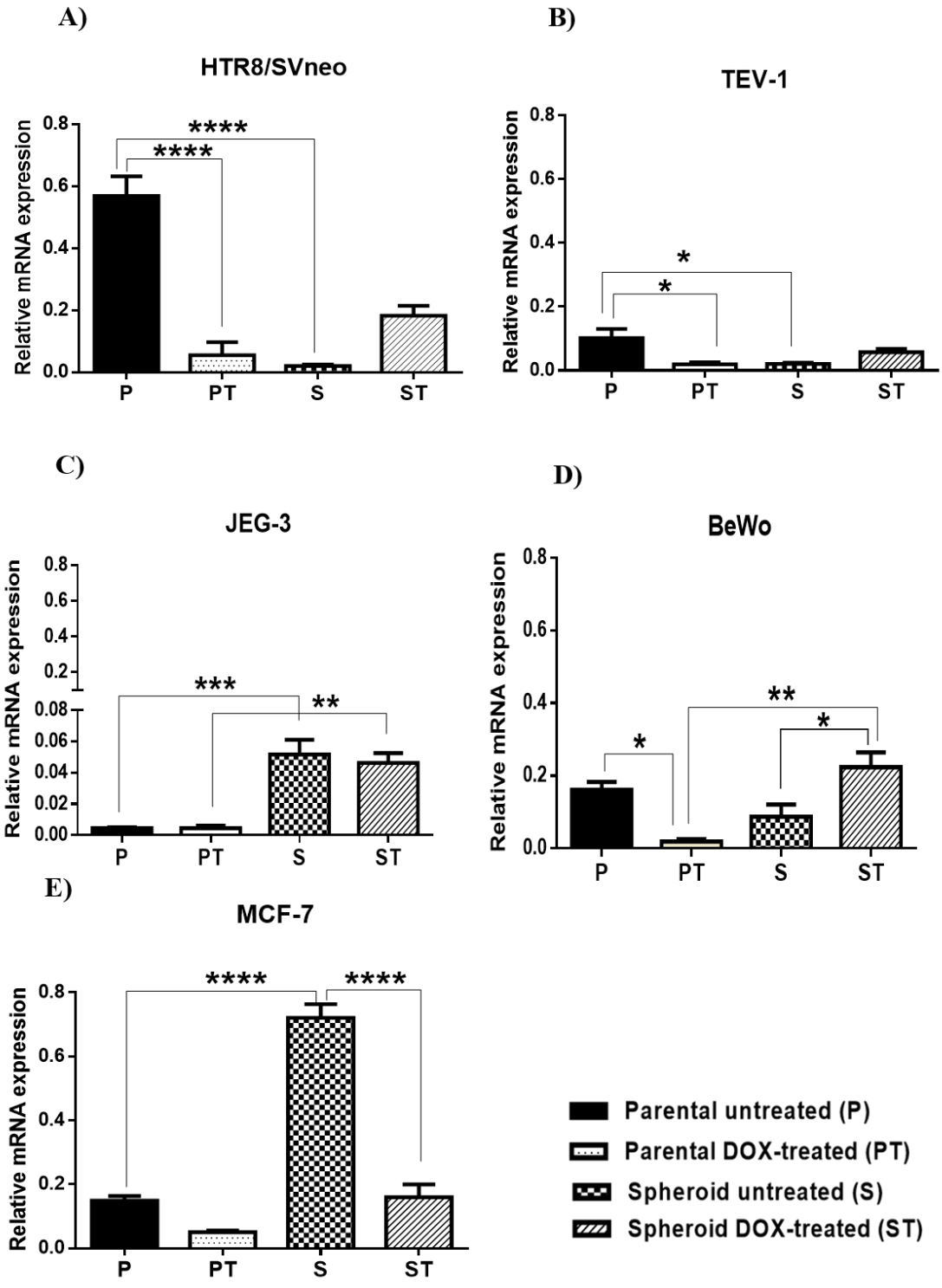

Figure 4.20: Relative mRNA expression of OCT4 in trophoblast and tumour cells.

The relative mRNA expression of OCT4 was compared between different conditions. The data from HTR8/SVneo and TEV-1 cells are given in panels **A** and **B** respectively. Likewise, data for JEG-3 and BeWo cells are presented in panels **C** and **D** respectively. Panel **E** shows the data from MCF-7 cells. Statistical significance was determined using a one-way ANOVA followed by Tukey's test for multiple comparisons. Data represent the mean ±SEM of three individual experiments, each performed in triplicate (****$p<0.0001$; ***$p<0.001$; **$p<0.01$; *$p<0.05$).

- **SOX2**

As can be observed from Figure 4.21, Panel **A**, there was no statistically significant difference in the relative expressions of SOX2 between all comparisons in HTR8/SVneo cells. However, a significant up-regulation of SOX2 mRNA expression was seen in TEV-1 between untreated spheroids and DOX-treated spheroids ($p<0.01$) (See Figure 4.21, Panel **B**). From Figure 4.21, panel **C**, JEG-3 cells showed significant up-regulation of SOX2 mRNA expression level of DOX-treated spheroids, in comparison with DOX-treated parental cells and untreated spheroids ($p<0.0001$). It was also observed that SOX2 mRNA expression in BeWo cells was significantly higher in untreated spheroidal cells, in comparison to both untreated parental cells and DOX-treated spheroids ($p<0.0001$) (See Figure 4.21, Panel **E**). As for MCF-7 cells, the mRNA expression level of SOX2 in untreated spheroidal cells was significantly higher than the untreated parental cells ($p<0.001$) (See Figure 4.21, Panel **F**).

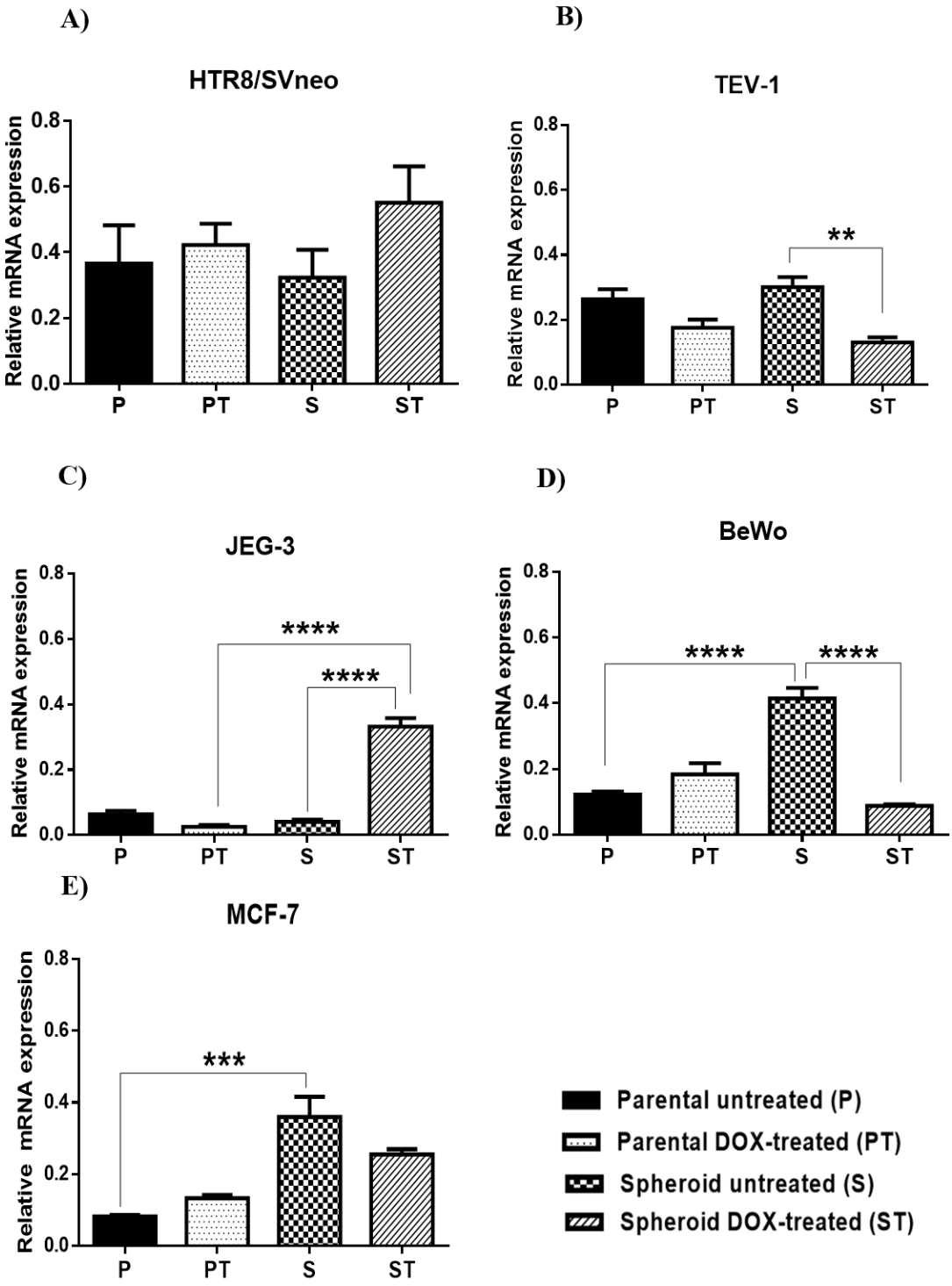

Figure 4.21: Relative mRNA expression of SOX2 in trophoblast and tumour cells.

The relative mRNA expression of SOX2 was compared between different conditions. The data from HTR8/SVneo and TEV-1 cells are given in panels **A** and **B** respectively. Likewise, the data for JEG-3 and BeWo cells are presented in panels **C** and **D** respectively. Panel **E** shows the data from MCF-7 cells. Statistical significance was determined using a one-way ANOVA followed by Tukey's test for multiple comparisons. Data represent the mean ±SEM of three individual experiments, each performed in triplicate (****$p<0.0001$; ***$p<0.001$; **$p<0.01$).

- **NANOG**

As seen in Figure 4.22, Panel **A**, DOX-treated parental HTR8/SVneo cells showed a significantly lower level of NANOG compared to untreated parental cells ($p<0.001$) and DOX-treated spheroidal cells ($p<0.0001$). Interestingly, in TEV-1 cells both DOX-treated parental and spheroids cells have shown a significant down-regulation in the NANOG mRNA expressions compared to their respective untreated cells (See Figure 4.22, Panel **B**). In contrast, JEG-3 showed a significant up-regulation of NANOG mRNA in untreated parental cells compared to DOX-treated parental cells ($p<0.001$) and spheroids ($p<0.05$). In the case of BeWo cells, the untreated parental cells showed a significant down-regulation of NANOG mRNA expression compared to (a) DOX-treated parental cells ($p<0.01$) and (b) spheroidal cells ($p<0.01$) (See Figure 4.22, Panels **C** and **D**).

In the MCF-7 cells, the overall mRNA expression levels of NANOG in untreated spheroids cells was found to be up-regulated in comparison with all other conditions types of this cells ($p<0.0001$) (See Figure 4.22, Panels **E**).

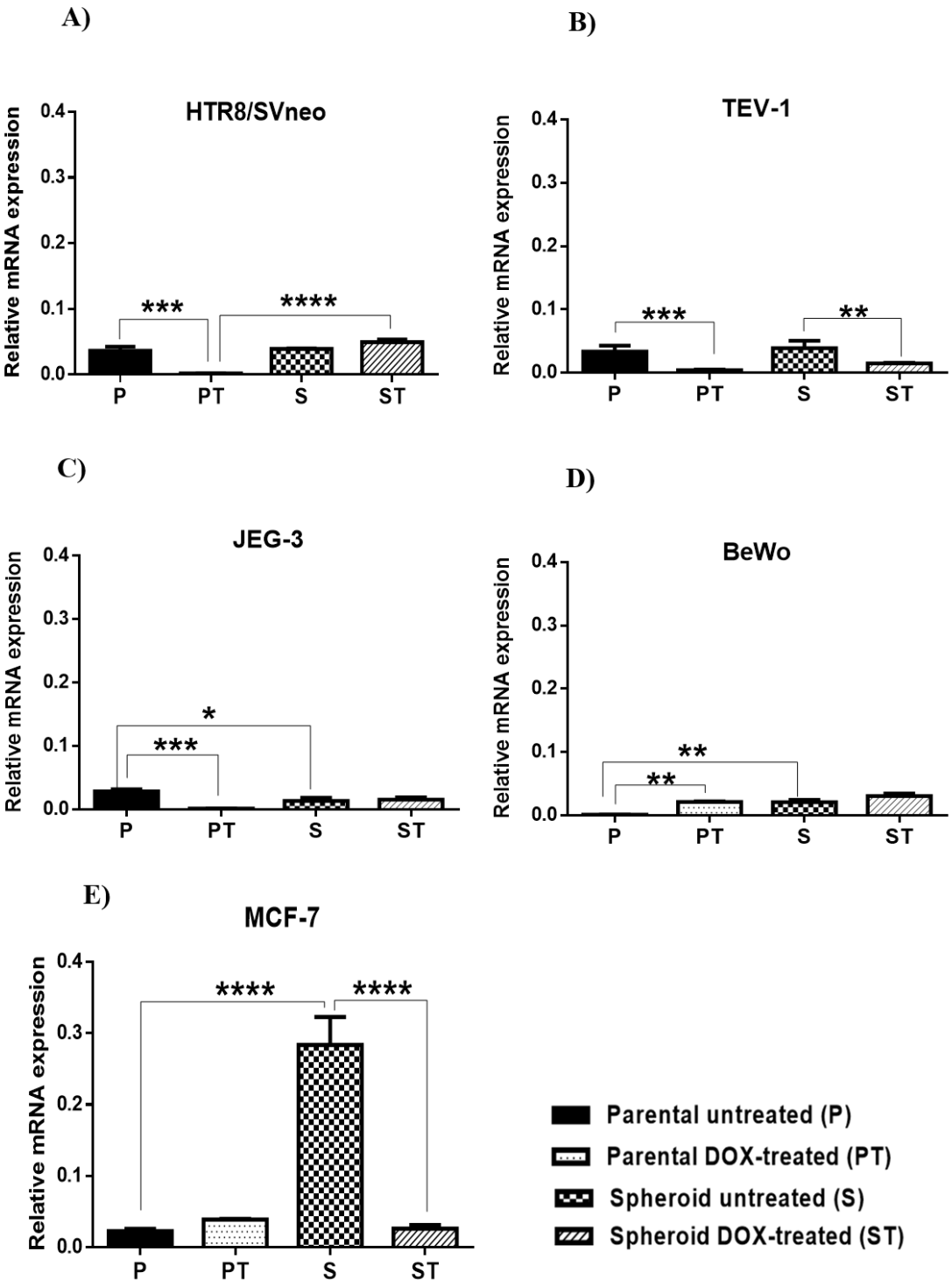

Figure 4.22: Relative mRNA expression of NANOG in trophoblast and tumour cells.

The relative in mRNA expression of NANOG was compared between different conditions. The data from HTR8/SVneo and TEV-1 cells are given in panels **A** and **B** respectively. Likewise, the data for JEG-3 and BeWo cells are presented in panels **C** and **D** respectively. Panel **E** shows the data from MCF-7 cells. Statistical significance was determined using a one-way ANOVA followed by Tukey's test for multiple comparisons. Data represent the mean ±SEM of three individual experiments, each performed in triplicate (****$p<0.0001$; ***$p<0.001$; **$p<0.01$; *$p<0.05$).

- **CDX2**

The first transformed trophoblast cell line, HTR8/SVneo, showed a significantly higher level of CDX2 mRNA expression in untreated parental compared to (a) DOX-treated parental ($p<0.01$); and (b) spheroidal cells ($p<0.001$). There was also a significant difference in DOX-treated spheroids compared to untreated spheroids ($p<0.001$) (See Figure 4.23, Panel **A**). The second transformed trophoblast cell line, TEV-1, showed a significantly higher level of CDX2 mRNA expressions in untreated parental compared to (a) DOX- treated parental ($p<0.001$); and (b) spheroidal cells ($p<0.01$). There was also a significant difference in untreated spheroids compared to DOX-treated spheroids ($*p<0.05$) (See Figure 4.23, Panel **B**).

Interestingly, both choriocarcinoma cell lines showed similar results to transformed trophoblast cell lines in untreated parental compared to (a) DOX-treated parental; and (b) spheroidal cells ($p<0.001$) (See Figure 4.23, Panel **C** and **D**).

Likewise, in MCF-7 cells there was a significant up-regulation of CDX2 mRNA expressions in untreated parental cells compared to untreated spheroids ($p<0.001$); and in DOX-treated parental cells in comparison to DOX-treated spheroids ($p<0.01$) (See Figure 4.23, Panel **E**).

Overall, there is a significant down-regulation of the mRNA expression of CDX2 in spheroid cells condition when compared with the parental cells conditions in four trophoblast and tumour cell lines.

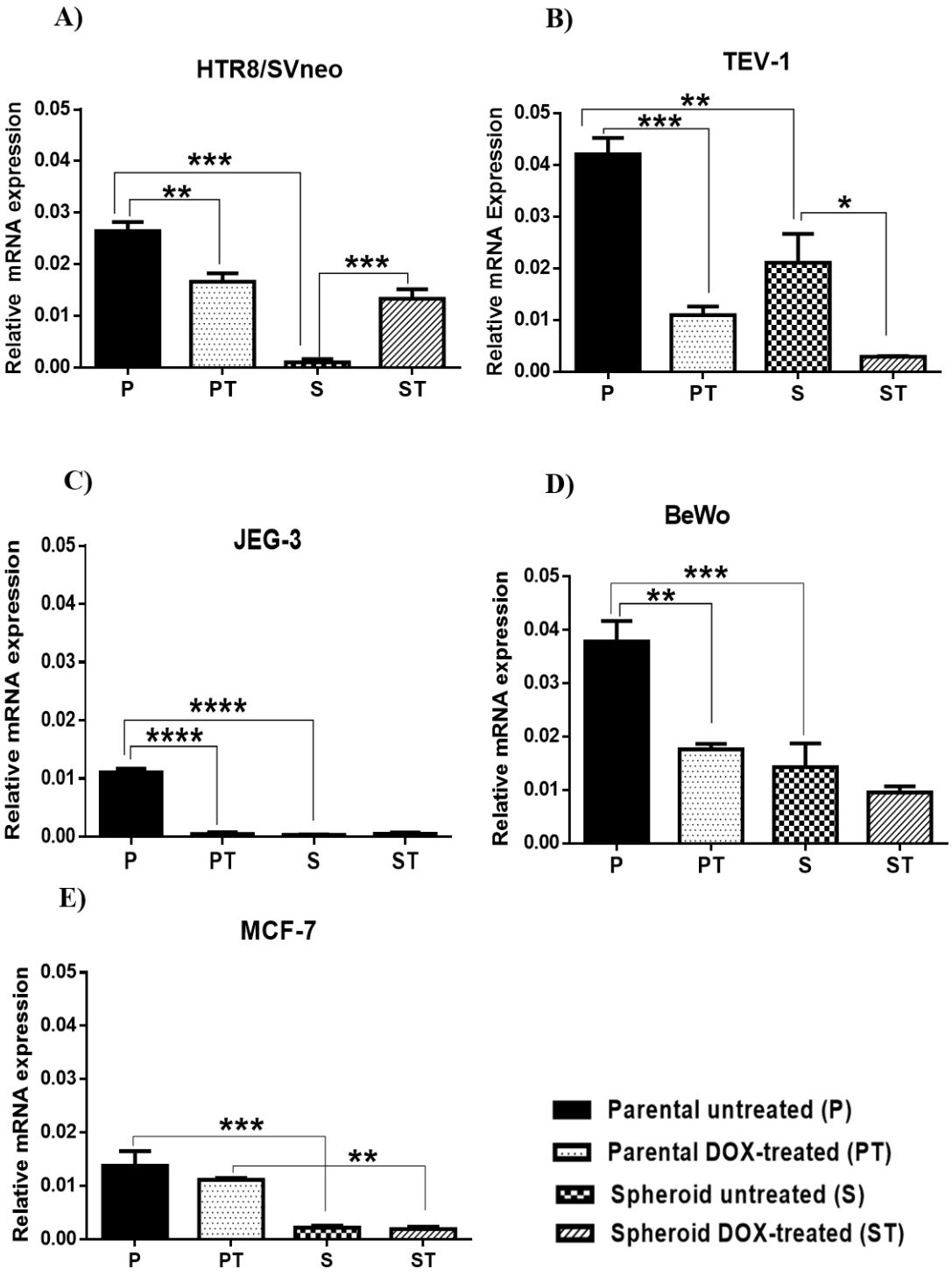

Figure 4.23: Relative mRNA expression of CDX2 in trophoblast and tumour cells.

The relative mRNA expression of CDX2 was compared between different conditions. The data from HTR8/SVneo and TEV-1 cells are given in panels **A** and **B** respectively. Likewise, the data for JEG-3 and BeWo cells are presented in panels **C** and **D** respectively. Panel **E** shows the data from MCF-7 cell. Statistical significance was determined using a one-way ANOVA followed by Tukey's test for multiple comparisons. Data represent the mean ±SEM of three individual experiments, each performed in triplicate (****$p<0.0001$; ***$p<0.001$; **$p<0.01$; *$p<0.05$).

- **NOTCH1**

HTR8/SVneo showed the mRNA expression of NOTCH1 was statistically increased in untreated parental cells compared to (a) DOX-treated parental ($p<0.001$) and (b) spheroidal cells ($p<0.0001$) (See Figure 4.24, Panel **A**). TEV-1 cells showed a significantly higher level of NOTCH1 mRNA expression in DOX-treated parental cells compared to (a) untreated parental cells ($p<0.05$) and (b) DOX-treated spheroids cells ($p<0.0001$). A significant difference in NOTCH1 expression was also observed between untreated parental cells when compared to untreated spheroids ($p<0.05$) (See Figure 4.24, Panel **B**).

In JEG-3 cells, no statistically significant difference in the relative expression of NOTCH1 was observed in any comparisons (See Figure 4.24, Panel **C**). However, the mRNA expression of NOTCH1 level in BeWo cells was significantly higher in (a) untreated parental cells when compared to spheroidal cells, and (b) DOX-treated parental cells compared to DOX-treated spheroidal cells ($p<0.0001$) (See Figure 4.24, Panel **D**). As seen from Figure 4.24, panel **E**, the relative mRNA expression level of NOTCH1 in MCF-7 was higher in untreated parental cells compared to DOX-treated parental cells and untreated spheroids ($p<0.0001$) (see Figure 4.24, Panel **E)**.

In general, there was a significant down-regulation of the mRNA expression of NOTCH1 in HTR8/SVneo, TEV-1, BeWo and MCF-7 cells under untreated and DOX-treated spheroidal cell conditions when compared with the parental cell conditions.

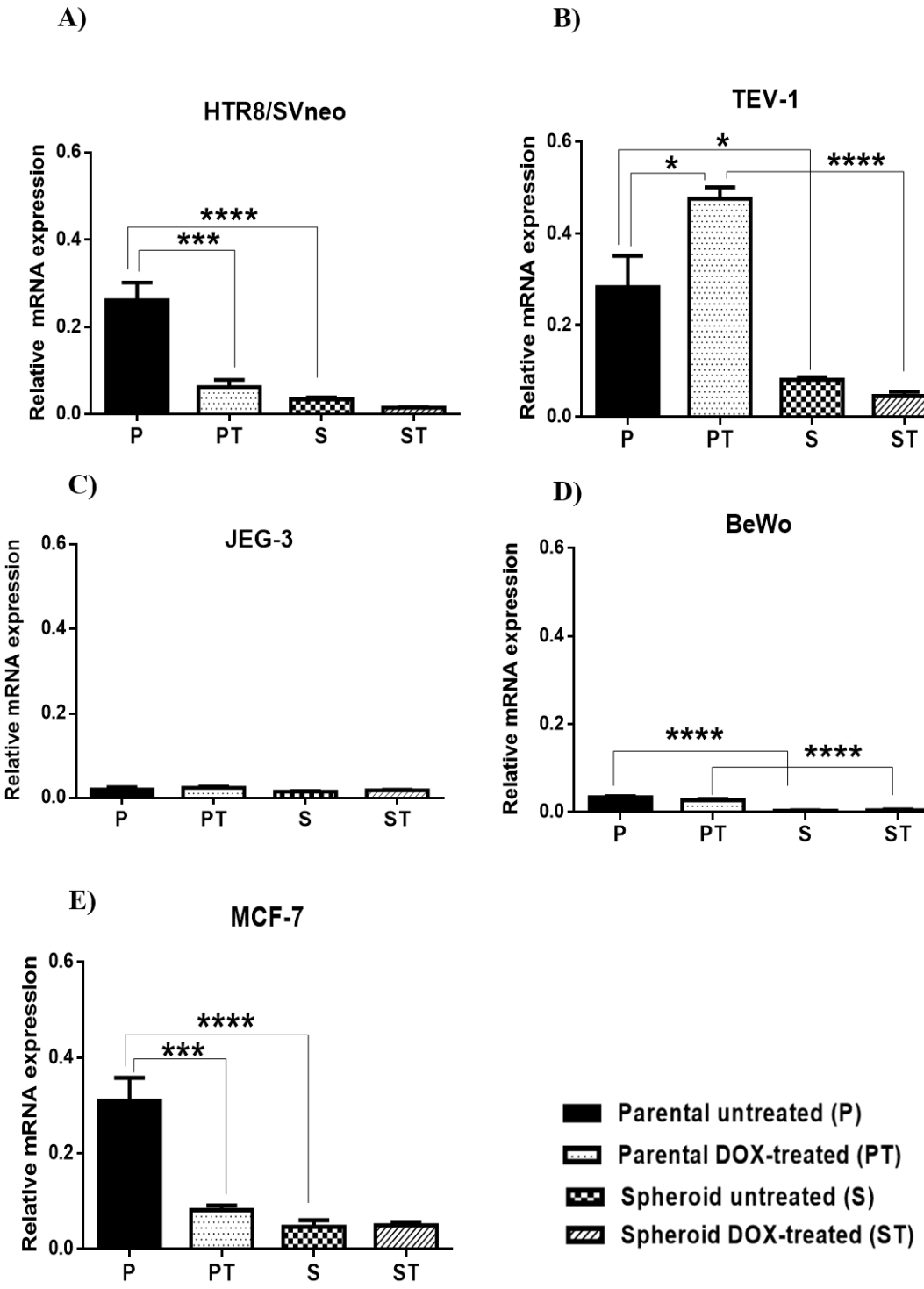

Figure 4.24: Relative mRNA expression of NOTCH1 in trophoblast and tumour cells.

The relative mRNA expression of NOTCH1 was compared between different conditions. The data from HTR8/SVneo and TEV-1 cells are given in panels **A** and **B** respectively. Likewise, the data for JEG-3 and BeWo cells are presented in panels **C** and **D** respectively. Panel **E** shows the data from MCF-7cell. Statistical significance was determined using a one-way ANOVA followed by Tukey's test for multiple comparisons. Data represent the mean ±SEM of three individual experiments, each performed in triplicate (****$p<0.0001$; ***$p<0.001$; *$p<0.05$).

4.2.6 Protein expression of stem cell markers

The relative protein expression was compared between: (a) untreated parental versus DOX-treated parental, (b) untreated parental versus untreated spheroid, (c) untreated spheroids versus DOX-treated spheroids, and (d) DOX-treated parental versus DOX-treated spheroids. The data were analysed using a one-way ANOVA followed by Tukey's post-hoc test for multiple comparisons. The equal amount of protein samples (30µg) from trophoblast and tumour cells were loaded onto the gel, as confirmed by the internal controls β-actin on the same blots. Specific positive controls were used for each factor as suggested by the antibody providers. Caco2 cells were used as a positive control for OCT4, NANOG and CDX2. While MCF-7 cell lines were used as positive control for NOTCH1 and SOX2. A lower level of the positive control (20µg) was loaded to avoid over-saturation of the blot. Protein expression levels were normalised using the housekeeping protein β-actin levels as an internal control.

4.2.6.1 Protein expression of OCT4

The OCT4 antibody produced a single band in spheroidal and parental (DOX-treated and untreated) samples in trophoblast cell lines, MCF-7 and the recommended positive control (Caco2 cell line). The detected bands were at 45 kDa which was within the predicted range for the protein (See Figure 4.25, Panel **A**). In contrast to mRNA expression, a significant increase in protein expression of OCT4 was observed in both HTR8/SVneo and TEV-1 spheroidal cells (untreated and DOX-treated) compared to their parental cell counterparts (see Figure 4.25, Panel **B** and **C**). In JEG-3 cells, both DOX-treated parental and untreated spheroids, showed a significant increase in OCT4 expression compared to untreated parental cells ($p<0.01$) (Figure 4.25, Panel **D**). However, the mRNA and protein expression were in agreement only in parental cells compared to untreated spheroids. From Figure 4.25, Panel **E**, a significant increase in protein expression of OCT4 was observed in BeWo cells between untreated parental with DOX-treated parental cells ($p<0.05$), and DOX-treated spheroids with DOX-treated parental cells ($p<0.001$). Interestingly, these differences in expression were also observed in mRNA expression (See Figure 4.20, Panel **D**). In MCF-7 cells (Figure 4.25, Panel **F**) the OCT4 protein expression was significantly different in untreated parental cells compared to (a) DOX-treated parental cells ($p<0.01$) and (b) untreated spheroids **(**$p<0.05$**)**. Likewise, only the OCT4 protein expression in DOX-treated spheroids was significantly higher than that of DOX-treated parental cells **(**$p<0.01$**)**. In summary, the expression of OCT4 protein in four trophoblast cell lines and MCF-7 tumour cell was significantly increased in untreated and DOX-treated spheroids cells compared to parental cells conditions.

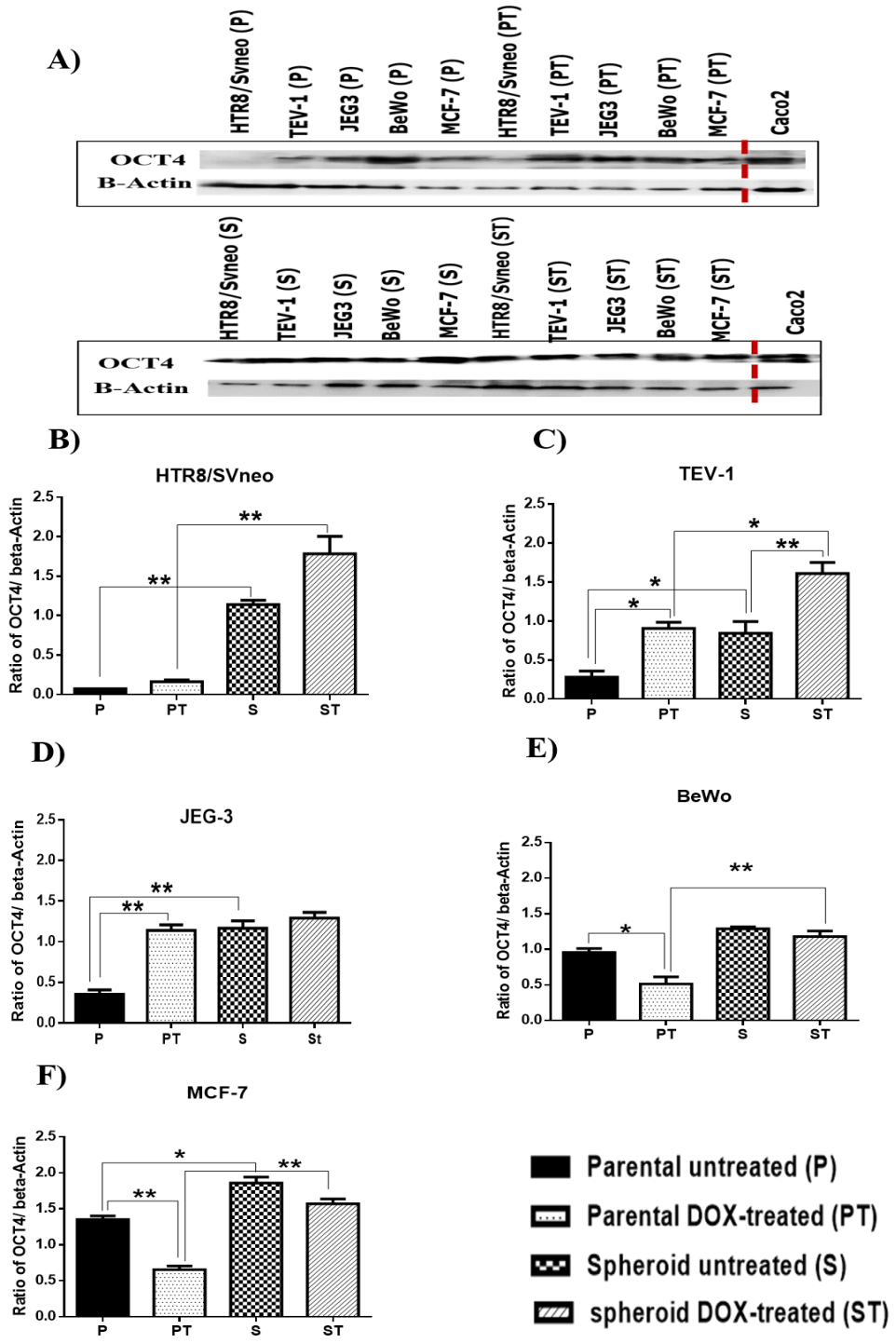

Figure 4.25: The expression of OCT4 protein in trophoblast and tumour cells.

Panel **A** represents a western blot showing the single bands detected by anti-OCT4 for trophoblast cell lines (HTR8/SVneo, TEV-1, JEG-3 and BeWo) and the breast cancer cell line MCF-7 under different conditions. Caco2 cell line used as the positive control and is separated with red dotted lines. Equal loading of protein was confirmed by β-actin expression. Panels **B, C, D, E** and **F** represents the ratio of OCT4 to β-actin densitometry readings for HTR8/SVneo, TEV-1, JEG-3, BeWo, and MCF-7 cells respectively. A one-way ANOVA followed by Tukey's test for multiple comparisons was carried out. Data represent the mean ±SEM of three individual experiments, each performed in triplicate (**p<0.01; *p<0.05).

4.2.6.2 Protein expression of SOX2

As seen from Figure 4.26, the SOX2 antibody produced a single band in almost all the protein samples from trophoblast cell lines and MCF-7 cells. These bands were detected at 37kDa, where the expected molecular weight of the band was in the range of 35-43 kDa. Interestingly, the overall protein expression of SOX2 was increased in the case of both untreated and DOX-treated spheroids (See Figure 4.26, Panel **A)**.

In HTR8/SVneo cells, the protein expression was significantly higher in untreated parental cells compared to DOX-treated parental cells ($p<0.01$) (See Figure 4.26, Panel **B**). Likewise, higher expression was observed in untreated spheroidal cells compared to untreated parental cells **(**$p<0.05$**)**. Moreover, the protein expression of DOX-treated spheroids was significantly higher than that of DOX-treated parental cells **(**$p<0.01$**)**.

In contrast to mRNA expression, a significant increase in protein expression of SOX2 in TEV-1 spheroids (both DOX-treated and untreated) was observed when compared to their parental cell counterparts ($p<0.01$) (See Figure 4.26, Panel **C**).

Also in contrast to mRNA expression data, a significant increase in protein expression of SOX2 was observed in both JEG-3 and BeWo cells between (a) untreated spheroids cells compared to untreated parental cells ($p<0.05$) and (b) DOX-treated spheroids compared to DOX-treated parental cell ($p<0.01$) (See Figure 4.26, Panel **D** and **E**).

There was a significant increase in protein expression of SOX2 observed in MCF-7 spheroids (both DOX-treated and untreated) compared to their parental cell counterparts (See Figure 4.26, Panel F). There was a correlation btween mRNA and protein expression in untreated parental compared to untreated spheroids (See Figure 4.21, Panel **F**).

Overall, the protein expression of SOX2 in four trophoblast cell lines and MCF-7 was significantly increased in spheroids compared to parental conditions.

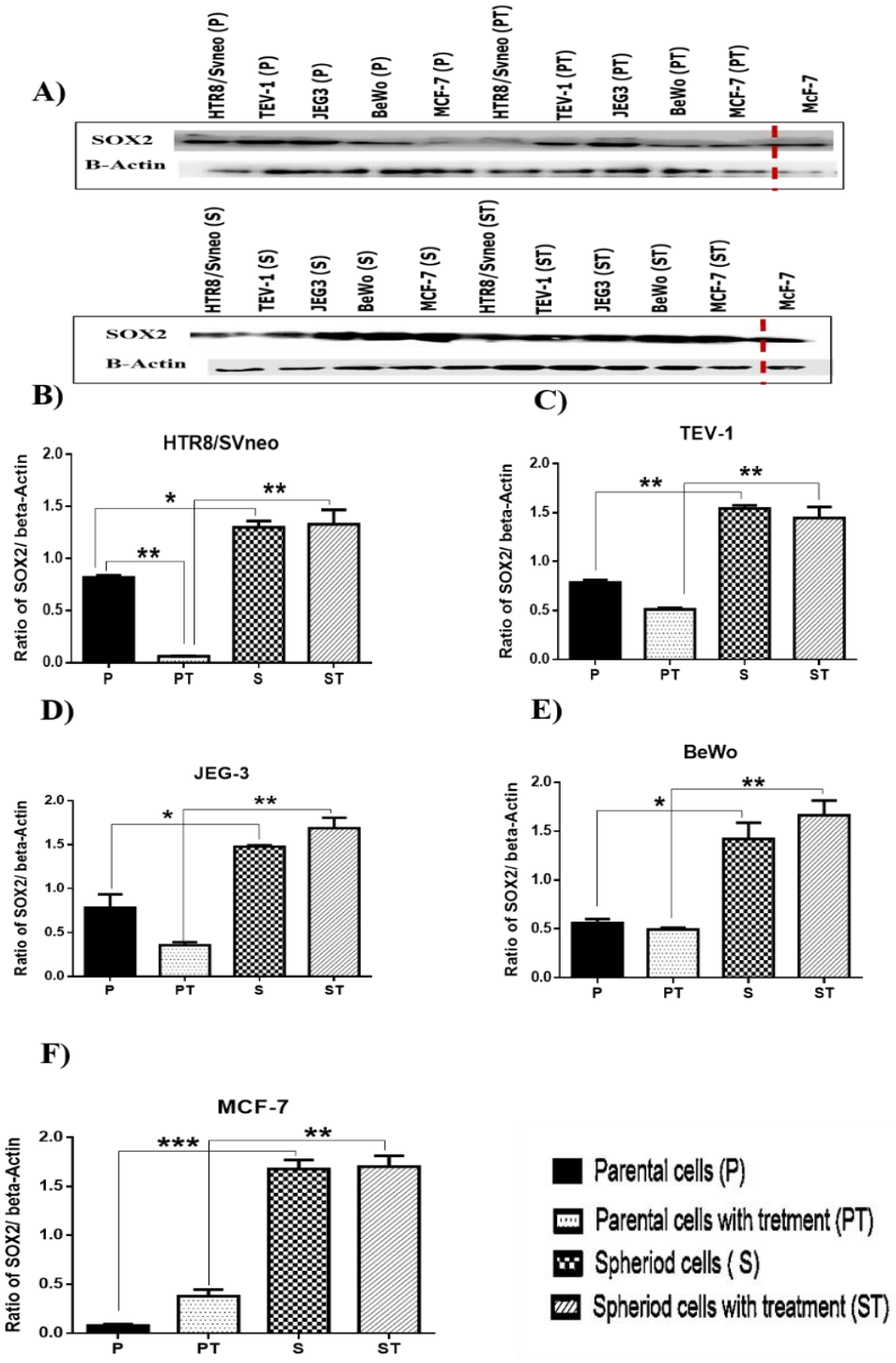

Figure 4.26: The expression of SOX2 protein in trophoblast and tumour cells.

Panel **A** represents a western blot showing the single bands detected by anti-SOX2 for trophoblast cell lines (HTR8/SVneo, TEV-1, JEG-3 and BeWo) and the breast cancer cell MCF-7 under different conditions. MCF-7 cell line used as the positive control and is separated with red dotted lines. Equal loading of protein was confirmed by β-actin expression. Panels **B, C, D, E** and **F** represents the ratio of SOX2 to β-actin densitometry readings for HTR8/SVneo, TEV-1, JEG-3, BeWo, and MCF-7 cells respectively. A one-way ANOVA followed by Tukey's test for multiple comparisons was carried out. Data represent the mean ±SEM of three individual experiments, each performed in triplicate (***p<0.001; **p<0.01; *p<0.05).

4.2.6.3 Protein expression of NANOG

The NANOG antibody produced a single band in almost all trophoblast cell lines, MCF-7cells and positive control (Caco2 cells). The expected molecular weight of the band was in the range of 36-55 kDa. Interestingly, the overall protein expression of NANOG was up-regulated in the case of spheroids (DOX-treated and untreated) in all cell lines. These bands were detected at 36 kDa (see Figure 4.27, Panel A).

In contrast to mRNA expression, a significant increase in protein expression of NANOG in both HTR8/SVneo and TEV-1 spheroidal cells (both DOX-treated and untreated) was observed, when compared to their parental cell counterparts (See Figure 4.27, Panel **B** and **C**). In the case of HTR8/SVneo DOX-treated parental cells compared to DOX-treated spheroids. There was a correlation in mRNA and protein expressions.

Similar results were observed in JEG-3 and BeWo cell lines. There was a significant increase in protein expression of NANOG in spheroidal cells (both DOX-treated and untreated) compared to their parental cell counterparts (See Figure 4.27, Panel **D** and **E**). Interestingly, the BeWo choriocarcinoma cell line showed there is correlation between mRNA and protein expressions in untreated spheroids versus untreated parental cells (See Figure 4.22, Panels **C** and **D**).

There was a significant increase in protein expression of NANOG observed in MCF-7 spheroidal cells (both DOX-treated and untreated) compared to their parental cell counterparts ($p<0.01$) (See Figure 4.27, Panel **F**). The difference observed in protein expression of NANOG between untreated parental versus untreated spheroids was also observed at the level of mRNA expressions (See Figure 4.22, Panel **E**).

Generally, all four trophoblast and MCF-7 cell lines showed a significant increase of NANOG protein expression in spheroid cells compared to parental conditions.

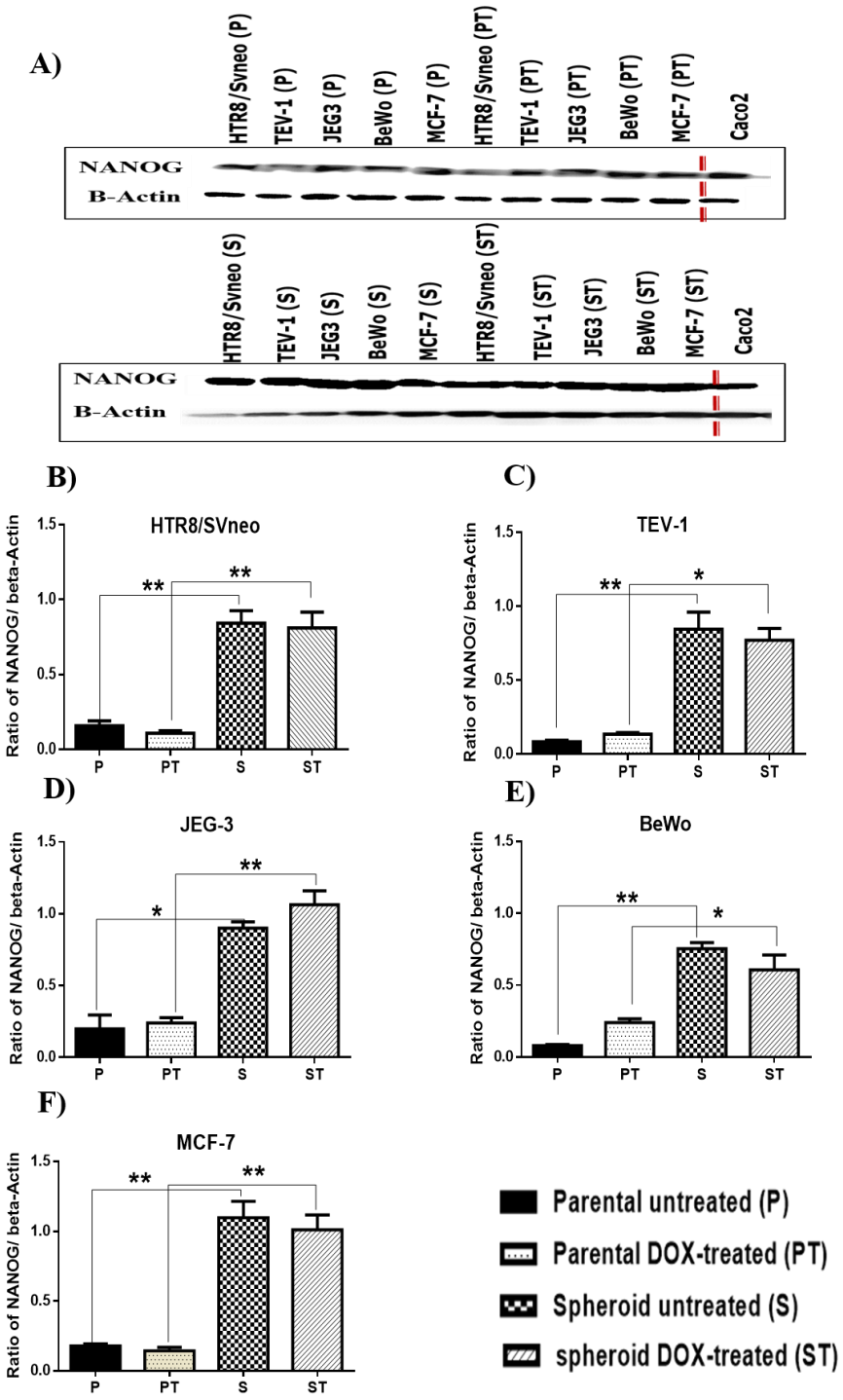

Figure 4.27: The expression of NANOG protein in trophoblast and tumour cells.

Panel **A** represents a western blot showing the single bands detected by anti-NANOG for trophoblast (HTR8/SVneo, TEV-1, JEG-3 and BeWo) and the breast cancer cell MCF-7 under different conditions. Caco2 cell line used as the positive control and is separated with red dotted lines. Equal loading of protein was confirmed by β-actin expression. Panels **B, C, D, E** and **F** represents the ratio of NANOG to β-actin densitometry readings for HTR8/SVneo, TEV-1, JEG-3, BeWo, and MCF-7 cells respectively. A one-way ANOVA followed by Tukey's test for multiple comparisons was carried out. Data represent the mean ±SEM of three individual experiments, each performed in triplicate (**p<0.01; *p<0.05).

4.2.6.4 Protein expression of CDX2

The CDX2 antibody produced a single band in most cell lines including positive control (Caco2 cells). The detected bands were at 42 kDa which is within the predicted range (30-42). The expression of CDX2 was minimal in parental DOX-treated and untreated trophoblast cells (see Figure 4.28, Panel **A**).

There were no significant changes observed in protein expression in both choriocarcinoma cell lines, However, CDX2 expression was increased in HTR8/SVneo DOX-treated spheroids compared to untreated spheroids ($p<0.05$) (See Figure 4.28, Panel **B)**. This difference in expression was also observed at the level of mRNA. Likewise, in TEV-1 cells the expression was found to be elevated in parental DOX-treated compared to untreated cells ($p<0.05$) (Figure 4.28, Panel **C**). On the other hand, in MCF-7 cells a significant increase in the expressions of CDX2 was observed in untreated parental cells compared to (a) DOX-treated parental and (b) untreated spheroids ($p<0.001$) (See Figure 4.28, Panel **F)**. This difference in the expression was also observed at the level of mRNA. Furthermore, there was significant increase in protein expression between versus DOX-treated spheroids untreated spheroids ($p<0.01$).

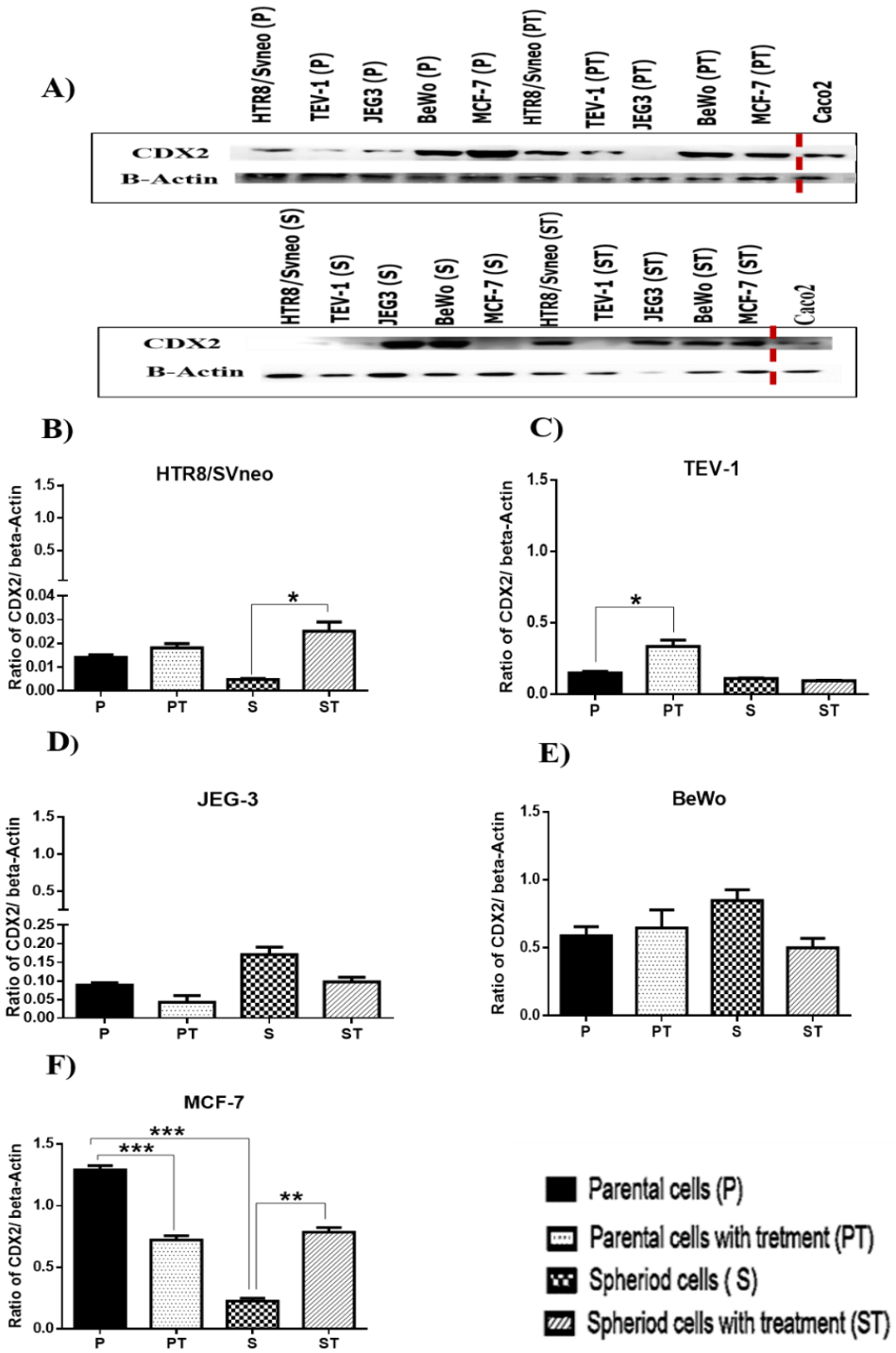

Figure 4.28: The expression of CDX2 protein in trophoblast and tumour cells.

Panel **A** represents a western blot showing the single bands detected by anti-CDX2 for trophoblast cell lines (HTR8/SVneo, TEV-1, JEG-3 and BeWo) and the breast cancer cell MCF-7 under different conditions. Caco2 cell line used as the positive control and is separated with red dotted lines. Equal loading of protein concentration was confirmed by β-actin expression. Panels **B, C, D, E** and **F** represents the ratio of CDX2 to β-actin densitometry readings for HTR8/SVneo, TEV-1, JEG-3, BeWo, and MCF-7 cells respectively. A one-way ANOVA followed by Tukey's test for multiple comparisons was carried out. Data represent the mean ±SEM of three individual experiments, each performed in triplicate (***p<0.001; **p<0.01; *p<0.05).

4.2.6.5 Protein expression of NOTCH1

The NOTCH1 antibody produced a single band in some trophoblast cell lines and MCF-7 (See Figure 4.29, Panel **A**). The predicated molecular weight of NOTCH1 protein as declared by the supplier (Abcam), was 125 kDa. However, a single band was observed at 100 kDa for NOTCH1 in all samples as well as in positive control (MCF-7 cells).

There was correlation between the mRNA and protein expression of NOTCH1 in HTR8/SVneo cells. It showed a significant increas in untreated parental compared to DOX-treated parental cells ($p<0.05$), and also between untreated parental versus untreated spheroids ($p<0.05$) (See Figure 4.29, Panel **B**). However, in TEV-1 cells there was no significant increase in the expression of NOTCH1 between all conditions.

In JEG-3 cells, a significant increase in protein expression of NOTCH1 was seen in parental untreated compared to DOX-treated parental cells and untreated spheroidal cells (See Figure 4.29, Panel **D**). This change was not apparent in mRNA expression. In BeWo cells the expression of NOTCH1 was reduced in untreated spheroids compared to respective parental cells ($p<0.05$). This change was also observed in mRNA expression.

In MCF-7 cells , there was a significant change in protein expression level of NOTCH1 especially in untreated parental cells compared to (a) DOX-treated parental cells ($p<0.001$) and (b) untreated spheroids ($p<0.01$). Moreover, in spheroid untreated compared to DOX-treated spheroids NOTCH1 protein level only were lower ($p<0.05$).

Overall, the protein expression of NOTCH1 in trophoblast cells was down-regulated in spheroids (both DOX-treated and untreated) compared to parental cell conditions.

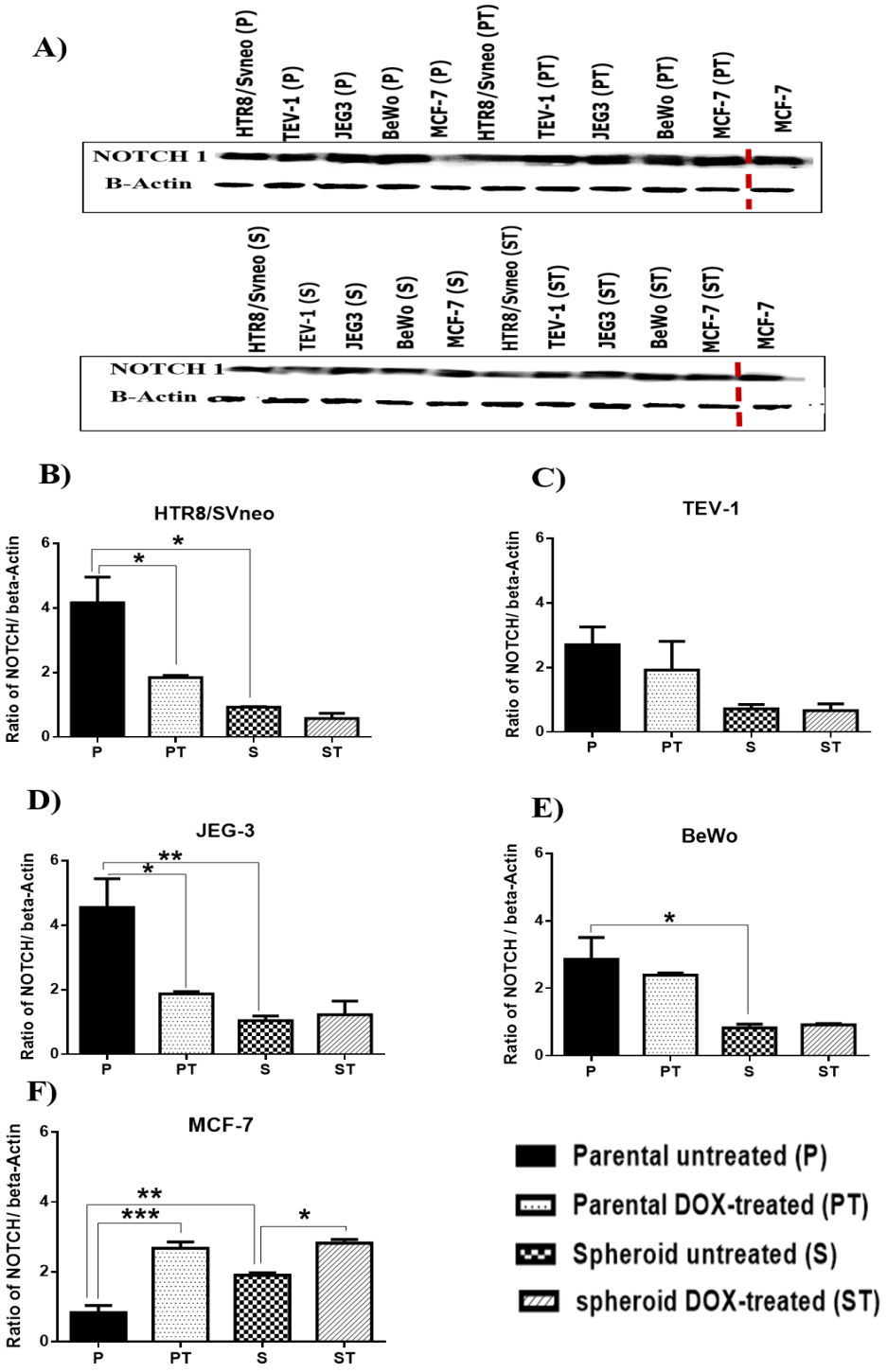

Figure 4.29: The expression of NOTCH1 protein in trophoblast and tumour cells.

Panel **A** represents a western blot showing the single bands detected by anti-NOTCH1 for trophoblast cell lines (HTR8/SVneo, TEV-1, JEG-3 and BeWo) and the breast cancer cell MCF-7 under different conditions. MCF-7 cell line used as the positive control and is separated with red dotted lines. Equal loading of protein was confirmed by β-actin expression. Panels **B, C, D, E** and **F** represents the ratio of NOTCH1 to β-actin densitometry readings for HTR8/SVneo, TEV-1, JEG-3, BeWo, and MCF-7 cells respectively.A one-way ANOVA followed by Tukey's test for multiple comparisons was carried out. Data represent the mean ±SEM of three individual experiments, each performed in triplicate (****p<0.0001; ***p<0.001; **p<0.01; *p<0.05).

4.3 Discussion

Methodical investigation of the status of any placental proteins, biomarkers and factors *in situ* has always been challenging due to ethical constraints. Moreover, the morphology of the placenta is clearly different from one individual to another even during normotensive pregnancies (Orendi *et al.,* 2011). To avoid these problems, placental explants and many different types of placental cells have been isolated and immortalised to be used as *in vitro* models (Orendi *et al.,* 2011). For this study, four placental cell lines were studied: HTR8/SVneo and TEV-1 (representing early first trimester trophoblast cells) together with JEG-3 and BeWo (choriocarcinoma cell lines) and MCF-7 (human breast adenocarcinoma cell line), which represents a tumour cell line of non-placental origins.

The trophoblast stem cells derived either from normal or choriocarcinoma placental cell lines are another powerful tool that can be used to understand the trophoblast cell immunology, biology, and placental development (King *et al.,* 2000). In addition, trophoblast spheroid generation is a useful method that can mimic and can be used to investigate the trophoblast during early differentiation stages, as these investigations are challenging in humans. Therefore, trophoblast cells have been cultured with other cell types in either two dimensional (2-D) or three dimensional (3-D) culture systems, where they are able to more to closely mimic the specialized features of trophoblast cells inside the uterus during pregnancy (Ji *et al.,* 2013).

The aims of this chapter were to generate and select spheroids from four trophoblast cell lines (HTR8/SVneo, TEV-1, JEG-3 and BeWo) and also from MCF-7 cells. To check the effects of chemotherapeutic agent (Doxorubicin) in producing drug resistant spheroids from all four trophoblast cell lines and MCF-7. After selection of spheroids from trophoblast cell lines, the expression of various stem cell markers was studied to determine the capacity for 'stemness' ability of these cell lines.

4.3.1 Effect of Doxorubicin on cell viability and toxicity

The first choice of assays to check cell viability and cytotoxicity were MTT and LDH assays, due to their quick and straight forward protocols, cost effectiveness and reliability. The data suggest that the lower concentrations of DOX do not affect mitochondrial activity; while at higher concentrations, DOX becomes cytotoxic to the cells used. The LDH assay showed minimum LDH release in cells treated with 250 and 500 ng/ml DOX concentrations compared to control.

There are two mechanisms by which DOX acts on cell cytotoxicity: (**1**) it has an ability to interact with plasma membranes, intercalate with DNA, and disrupt topoisomerase-II, (**2**) generation of the free radicals and their damage to cellular membranes, DNA and proteins (Gewirtz, 1999).

4.3.2 Generation of non-resistant (normal) spheroids

As explained in Section 4.2.3.1, both the first trimester transformed trophoblast and choriocarcinoma cells have shown the ability to form spheroids. From literature searches, it is clear that this is the first successful attempt to produce spheroid bodies in the transformed first trimester trophoblast cell line TEV-1. In fact, there is only one recent study, which has managed to produce spheroids from other placental cell lines (Webber *et al.,* 2013). They illustrated that HTR8/SVneo cells have a high ability to form spheroid bodies and was in agreement with the present study. However, they reported that JEG-3 cells have only a limited ability to form spheroid bodies, while in this study, JEG-3 cells were found to have produced spheroids. The difference between the two studies may depend on the methodology used to produce spheroids. The previous study used hanging drops, which is a simple and inexpensive method to produce spheroid. However, it is difficult to change media, add drugs and track the spheroid behaviour during formation (Achilli *et al.,* 2012; Mehta *et al.,* 2013). In contrast, this study as explained before in (Section 2.9) used non-adherent flasks with a cocktail of growth factors to induce spheroid formation. Furthermore, Grummer *et al.* 1994 reported the formation and properties of spheroids produced from the BeWo and JEG-3 cell lines. The present study also prove the formation of spheroids from BeWo cells. 3-D culture can be a useful model to studying the differentiation, attachment and invasion potential of trophoblast.

Overall, the findings of this study indicate that, all four trophoblast cell lines are capable of producing spheroids under non-adherent conditions and re-grow again under normal conditions (See Section 4.2.3.1).

4.3.3 Generation of resistant spheroids from trophoblast and tumour cell lines

Spheroids were aggregated as clusters of cells, formed by self-assembly with the help of growth factors and non-adherent culture flasks. Compared to 2-D cell monolayer cultures, spheroidal 3-D models can closely replicate essential physiological conditions and *in vivo* cellular responses to external motivations (Mehta *et al.,* 2013). 3-D cultures offer many physiological advantages for testing of drug delivery and toxicity, by allowing the study about their *in vivo* metabolism *in vitro*. In addition, the cellular heterogeneity of spheroid produced from 3-D culture can closely mimic the cell morphology *in vivo* as well as their

functions such as proliferation, differentiation, gene expression, etc. However, 3-D cell culture can be expensive for large-scale production and time consuming (Mehta *et al.,* 2013). Furthermore, the 3-D systems still lack the complex vascular systems which support tissues *in vivo* for nutrients, oxygenation, and removal of waste (Edmondson *et al.*, 2014). Cells grown in this system perform these functions only by diffusion processes.

The drug-resistant spheroid bodies were generated using DOX. All concentrations above 1000 ng/ml of DOX showed reduced cell viability in all four trophoblast cell lines (HTR8/SVneo, TEV-1, JEG-3 and BeWo). In addition, the small cells resulting from DOX treatment did not revert back to a monolayer morphology, when cultured back into adherent cell culture flasks. However, the spheroids produced from 250 and 500 ng/ml DOX were larger in size and also reverted back into a monolayer upon growing in adherent cell culture flasks. Similar results could be observed in the MCF-7 cell line. Nevertheless, the spheroids produced by MCF-7 cells were bigger in size compared to the trophoblast cell lines. Additionally, the DOX resistant spheroids generated from all four trophoblast cell lines were smaller when compared with the non-treated spheroids. However, the DOX treatment did not affect the ability of MCF-7 cell line to produce larger spheroids.

These preliminary results indicate that the trophoblast cells lines exhibit "stemness" features in spheroid bodies, such as self-renewal, as they possessed the ability to re-grow again under normal conditions. Although the MCF-7 cells treated with 1000 ng/ml of DOX were able to produce small spheroids, considering a uniform selection criteria, 250 ng/ml DOX treatment was selected as the optimum dose to generate drug resistant spheroids in all five cell lines.

4.3.4 Characterization of stem cell markers by Immunofluorescence

The expression of transcription factors (such as SOX2, NANOG) that are associated with "stemness" were clearly observed in all the cell lines used (under all conditions). In the case of OCT4, there was no staining in parental (both DOX-treated and untreated) TEV-1, JEG-3 and MCF-7 cells. On the other hand, both parental cells of HTR8/SVneo and BeWo have shown immunofluorescence for OCT4. This shows OCT4 expression was cell lines dependent for parental cells type. However, the presence of OCT4 in the spheroidal cells generated from all trophoblast cells and MCF-7 suggests that these cell lines have transformed into stem-like cells upon spheroid formation.

OCT4, SOX2 and NANOG form a core regulatory network that coordinates to determine the self-renewal and differentiation of embryonic stem cells (ESCs) which can contribute to tumorigenesis (Chang *et al.,* 2008). Interestingly, the expression of OCT4, SOX2 and NANOG in MCF-7 have already been reported by Ling *et al.* (2012) using

immunohistochemistry. Likewise, Webber *et al.* (2013) have confirmed the expression of SOX2, NANOG, and NOTCH1 in HTR8/SVneo spheroid cells. Although these findings support the present finding partially, the data from Webber *et al.* (2013) have not shown the expression of OCT4 in HTR8/SVneo spheroid cells and expressions in JEG-3 were not reported. These differences may be attributed to the use of different antibodies, and differences in the experimental procedure for producing spheroids.

However, the staining for the trophoblast transcription marker CDX2, was absent in the spheroidal cells generated from all cell lines. Interestingly, staining for CDX2 was detected in the parental cells of HTR8/SVneo and TEV-1. Since CDX2 is a specific trophoblast transcription factor. This finding suggests that CDX2 is a sign of trophoblast lineage derivation instead of a trophoblast stem cell differentiation. Jia *et al.* (2014) have shown CDX2 overexpression in HTR-8/SVneo cells enhanced the cell invasion by promoting MMP-9 expression and inhibiting TIMP-1 expression. The fact that the expression of CDX2 was lost in spheroidal cells was contradictory with Webber *et al.* (2013) investigation, where they showed HTR8/SVneo and JEG-3 spheroid bodies expressed CDX2. These differences may be attributed to the use of different antibodies. Additional, differences in the experimental methods to produce spheroids such as hanging drop was used by Webber *et al.* (2013).

NOTCH1 was detected in all four trophoblast cell lines (HTR8/SVneo, TEV-1, JEG-3 and BeWo) and MCF-7 in both parental and spheroidal cells (DOX-treated and untreated). NOTCH1 have been reported to be expressed in trophoblast stem cells and in differentiated trophoblast cells, and has been associated with "stemness" properties such as stem cell self-renewal (Sarikaya and Jerome-Majewska, 2011; Bolós *et al.*, 2013). NOTCH1 activity was also associated positively with cancer growth or initiation of pro-tumorigenic activities in breast cancer cell lines such as MCF-7 (Bolós *et al.*, 2013). Although the expression/localisation of these factors are not clear in spheroidal cells (due to the spheroidal nature), the parental cells show a clear cytoplasmic staining. Other studies using gastric cancer cell lines have also shown the cytoplasmic and perinuclear distribution of these factors (Liu *et al.*, 2013).

Overall, both un-treated and DOX-treated spheroids showed positive staining for most of these factors except CDX2. Since spheroidal cells are associated as clusters, they might have complemented signals to each other, whilst monolayer cell cultures of parental cells may not have these signals (Liu *et al.*, 2013). Moreover, the culture medium used for spheroids contained growth factors which may also contribute to the increased intensity of staining. It should be noted that in immunofluorescence studies, the intensity of staining is not

proportional to the expression levels. Especially in spheroidal cells, the staining intensity was affected by the clustering nature of the cells.

4.3.5 Relative mRNA/protein expressions of stem cell markers

The relative mRNA and protein expression level of each marker (OCT4, SOX2, NANOG, CDX2 and NOTCH1) was compared between the different conditions used in this study. Some comparisons showed a correlation between relative mRNA expression and protein level (especially in MCF-7 cells), whereas others results did not show this correlation. The reason for the mismatch correlation between mRNA and protein levels was not entirely explainable. It may be that expression of mRNAs are reciprocally reduced as a result of the high levels of protein expression. Another potential reason is that the half-life of some mRNA transcripts is extremely short due to RNA degradation. For data showing relatively high levels of mRNA compared to their protein counterpart; it can be argued that some transcripts have an extremely long half-life (Wang *et al.,* 2002; Yang *et al.,* 2003) Either way it is suggested that the correlation between transcript and protein level can be as little as 40% for factors that have regulatory functions. This was also ascertained by Schwanhausser *et al.* (2013) who argued that there is poor genome-wide correlations between some mRNA and proteins, mainly between those factors involved in the regulation of cell division and differentiation (Schwanhausser *et al.,* 2013)

- **OCT4**

In this study, spheroids (DOX-treated and untreated) from four trophoblast cell lines (HTR8/SVneo, TEV-1, JEG-3 and BeWo) and MCF-7 cells have shown an increase in the protein expression of OCT4 compared with the parental cells conditions of these cell lines. Similar results were observed in mRNA expression of OCT4 under spheroid (treated and untreated) when compared with the parental condition only in the JEG-3, BeWo and MCF-7 cells. Li *et al.* (2012) recognized that SOX2 and OCT4 are associated with "stemness" characteristics in cancer cells, therefore, they could lead to cells immortality, as well as self-renewable and invasive properties of cancer cells. Different studies have confirmed that OCT4 is responsible for the stemness properties and it is regulator expression and protects embryonic stem cells in an undifferentiated state (Boyer *et al.,* 2005; Shi and Jin, 2010; Zhang *et al.,* 2015). Therefore, the high expression of OCT4 in the spheroids in this study suggests the "stemness" characteristic of these cells.

- **SOX2**

SOX2 is an important transcription factor which is involved in many physiological processes including normal and pathological development such as maintenance the pluripotency of human ESC, and cancer (Liu *et al.*, 2013: Wu *et al.*, 2013).

In addition, it may have an essential role in trophoblast development. However, the role of SOX2 in human ESCs is not fully understood (Adachi *et al.,* 2010). SOX2 protein has been implicated in many processes of cancer including proliferation, growth, cellular migration and invasion, maintenance of the stemness of CSCs or TICs (tumour-initiating cells), and chemo-resistance (Liu *et al.,* 2013). It has been reported that the placenta contain a population of multipotent stem cells which show expression of embryonic stem cells markers, such OCT4 and SOX2 (Miki and Strom, 2006). This supports the present findings which showed an increased protein expression of SOX2 in spheroids (DOX-treated and untreated) in almost all trophoblast cell lines used. The increased expression of SOX2 in spheroids also indicated its stem-like features. In addition, SOX2 expression in cancer cells has been found to correlate with the invasiveness of several types of solid tumours, such as breast cancer (Wu *et al.,* 2013). It has been demonstrated that SOX2 was expressed in most of the human breast cancer cell lines such as MCF-7, T-47D and MDA-MB-231 cell lines (Chen *et al.*, 2008). This agreed with current findings with SOX2 expressions in case of MCF-7 cells.

- **NANOG**

The transcription factors such as OCT4, SOX2 and NANOG have critical molecular switches regulating ESC fate, which might also operate in renewing cancer stem cells. They play a role in determining the self-renewal and differentiation of ESCs (Ling *et al.*, 2012). The current study shows NANOG protein expression was up-regulated in spheroids (DOX-treated and untreated) in all cell lines indicating that they have self-renewal properties. The mechanism of NANOG on stem cell pluripotency are still unknown (Miyazawa *et al.*, 2014). Previous findings by Siu *et al*. (2008) reported that the knock down of the NANOG genes decreased mobility and invasion potential of trophoblast cells; suggesting NANOG may be involved in the malignant progression of trophoblast especially in the choriocarcinoma cell line JEG-3. The current study has shown that up-regulation of NANOG is common during the spheroidal transformation of all trophoblast cell lines suggesting NANOG expression may be linked to invasive properties (see Chapter 5).

- **CDX2**

CDX2 plays an essential role during embryonic development and is involved in the processes of intestinal cell proliferation, differentiation, adhesion, and apoptosis (Bai *et al.*, 2003). It is also a transcriptional regulator essential for the trophoblast lineage (Tolkunova *et al.*, 2006). However, the specific role of CDX2 in trophoblast invasion is still unclear; although it has been shown that aberrant expression of CDX2 is associated with intestinal inflammation and tumorigenesis (Coskun *et al.,* 2011). The data from the current study have shown that there was no significant difference in the protein expression levels of CDX2 during spheroidal transformation in all cell lines. This could be because the CDX2 expression is repressed and regulated by the high expression of pluripotent OCT4 and NANOG transcription factors. The correlation of NANOG and OCT4 expressions to CDX2 expression level during specialisation of the pluripotent trophoblast stem cell TSC have also been reported (Marchand *et al.*, 2011). Interestingly there was a decrease in the protein expression level of CDX2 under untreated spheroids compared to the parental cells in MCF-7 cells. This may be due to the tumour suppressive role of CDX2 by inhibiting cell proliferation (Saad *et al.*, 2011).

- **NOTCH1**

NOTCH1 plays important roles in many cellular processes, such as regulating proliferation, cell fate determination, differentiation, cell death and cell type specification that is critical for organogenesis (Zhao and Lin, 2012). It isassociated with "stemness" properties, as well as with the differentiation of cancer stem cells (Prasad *et al.,* 2009; Webber *et al.,* 2013). There was a clear IF staining of NOTCH1 observed in four trophoblast cell lines under different conditions. However, the protein expression of NOTCH1 was decreased in spheroidal cells (both DOX-treated and untreated) compared to parental cells in four trophoblast cell lines. A previous study has also reported NOTCH1 expression in both trophoblast stem cells and in differentiated trophoblast cells (Sarikaya *et al.*, 2011). However, the result from this study in the case of spheroidal cells was not as expected.

4.4 Conclusions

The data from this chapter showed the ability of four trophoblast cell lines (HTR8/SVneo, TEV-1, JEG-3 and BeWo) to produce spheroids under 3-D culture. Re-grown under normal conditions, they were able to produce monolayer of cells. Overall, the data in this study suggest that compared to parental cells there was an increased protein expression of stem cell markers (such as OCT4, SOX2 and NANOG) in spheroidal cells (DOX-treated and untreated); as they are required to maintain the stemness properties. Moreover, the positive staining for these factors could provide evidence that the spheroids generated from four trophoblast cell lines possess "stem-like cells" characteristics. The data suggests that these cells could be used as an *in vitro* model representing physiologically rapidly dividing cells.

Chapter 5
Understanding the cellular behaviour of spheroidal cells derived from trophoblast and tumour cell lines

5.1 Introduction

Uncontrolled cell proliferation along with cell invasion is important for aggressive tumour metastasis (Curran and Murray, 2000). Interestingly, during development of the human placenta, the trophoblast cells share some properties with tumour cells; for instance, differentiation, rapid proliferation, the ability to invade the surrounding tissue (including the basement membrane), migration and formation of new blood vessels (or angiogenesis) (Yagel *et al*., 1988). During the first trimester of pregnancy, extra-villous trophoblast cells invade into the maternal spiral arteries and into the uterine wall, which is essential for foetal development and normal pregnancy. Normally, the invasion of trophoblasts is controlled by several cellular interactions and/or molecular events such as extracellular matrix degradation, trophoblast differentiation and transcriptional regulation (Goldman-Wohl and Yagel, 2002). However, pre-eclampsia is characterized by shallow, insufficient trophoblast invasion, which leads to unmodified narrow spiral arteries and results in foetal hypoxia. This causes endothelial damage and finally leads to maternal symptoms such as hypertension, oedema, and proteinuria (Goldman-Wohl and Yagel, 2002). Interestingly, in the early 18th Century, John Beard (1911) developed the idea that the trophoblast can be used as an ideal model for cancer, to study the regulation of cell growth and differentiation, as well as invasion. Therefore, a better understanding of all aspects of trophoblast invasion may result in the development of new therapies to treat diseases of pregnancy associated with over (such as choriocarcinoma) or under invasion (e.g. PE) (Graham and Lala, 1992). Furthermore, the understanding of trophoblast invasion may not only pave the way to unravel the molecular mechanisms involved in metastatic tumour cells, but also lead to identification of new therapeutic targets for inhibiting proliferation and invasion (Anin *et al.,* 2004: Holtan *et al.*, 2009).

In order to understand tumour development, spheroid models have been used to understand the inter-relationship between tumour and endothelial cells (Oudar, 2000). These models have been used to study aspects such as wound healing, invasion, metastasis and angiogenesis. According to Oudar (2000), spheroid cells are powerful tools that reflect the degree of complexity and tumourigenicity *in vivo* when compared with monolayer cells. Grummer *et al.* 1994 reported the formation and properties of spheroids produced from the BeWo and JEG-3 cell lines. However, the invasive properties of these spheroids were not investigated.

To the best of the author's knowledge, this is the first study which shows the invasive properties of spheroids formed from trophoblast cell lines.

The present study aims to generate spheroids and characterise "stem-like cells" from transformed trophoblast cell lines (HTR8/SVneo, TEV-1) and trophoblast choriocarcinoma cells (JEG-3, BeWo) and MCF-7 cells. This comparative analysis of the migration and invasive potentials of parental and spheroidal cells was carried out to understand the behaviour of the spheroids produced from cells of trophoblast cells.

5.2 Results

The wound healing (scratch) assay was carried out at first, followed by invasion assays using 2-D matrigel and by 96 well 3-D spheroid BME. As mentioned in Section 2.12-2.14 assays were performed on both the parental cells from 2-D adherent flasks in DOX-treated and untreated conditions, along with the spheroids selected by using 3-D culture with or without DOX-treatment. The results are described below.

5.2.1 *In vitro* cell migration by scratch/wound healing assay

This assay was carried out to study the migration potential of transformed trophoblast cell lines (HTR8/SVneo and TEV-1), choriocarcinoma cell lines (JEG-3 and BeWo) and MCF-7, amongst parental DOX-treated and untreated, spheroids DOX-treated and untreated, each at 24 and 48 hours. Spheroids were used after being harvested from non-adherent flasks and disrupted by trypsin for plating into adherent 24 well plates under normal growth conditions before migration (as described in Section 2.12). WimScratch/Wimasis® software was used to analyse all confocal images, to calculate percentage wound closure. The experiment was repeated three times in quintuplicates. A two-way ANOVA followed by Tukey's post-hoc test was performed for multiple comparisons between: (a) parental untreated cells versus parental DOX-treated, (b) parental untreated cells versus spheroid untreated cells, (c) spheroid untreated versus spheroid DOX-treated cells and (d) parental DOX-treated cells versus spheroid DOX-treated cells.

5.2.2.1 Migration of transformed trophoblast cell lines

According to Figure 5.1, the HTR8/SVneo parental cells have covered 75% of the area at 24 hours, and at 48 hours cells covered almost 95% of the scratch area. In the case of the DOX-treated parental cells, almost 98% of wound closure was observed at 24 hours and a gradual decrease to 80% was observed at 48 hours. Therefore, DOX showed an inhibitory effect on the cell migration only after 48 hours of HTR8/SVneo cells [Figure 5.1, Panel **A** (red arrow)]. In the case of untreated spheroids, wound closure of 45% was observed at 24 hours which was increased to 98% at 48 hours. In contrast, the DOX-treated spheroid covered 55% of the area in 24 hours and decreased to 49% of the area in 48 hours [Figure 5.1, Panel **A** (white arrow)].

At 24 hours, there was a significant increase in wound closure in parental cells (both DOX-treated and untreated) compared to their spheroidal cell counterparts ($p<0.01$). Likewise, a significant increase in wound closure was observed in untreated spheroids versus DOX-treated spheroids at 48 hours ($p<0.01$) (Figure 5.1, Panel **B**).

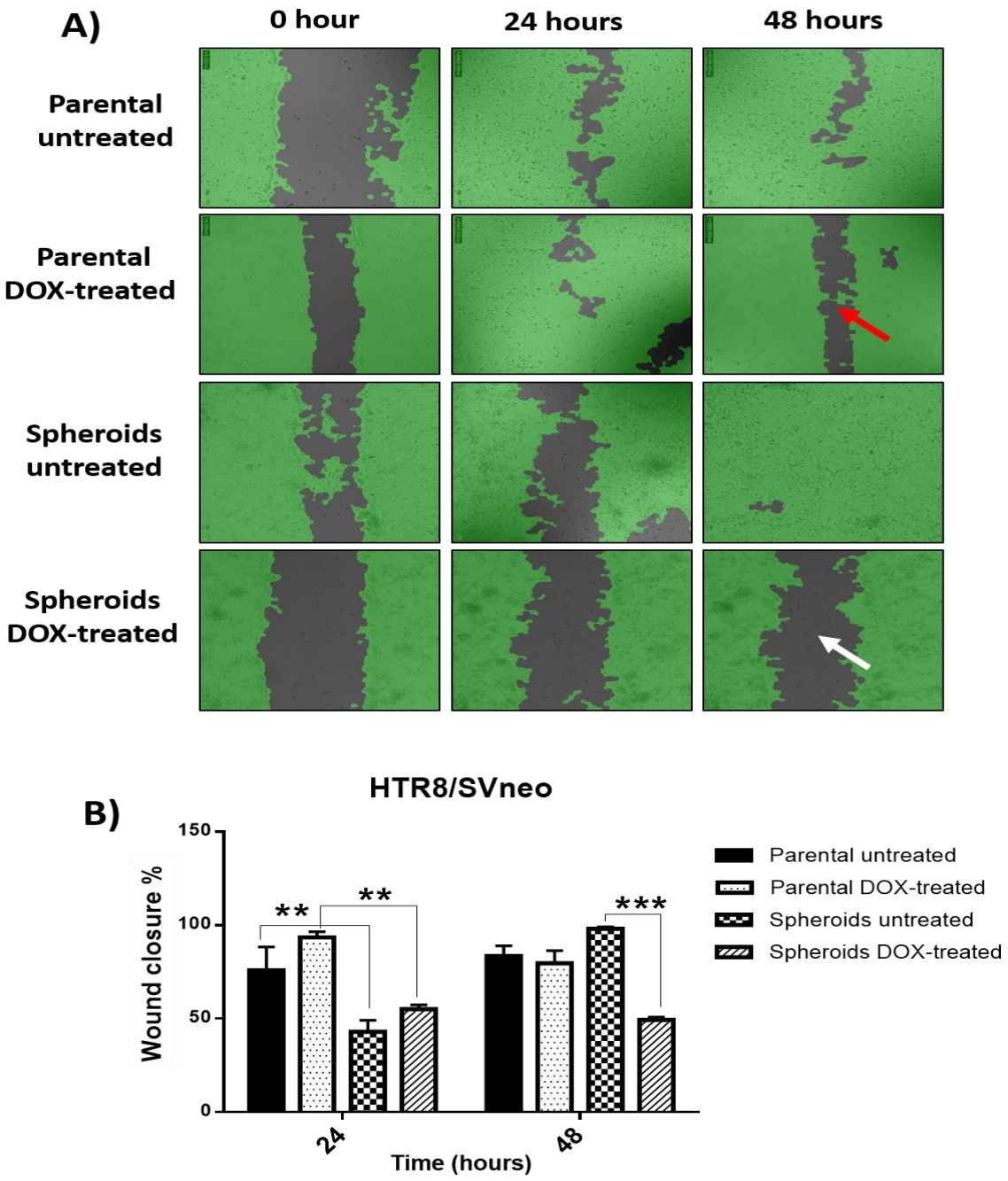

Figure 5.1: Migration of the HTR8/SVneo cell line.

Panel **A:** Represents the percent (%) wound closure at 0, 24 and 48 hours. The red arrow is pointing to the delayed effect of DOX on parental cells under treated conditions. The white arrow shows the effect of DOX on spheroidal cells. Panel **B**: Represents the quantitative analysis of wound closure using WimScratch/Wimasis® at 24 and 48 hours. Statistical significance was determined using a two-way ANOVA followed by Tukey's test for multiple comparisons between each condition. Data represent the mean ±SEM of three individual experiments, each performed in quintuplicate (**p<0.01).

In the case of TEV-1 cells, untreated parental cells covered almost 100% of the scratch area within 48 hours. In contrast, when the parental cells were treated with DOX at 24 hours the closure was found to be 98%. Interestingly, the wound re-opened and showed only 86% healing at 48 hours [see Figure 5.2, Panel **A** (red arrow)].

The migration of untreated spheroids was 90% at 24 hours and increased to 100% at 48 hours. The migration of DOX-treated spheroids covered around 55% at 24 hours and the covered area was reduced to 40% at 48 hours, which shows limited migration even after 48 hours [Figure 5.2, Panel **A** (white arrow)].

There was a significant increase in wound closure in the case of DOX-treated parental versus DOX-treated spheroids. Similarly, there was an increase in wound closure between untreated spheroids and DOX-treated spheroids at 24 and 48 hours ($p<0.0001$). At 48 hours, a significant increase in wound closure was observed between untreated parental and DOX-treated parental ($p<0.01$) (Figure 5.2, Panel **B**).

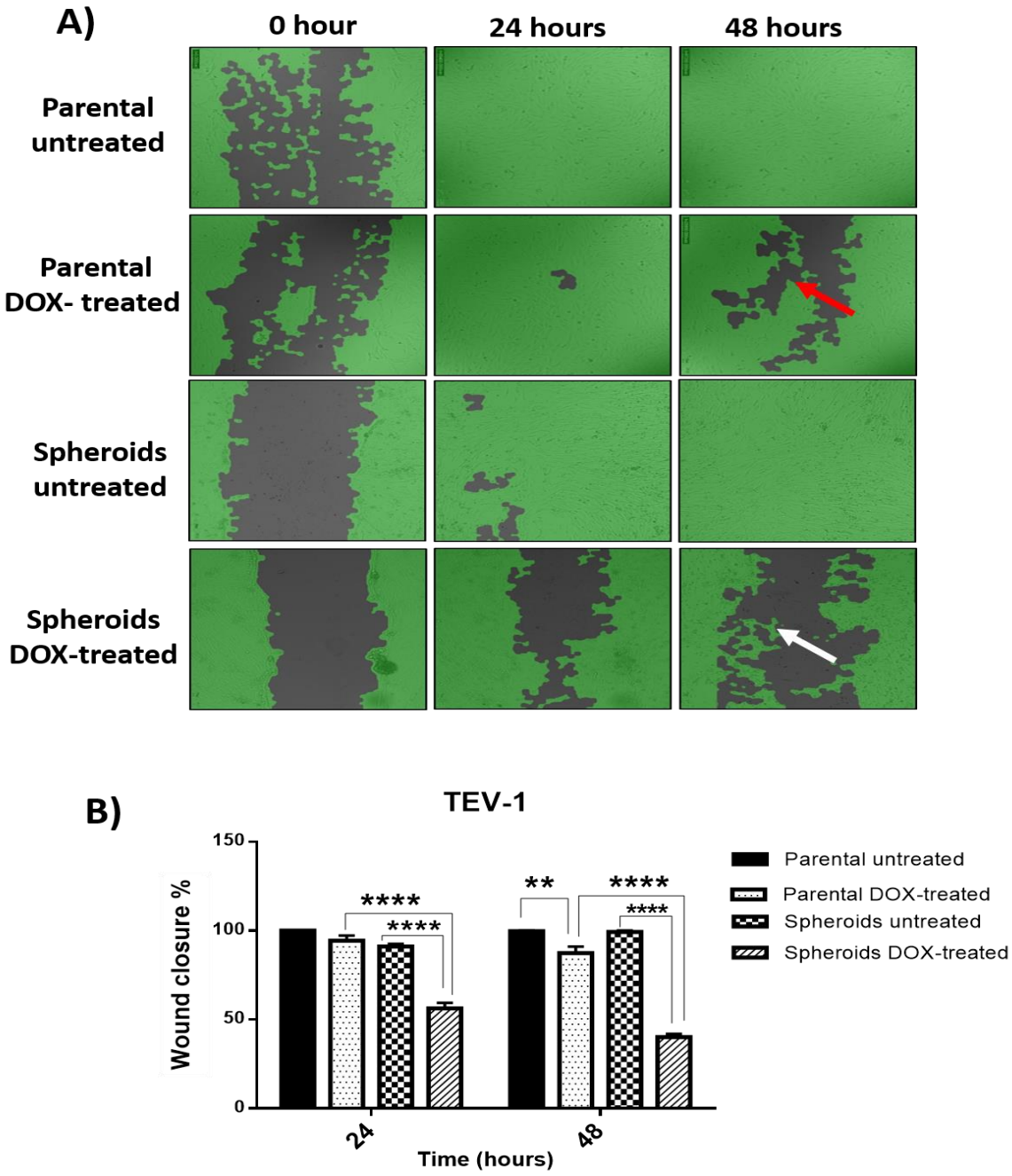

Figure 5.2: Migration of the TEV-1 cell line.

Panel **A:** Represents the percent (%) wound closure at 0, 24 and 48 hours. The red arrow is pointing to the delayed effect of DOX on parental cells under treated conditions. The white arrow shows the effect of DOX on spheroidal cells. Panel **B**: Represents the quantitative analysis of wound closure using WimScratch/Wimasis® at 24 and 48 hours. Statistical significance was determined using a two-way ANOVA followed by Tukey's test for multiple comparisons between each condition. Data represent the mean ±SEM of three individual experiments, each performed in quintuplicate (****$p<0.0001$; **$p<0.01$).

5.2.2.2 Migration of choriocarcinoma cell lines

Figure 5.3, Panel **A**, shows that the parental cells of JEG-3 covered 77% of the scratch wound area at 24 hours which was increased to 89% at 48 hours. A similar trend was observed for the DOX-treated parental cells, which covered almost 81% of the scratch area at 24 hours. However, the wound healed area was decreased to 61% at 48 hours [See Figure 5.3, Panel **A** (red arrow)]. In untreated spheroidal cells, the covered area remained 81% at 24 hours, but at 48 hours healing showed a slight increase to 85% in covered area. In the case of spheroidal cells under DOX treatment the covered area was 60% at 24 hours. Again like DOX-treated parental cells, at 48 hours, the cell covered area was reduced to 55% [See Figure 5.3, Panel **A** (white arrow)].

There was a significant reduction in the covered area of DOX-treated spheroids compared to both (a) DOX-treated parental ($p<0.01$) and (b) untreated spheroidal cells ($p<0.01$) at 24 hours. Moreover, there was a significant increase in wound closure of untreated parental versus DOX-treated parental cells ($p<0.01$). Likewise, the wound closure in untreated spheroidal cells was higher than in DOX- treated spheroids cells ($p<0.0001$) at 48 hours (See Figure 5.3, Panel **B**).

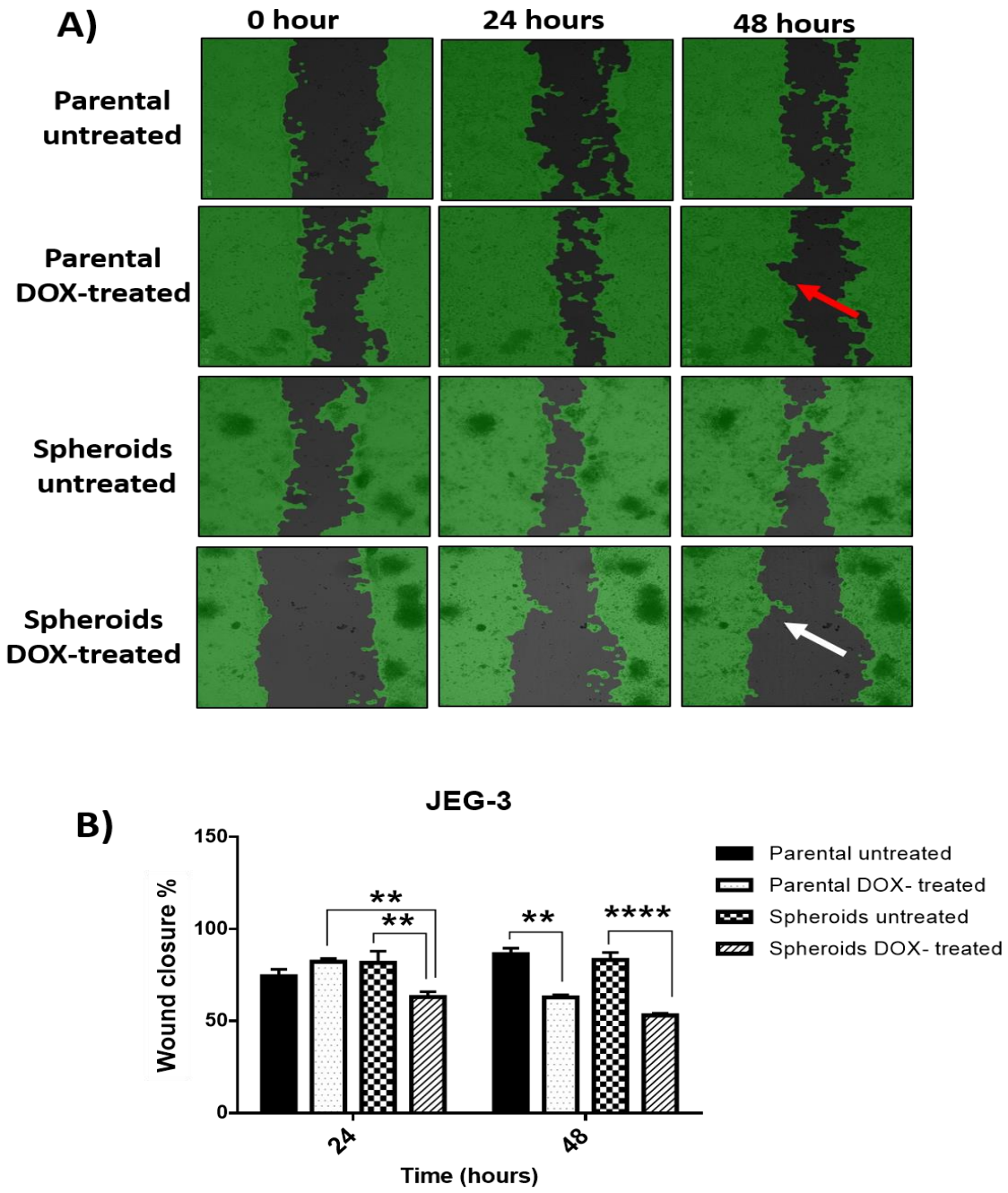

Figure 5.3: Migration of the JEG-3 cell line.

Panel **A:** Represents the percent (%) wound closure at 0, 24 and 48 hours. The red arrow is pointing to the delayed effect of DOX on parental cells under treated conditions. The white arrow shows the effect of DOX on spheroidal cells. Panel **B**: Represents the quantitative analysis of wound closure using WimScratch/Wimasis® at 24 and 48 hours. Statistical significance was determined using a two-way ANOVA followed by Tukey's test for multiple comparisons between each condition. The data is a mean representative of three individual experiments each for two different passages performed in quintuplicate (n=3±SEM; ****p<0.0001; **p<0.01).

In the case of BeWo cells, the untreated parental cells covered around 71% of the scratch area at 24 hours. At 48 hours it was increased to 80%. Whilst, DOX-treated parental cells covered 85% of the area at 24 hours, which was then decreased to 63% at 48 hours [see Figure 5.4, Panel **A** (red arrow)]. In the case of untreated spheroids, at 24 hours the cell covered area was 55% and this increased to 60% at 48 hours. On the other hand, in the DOX-treated spheroidal cells, the covered area at 24 hours was 45% and this decreased to 36% at 48 hours [see Figure 5.4, Panel **A** (white arrow)].

Overall, the cell migration was reduced in DOX-treated spheroidal cells compared to DOX-treated parental cells ($p<0.001$) at 24 hours. There was a significant increase in untreated parental cells compared to both DOX-treated parental cells and untreated spheroids ($p<0.05$). However, a significant reduction in cell migration was also observed in DOX-treated spheroidal cells compared to both untreated spheroidal cells and DOX-treated parental cells ($p<0.01$). (See Figure 5.4, Panel **B**).

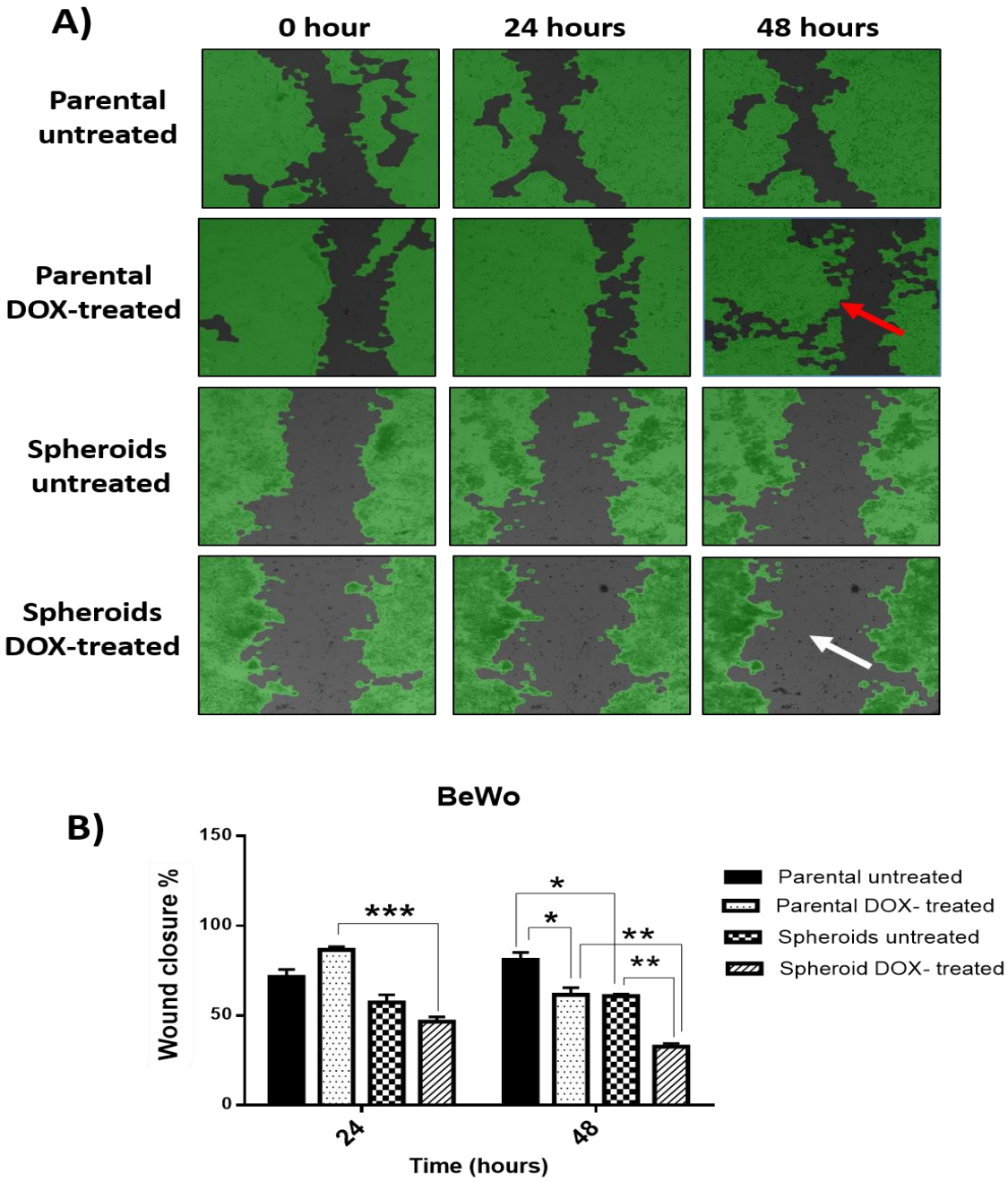

Figure 5.4: Migration of the BeWo cell line.

Panel **A:** Represents the percent (%) wound closure at 0, 24 and 48 hours. The red arrow is pointing to the delayed effect of DOX on parental cells under treated conditions. The white arrow shows the effect of DOX on spheroidal cells. Panel **B**: Represents the quantitative analysis of wound closure using WimScratch/Wimasis® at 24 and 48 hours. Statistical significance was determined using a two-way ANOVA followed by Tukey's test for multiple comparisons between each condition. Data represent the mean ±SEM of three individual experiments, each performed in quintuplicate (***$p<0.001$; **$p<0.01$;*$p<0.05$).

5.2.2.3 Migration of MCF-7 tumour cells

In the case of MCF-7cells, the parental MCF-7 cells covered 63% of the wound at 24 hours, and at 48 hours this was slightly increased to 69%. In DOX-treated parental MCF-7, the cell covered area observed was 70% at 24 hours. A slight increase to 73% in wound closure was observed at 48 hours [Figure 5.5, Panel **A** (red arrow)].

The wound closure observed in untreated spheroids cells at 24 and 48 hours, were 55% and 58% respectively. In the case of DOX-treated spheroidal MCF-7 cells, the cells covered area was 58% at 24 hours and this was slight decreased to 50% at 48 hours [Figure 5.5, Panel **A** (white arrow)].

There was a significant increase in wound closure in parental cells (both DOX-treated and untreated) compared to their spheroidal cell counterparts at 24 and 48 hours. Moreover, the wound closure in DOX-treated parental cells was faster than DOX-treated spheroids (See Figure 5.5, Panel **B**).

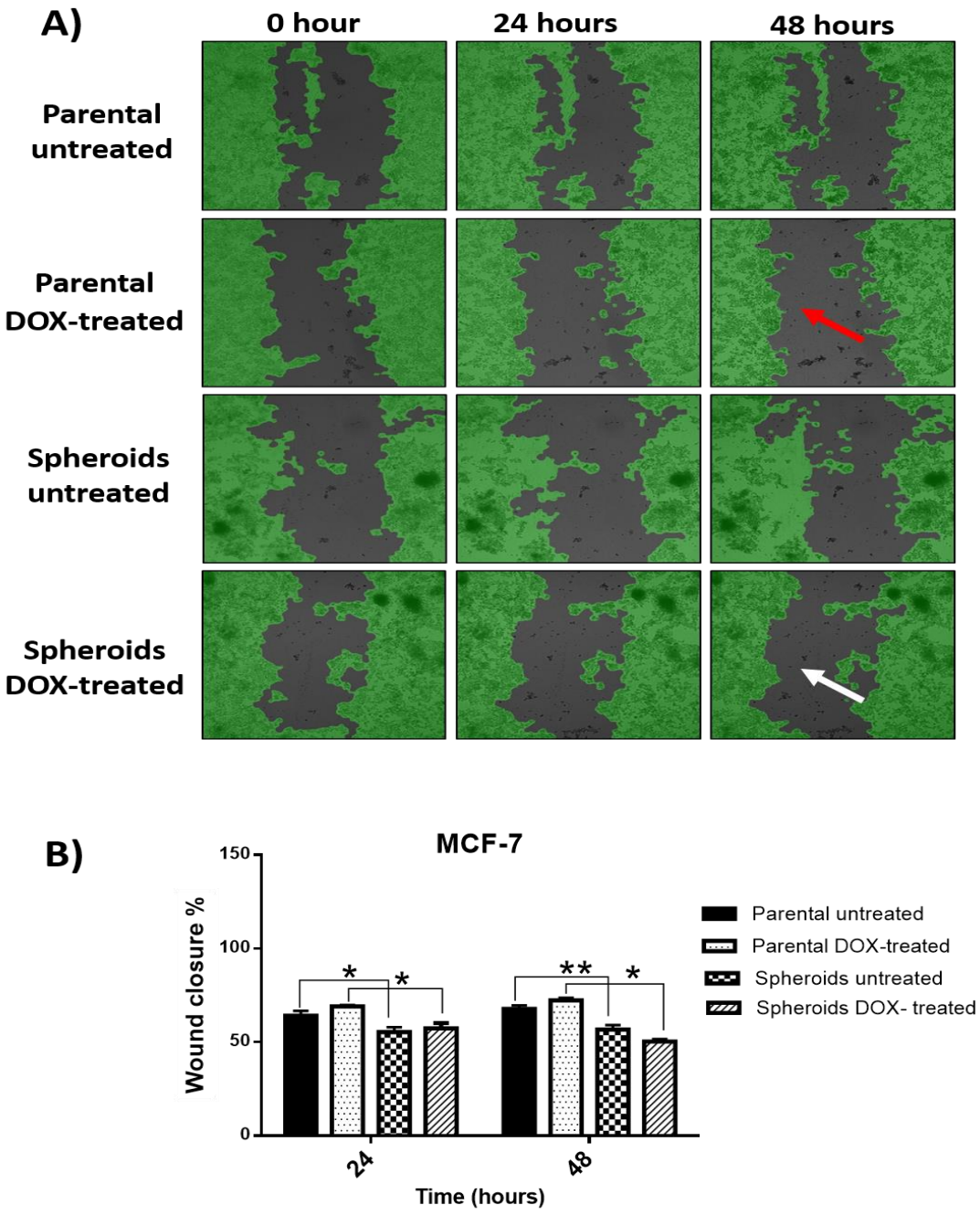

Figure 5.5: Migration of the MCF-7cell line

Panel **A:** Represents the percent (%) wound closure at 0, 24 and 48 hours. The red arrow is pointing to the delayed effect of DOX on parental cells under treated conditions. The white arrow shows the effect of DOX on spheroidal cells. Panel **B**: Represents the quantitative analysis of wound closure using WimScratch/Wimasis® at 24 and 48 hours. Statistical significance was determined using a two-way ANOVA followed by Tukey's test for multiple comparisons between each condition. Data represent the mean ±SEM of three individual experiments, each performed in quintuplicate (**p<0.01; *p<0.05).

5.2.2 Cell invasion Assay

The cell migration assay was followed by an invasion assay using BD Falcon ™ BioCoat tumour invasion plates as explained in Section 2.13. This experiment was carried out to study the invading capacity of cells by comparing the number of cells invaded under different conditions. In this present study, spheroid cells which have a total diameter above 8.0 μm were involved. Therefore, the spheroids were disintegrated by using trypsin into single cells before performing the invasion assay. Image J software analysis was used to analyse the images taken using Olympus microscope of the bottom coated membrane. As in the migration assay, the invasion capacity of cells was compared between (a) untreated parental versus DOX-treated parental; (b) untreated parental versus untreated spheroidal cells; (c) untreated spheroidal versus DOX-treated spheroid and (d) DOX-treated parental versus DOX-treated spheroidal cells. This comparisons were performed by using a one-way ANOVA followed by Tukey's post-hoc test for multiple comparisons. Micrographs obtained from the cell invasion study, together with the quantitative analysis of number of cells invaded and percentage of cell invasion are given in Figures 5.6 to 5.10. The number of cells invaded and percentage of cells invasion were two different methods to calculate this property.

5.2.2.1 The invasion of transformed trophoblast cell lines

Both the transformed cell lines, HTR8/SVneo and TEV-1, were initially analysed for their invasive capacity. HTR8/SVneo cells showed a higher invasion capacity in untreated spheroids compared to other conditions of this cells. Moreover, there was also a significant increase in the number of cells invaded by untreated parental compared to DOX-treated parental cells ($p<0.05$). There was a highly significant increase in the number of untreated spheroid cells invaded compared to all other cells/treatments (See Figure 5.6, Panel **A** and **B**). However, the percentage invaded of untreated spheroidal cells (that cell invasion in comparison to migration) was significantly lower than untreated parental and DOX-treated spheroidal cells ($p<0.05$) (See Figure 5.6, Panel **C)**.

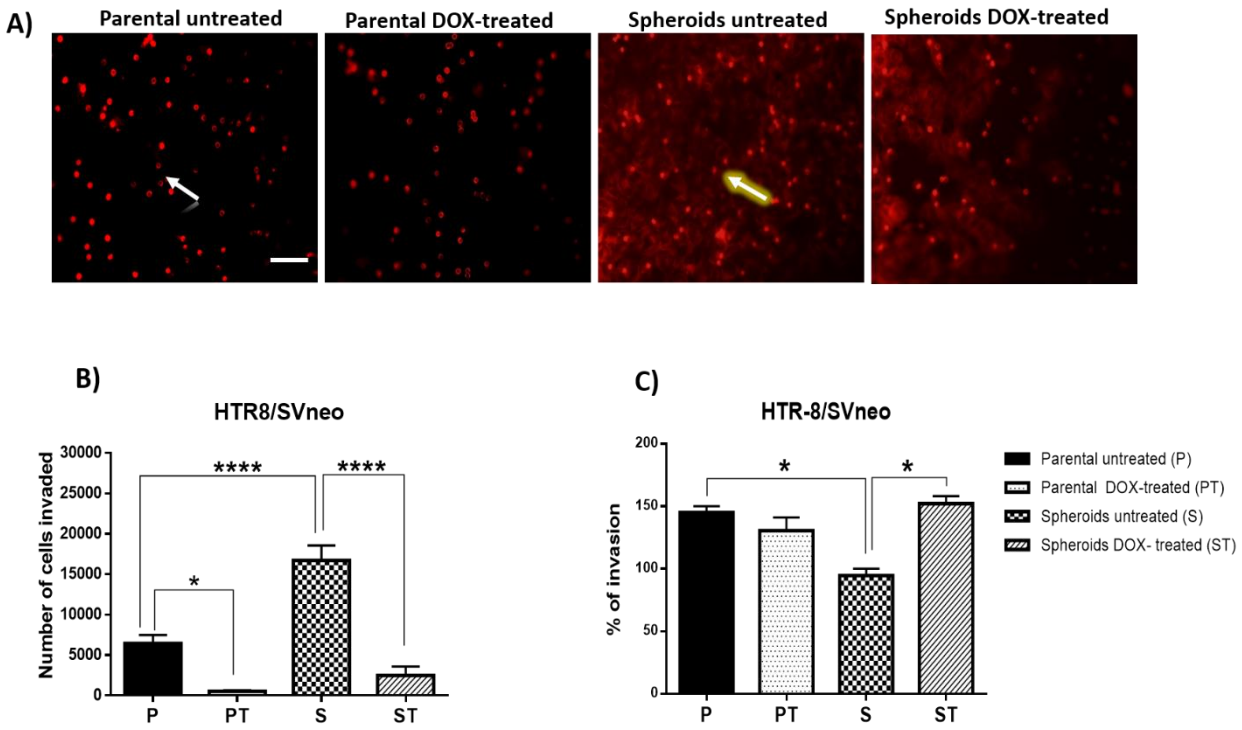

Figure 5.6: HTR8/SVneo invasion.

Panel **A**: Represents the number of HTR8/SVneo cells invaded at 24 hours. Image was taken of the bottom coated membrane using an Olympus fluorescence microscope. Objective magnification 20X (Scale bar = 100 μm). Panel **B**: Represents the quantitative analysis of number of cells invaded using ImageJ and Graphpad software. Panel **C**: Represents the percentage of invasion calculated using the formula described in Section 2.13. The white bold arrow and glowing arrow are pointing towards parental invaded cells and invaded spheroids respectively. Statistical significance was determined using a one-way ANOVA followed by Tukey's test for multiple comparisons. Data represent the mean ±SEM of three individual experiments, each performed in quintuplicate (****$p<0.0001$; *$p<0.05$).

In the case of TEV-1 cells (see Figure 5.7, Panel **A** and **B**), there was a highly significant increase in the number of cells invaded by untreated spheroids compared to both untreated parental ($p<0.0001$) and DOX-treated spheroids ($p<0.05$). In addition, there was a significant reduction in the number of cells invaded by DOX-treated parental compared to DOX-treated spheroidal cells ($p<0.05$). However, there was no statistically significant increase in the percentage invasion under all conditions except in untreated parental versus DOX-treated parental cells ($p<0.05$) (Figure 5.7, Panel **C**).

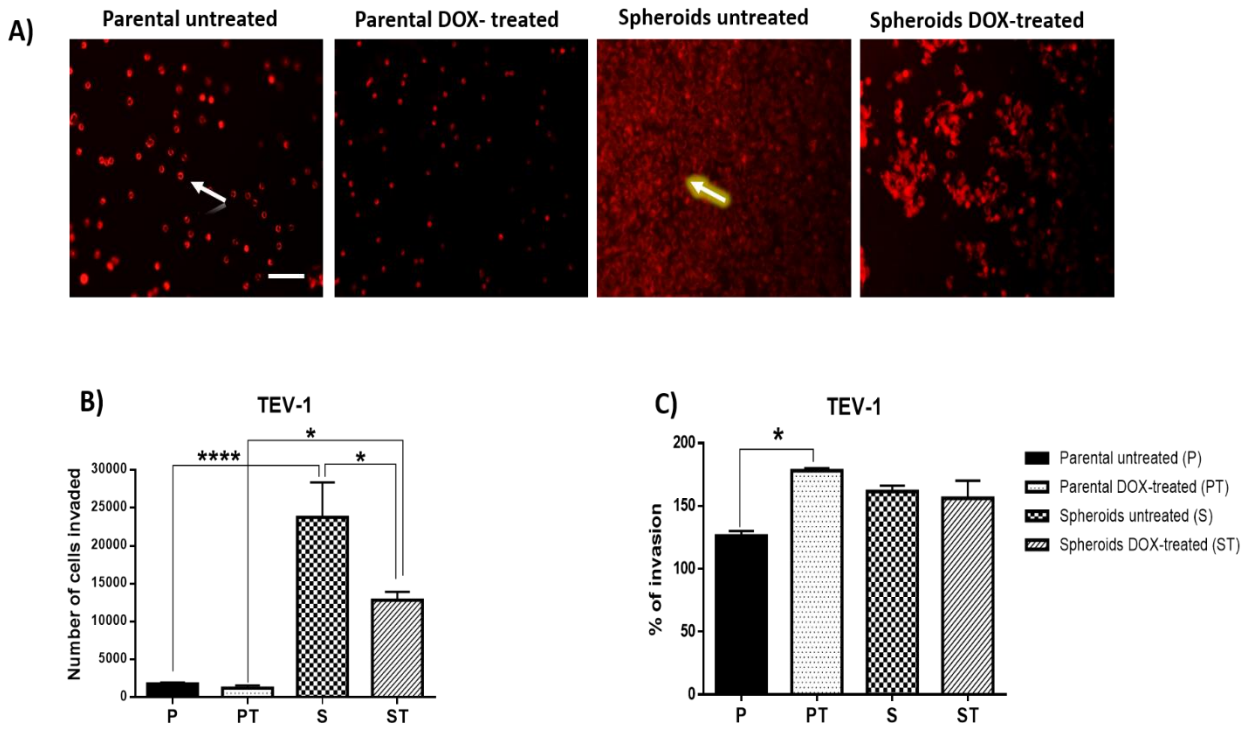

Figure 5.7: TEV-1 invasion.

Panel **A**: Represents the number of TEV-1 cells invaded at 24 hours. Image was taken of the bottom coated membrane using an Olympus fluorescence microscope. Objective magnification 20X (Scale bar = 100 µm). Panel **B**: Represents the quantitative analysis of number of cells invaded using ImageJ and Graphpad software. Panel **C**: Represents the percentage of invasion calculated using the formula described in Section 2.13. The white bold arrow and glowing arrow are pointing towards parental invaded cells and invaded spheroids respectively. Statistical significance was determined using a one-way ANOVA followed by Tukey's test for multiple comparisons. Data represent the mean ±SEM of three individual experiments, each performed in quintuplicate (****$p<0.0001$; *$p<0.05$).

5.2.2.2 The invasion of choriocarcinoma cell lines

Figure 5.8, Panels **A** and **B**, represent the invasion by JEG-3 cells. The data were similar to TEV-1 cells. There was a highly significant increase in the number of cells invaded by untreated spheroid compared to both untreated parental cells and DOX- treated spheroids ($p<0.0001$). Moreover, there was a significant reduction in the number of cells invaded by DOX-treated parental compared to DOX-treated spheroid cells ($p<0.01$) (See Figure 5.8, Panel **A** and **B**). There was no statistically significant increase in the percentage invasion under all conditions except in untreated parental verses DOX-treated parental cells ($p<0.05$) (See Figure 5.8, Panel **C**).

In the BeWo cell line (see Figure 5.9, Panel A and B), there was only a significant increase in the number of cells invaded in untreated spheroids compared to untreated parental cells ($p<0.05$). The percentage of invasion followed the same pattern (See Figure 5.9, Panel C).

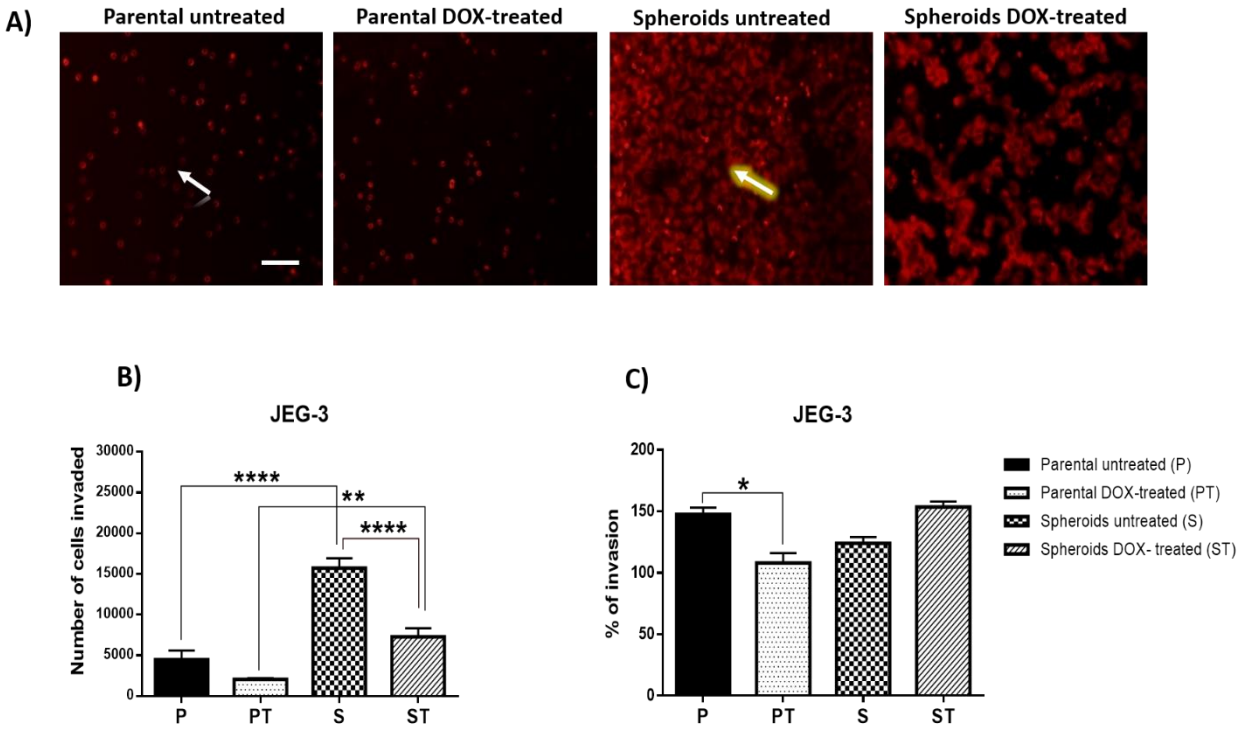

Figure 5.8: JEG-3 invasion.

Panel **A**: Represents the number of JEG-3 cells invaded at 24 hours. Image was taken of the bottom coated membrane using an Olympus fluorescence microscope. Objective magnification 20X (Scale bar = 100 μm). Panel **B**: Represents the quantitative analysis of number of cells invaded using ImageJ and Graphpad software. Panel **C**: Represents the percentage of invasion calculated using the formula described in Section 2.13. The white bold arrow and glowing arrow are pointing towards the parental invaded cells and invaded spheroids respectively. Statistical significance was determined using a one-way ANOVA followed by Tukey's test for multiple comparisons. Data represent the mean ±SEM of three individual experiments, each performed in quintuplicate (****$p<0.0001$; **$p<0.01$; *$p<0.05$).

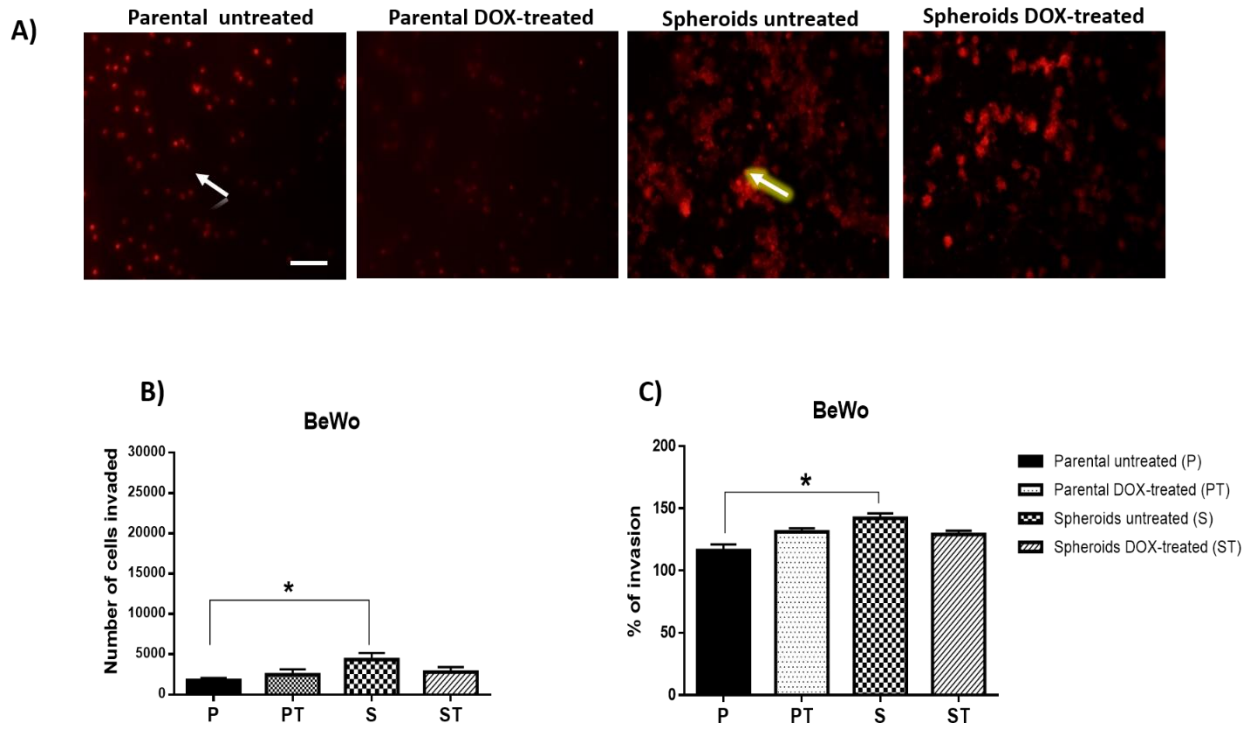

Figure 5.9: BeWo invasion.

Panel **A**: Represents the number of BeWo cells invaded at 24 hours. Image was taken of the bottom coated membrane using an Olympus fluorescence microscope. Objective magnification 20X (Scale bar = 100 μm). Panel **B**: Represents the quantitative analysis of number of cells invaded using ImageJ and Graphpad software. Panel **C**: Represents the percentage of invasion calculated using the formula described in Section 2.13. The white bold arrow and glowing arrow are pointing towards the parental invaded cells and invaded spheroids respectively. Statistical significance was determined using a one-way ANOVA followed by Tukey's test for multiple comparisons. Data represent the mean ±SEM of three individual experiments, each performed in quintuplicate (n=; *p<0.05).

5.2.2.3 The invasion of MCF-7 cell line

In MCF-7 cells, there was a significantly higher number of cells invading in spheroids (untreated and DOX-treated) compared to parental cells (untreated and DOX-treated). Moreover, there was a significant reduction in the number of cells invaded by DOX-treated parental cells compared to DOX-treated spheroidal cells ($p<0.0001$) (See Figure 5.10, Panel **A** and **B**). The percentage of invasion showed a statistically significant increase between parental cells (both DOX-treated and untreated) compared to their spheroidal cell counterparts ($p<0.01$) (See Figure 5.10, Panel **C**).

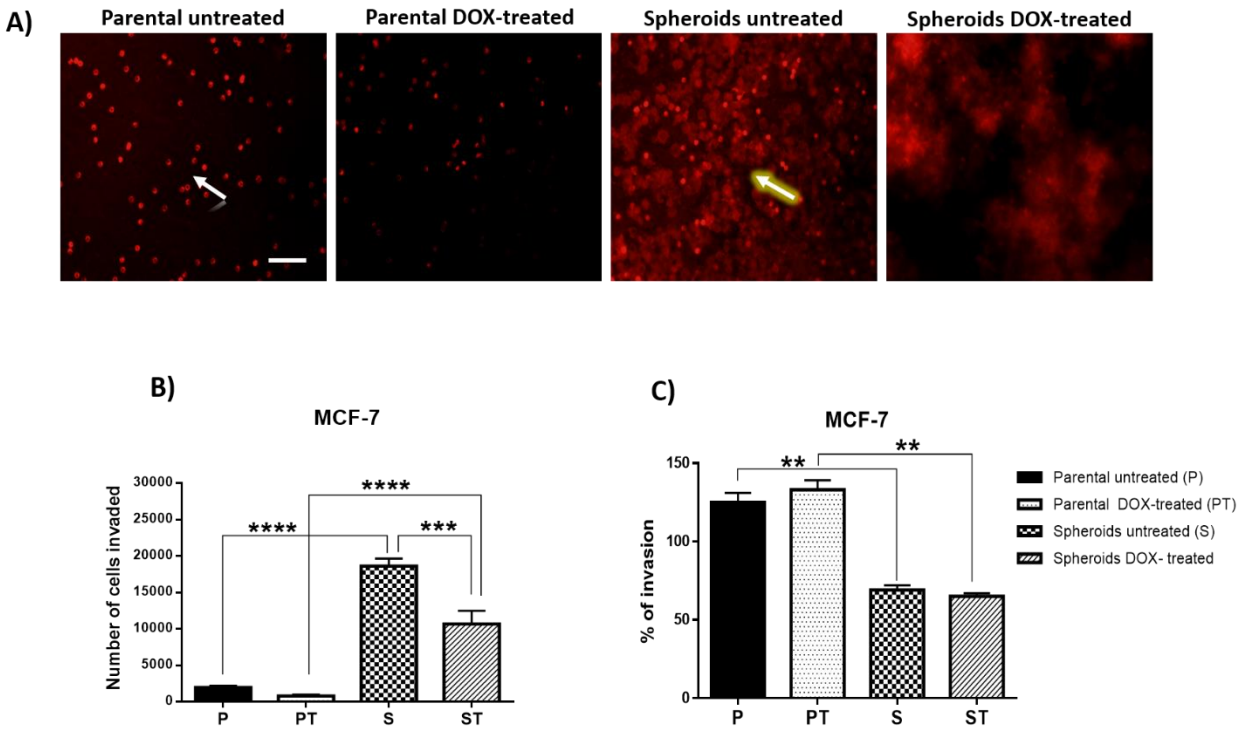

Figure 5.10: MCF-7 invasion.

Panel **A**: Represents the number of MCF-7 cells invaded at 24 hours. Image was taken of the bottom coated membrane using an Olympus fluorescence microscope. Objective magnification 20X (Scale bar = 100 µm). Panel **B**: Represents the quantitative analysis of number of cells invaded using ImageJ and Graphpad software. Panel **C**: Represents the percentage of invasion calculated using the formula described in Section 2.13. The white bold arrow and glowing arrow are pointing towards the parental invaded cells and invaded spheroids respectively. Statistical significance was determined using a one-way ANOVA followed by Tukey's test for multiple comparisons. Data represent the mean of three individual experiments, each performed in quintuplicate (n=3±SEM; ****p<0.0001; ***p<0.001; **p<0.01).

5.2.3 3-D Spheroid BME cell invasion assay

3-D Spheroid BME cell invasion assays were carried out to compare the invasive potential of untreated and DOX-treated spheroidal cells. ImageJ software was used to analyse all confocal images, to measure changes in the invasion area at 12, 24 and 48 hours.

5.2.3.1 3-D invasion by spheroids produced from transformed trophoblast cell lines

In HTR8/SVneo cells, there was a significant increase in invasion potential observed for untreated spheroid compared to DOX-treated spheroids (see Figure 5.11). The significance was proportional with time. At 12 hours, there was no significant difference in the invasion capacity between untreated and DOX-treated spheroids. On the other hand, a significant increase was observed in invasion capacity of the cells at 24 and 48 hours.

This pattern of invasion was also noticed in the TEV-1 cell line. Untreated spheroids showed significant increases in invasion area compared to DOX-treated spheroids at 24 and 48 hours. In both transformed trophoblast cell lines (HTR8/SVneo and TEV-1), the size of the untreated spheroids were found to be larger than DOX-treated spheroids. Furthermore, a polygonal morphology with stretched protrusions was formed by the cells, which was clear in the untreated spheroid condition (See Figure 5.11 and 5.12, Panel **A**). In untreated spheroids invasion increased with time but these invasive characteristics were minimal (at 24 and 48 hours) or absent (at 12 hours) in DOX-treated spheroids. See Figure 5.11 and 5.12, Panel **B**).

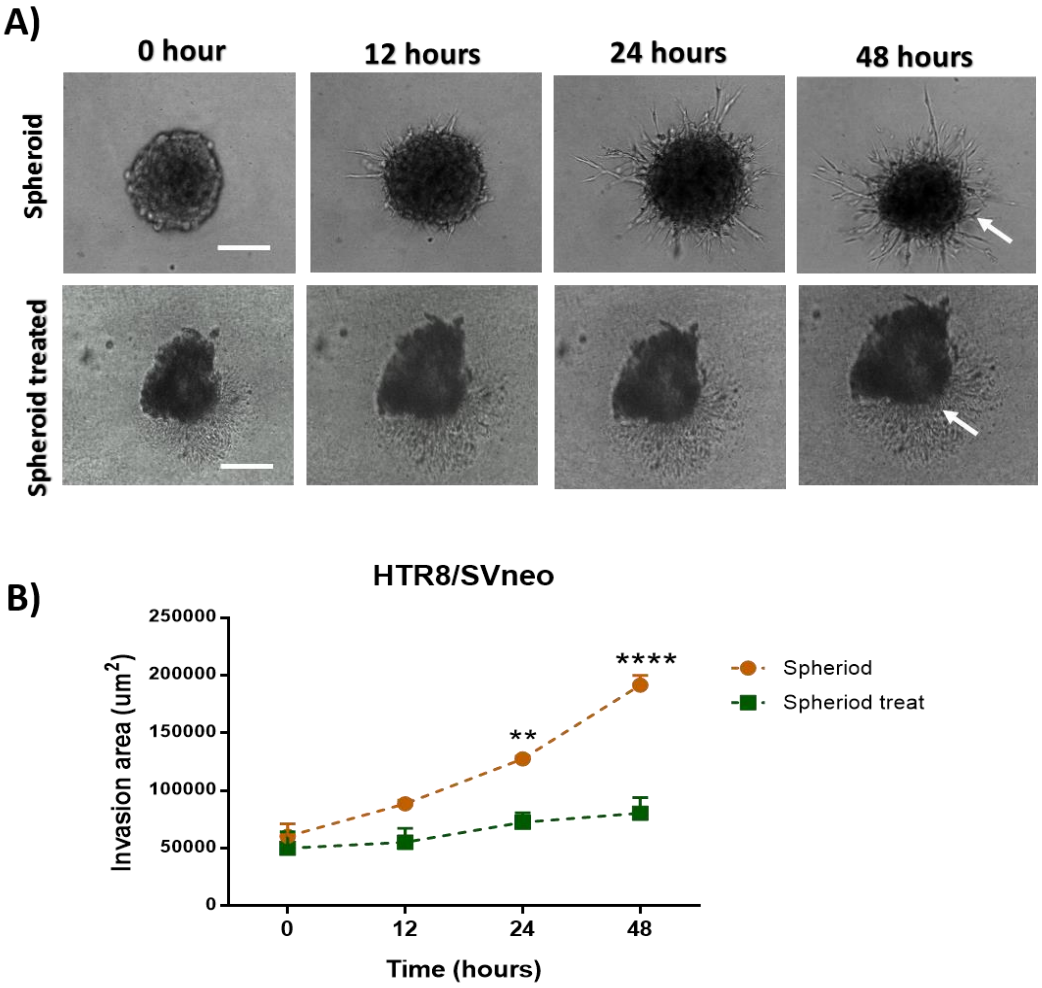

Figure 5.11: Invasion potential of untreated and DOX-treated spheroids of HTR8/SVneo.

Panel **A**: Represents images of invasion pattern of HTR8/SVneo untreated and DOX-treated spheroidal cells using confocal microscopy. Objective magnification=10X. Panel **B**: Represents the quantitative analysis of invasion area of untreated and DOX-treated spheroidal cells using ImageJ and Graphpad software. White bold arrow indicates active protrusions from spheroid untreated, which was clearer than in spheroid DOX-treated. Statistical significance was determined using two-way ANOVA followed by Sidak's multiple comparisons test performed to compare invasion area between untreated and DOX-

treated spheroids at different times. Data represent the mean ±SEM of three individual experiments, each performed in quintuplicate (****p<0.0001; **p<0.01).

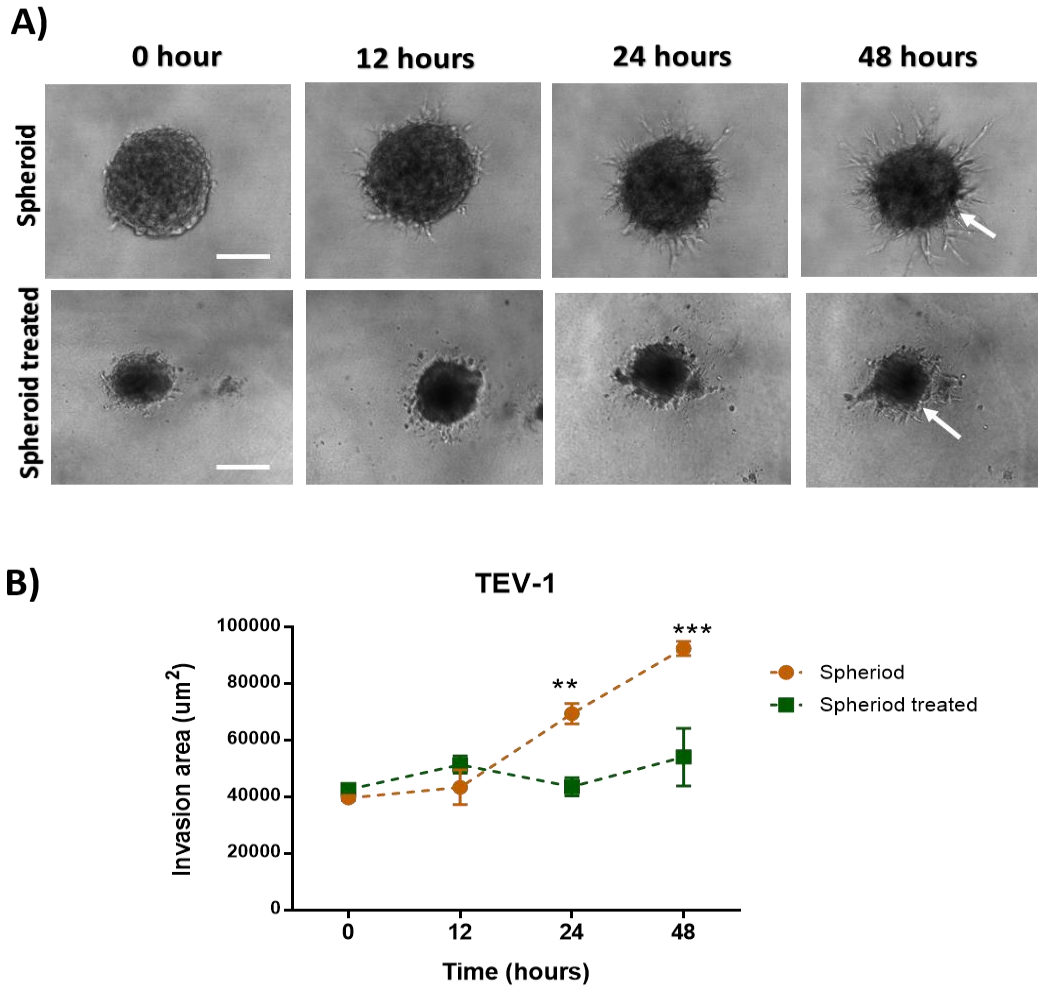

Figure 5.12: Invasion potential of untreated and DOX-treated spheroids of TEV-1.

Panel **A**: Represents images of invasion pattern of TEV-1 spheroids untreated and DOX-treated cells using confocal microscopy. Objective magnification=10X. Panel **B**: Represents the quantitative analysis of invasion area of untreated and DOX-treated spheroid cells using ImageJ and Graphpad software. White bold arrow indicates active protrusions from spheroid untreated, which was clearer than in spheroid DOX-treated. Statistical significance was determined using two-way ANOVA followed by Sidak's multiple comparisons test performed to compare invasion area between untreated and DOX-treated spheroids at different times. Data represent the mean ±SEM of three individual experiments, each performed in quintuplicate (***p<0.001; **p<0.01).

5.2.3.2 3-D invasion by spheroids produced from choriocarcinoma cell lines

Both choriocarcinoma cell lines (JEG-3 and BeWo) were developed from trophoblast tumours. The size of the untreated spheroids were found to be larger than that of transformed trophoblast cells (See Figures 5.13 and 5.14, Panel **A** respectively). In the case of JEG-3 cells, there was a significant increase in invasion potential observed in untreated spheroids

compared to DOX-treated spheroids at 12, 24 and 48 hours. However, the DOX-treated spheroids from JEG-3 cells only produced a collection of spheroid like bodies without any invasive properties (see Figure 5.13, Panel **B**). Similarly, in BeWo cells, the untreated spheroids showed a higher invasion potential than DOX-treated spheroids at 12, 24 and 48 hours (See Figure 5.14, Panel **B**). In contrast, the DOX-treated cells failed to produce any effective spheroids. In both choriocarcinoma cell lines (JEG-3 and BeWo), the size of the untreated spheroids were found to be larger than the DOX-treated spheroids.

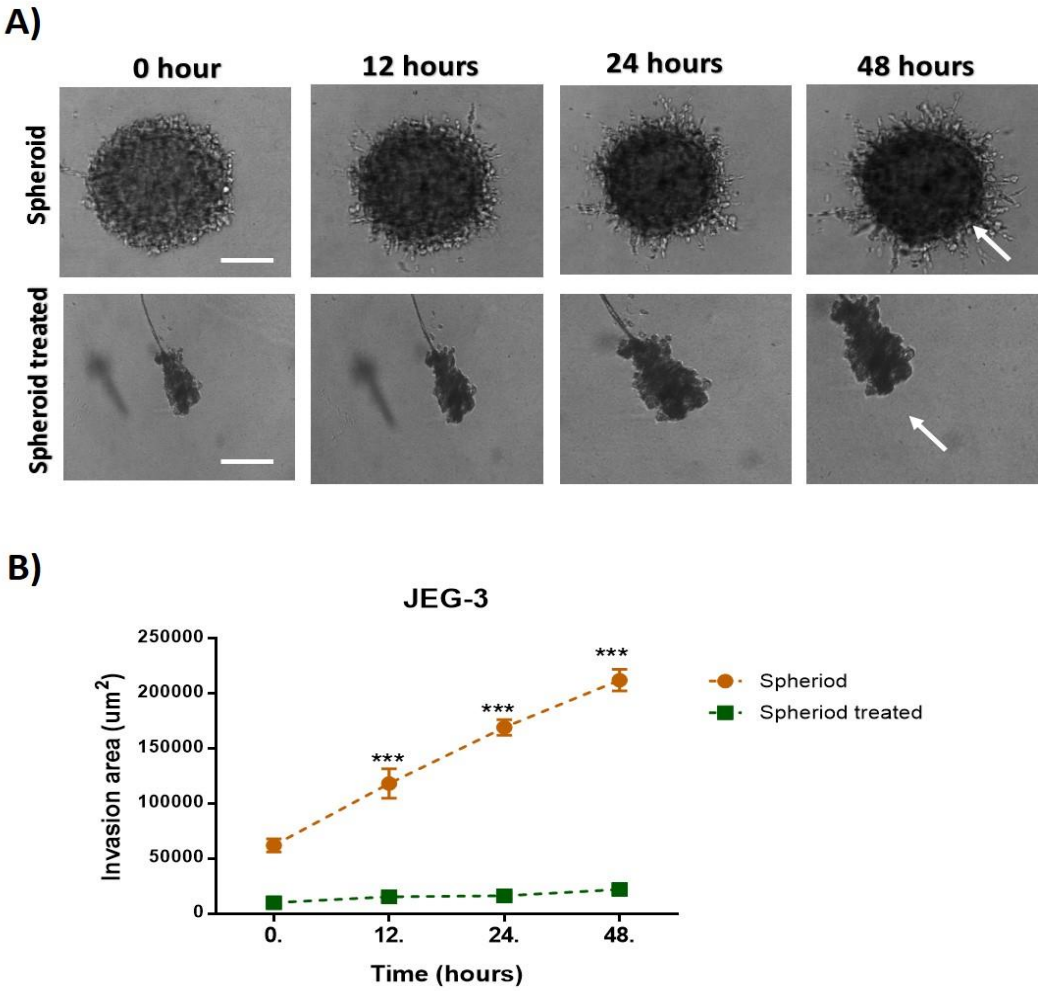

Figure 5.13: Invasion potential of untreated and DOX-treated spheroids of JEG-3.

Panel **A**: Represents images of invasion pattern of JEG-3 spheroids untreated and DOX-treated cells using confocal microscopy. Objective magnification=10X. Panel **B**: Represents the quantitative analysis of invasion area of spheroid untreated and DOX-treated cells using ImageJ and Graphpad software. White bold arrow indicates active protrusions from spheroid untreated, which was clearer than in spheroid treated. Statistical significance was determined using two-way ANOVA followed by Sidak's multiple comparisons test performed to compare invasion area between untreated and DOX-treated spheroids at different times. Data represent the mean ±SEM of three individual experiments, each performed in quintuplicate (***$p<0.001$).

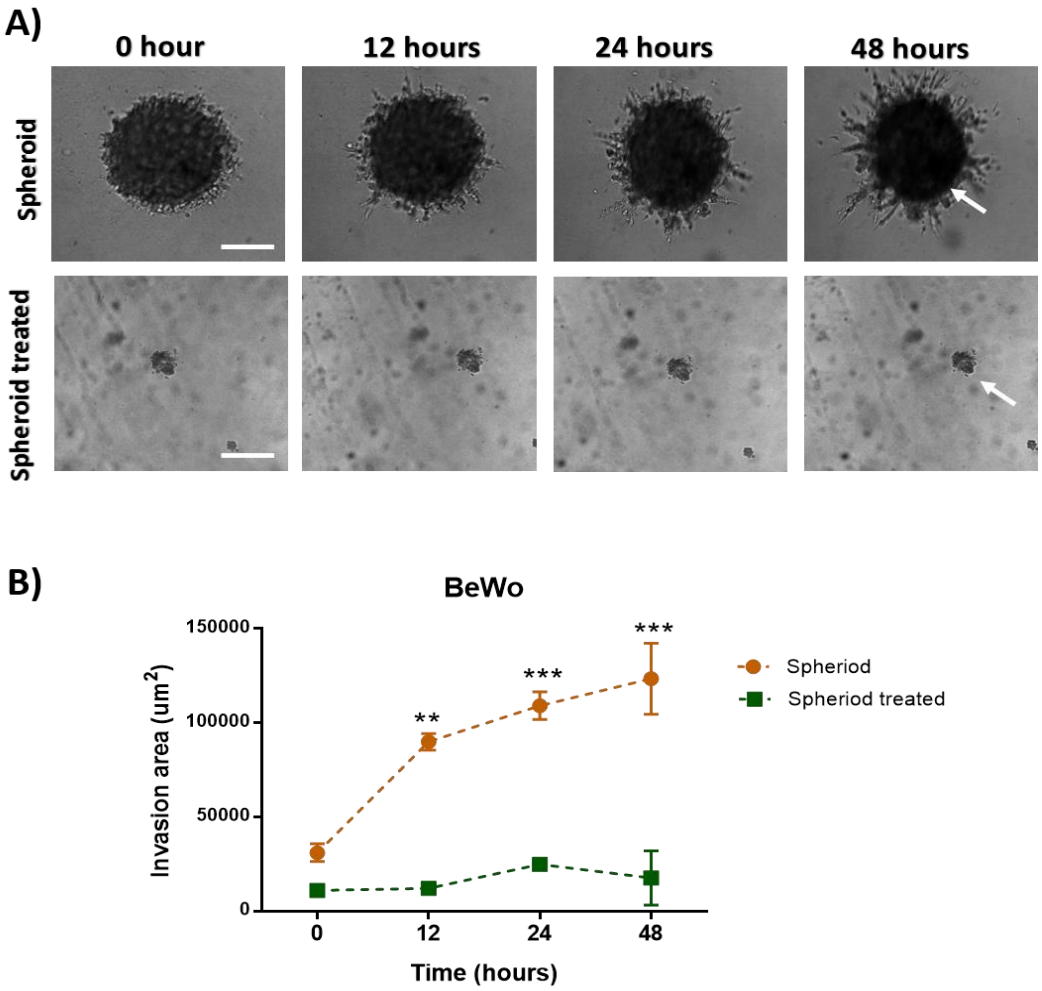

Figure 5.14: Invasion potential of spheroids untreated and DOX-treated of BeWo.

Panel **A**: Represents images of invasion pattern of BeWo spheroids untreated and DOX-treated cells using confocal microscopy. Objective magnification=10X. Panel **B**: Represents the quantitative analysis of invasion area of spheroid untreated and DOX-treated cells using ImageJ and Graphpad software. White bold arrow indicates active protrusions from spheroid untreated, which was clearer than in spheroid DOX-treated. Statistical significance was determined using two-way ANOVA followed by Sidak's multiple comparisons test performed to compare invasion area between untreated DOX-treated spheroids at different times. Data represent the mean ±SEM of three individual experiments, each performed in quintuplicate (***p<0.001; **p<0.01).

5.2.3.3 3-D invasion by spheroids produced from adenocarcinoma breast cancer cell line.

In MCF-7 cells, untreated and DOX-treated spheroids remained as cell aggregates and did not invade into the surrounding invasion matrix. It has failed to produce effective spheroids in 3-D culture. The analysis showed no significant difference in invasion potential of untreated and DOX-treated spheroids. It was also evident in the micrographs that the

spheroids had failed to produce a polygonal morphology or an even network structure (See Figure 5.15, Panel **A** and **B**).

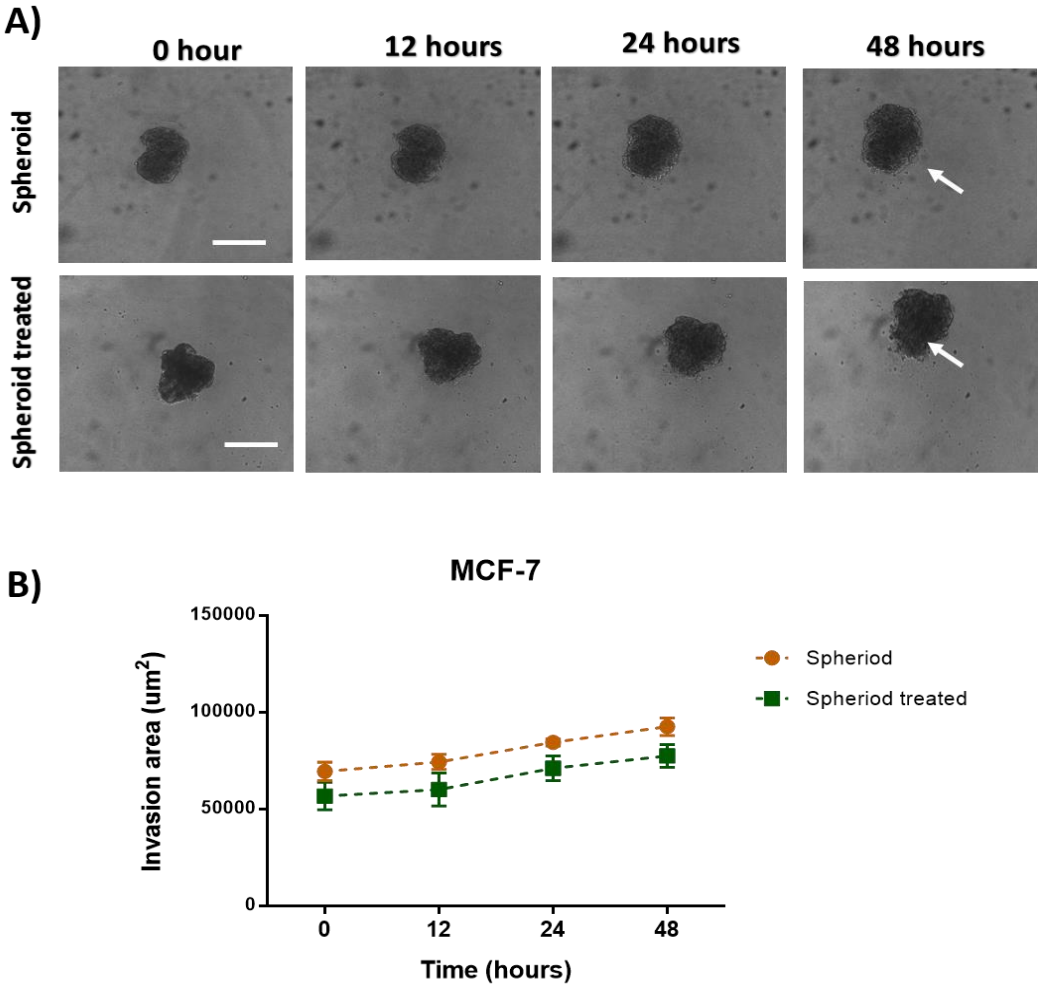

Figure 5.15: Invasion potential of untreated and DOX-treated spheroids of MCF-7.

Panel **A**: Represents images of invasion pattern of MCF-7 spheroids untreated and DOX-treated cells using confocal microscopy. Objective magnification=10X. Panel **B**: Represents the quantitative analysis of invasion area of spheroid untreated and DOX-treated cells using ImageJ and Graphpad software. White bold arrow indicates active protrusions from spheroid untreated, which was not pronounced in DOX-treated spheroids). There was no statistically significant difference determined by using two-way ANOVA followed by Sidak's multiple comparisons test performed to compare invasion area between untreated and DOX-treated spheroids at different times. Data represent the mean ±SEM of three individual experiments, each performed in quintuplicate.

5.3 Discussion

Successful placental implantation requires distinct cellular functions including attachment, migration and invasion of EVTs into the uterine endometrium (Norwitz *et al.,* 2001). Reduced or aggressive invasion can cause gestational complications such as placental accreta (or choriocarcinoma) and PE or intrauterine growth restriction (IUGR) respectively (Graham and Lala, 1992). Spheroids produced from 3-D cultures are a useful method to investigate the physiological events such as wound healing, invasion and metastasis (Oudar, 2000). Therefore, the aim of this chapter was to investigate and comparatively analyse the invasive potentials of parental and spheroidal cells from transformed trophoblast (HTR8/SVneo and TEV-1), choriocarcinoma cell lines (JEG-3 and BeWo) and MCF-7 cell line.

5.3.1 *In vitro* cell migration analysis using scratch /wound healing assay

Migration is a key property of living cells and plays a critical role in embryonic development, immune response, vascular morphogenesis and tissue repair (Kramer *et al.,* 2011). Many pathological processes, such as cancer metastasis and inflammation, also involve cell migration (Kramer *et al.,* 2011). Wound healing assays are suitable methods for studying the effects of cell–to-matrix and cell–to-cell interactions during migration (Liang *et al.,* 2007). It is a simple, common and economical technique for studying cell migration *in vitro*. Therefore, it is an important and useful tool in biomedical research such as cancer biology and cell biology (Jain *et al.,* 2012). In fact, the comparative study of migratory behaviour of malignant cells and non-malignant trophoblast cells can shed light onto the prognosis of tumour metastasis (Kramer *et al.,* 2011). The present study, combines 3-D and 2-D cell culture techniques by producing spheroids to mimic the *in vivo* situation.

5.3.1.1 Migration of transformed trophoblast cell lines

HTR8/SVneo cell line has been previously used to study cell adhesion and migration (Hannan, 2010). The results explained herein showed that the migration of HTR8/SVneo parental cells was increased at 24 and 48 hours. As there was no treatment given to the parental cells, they may have proliferated and migrated at normal speed. In contrast, migration was greater in HTR8/SVneo DOX-treated parental than untreated parental cells at 24 hours. However, the wound re-opened at 48 hours. This could be because 250 ng of DOX may have showed a delayed inhibitory effects on the cell migration. DOX has been reported to develop resistance in tumour cells, and toxicity in healthy tissues and cells (Gajewski, 2007). Therefore, DOX maybe producing delayed anoikis in these cells by disrupting their contact with the ECM as explained by Gilmore (2005). Interestingly, the rate of migration in

untreated spheroids was higher at 48 hours. Spheroidal cells migrate faster than the parental cells. Since spheroids, act like solid tumours *in vivo*, the observed high migration by spheroidal cells may be due to their deregulated proliferation and an uncontrolled speed of migration (Ferretti *et al.,* 2007). However, DOX-treated spheroidal cells showed a lower rate of migration than untreated spheroids at 48 hours. Furthermore, the monolayers produced by the spheroidal cells have the ability to re-grow under normal conditions, as clusters which are different from the normal cell monolayers [see section 4.2.3.2, Figures 4.6 to 4.10 Panel **D** (chapter 4)]. This might have affected the migration of spheroidal, especially DOX-treated cells.

The migration of parental TEV-1 cells increased and covered almost 100% of the wound area within 24 and 48 hours. This could suggest a high proliferative and migratory capacity of these cells. In contrast, after treating with DOX, the wound initially healed well (95% by 24 hours), but re-opened by 48 hours. This may suggest that DOX produces delayed anoikis in these cells by disrupting their contact with the ECM (Gilmore, 2005), and also affects the proliferation or migration of the cells (Denard *et al.*, 2012).

Data from this study showed that spheroids derived from TEV-1 show high migration and covered most of the scratch area at 24 and 48 hours. However, DOX-treated spheroid cells showed a lower rate of migration at 48 hours, perhaps because of DOX mediated effects on spheroidal migration speed, as these cells are plated as single cells and grow as monolayers.

5.3.1.2 Migration of choriocarcinoma cell lines

The migration of JEG-3 parental cells showed the wounds healed within 48 hours. However, after treating with DOX, the wound healing increased at 24 hours, interestingly, the wound re-opened at 48 hours. This reduction in wound covered area by the DOX indicates an effect of DOX on proliferation or migration of these cell. There was a slight increase in wound covered area in untreated spheroids. In contrast, the migration was slightly decreased in DOX-treated spheroids at 48 hours compared to 24 hours. In BeWo cells, the migration of parental cells was increased at 48 hours. This may be due to the slow growing nature of the BeWo cell line (Aplin *et al.,* 1992). Since the cells are slow growing, the syncytial nature of the cell was unpredictable and as a result the scratch was not 100% covered. However, in parental DOX-treated cells the wound covered area was increased at 24 hours but decreased at 48 hours. This may be due to the slow effects of DOX. Untreated spheroids showed increased wound coverage at 48 hours. Overall, the wound healing of transformed trophoblast cells in both parental untreated and spheroids cells showed higher wound coverage than placental choriocarcinoma cell lines. This unexpectedly reduced rate of

wound healing in JEG-3 and BeWo cells may be due to the fact that these cell lines (despite having originated from choriocarcinoma), have a syncytial-like morphology. That is, they both grow in clusters of cells and migrate as sheets or clumps. Therefore, difference in cell motility cannot be observed as in transformed trophoblast cells.

5.3.1.3 Migration of MCF-7 tumour cell line.

The increase of cell covered area in the parental MCF-7 cell experiments was lower than for the trophoblast cell lines. The parental MCF-7 under DOX-treated condition, showed no significant change in cell covered area at 24 and 48 hours. This may be because the cells develop resistance to DOX over several sub-culture. Although the speed of migration of DOX-treated parental cells was low, the wound showed no signs of "re-opening" as in transformed trophoblast cells. Therefore, it is possible that the effects of DOX are somewhat resisted by the transformed trophoblast cells until 24 hours. However, long term exposure of DOX would have disrupted the cell-to-ECM contact. This phenomenon was not shown in MCF-7.

DOX is an anthracycline antibiotic which can inhibit cell proliferation and induce apoptosis in tumour cells (Wang *et al.,* 2004). Despite the fact that DOX is an active drug for breast cancer therapy and the best effect is only seen when used in combination of cyclophosphamide, Adriamycin, 5-Fluorouracil (CAF) (Czeczuga-Semeniuk *et al.,* 2004). Ciftci and colleagues (2003), have demonstrated that DOX can inhibit cell proliferation up to 70-80% in 24 hours in the MCF-7 cell line regardless of concentration. There was no significant change observed in covered area by spheroids at 24 and 48 hours. DOX-treated spheroids of MCF-7 showed there was a slight increase in wound coverage at 48 hours compared to 24 hours, which may be due to the delayed effect of DOX. Studies by Bartholoma and colleagues, (2005) have demonstrated that spheroids of breast cancer cell lines (mainly MCF-7) can be used to study the cytotoxic effects of different drugs.

5.3.2 Cell invasion Assay

This assay is designed to monitor cell invasion by using the BD Falcon™ BioCoat tumour invasion system. This assay kit contains a FluoroBlok™ 96 well insert plate with a membrane (8.0 μm pore size). This membrane is coated with matrigel matrix that only allows single cells to pass. However, in this present study, spheroids which have a total size greater than 8.0 μm were involved. Therefore, the spheroids were dispersed using trypsin into single cells before performing the invasion assay. Also, in order to differentiate cell migration from invasion the experiment was duplicated in a control migration plate with a porous membrane. Hence, the migration plate will only measure the number of cells travelling through this

porous membrane. On the other hand, the cell invasion assay monitors the cell movement through the matrigel (Kramer *et al.,* 2013). The quantitation of this assay is achieved by pre-labelling cells with a fluorescent dye as only labelled cells passing through the matrigel can be detected.

5.3.2.1 2-D Invasion by transformed trophoblast cell lines

In this study, HTR8/SVneo cells showed a higher invasion capacity in untreated spheroids compared to other conditions. Previous studies have used HTR8/SVneo cell line as a model to investigate the proliferation and invasion of trophoblast cells (Zuo *et al.,* 2014). While, TEV-1 cell line showed a highly significant difference in invasive capacity of untreated and DOX-treated spheroids compared to their respective parental counterparts. Previously, the TEV-1 cell line has been shown to have a higher invasive potential in response to TGFβ1 treatment *in vitro* (Feng *et al.,* 2005). TGFβ1 under *in vivo* conditions is reported to play a significant role in regulating extravillous trophoblast invasion, migration and proliferation (Graham and Lala, 1991; Peng, 2003). Therefore, TEV-1 may be highly useful as a cell model to study the physiological and functional properties of human extravillous trophoblast invasion (Feng *et al.,* 2005). Interestingly, the invasion by DOX-treated spheroids was lower than the untreated spheroids in TEV-1. Therefore, it can be suggested that the treatment with DOX has reduced the invasion capacity of cells. However, the mechanism through which DOX inhibits invasion of cells is not completely understood (Denard *et al.,* 2012). It is known that the trophoblast-derived proteinases (MMPs and the serine proteases) are essential for trophoblast invasion (Librach *et al.,* 1991). Also it has been previously shown that DOX treatment reduced the production of pro-MMP-2 and pro-MMP-9 at 24 hours of treatment, resulting in reduced cell proliferation along with reduced invasion. However, the status of MMPs in this study is yet to be investigated (Shen *et al.,* 2009).

5.3.2.2 2-D Invasion by choriocarcinoma cell lines

JEG-3 cells showed similar result to TEV-1 cells, in that there was a highly significant increase in invasion capacity of untreated and DOX-treated spheroids compared to their respective parental cells. This confirms the findings by Buck and colleagues (2015), who have shown that the linear growth and invasion potential of spheroids from the hybridoma cell line, AC-1M88 (a fusion of primary EVT cells and the JEG-3 choriocarcinoma cell line), are much higher than differentially grown single cells. The invasion potential of untreated and DOX-treated spheroids was increased due to the spheroidal features, as they act as solid tumour.

In the case of BeWo, the only significant increase in invasion capacity was observed in untreated spheroids compared to untreated parental cells. The invasiveness of spheroids produced from JEG-3 and BeWo, as an *in vitro* model have been previously studied (Grummer *et al.,* 1989). According to their experiment, differences in the adhesion and invasion processes were observed. JEG-3 cells showed the highest adhesion rate to endometrial epithelium and a fast/deep invasion into stroma. However, BeWo cells showed low adhesion rate to endometrial epithelium and shallow invasion into stroma. The data from this current study also confirmed the fact that the invasion potential of JEG-3 (both parental and spheroidal cells) was found to be higher than that of BeWo cells.

5.3.2.3 2-D Invasion of the MCF-7 cell line

Although, MCF-7 cells are derived from a non-invasive breast cancer compared to invasive cell line MDA-MB-231(Nagaraja *et al.,* 2006), the MCF-7 cell line demonstrated similar results to TEV-1 and JEG-3 cells. There was a significantly high invasion capacity of untreated and DOX-treated spheroids compared to their respective parental cells. This could be that the MCF-7 spheroids after dispersion into monolayers exert invasive properties as they still have stem-like features. However, DOX-treated parental cells showed lower numbers of cells invading than untreated parental cells. Several studies have shown that DOX inhibits the growth of breast cancer cell lines in a dose and time dependant manner (Sharma *et al.,* 2004). Therefore, the observed results were expected. It is known that DOX can reduce the invasion potential of MCF-7 cells by reducing the rate of proliferation (Pichot *et al.,* 2009) and also reduce the invasion potential of spheroids produced by MCF-7 (Doillon *et al.,* 2004). MCF-7 spheroids after dispersal showed higher number of cells invading the matrix when compared with the parental cells. This may be due to the nature of spheroids which act like solid tumours (Khanna *et al.,* 2014).

Overall, it is clear that the spheroids produced from both transformed trophoblast cell lines (HTR8/SVneo and TEV-1) and choriocarcinoma (JEG-3 and BeWo) cell lines were capable of invasion. The results of the present study are in general agreement with another study, which showed that there were potentially different invasive properties of HTR8/SVneo, JEG-3 and BeWo dependent on the cell type (Lash *et al.,* 2007). However, monolayer cell invasion systems are commonly used to evaluate invasion of single cells. Therefore, this method is not competent enough to study the invasion potential of a spheroid. Although the spheroids were artificially separated into single cells to suit the 2-D invasion assay, it is not entirely appropriate to study the interactions between the invasive spheroid and the basement membranes. In order to compare the invasive behaviour of untreated and DOX-treated spheroids a further experiment 3-D invasion assay experiment is necessary.

5.3.3 3-D Spheroid BME cell invasion assay

The 3-D spheroid BME cell invasion assay provides an easy, quick and quantitative process to compare morphological patterns as well as the speed of invasion. The study of parameters related to how cells can invade an artificial basement membrane acting as ECM in response to chemoattractants and/or inhibiting compounds, is important for embryonic development, immune response and tumour metastasis (**www[21])** . In this assay spheroids produced within each well can invade the surrounding matrix resulting in spindle-like formation, and the absence of this would indicate that there is less or no invasion (**www[21])**. This assay is commonly used in *in vitro* drug testing to compare the invasive patterns of aggressive tumours with and without drug intervention. The main advantage of this assay is that cell movement through a 3-D matrix closely mimics invasion *in vivo* (**www[21])**. Interestingly, the invasion process occurs from cell clusters with well-established cell–cell interactions rather than from single cells, closely reflecting the *in vivo* situation in cancer. However, to the author's knowledge this is the first study that has used this assay to compare the invasive potential of spheroids originating from transformed trophoblast and choriocarcinoma placental cells.

5.3.3.1 3-D invasion of spheroids produced from transformed trophoblast cell lines

In the case of HTR8/SVneo, the size of both untreated and DOX-treated spheroids were initially almost equal. However, with increasing time untreated spheroids invaded a large surface area with a more consistent growth trend than treated spheroids (viewed under time-lapse images). However, DOX-treated spheroids showed minimal growth and invasion (Figure 5.11).

It is also possible that the cells may have produced a mass to compensate for the effects of DOX, but that they retained some properties of invasion. For TEV-1 cells, the initial size of DOX-treated spheroids was smaller than that of untreated spheroids (Figure 5.12). However, untreated spheroid invasion increased with time. In contrast, compared to untreated spheroids, the invasion of DOX-treated spheroids was found to be low; yet they did show limited invasive potential in 3-D. Further investigations are needed to understand the survival mechanisms of these cell types after treatment.

5.3.3.2 3-D invasion of spheroids produced from choriocarcinoma cell lines

In the case of JEG-3 and BeWo cells, untreated spheroids showed a distinct increase in invading area with time (See Figure 5.13 and 5.14). These data suggest that spheroids derived from choriocarcinoma cell lines can potentially invade faster than those of transformed trophoblast cells. It is worth noting that a previous study has shown that BeWo cells can produce spheroids *in vitro*, (Grummer *et al.,* 1994). In this present study, BeWo

cells were able to form spheroids (See Figure 5.14 Panel **A**). However, DOX-treated spheroids from both JEG-3 and BeWo cells have shown an unusual profile. The distorted shape of spheroids did not show any invasion in either cell line. This may be due to the persisting effect of the DOX treatment in these cell lines.

5.3.3.3 3-D invasion of spheroids produced from the MCF-7 cell line

According to the supplier's (Amsbio) result (they used the same kit to test the morphology of 3-D invasion and to analyse the surface area of the MCF-7 cell line during 4 days), MCF-7 cells remained as aggregates and did not invade into the surrounding invasion matrix. In contrast, invasive cells such as MDA-MB-231 did invade. The results in this study showed similar results and there was no significant difference in invasion capacity between MCF-7 spheroids that were DOX-treated and untreated. Data from the current study also confirmed that both untreated and DOX-treated spheroids of MCF-7 cells did not show any ability to invade. They formed an irregular mass of cells which were incapable of invasion. Non-invasive cancer cell lines stay as compact spheroids with a distinct border to the surrounding ECM and do not show any signs of invasion even after a long period of cultivation. However, invasive cell lines (such as the breast cancer line MDA-MB-231) start to invade into the surrounding matrix and show astral outgrowth from the spheroid (Kramer *et al.* 2013).

Almost all of the cell lines used in this study were able to produce spheroids with DOX treatment with different morphologies. However, the DOX-treated spheroids are found to be small with lower invasion capacity. Therefore, it can be suggested that DOX-treatment, due to its toxicity, has produced an accumulation of cells (instead of true spheroidal cells), that are trying to survive in the stressed cellular microenvironment to avoid apoptosis. Further detailed study is necessary to understand the underlying mechanisms of invasion by spheroids produced from trophoblast (HTR-8/SVne, TEV-1, JEG-3 and BeWo) cell lines.

5.4 Conclusions

The data obtained from this chapter suggest that the transformed trophoblast (HTR8/SVneo and TEV-1) and choriocarcinoma (JEG-3 and BeWo) cell lines are capable of producing spheroids with different invasive properties. There was no significant difference in invasion ability of both untreated and DOX-treated spheroidal cells generated from MCF-7. The wound healing of transformed trophoblast cells in both parental untreated and spheroids cells showed higher healing coverage than placental choriocarcinoma cells. Moreover these spheroids have shown the potential to invade under 2-D culture conditions, with different invasive properties. As for 3-D cell culture a time dependant increase in the invasion was observed especially in non-resistant spheroids confirming their "stem-like" attributes.

Most of the previous studies focussed on JEG-3 and BeWo cells as a model of the invasive trophoblast. However, present study have shown HTR8/SVneo and TEV1 may also be used as additional models to represent physiologically rapidly dividing cells in the toxicological studies of chemotherapeutic agents.

Chapter 6

Comparative expression analysis of tumour associated factors in trophoblast cell lines under different conditions

6.1 Introduction

Human placenta is a multifaceted and poorly understood organ, which has an essential role not only in the supply of nutrients to the foetus but also in the maintenance of pregnancy (Ji *et al.,* 2013; **www[22])**. Primary human trophoblast cultures (CTBs and EVTs) may be ideal to study the molecular regulation of trophoblast invasion (Bilban *et al.,* 2010). They provide critical insights into placental function in normal and abnormal development (Rosario *et al.,* 2012). Furthermore, EVT cells that are derived from early pregnancy are much more invasive than those from term placentae (Ji *et al.,* 2013). Although, primary trophoblast cultures are useful tools to examine the differentiation and functions of the trophoblast, there are many major limitations to the use of these cells as *in vitro* models. Firstly, due to ethical constraints these cells are more difficult to obtain, and secondly, fresh primary cells have a very limited lifespan. Furthermore, they have limited ability to proliferate in culture, and hence, difficult to study the biochemical pathways and placental function (Ji *et al.,* 2013**)**. These limitations have hampered the use of these cells in standard molecular manipulation experiments, such as overexpression/silencing through plasmid DNA transfection etc.

In addition, the gestational age of the placental tissue can influence the differentiation potential of CTBs and must be taken into account when primary cultured trophoblast cells are used as an *in vitro* model (Ji *et al.,* 2013). In order to avoid these issues, several transformed model cell lines have been established over many years using different approaches. For example, trophoblast derived cell lines were used in an attempt to identify functional pathways differentially regulated by epigenetic modification (Novakovic *et al.,* 2011).

Trophoblast cell lines can be used as an alternative to primary trophoblast cells to study placental function *in vitro* including, the processes of differentiation/invasion, hypoxia/oxidative stress responses, and foeto-maternal immunology (Burleigh *et al.,* 2007). Since the cellular origins of transformed trophoblasts are likely to be diverse, it may be of value to increase the understanding of the unique and shared phenotypes of these cells on a global scale (Burleigh *et al.,* 2007).

Most of the available cell lines can be separated into three main groups: (1) cell lines originating from normal tissue, such as HTR8/SVneo, SGHPL-4 and RSVT-2; (2) cell lines originating from malignant tissue, such as BeWo, JEG-3 and JAR; and (3) cell lines originating from embryonic carcinomas which have evidence of trophoblast differentiation, such as H9, NCR-G3 and NCCIT (King *et al.,* 2000).

As explained in chapter 1, several tumour associated factors may also be expressed in human placenta. Cellular expression of these novel factors: ALDH3A1, AURK-A/C, PDGFRα, TWIST1, and JAG1 have been compared between NT and PE placentae in chapter 3. It would be interesting to study the changes in the expressions of these factors after spheroidal transformation. Apart from this it would be worth analysing the global changes in the protein/peptide expression between parental and spheroidal cells obtained in this study (Chapter 4). Recently, a new technique called SWATH-MS (Sequential Windowed Acquisition of All Theoretical Fragment Ion Mass Spectra), is being used for identification and quantification of a large number of proteins and proteomes from a complex mixture (Wang *et al.*, 2015). SWATH is a suitable tool for identifying more differential ratios, being (a) more sensitive in the detection of small differential ratios, and (b) capable to cover a larger dynamic range (Bourassa *et al.*, 2015). This could help to quantify dynamic changes in protein complex interaction level, for each different cell lines under different conditions.

The first aim of this chapter was to compare the status of the tumour associated factors, such as ALDH3A1, AURK- A/C, PDGFRα, TWIST1, and JAG1, in parental and spheroidal cells (untreated and DOX-treated) produced from trophoblast cell lines (HTR8/SVneo, TEV-1, JEG-3 and BeWo) and MCF-7 cell line.

The second aim was to investigate the changes in the global protein (peptide) expression profiles of non-resistant, and drug-resistant spheroids originated from transformed trophoblast cell lines (HTR8/SVneo and TEV-1) by using SWATH-MS.

6.2 Results

6.2.1 Relative mRNA expression

The relative expression of these factors were studied by comparing mRNA (qRT-PCR) expression under different conditions. Analysis was performed by using a one-way ANOVA followed by Tukey's Post-hoc test for multiple comparisons between (a) untreated parental versus DOX-treated parental, (b) untreated parental versus untreated spheroid, (c) untreated versus DOX-treated spheroids, and (d) DOX-treated parental versus DOX-treated spheroids.

6.2.1.1 Relative mRNA expression of ALDH3A1

HTR8/SVneo cells lines showed significant up-regulation of ALDH3A1 mRNA expression in untreated parental cells compared to (a) DOX-treated parental cells ($p< 0.0001$) and (b) untreated spheroids ($p<0.001$). Similarly, compared to DOX-treated spheroids, the untreated spheroidal cells showed an up-regulation of ALDH3A1 mRNA expression ($p<0.001$) (See Figure 6.1, Panel **A**). TEV-1 showed a significant in increase in mRNA expression of parental cells (both DOX-treated and untreated) compared to spheroidal cells counterparts. Moreover, there was a significant increase in mRNA expression in untreated spheroids of TEV-1 compared to DOX-treated spheroids ($p<0.05$) (See Figure 6.1, Panel **B**). On the other hand, the mRNA expression of ALDH3A1 in JEG-3 cells was significantly up-regulated in untreated spheroids compared to untreated parental cells ($p<0.01$) (See Figure 6.1, Panel **C**). BeWo cells showed a significantly higher level of ALDH3A1 mRNA expression in untreated parental compared to DOX-treated parental cells ($p<0.05$). Moreover, there was a significant up-regulation of ALDH3A1 mRNA expression level in DOX-treated BeWo spheroids compared to both DOX-treated parental and untreated spheroids ($p<0.001$) (See Figure 6.1, Panel **D**). As for MCF-7 cells, the mRNA expression levels in untreated spheroidal cells was significantly higher compared to its parental counterpart ($p<0.001$) and DOX-treated spheroids ($p<0.0001$) (See Figure 6.1, Panel **E**). There was also a significant difference in mRNA expression level in the same cell line between untreated parental and DOX-treated parental cells ($p<0.01$).

.

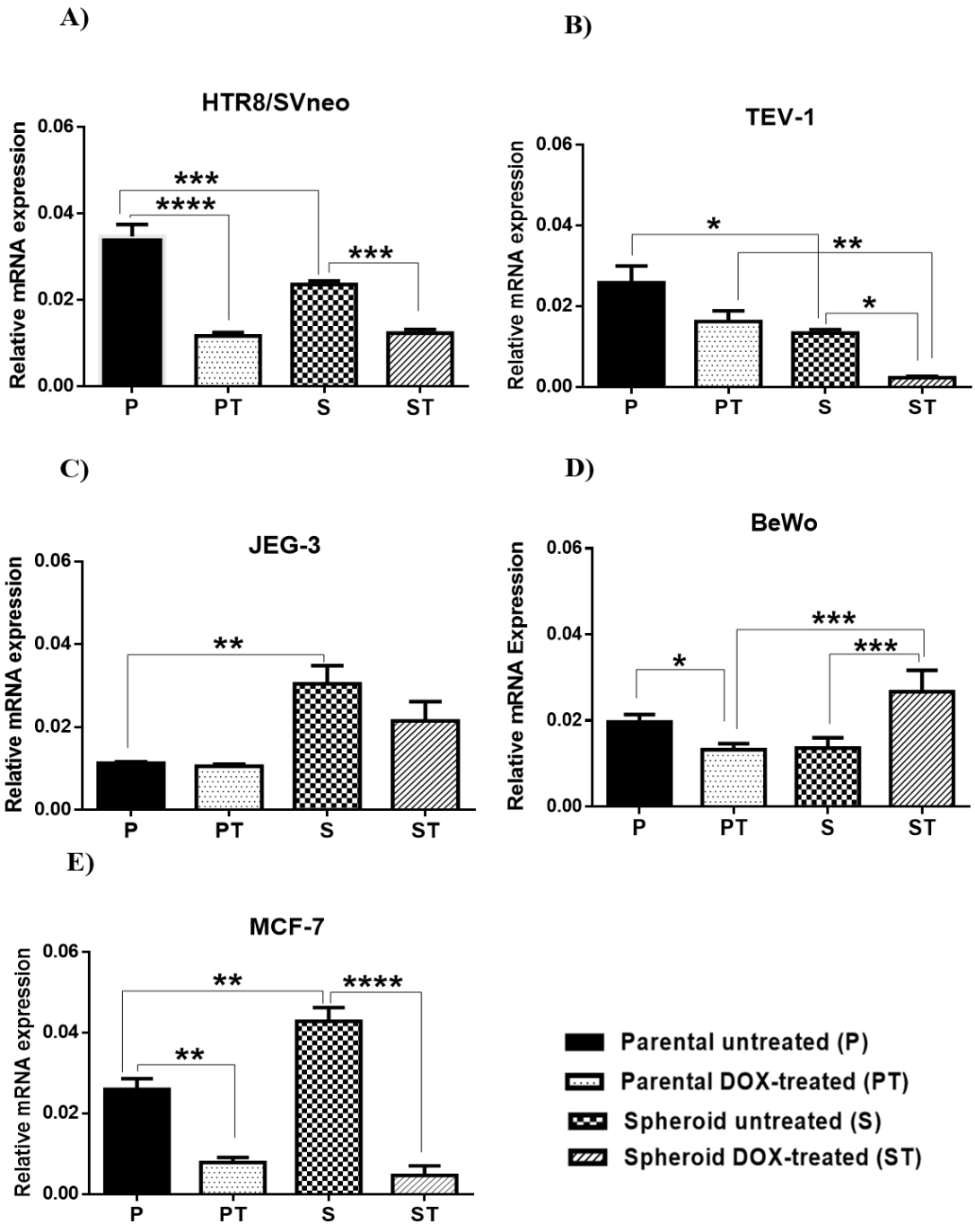

Figure 6.1: Relative mRNA expression of ALDH3A1.

The variance in mRNA expression was compared between different conditions. The data from HTR8/SVneo and TEV-1 cells are given in panels **A** and **B** respectively. Likewise, JEG-3 and BeWo cells data are presented in panels **C** and **D** respectively. Panel **E** shows the data from MCF-7 cells. Statistical significance was determined using a one-way ANOVA followed by Tukey's test for multiple comparisons. Data represent the mean ±SEM of three individual experiments, each performed in triplicate (****$p<0.0001$; ***$p<0.001$; **$p<0.01$; *$p<0.05$).

6.2.1.2 Relative mRNA expression of Aurora kinase A (AURK-A)

Figure 6.2 shows the relative mRNA expression of AURK-A in HTR8/SVneo, TEV-1, JEG-3, BeWo and MCF-7 cells. As seen in Panel **A,** HTR8/SVneo showed significantly higher AURK-A mRNA expression in untreated parental compared to DOX-treated parental cells ($p<0.01$); and between untreated spheroids compared to DOX-treated spheroids ($p<0.01$). In TEV-1 cells, there was a significantly higher level of mRNA expression in untreated parental compared to both DOX-treated parental and untreated spheroids ($p<0.0001$). Also, there was a significant up-regulation in untreated spheroids compared to DOX-treated spheroids ($p<0.01$) (See Figure 6.2, Panel **B**). However, there was no a statistically significant difference in the relative expression of AURK-A between any comparison in both choriocarcinoma cell lines (BeWo and JEG-3) (See Figure 6.2, Panel **C** and **D**). In the MCF-7 cell line, there was a significant up-regulation observed in untreated parental compared to both DOX-treated parental and untreated spheroids ($p<0.0001$). Also, there was a significant difference in mRNA expression in DOX-treated parental versus DOX-treated spheroids ($p<0.0001$) (See Figure 6.2, Panel **E)**.

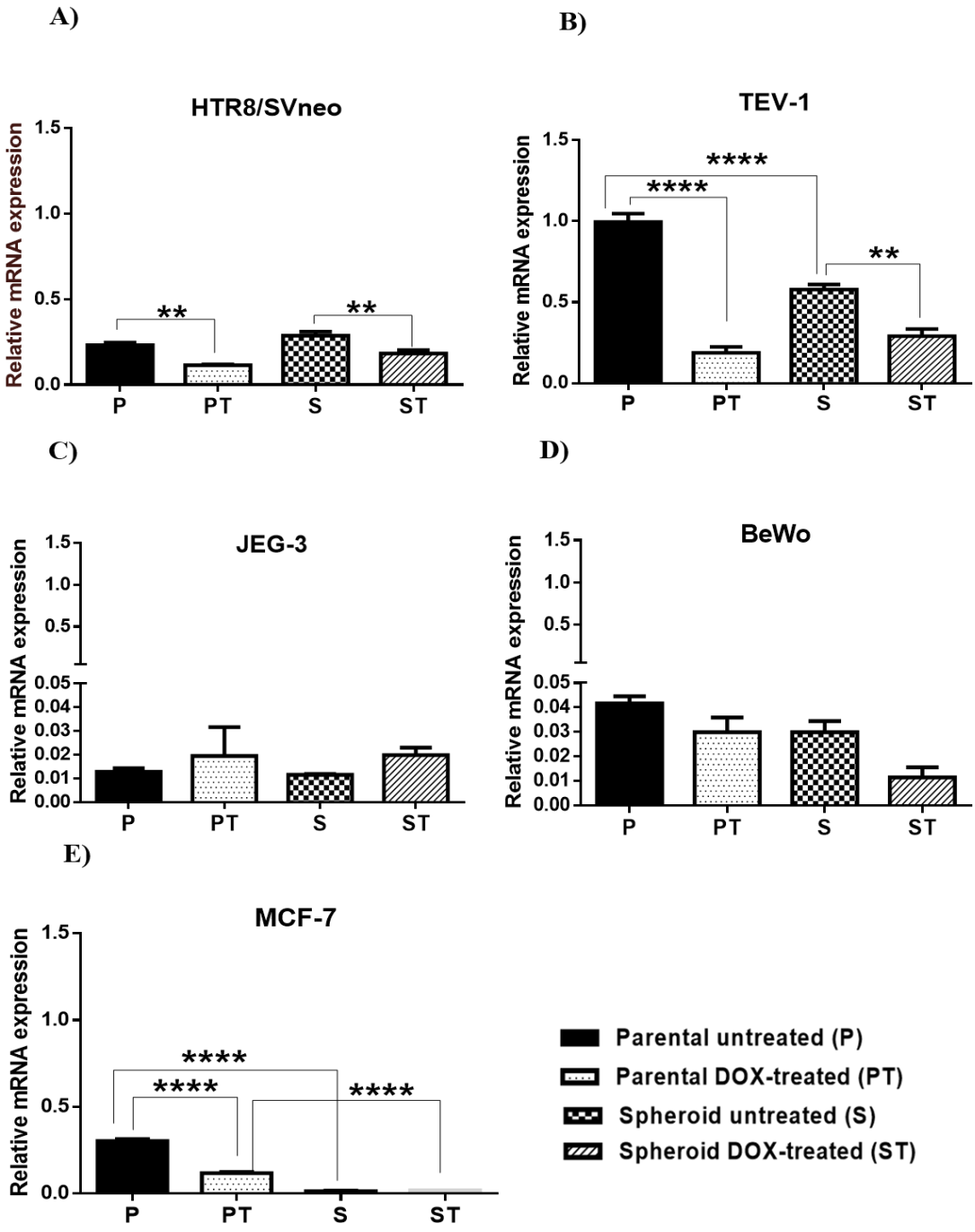

Figure 6.1: Relative mRNA expression of AURK-A.

The variance in mRNA expression was compared between different conditions. The data from HTR8/SVneo and TEV-1 cells are given in panels **A** and **B** respectively. Likewise, JEG-3 and BeWo cells data are presented in panels **C** and **D** respectively. Panel **E** shows the data from MCF-7cells. Statistical significance was determined using a one-way ANOVA followed by Tukey's test for multiple comparisons. Data represent the mean ±SEM of three individual experiments, each performed in triplicate (****$p<0.0001$; **$p<0.01$).

6.2.1.3 Relative mRNA expression of Aurora kinase C (AURK-C)

Compared to other factors the mRNA expression of AURK-C was relatively low in all five cell lines. The HTR8/SVneo cell line showed a significantly higher level of AURK-C mRNA expression in untreated parental compared to DOX-treated parental cells ($p<0.01$). There was a significant down-regulation of mRNA expression in DOX-treated spheroids compared to both DOX-treated parental ($p<0.05$) and untreated spheroids ($p<0.001$) (See Figure 6.3, Panel **A**). TEV-1 cells showed a significant up-regulation of AURK-C mRNA expression level in untreated parental compared to both DOX-treated parental and untreated spheroidal cells($p<0.0001$). Moreover, there was a significant down-regulation in DOX-treated spheroids compared to untreated spheroids ($p<0.05$) (See Figure 6.3, Panel **B**). Interestingly, the JEG-3 cell line showed similar result to the TEV-1cell line, while the BeWo cell line showed a similar result to HTR8/SVneo only in untreated parental compared to DOX-treated parental cells (See Figure 6.3, Panel **C** and **D**). From Panel **E**, the relative mRNA expression of AURK-C in MCF-7 was down-regulated in untreated parental cells compared to untreated spheroidal cells ($p<0.0001$) and DOX-treated parental compared to DOX-treated spheroidal cells ($p<0.001$).

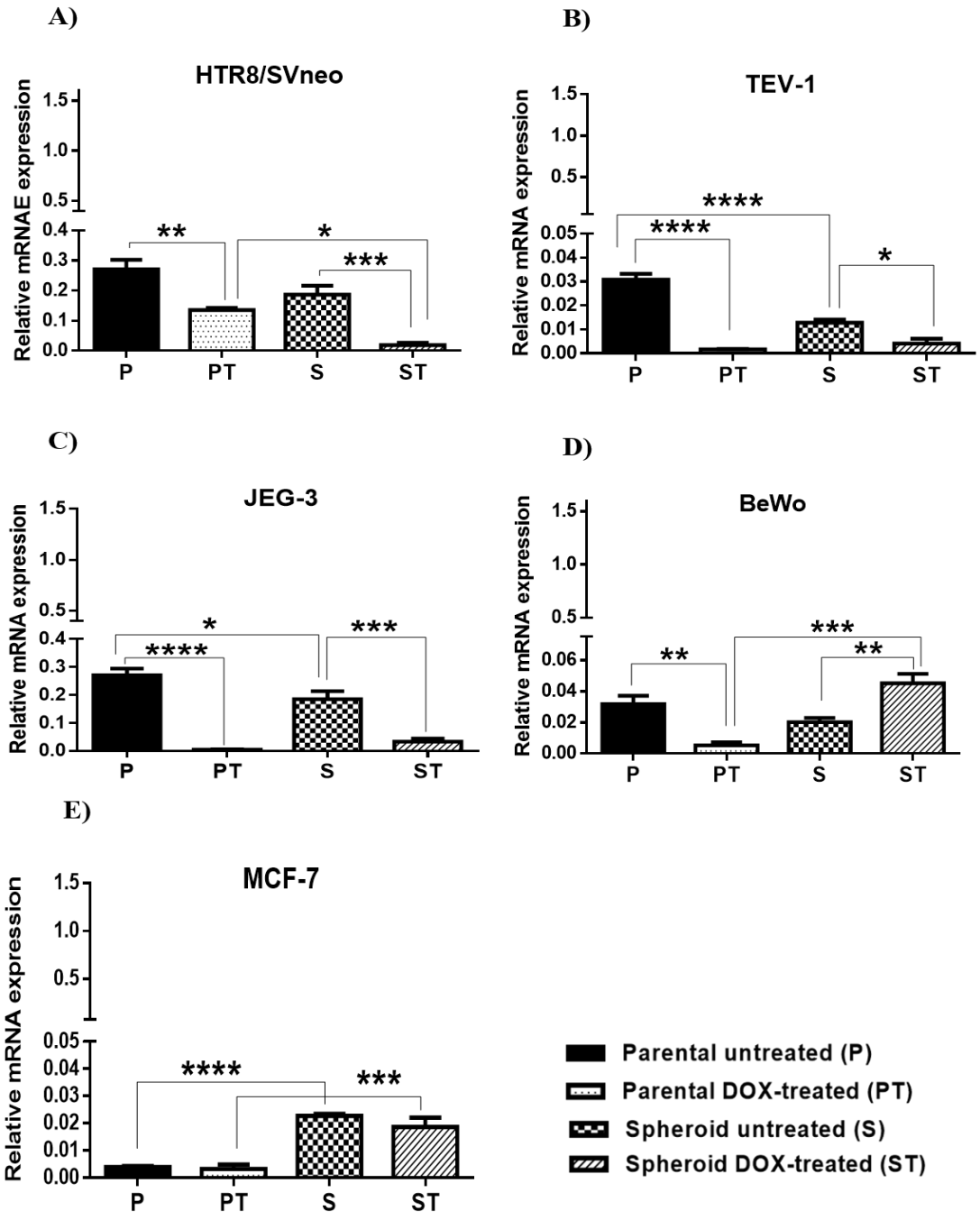

Figure 6.3: Relative mRNA expression of AURK-C.

The variance in mRNA expression was compared between different conditions. The data from HTR8/SVneo and TEV-1 cells are given in panels **A** and **B** respectively. Likewise, JEG-3 and BeWo cells data are presented in panels **C** and **D** respectively. Panel **E** shows the data from MCF-7 cells. Statistical significance was determined using a one-way ANOVA followed by Tukey's test for multiple comparisons. Data represent the mean ±SEM of three individual experiments, each performed in triplicate (****$p<0.0001$; ***$p<0.001$; **$p<0.01$; *$p<0.05$).

6.2.1.4 Relative mRNA expression of PDGFRα

There was a significant up-regulation of PDGFRα mRNA expression in HTR8/SVneo untreated parental cells compared to DOX-treated parental ($p<0.0001$) and in untreated spheroids compared with DOX-treated spheroidal cells ($p<0.0001$) (See Figure 6.4, Panel **A**). In TEV-1 there was a significant up-regulation in mRNA expression in untreated spheroids compared to both untreated parental and DOX-treated spheroids ($p<0.0001$) (See Figure 6.4, Panel **B**).

For JEG-3 cells (Panel **C**), there was a significant up-regulation of PDGFRα mRNA expression level of DOX-treated parental cells in comparison to both (a) untreated parental cells ($p<0.01$), and (b) DOX-treated spheroids ($p<0.001$). Also, there was a significant down-regulation in untreated spheroids compared with untreated parental cells ($p<0.0001$). In BeWo cells, a significant down-regulation of mRNA expression was observed in DOX-treated parental cells compared to (a) untreated parental cells ($p<0.001$) and (b) DOX-treated spheroids ($p<0.05$) (See Figure 6.4, Panel **D**).

MCF-7 cells (Figure 6.4 Panel **F**), showed higher mRNA expression levels in (a) untreated parental cells in comparison to untreated spheroids ($p<0.05$) and also in DOX-treated parental compared with DOX-treated spheroids ($p<0.01$). However, a lower mRNA expression was observed in DOX-treated spheroids cells compared to untreated spheroids ($p<0.01$).

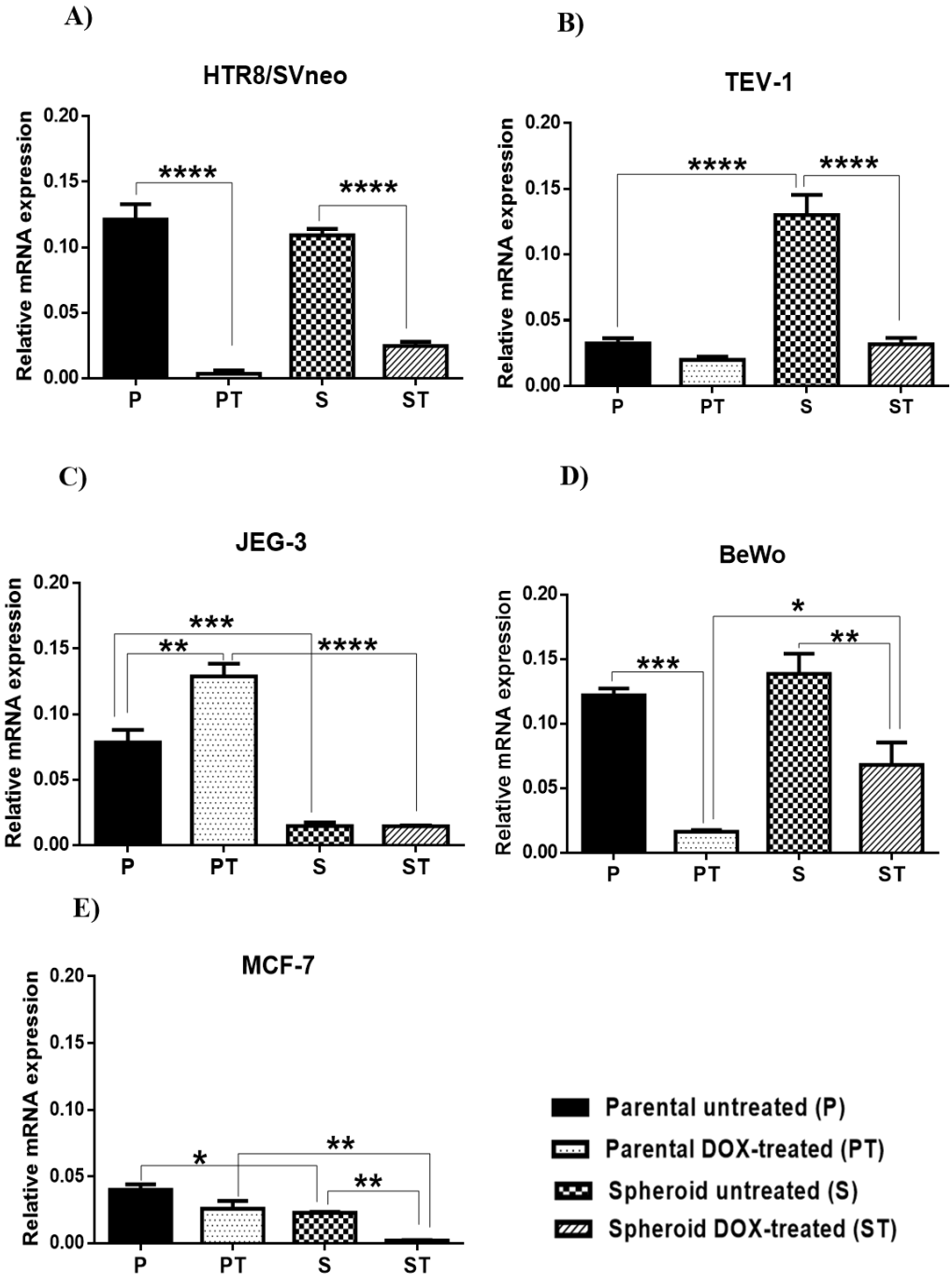

Figure 6.4: Relative mRNA expression of PDGFRα.

The variance in mRNA expression was compared between different conditions. The data from HTR8/SVneo and TEV-1 cells are given in panels **A** and **B** respectively. Likewise, JEG-3 and BeWo cells data are presented in panels **C** and **D** respectively. Panel **E** shows the data from MCF-7cells. Statistical significance was determined using a one-way ANOVA followed by Tukey's test for multiple comparisons. Data represent the mean ±SEM of three individual experiments, each performed in triplicate (****$p<0.0001$; ***$p<0.001$; **$p<0.01$; *$p<0.05$).

6.2.1.5 Relative mRNA expression of TWIST1

From Figure 6.5, Panel **A**, the HTR8/SVneo cell line showed a significant down-regulation of TWIST1 mRNA expression in DOX-treated parental cells compared to untreated parental cells ($p<0.01$). Similar changes were observed in DOX-treated spheroids compared to untreated spheroids ($p<0.01$). It was also observed that TWIST1 mRNA expression in TEV-1 cells was significantly higher in untreated parental cells in comparison to both (a) DOX-treated parental, and (b) untreated spheroidal cells ($p<0.001$). Likewise in panel **B**, the mRNA expressions in untreated spheroids was found to be higher than that of DOX-treated spheroidal cells ($p<0.01$).

Similar result to the HTR8/SVneo cell line was observed in the JEG-3 cell line. Additionally, BeWo cells showed similar results to TEV-1 cell line (See Figure 6.5, Panel **C** and **D)**. In the MCF-7 cell line, a significant difference in mRNA expression of TWIST1 was observed in untreated parental compared to both (a) DOX-treated parental and (b) untreated spheroidal cells ($p<0.0001$).

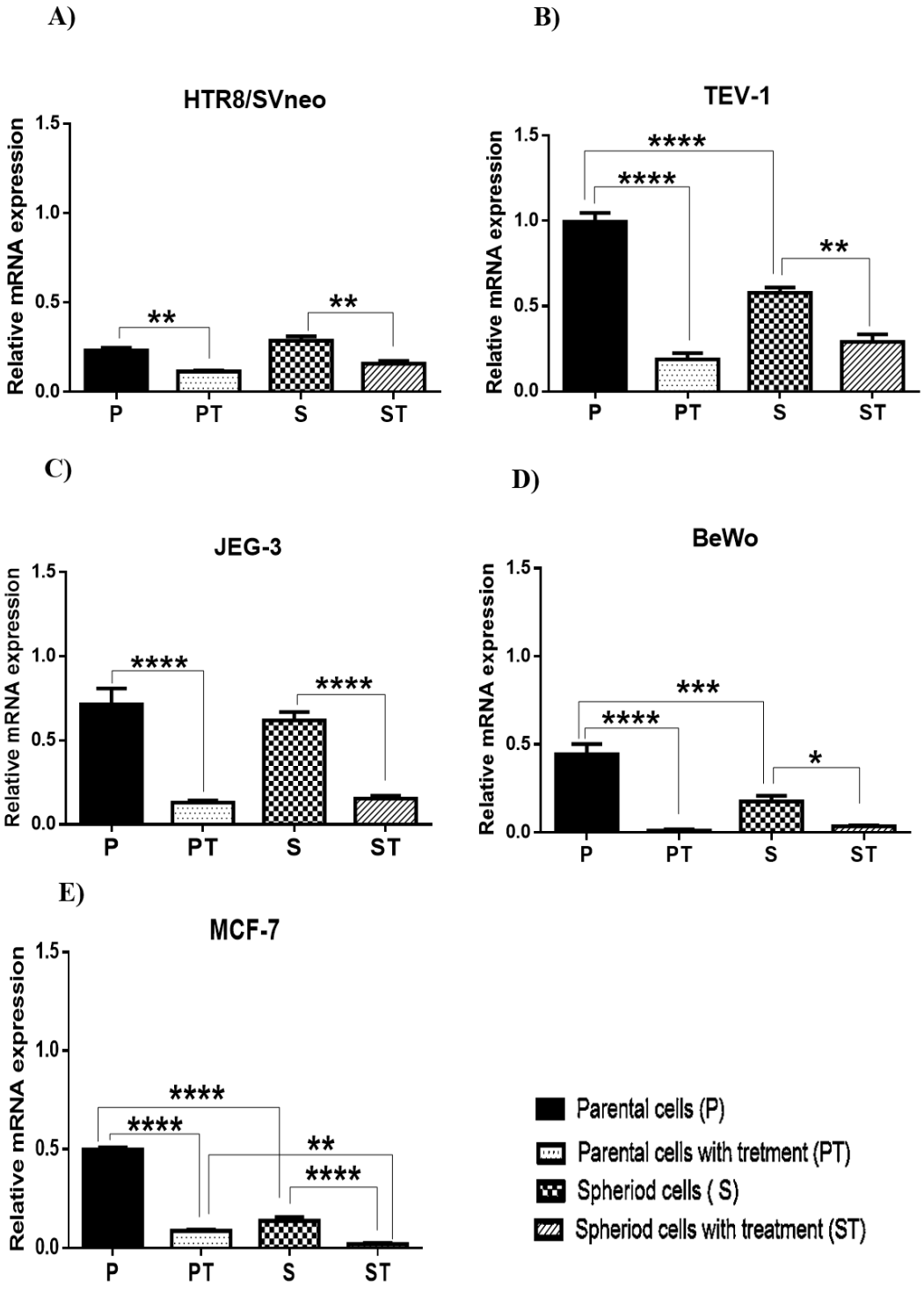

Figure 6.2: Relative mRNA expression of TWIST1.

The variance in mRNA expression was compared between different conditions. The data from HTR8/SVneo and TEV-1 cells are given in panels **A** and **B** respectively. Likewise, JEG-3 and BeWo cells data are presented in panels **C** and **D** respectively. Panel **E** shows the data from MCF-7cells. Statistical significance was determined using a one-way ANOVA followed by Tukey's test for multiple comparisons. Data represent the mean ±SEM of three individual experiments, each performed in triplicate (****$p<0.0001$; ***$p<0.001$; **$p<0.01$; *$p<0.05$).

6.2.1.6 Relative mRNA expression of JAG1 (Jagged 1)

There were no statistically significant differences observed in the relative expression of JAG1 between all comparisons in either HTR8/SVneo or BeWo cell lines (see Figure 6.6 Panel **A** and **D)**. However, in TEV-1, there was a significant up-regulation in untreated parental compared to both DOX-treated parental and untreated spheroidal cells ($p<0.0001$). Also, untreated spheroids expressed a higher level of JAG1 mRNA than DOX-treated spheroids ($p<0.05$) (Figure 6.6 Panel **B)**. A similar profile to that seen in TEV-1 cells was also observed in JEG3 cells, where untreated parental cells expressed significantly higher levels of JAG1 mRNA than either DOX-treated parental or untreated spheroidal cells ($p<0.0001$) (Figure 6.6 Panel **C**). Interestingly, MCF-7 cells showed a similar result to both trophoblast cell lines (HTR8/SVneo and BeWo) (Figure 6.6 Panel **E)**.

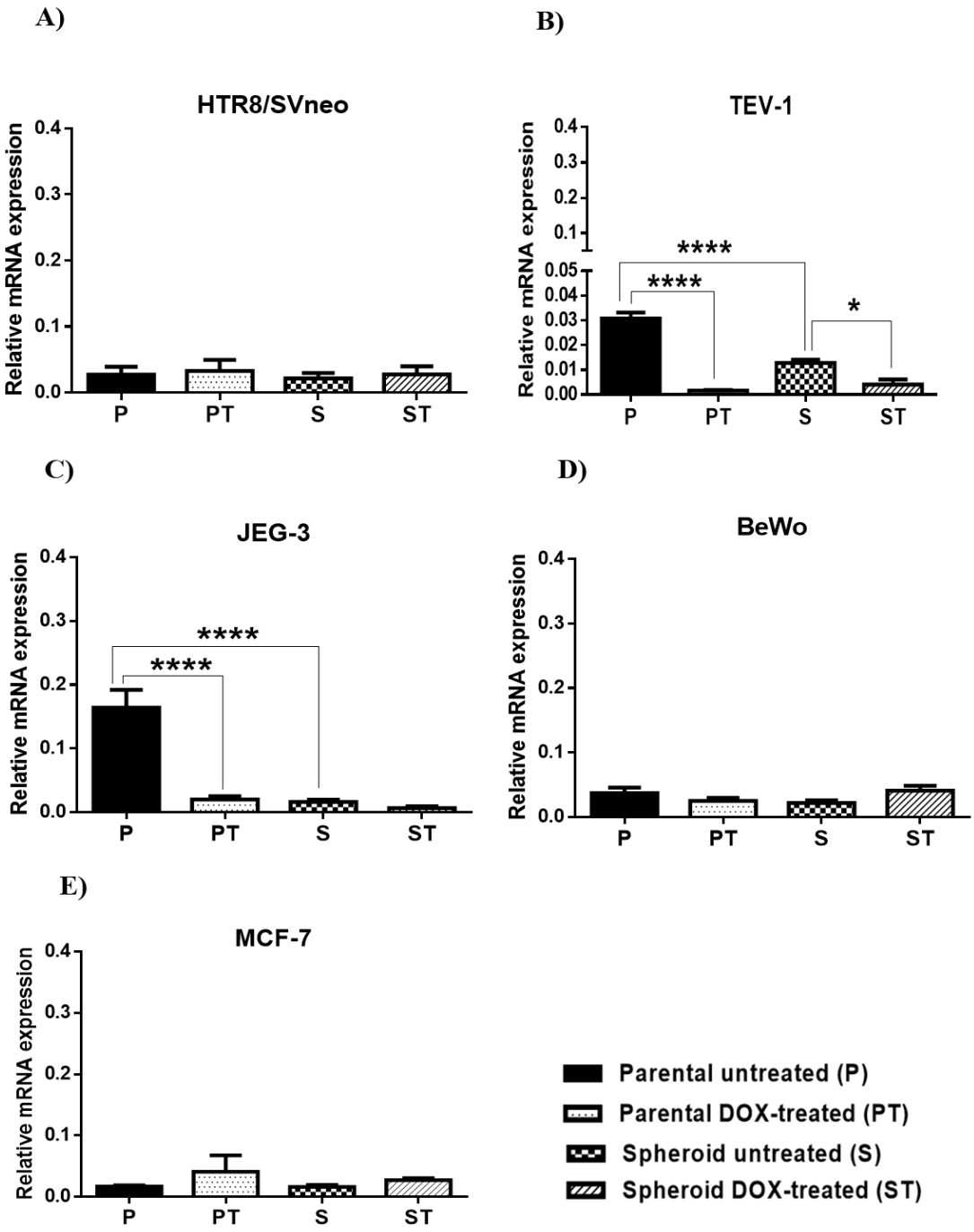

Figure 6.3: Relative mRNA expression of JAG1.

The variance in mRNA expression was compared between different conditions. The data from HTR8/SVneo and TEV-1 cells are given in panels **A** and **B** respectively. Likewise, JEG-3 and BeWo cells data are presented in panels **C** and **D** respectively. Panel **E** shows the data from MCF-7cells. Statistical significance was determined using a one-way ANOVA followed by Tukey's test for multiple comparisons. Data represent the mean ±SEM of three individual experiments, each performed in triplicate (****$p<0.0001$; *$p<0.05$).

6.2.2 Protein expression analysis

Protein expression level were compared between different conditions as explained earlier in Section 6.2.1 Different positive controls, as suggested by the supplier (Abcam, UK), were used (separated by red dotted lines in the blot). The protein expression levels were normalised by using housekeeping protein β-actin levels as an internal control.

6.2.2.1 Protein expression of ALDH3A1

The predicated molecular weight of ALDH3A1 protein was 50 kDa. The single band was observed at 49kDa in untreated and DOX-treated parental and spheroidal cells. The ALDH3A1 antibody produced a single band in most samples from four trophoblast and tumour MCF-7) cell lines (see Figure 6.7).

In HTR8/SVneo cells (Figure 6.7 Panel **A**), the ALDH3A1protein expression was significantly higher in DOX-treated parental cells compared to both (a) untreated parental cells; (b) DOX-treated spheroidal cells ($p<0.001$). Likewise, ALDH3A1 expression in untreated spheroids was found to be higher than untreated parental cells and DOX-treated spheroids ($p<0.01$). However, there were no statistically significant differences observed in the protein expression of ALDH3A1 between any conditions in TEV-1 cells (see Figure 6.7 Panel **B**). In JEG-3 cells, there was a significant up-regulation in DOX-treated parental verses untreated parental cells and in DOX-treated spheroids versus untreated spheroids ($p<0.01$) (Figure 6.7 Panel **C**). In BeWo cells, there was a significant up-regulation in protein expression in DOX-treated parental cells versus DOX-treated spheroidal cells ($p<0.05$) (Figure 6.7 Panel **D**).

The MCF-7 cells showed a significant up-regulation of protein expression in untreated spheroids compared to (a) untreated parental cells ($p<0.001$) and (b) DOX-treated spheroids ($p<0.05$). Interestingly, these differences in expression were also observed in mRNA expression. Likewise, there was also a significant difference in DOX-treated spheroids versus DOX- treated parental cells ($p<0.01$). In general, the protein expression of ALDH3A1 was significant higher in MCF-7 untreated spheroids compared to other conditions.

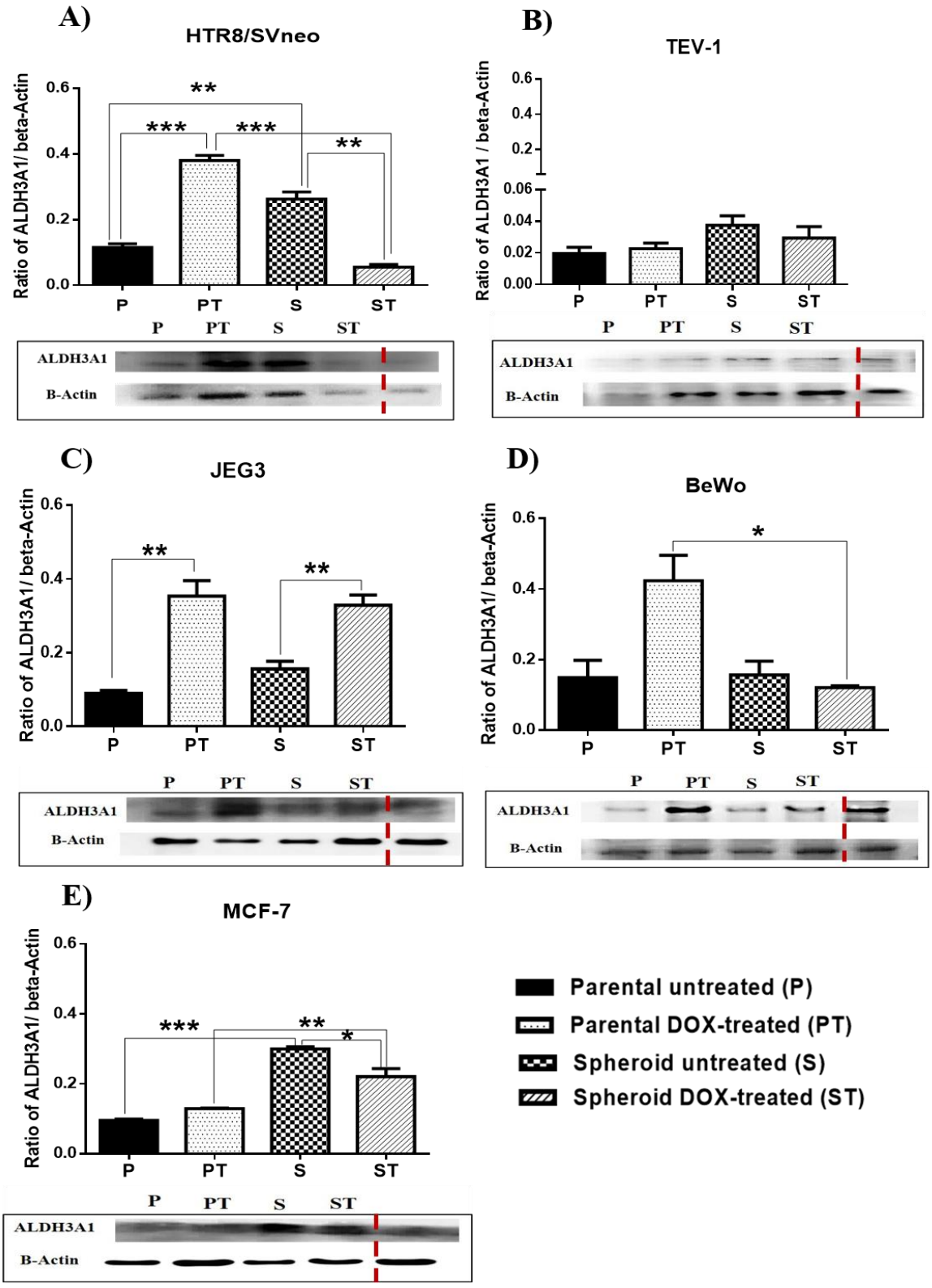

Figure 6.7: The expression of ALDH3A1 protein.

The ratio of ALDH3A1 to β-actin densitometry readings are given for the HTR8/SVneo and TEV-1 cell lines in panels **A** and **B** respectively. Likewise Panel **C** and **D** represent JEG-3 and BeWo cell lines; and Panel **E** shows the data for the MCF-7 cell line. MCF-7 cell line used as the positive control and is separated with red dotted lines. A one-way ANOVA followed by Tukey's test for multiple comparisons between different conditions was carried out. Data represent the mean ±SEM of three individual experiments, each performed in triplicate (***p<0.001; **p<0.01; *p<0.05).

6.2.2.2 Protein expression of AURK-A

The AURK-A antibody produced single band at 48 kDa in most of the trophoblast cell lines, MCF-7 cells and positive control (Hela cells) (See Figure 6.8).

There was correlation between mRNA and protein expression profile for AURK-A in HTR8/SVneo cells. There was a significant increase in untreated parental compared to DOX-treated parental cells ($p<0.05$) and also between untreated spheroids and DOX-treated spheroids ($p<0.001$) (See Figure 6.8, Panel **A**). TEV-1 cells showed a significant up-regulation in AURK-A protein level in DOX-treated spheroids compared to both (a) DOX-treated parental cells ($p<0.001$) and (b) untreated spheroids cells ($p<0.05$) (Figure 6.8, Panel **B**).

In JEG-3 cells, there were no significant changes in the expression of AURK-A between all conditions. On the other hand, a significant increase in protein expression was seen in BeWo DOX-treated parental cells compared to untreated parental cells ($p<0.05$) (See Figure 6.8, Panel **C** and **D**). This change was not seen in mRNA expression comparisons. The protein expression of AURK-A was increased in MCF-7 untreated spheroids compared to parental cells ($p<0.05$). Also, there was a significant change in untreated spheroidal cells versus DOX-treated spheroidal cells ($p<0.05$) (See Figure 6.8, Panel **E).**

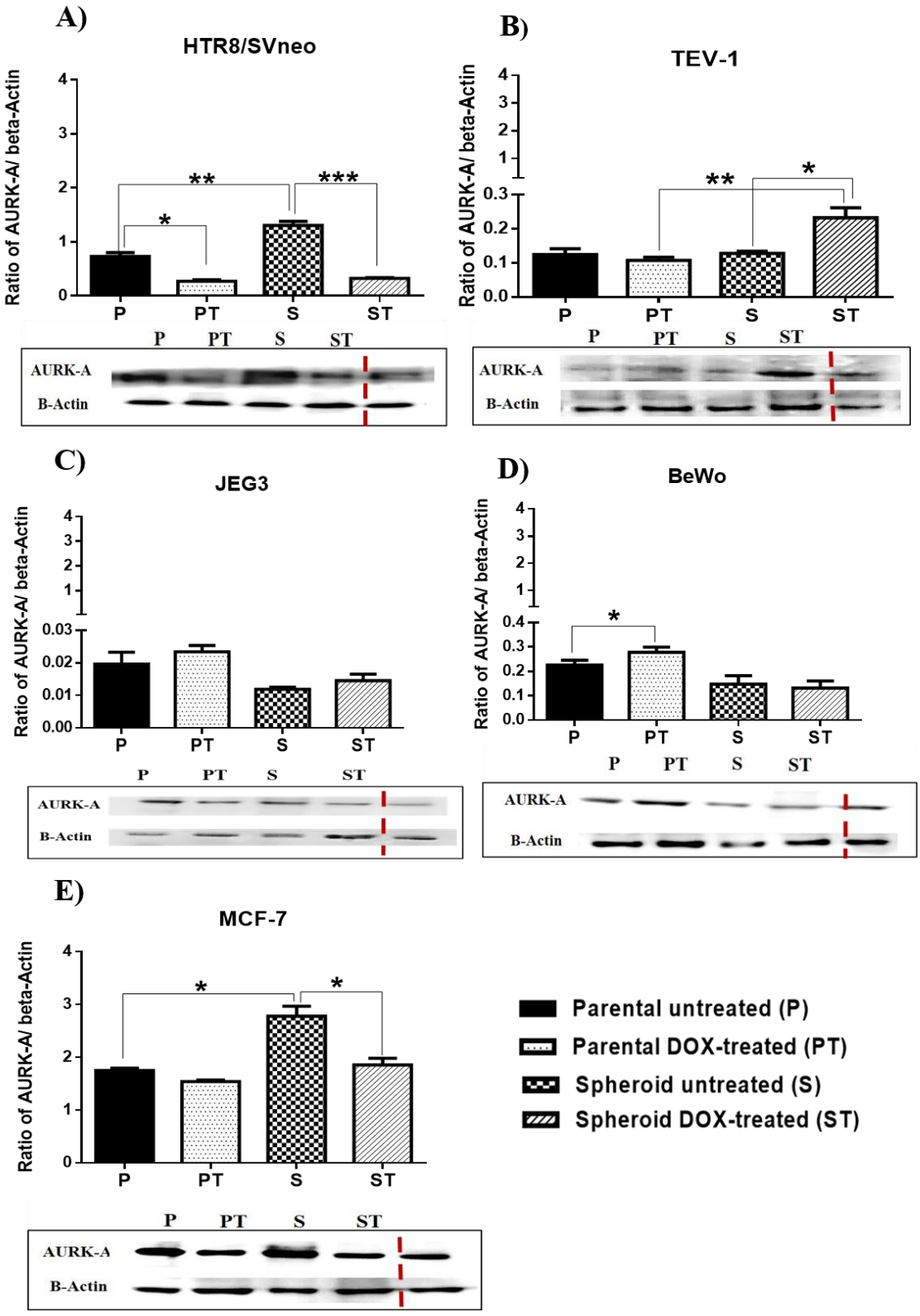

Figure 6.8: The expression of AURK-A protein.

The ratio of AURK-A to β-actin densitometry readings are given for the HTR8/SVneo and TEV-1 cell lines in panels **A** and **B** respectively. Likewise Panel **C** and **D** represent JEG-3 and BeWo cell lines; and Panel **E** shows the data for the MCF-7 cell line. Hela cell line used as the positive control and is separated with red dotted lines. A one-way ANOVA followed by Tukey's test for multiple comparisons between different conditions was carried out. Data represent the mean ±SEM of three individual experiments, each performed in triplicate (***p<0.001; **p<0.01; *p<0.05).

6.2.2.3 Protein expression of AURK-C

The AURK-C antibody produced single bands at 36 kDa in almost all the four trophoblast cell lines, MCF-7 samples and positive control (Hela cells) (See Figure 6.9).

There was a significant increase in protein expression of AURK-C observed in HTR8/SVneo DOX-treated parental cells compared with (a) their untreated counter parts ($p<0.05$), and (b) DOX-treated spheroidal cells ($p<0.01$). On the other hand, there was a significant reduction in protein expression in untreated spheroid compared to untreated parental cells ($p<0.01$) (See Figure 6.9, Panel **A**). The TEV-1 cell line showed a significant increase in DOX-treated parental cells compared to untreated parental cells. (See Figure 6.9, Panel **A**).

There was a correlation between mRNA and protein expression in JEG-3 untreated parental compared to untreated spheroidal cells ($p<0.01$). Difference in protein expression level were only observed in DOX-treated parental compared to DOX-treated spheroidal cells ($p<0.01$) (See Figure 6.9, Panel **C**). The BeWo cells derived untreated spheroids showed a higher protein expression level of AURK-C than DOX-treated spheroids ($p<0.01$) (See Figure 6.9, Panel **D**).

There was a significant increase in mRNA and protein expression of AURK-C observed in MCF-7 spheroidal cells (both DOX-treated and untreated) compared to their parental cell counterparts ($p<0.01$) (See Figure 6.9, Panel **E**).

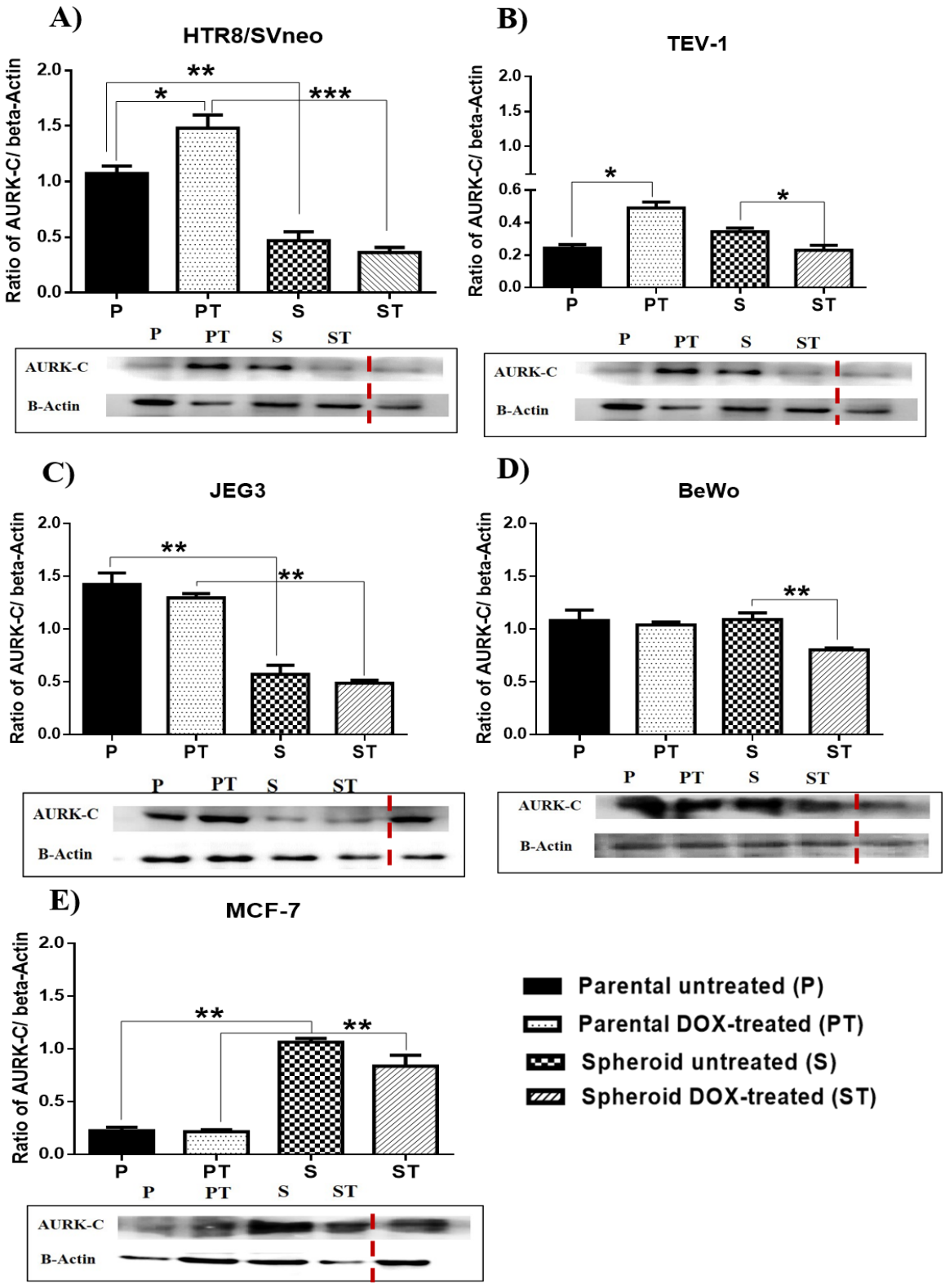

Figure 6.9: The expression of AURK-C protein.

The ratio of AURK-C to β-actin densitometry readings are given for the HTR8/SVneo and TEV-1 cell lines in panels **A** and **B** respectively. Likewise Panel **C** and **D** represent JEG-3 and BeWo cell lines; and Panel **E** shows the data for the MCF-7 cell line. Hela cell line used as the positive control and is separated with red dotted lines. A one-way ANOVA followed by Tukey's test for multiple comparisons between different conditions was carried out. Data represent the mean ±SEM of three individual experiments, each performed in triplicate (***p<0.001; **p<0.01; *p<0.05).

6.2.2.4 Protein expression of PDGFRα

The PDGFRα antibody produced a single band at 36kDa in all four trophoblast, MCF-7 samples and positive control (PDGF protein), whilst the expected molecular weight of the band was in the range of 14-20kDa (Figure 6.10).

In HTR8/SVneo cells (Figure 6.10, Panel **A**) the protein and mRNA expression of PDGFRα was significantly higher in untreated parental cells compared to DOX-treated parental cells ($p<0.001$). The protein expression in DOX-treated spheroids was significantly higher than that of DOX-treated parental cells ($p<0.001$). In TEV-1 cells, compared to parental cells spheroids showed a significant increase in protein expression of PDGFRα ($p<0.01$) (see Figure 6.10, Panel **B)**.

In JEG3 cells, a significant increase in protein expression of PDGFRα was seen in DOX-treated parental cells compared to (a) untreated parental cells ($p<0.001$) and (b) DOX-treated spheroids ($p<0.05$) (Figure 6.10, Panel **C)**.

In BeWo cells, the expression of protein was reduced in DOX-treated parental cells compared to parental cells ($p<0.001$). Furthermore, a significant reduction was observed in untreated spheroids compared to parental cells ($p<0.001$) (Figure 6.10, Panel **D)**. These changes were not observed in mRNA expression comparisons

In MCF-7 cells (Figure 6.10, Panel **E**), the protein expression was higher in untreated parental cells compared to DOX-treated parental cells ($p<0.001$). Also, there was a significant difference between untreated parental and untreated spheroidal cells ($p<0.001$).

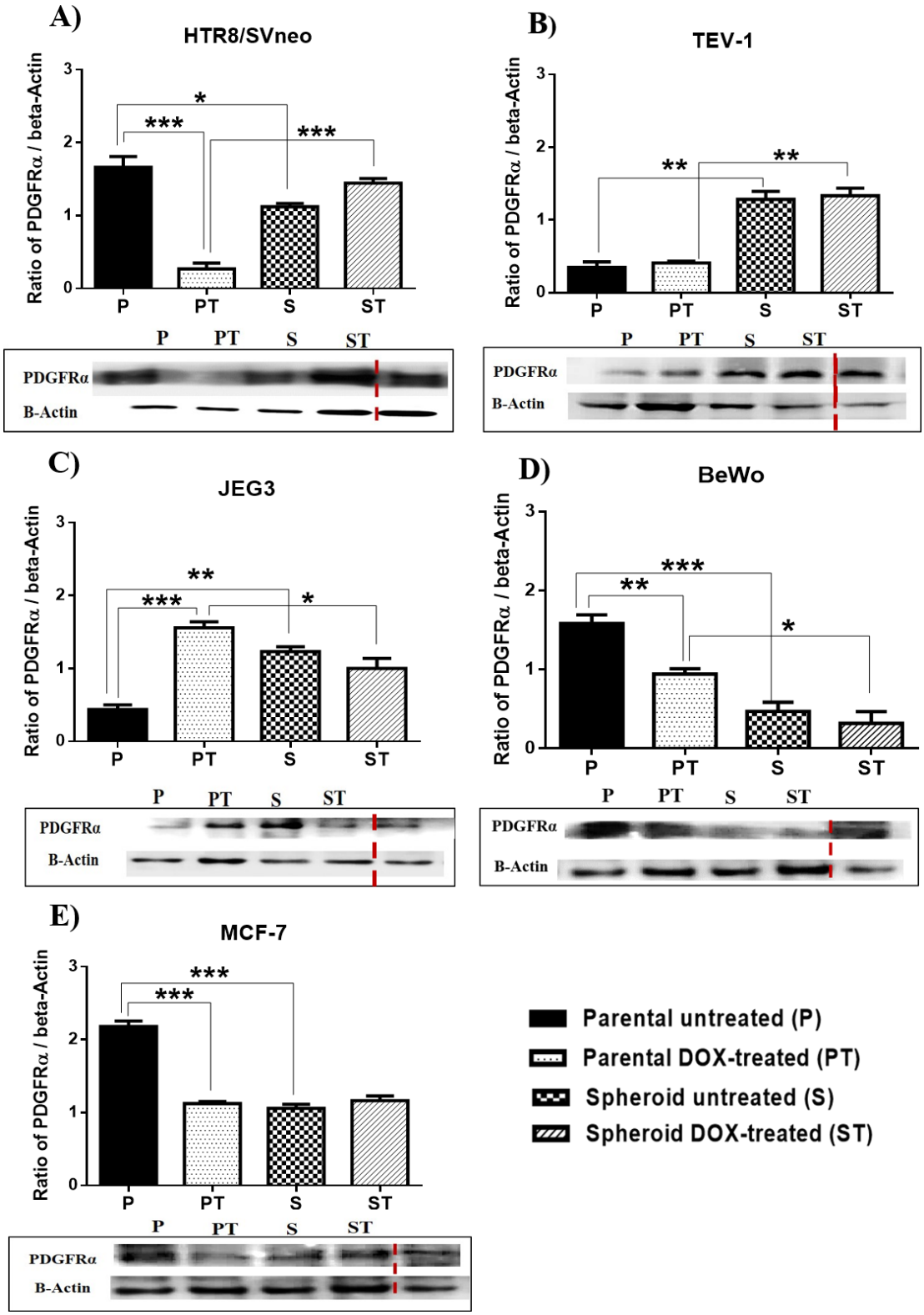

Figure 6.10: The expression of PDGFRα protein.

The ratio of **PDGFRα** to β-actin densitometry readings are given for the HTR8/SVneo and TEV-1 cell lines in panels **A** and **B** respectively. Likewise Panel **C** and **D** represent JEG-3 and BeWo cell lines; and Panel **E** shows the data for the MCF-7 cell line. PDGF (protein) used as the positive control and is separated with red dotted lines. A one-way ANOVA followed by Tukey's test for multiple comparisons between different conditions was carried out. Data represent the mean ±SEM of three individual experiments, each performed in triplicate (***p<0.001; **p<0.01; *p<0.05).

6.2.2.5 Protein expression of TWIST1

The TWIST1 antibody produced single bands at 49kDa in all four trophoblast, MCF-7 samples and positive control (Hela cells), whilst the expected molecular weight of the band was between 21- 36 kDa (Figure 6.11).

Figure 6.11 Panel **A** shows that protein expression was lower in HTR8/SVneo DOX-treated parental cells compared (a) untreated parental and (b) DOX-treated spheroids ($p<0.01$). In TEV-1 cells (Figure 6.11, Panel **B**), the protein expression was significantly higher in DOX-treated parental cells compared to untreated parental ($p<0.05$) and in DOX- treated parental cells versus untreated spheroids ($p<0.01$).

The JEG-3 cells showed a significant change in protein expression in untreated parental cells compared to DOX-treated parental cells and untreated spheroidal cells ($p<0.05$) (Figure 6.11, Panel **C**). In the BeWo cells, a significant reduction in protein expression of TWIST1 was observed in untreated spheroidal cells compared to (a) untreated parental cells and (b) DOX-treated spheroids ($p<0.05$) (Figure 6.11, Panel **D**).

MCF-7 cells exhibited a high level of protein and mRNA expression of TWIST1 in DOX-treated parental cells compared to DOX-treated spheroids ($p<0.05$) (Figure 6.11, Panel **E**).

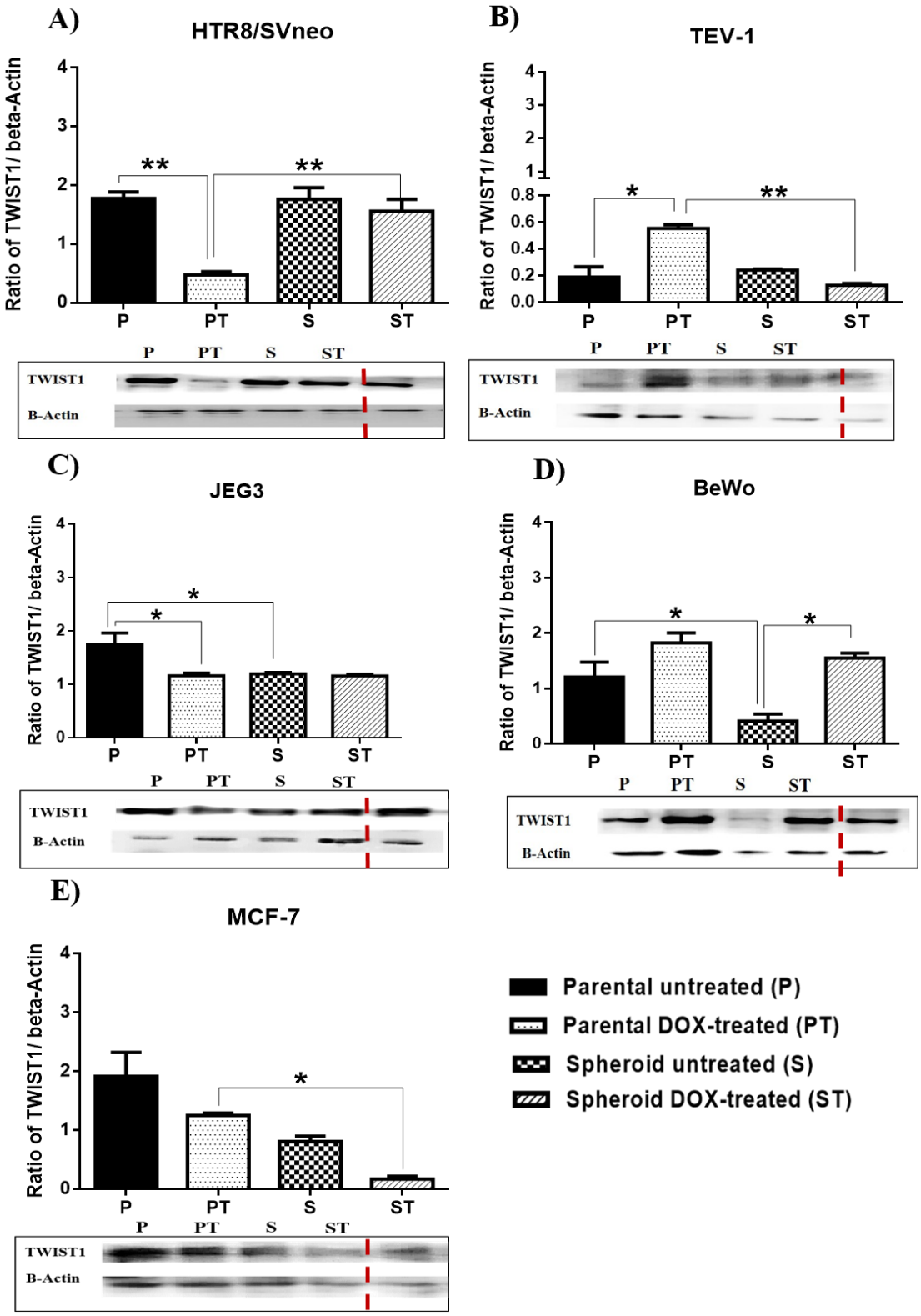

Figure 6.14: The expression of TWIST1 protein.

The ratio of **TWIST1** to β-actin densitometry readings are given for the HTR8/SVneo and TEV-1 cell lines in panels **A** and **B** respectively. Likewise Panel **C** and **D** represent JEG-3 and BeWo cell lines; and Panel **E** shows the data for the MCF-7 cell line. Hela cell line used as the positive control and is separated with red dotted lines. A one-way ANOVA followed by Tukey's test for multiple comparisons between different conditions was carried out. Data represent the mean ±SEM of three individual experiments, each performed in triplicate (**p<0.01; *p<0.05).

6.2.2.6 Protein expression of JAG1

The JAG1 antibody produced single band at 75 kDa in all the four trophoblast cells, MCF-7 and positive control (Hela cells) under different conditions (See Figure 6.12). There were no significant changes observed in JAG1 protein expression level in HTR8/SVneo, TEV-1, BeWo and MCF-7 cell lines (See Figure 6.12, Panel **A**, **B**, **D** and **E**). However, in JEG-3 the protein expression of JAG1 was increased in DOX-treated parental cells compared to both (a) untreated parental, and (b) DOX-treated spheroids ($p<0.01$) (See Figure 6.12, Panel **C**).

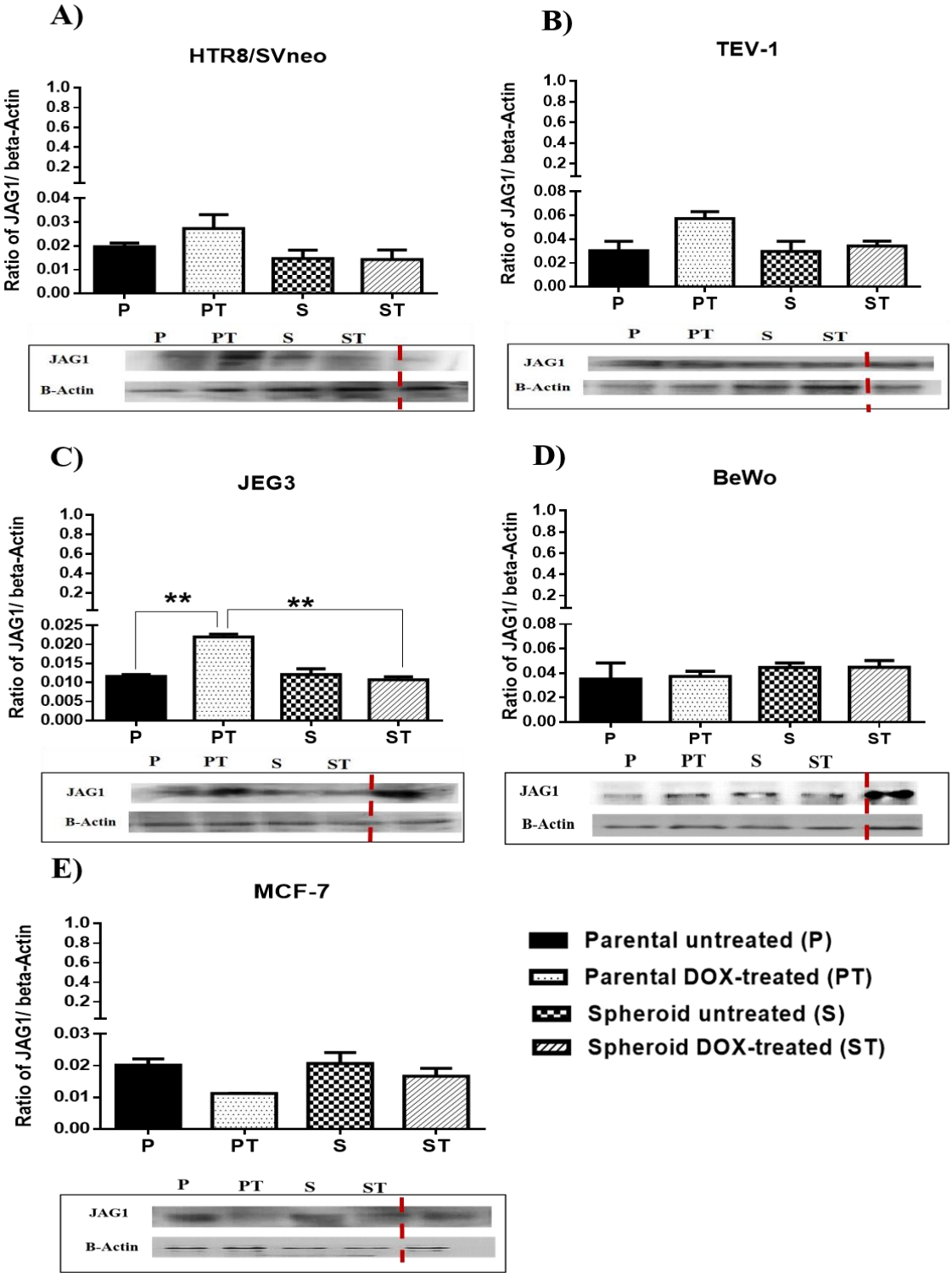

Figure 6.12: The expression of JAG1 protein.

The ratio of **JAG1** to β-actin densitometry readings are given for the HTR8/SVneo and TEV-1 cell lines in panels **A** and **B** respectively. Likewise Panel **C** and **D** represent JEG-3 and BeWo cell lines; and Panel **E** shows the data for the MCF-7 cell line. Hela cell line used as the positive control and is separated with red dotted lines. A one-way ANOVA followed by Tukey's test for multiple comparisons between different conditions was carried out. Data represent the mean ±SEM of three individual experiments, each performed in triplicate (**p<0.01).

6.2.3 Proteomic analysis of global protein/peptide expressions

Sequential Windowed Acquisition of All Theoretical Fragment Ion Mass Spectra (SWATH-MS) was carried out to identify novel proteins, whose expression is affected by spheroidal transformation. As the analyses have produced a very large data set, this chapter focuses only on the changes identified in the transformed trophoblast cell lines (HTR8/SVneo and TEV-1). SWATH-MS analysis is a recently developed technique, which enables quantification of mass spectrometry data (Wang *et al.,* 2015). These proteins were selected from a long list of proteins identified according to their fold change only up-regulated proteins and functions related to cell division, proliferation and invasion.

6.2.3.1 Identification of altered proteins in HTR8/SVneo cells

A list of the most up-regulated proteins and their fold change in HTR8/SVneo cells are summarised in Table 6.1 [6.1A - untreated parental versus untreated spheroids; 6.1B untreated parental versus DOX-treated parental; 6.1C untreated spheroid versus DOX-treated spheroids; and 6.1D. DOX-treated parental versus DOX-treated spheroids]. As can be seen in Table 6.1A, eight of the proteins with different fold changes were observed to be up-regulated in untreated spheroids compared to their parental counterparts. Interestingly, plasminogen, vitronectin, cysteine rich protein 2 and AL1A3 were all up-regulated in untreated spheroidal cells (6.1A). Many of these proteins are involved in cells differentiation and proliferation. In addition, the cell adhesion factor vitronectin and plasminogen were found to be up-regulated in both untreated and DOX-treated spheroidal cells. The details of fold changes with cells involved are summarised in table 6.1 (A) to (D). The most interesting proteins that have been identified in different cell populations of HTR8/Svneo and TEV-1 by SWATH-MS are summarised in Table 6.3.

Table 6. 1: Identification of up-regulated proteins/peptide in HTR8/SVneo cells.

HTR8/SVneo cells were collected from adherent and non-adherent flasks. The proteins were analysed by SWATH-MS using the following comparisons; untreated parental Vs untreated spheroids (6.1A); untreated parental Vs DOX-treated parental) (6.1B); untreated spheroids Vs DOX-treated spheroidal cells (6.1C) and parental cells Vs DOX-treated spheroidal cells (6.1D).

(A) Untreated parental versus untreated spheroids

Protein Name	Accession number	Uniprot name	Absolute fold change	Up -regulated expression	Function of the protein
Plasminogen	P00747	PLMN_HUMAN	3.579	untreated spheroids	It plays role in embryonic development, tissue remodelling, tumour invasion, and inflammation.
Vitronectin	P04004	VTNC_HUMAN	2.878	untreated spheroids	It is a cell adhesion and spreading factor found in serum and tissues. Is recognized by certain members of the integrin family and serves as a cell-to-substrate adhesion molecule.
Protein NDRG1	Q92597	NDRG1_HUMAN	2.471	untreated spheroids	Plays roles in hormone responses, cell growth, and differentiation. Acts as a tumour suppressor in many cell types.
Cysteine-rich protein 2	P52943	CRIP2_HUMAN	2.097	untreated spheroids	Positive regulation of cell proliferation
SAP domain-containing ribonucleoprotein	P82979	SARNP_HUMAN	1.284	untreated spheroids	May participate in important transcriptional or translational control of cell growth, metabolism and carcinogenesis.
Cathepsin B	P07858	CATB_HUMAN	1.214	untreated spheroids	It participate in intracellular degradation and turnover of proteins. Has been implicated in tumour invasion and metastasis.
Deoxyribonuclease-2-alpha	O00115	DNS2A_HUMAN	1.662	untreated spheroids	plays a major role in the degradation of nuclear DNA in cellular apoptosis during development. Necessary for proper foetal development
Aldehyde dehydrogenase family 1 member A3	P47895	AL1A3_HUMAN	1.5	untreated spheroids	plays important role in cell proliferation, differentiation and survival especially during the cellular responses to oxidative stress.

(B) Untreated parental versus DOX-treated parental cells

Protein Name	Accession number	Uniprot name	Absolute fold change	Up -regulated expression	Function of the protein
Collagen alpha-1(I) chain	P02452	CO1A1_HUMAN	3.28	DOX-treated parental	Type I collagen is a member of group I collagen (fibrillar forming collagen)
Collagen alpha-2(I) chain	P08123	CO1A2_HUMAN	2.268	untreated parental	Type I collagen is a member of group I collagen (fibrillar forming collagen)
Cysteine-rich protein 2	P52943	CRIP2_HUMAN	2.084	DOX-treated parental	Positive regulation of cell proliferation
Stress-70 protein, mitochondrial	P38646	GRP75_HUMAN	1.078	untreated parental	Implicated in the control of cell proliferation and cellular aging

The data were summarised after 4 individual experiments with different passage numbers (n=4) using SCIEX OneOmics with the following parameters: MLR weight >0.15, confidence >70%, algorithms. Both accession numbers and protein names are from the Uniprot database. The common proteins that were found among all the comparisons were encircled with red colour.

Table 6.1: Identification of up-regulated proteins/peptide in HTR8/SVneo cells.

(C) Untreated spheroids versus DOX-treated spheroids

Protein Name	Accession number	Uniprot name	Absolute fold change	Up -regulated expression	Function of the protein
Basigin	P35613	BASI_HUMAN	1.868	DOX-treated spheroids	Plays pivotal roles in spermatogenesis, embryo implantation, neural network formation and tumour progression.
Plasminogen	P00747	PLMN_HUMAN	1.255	DOX-treated spheroids	It plays role in embryonic development, tissue remodelling, tumour invasion, and inflammation.
Alpha-parvin	Q9NVD7	PARVA_HUMAN	1.085	DOX-treated spheroids	Required for normal development of the embryonic cardiovascular system, and for normal Plays a role in the establishment of cell polarity, cell adhesion, cell spreading, and directed cell migration
Vitronectin	P04004	VTNC_HUMAN	1.25	DOX-treated spheroids	It is a cell adhesion and spreading factor found in serum and tissues. Is recognized by certain members of the integrin family and serves as a cell-to-substrate adhesion molecule.

(D) DOX-treated parental versus DOX- treated spheroids

Protein Name	Accession number	Uniprot name	Absolute fold change	Up -regulated expression	Function of the protein
Vitronectin	P04004	VTNC_HUMAN	4.239	DOX-treated spheroids	It is a cell adhesion and spreading factor found in serum and tissues. Is recognized by certain members of the integrin family and serves as a cell-to-substrate adhesion molecule.
Plasminogen	P00747	PLMN_HUMAN	5.696	DOX-treated spheroids	It plays role in embryonic development, tissue remodelling, tumour invasion, and inflammation
Thrombospondin-1	P07996	TSP1_HUMAN	2.53	DOX-treated spheroids	Adhesive glycoprotein that mediates cell-to-cell and cell-to-matrix interactions. Ligand for CD36 mediating antiangiogenic properties.

The data were summarised after 4 individual experiments with different passage numbers (n=4) using SCIEX OneOmics with the following parameters: MLR weight >0.15, confidence >70%, algorithms. Both accession numbers and protein names are from the Uniprot database. The common proteins that were found among all the comparisons were encircled with red colour.

6.2.3.2 Identification of altered proteins in TEV-1 cells

A list of the most up-regulated proteins and their fold changes are summarised in Table 6.2 [6.2A untreated parental versus untreated spheroids; 6.2B untreated parental versus DOX-treated parental; 6.2C untreated spheroids versus DOX-treated spheroids; and 6.2D DOX-treated parental versus DOX-treated spheroids. An overall two-fold up-regulation of AL1A3 (Aldehyde dehydrogenase family 1 member A3) was observed in untreated parental versus spheroidal cells and in untreated parental versus DOX-treated parental cells [see tables 6.2(A) and (B)]. Furthermore, there was a more than three fold up-regulation of proteolytic enzyme plasminogen in untreated spheroids in comparison with untreated parental cells [(Table 6.2(B)]. Interestingly, the three-fold up-regulation of plasminogen in untreated spheroids was also observed when compared to DOX-treated spheroids [Table 6.2(C)]. In contrast, the less than two-fold up-regulation of Galectin-1 (LEG1) was observed in untreated spheroids compared to DOX-treated spheroids [Table 6.2(C)] and in DOX-treated parental compared to DOX-treated spheroids [Table 6.2(D)]. The details of fold changes with cells involved are summarised in Table 6.2 (A) to (D). The most interesting proteins that have been identified in different cell populations of HTR8/SVneo and TEV-1 by SWATCH-MS are summarised in Table 6.3.

Table 6. 2: Identification of up-regulated proteins/peptide in TEV-1 cells.

TEV-1 cells were pre-collected from adherent and non-adherent flask. The up-regulated proteins were analysed by SWATH-MS using following comparisons; untreated parental Vs untreated spheroids (6.2A); untreated parental Vs DOX-treated parental) (6.2B); untreated spheroids Vs DOX-treated spheroidal cells (6.2C) and parental cells Vs DOX-treated spheroidal cells (6.2D).

(A) Untreated parental versus untreated spheroids

Protein Name	Accession number	Uniprot name	Absolute fold change	Up -regulated expression	Function of the protein
Vitronectin	P04004	VTNC_HUMAN	3.213	untreated spheroids	It is a cell adhesion and spreading factor found in serum and tissues. Is recognized by certain members of the integrin family and serves as a cell-to-substrate adhesion molecule
Plasminogen	P00747	PLMN_HUMAN	3.049	untreated spheroids	It plays role in embryonic development, tissue remodelling, tumour invasion, and inflammation
Aldehyde dehydrogenase family 1 member A3	P47895	AL1A3_HUMAN	2.199	untreated spheroids	plays important role in cell proliferation, differentiation and survival especially during the cellular responses to oxidative stress
Caprin-1	Q14444	CAPR1_HUMAN	1.368	untreated parental	It may regulate the transport and translation of mRNAs of proteins involved in cell proliferation and migration in multiple cell types

(B) Untreated parental versus DOX-treated parental cells

Protein Name	Accession number	Uniprot name	Absolute fold change	Up -regulated expression	Function of the protein
Glucose-6-phosphate isomerase	P06744	G6PI_HUMAN	3.033	DOX-treated parental	It function as a tumour-secreted cytokine and an angiogenic factor (AMF) that stimulates endothelial cell motility
Cellular tumour antigen p53	P04637	P53_HUMAN	2.224	untreated parental	Acts as a tumour suppressor in many tumour types; induces growth arrest or apoptosis depending on the physiological circumstances and cell type. Involved in cell cycle regulation as a trans-activator that acts to negatively regulate cell division by controlling a set of genes required for this process
Aldehyde dehydrogenase family 1 member A3	P47895	AL1A3_HUMAN	2.056	untreated parental	plays important role in cell proliferation, differentiation and survival especially during the cellular responses to oxidative stress

The data were summarised after 4 individual experiments with different passage numbers (n=4) using SCIEX OneOmics with the following parameters: MLR weight >0.15, confidence >70%, algorithms. Both accession numbers and protein names are from the Uniprot database. The common proteins that were found among all the comparisons were encircled with red colour.

Table 6.2: Identification of up-regulated proteins/peptide in TEV-1 cells.

(C) Untreated spheroids versus DOX-treated spheroids

Protein Name	Accession number	Uniprot name	Absolute fold change	Up -regulated expression	Function of the protein
Prelamin-A/C	P02545	LMNA_HUMAN	5.648	untreated spheroids	Plays an important role in nuclear assembly, chromatin organization, nuclear membrane and telomere dynamics.
Plasminogen	P00747	PLMN_HUMAN	3.646	untreated spheroids	It plays role in embryonic development, tissue remodelling, tumour invasion, and inflammation.
Galectin-1	P09382	LEG1_HUMAN	1.249	untreated spheroids	Plays a role in regulating apoptosis, cell proliferation and cell differentiation.

(D) DOX-treated parental versus DOX- treated spheroids

Protein Name	Accession number	Uniprot name	Absolute fold change	Up -regulated expression	Function of the protein
Plasminogen	P00747	PLMN_HUMAN	2.135	DOX-treated parental	It plays role in embryonic development, tissue remodelling, tumour invasion, and inflammation
Complement component 1 Q subcomponent-binding protein, mitochondrial	Q07021	C1QBP_HUMAN	1.945	DOX-treated spheroids	it is believed to be a multifunctional and multicompartmental protein involved in inflammation and infection processes, ribosome biogenesis, regulation of apoptosis, transcriptional regulation and pre-mRNA splicing.
Galectin-1	P09382	LEG1_HUMAN	1.535	DOX-treated parental	Plays a role in regulating apoptosis, cell proliferation and cell differentiation

The data were summarised after 4 individual experimentations with different passage numbers (n=4) using SCIEX OneOmics with parameters MLR weight >0.15, confidence >70% algorithms used mentioned as detailed. Both accession numbers and protein names are from the Uniprot database. Any protein found in both conditions were encircled with red colour.

Table 6. 3: Protein changes that are common to HTR/SVneo and TEV-1 cells.

Protein Name	HTR8/SVneo and TEV-1(Comparison)
Plasminogen (PLMN_HUMAN)	Up-regulated in untreated spheroids compared to its parental counterpart
Vitronectin (VTNC_HUMAN)	Up-regulated in untreated spheroids compared to its parental counterpart
Aldehydedehydrogenase family 1 member A3 (AL1A3_HUMAN)	Up-regulated in untreated spheroids compared to its parental counterpart

6.3 Discussion

The aim of this chapter was to investigate and compare the status of the tumour associated factors ALDH3A1, AURK-A and C, PDGFRα, TWIST1, and JAG1 in four trophoblast cell lines (HTR8/SVneo, TEV-1, JEG-3 and BeWo) and MCF-7cells under different conditions. The expression of these factors have been investigated in placental tissues (NT and PE) in Chapter 3. In this chapter, the status of the same factors were analysed in different trophoblast cell lines and the spheroidal cells generated from them. Both mRNA and protein expression were compared by qRT-PCR and semi-quantitative western blotting respectively. To the best of author's knowledge, this is the first study that has attempted to comparatively analyse the protein and mRNA expressions of these factors in (trophoblast) placental derived cells. Since some of the factors related to tumourigenesis have been shown to be changed with spheroidal transformation, it was also decided to compare the global protein expression (proteome) during spheroidal transformation.

As mentioned in Section 6.1, there are many difficulties in using primary cell cultures. To elaborate further, the purity of primary trophoblasts are always questionable as these cultures readily become contaminated with other cell types such as fibroblasts, endothelial and mesenchymal cells (Zuo *et al.,* 2014). Furthermore, they cannot be maintained for long periods in culture. Therefore, several trophoblast cell lines have been established and characterised to investigate the proliferation and invasion of both placenta and placental tumours (Zuo *et al.,* 2014). These cells have different features and they share some molecular markers with their primary counterparts. However, they are of limited value for studying the paracrine/autocrine interaction between sub-populations of trophoblast because all these cell lines differ from each other as they: a) do not comprise the sub-populations, b) have differing genetic backgrounds, and c) have been immortalised under different procedures or obtained after tumorigenic transformation strategies (Hiden *et al.,* 2007).

Some of these cells have been used in this study, such as HTR8/SVneo, which is a human immortal first-trimester EVT cell line, originated from extravillous cytotrophoblast and exhibits similar *in vitro* invasive properties to the parental cells (Lala *et al.,* 2002).The TEV-1 cell line was established from a human first-trimester extravillous trophoblast cell line. It resembles EVTs in the expression of immunological antigens and phenotypic characteristics (Feng *et al.,* 2005). JEG-3 is a choriocarcinoma cell line, used as a trophoblast cell model to study placental function and presents many of the biological and biochemical characteristics associated with syncytiotrophoblasts (Matsuo and Strauss, 1994). BeWo is another type of choriocarcinoma cell line, used *in vitro* as a model to mimic *in vivo* syncytialisation of

placental villous trophoblasts, to study villous trophoblast differentiation and fusion (Orendi *et al.,* 2010).

6.3.1 Relative mRNA/protein expressions of factors of interest

The variance in mRNA and protein expression level of these factors (ALDH3A1, AURK- A and C, PDGFRα, TWIST1, and JAG1) were compared between different conditions. It is worth noting that data from different cell lines were found to be different to each other. This shows that the observations are cell line specific and might have been influenced by the way they were immortalised. Also, compared to the house-keeping proteins, the expression of these factors are low, both at mRNA and protein levels. Some comparisons showed a correlation between relative mRNA expression and protein level (especially in MCF-7 cells), whereas other results did not show this correlation. As mentioned in Chapter4 (Section 4.3.5), the reason for the mismatch correlation between mRNA and protein levels is not fully clear, but it may be possible that expression of mRNA is reciprocally reduced as a result of the high levels of protein expression. Moreover, it could be because of the half-life of some mRNA transcripts is extremely low due to RNA degradation.

- **ALDH3A1**

ALDH is also found in stem cells during early life and was demonstrated as an important marker for identification of SCs (Douville *et al.,* 2009). Also ALDH1 can be a better marker of breast cancer SCs than CD44+/CD24- (Tanei *et al.,* 2009). It has also been described as a stem cell marker in various solid tumours including lung cancer (Jiang *et al.,* 2009), breast carcinoma (Ginestier *et al.,* 2007), and colorectal cancer (Huang *et al.,* 2009). ALDH1A3 may influence cell activity and proliferation by controlling intracellular retinoid concentrations and play important roles in stem cell biology (Balber, 2011). It also plays an essential role in the cell proliferation, drug metabolism and regulation of growth and differentiation in both normal and cancer cells (Muzio *et al.,* 2012). The mRNA of a specific isoform ALDH3 has been found to be expressed in placental tissue (Alnouti and Klaassen, 2007). In this investigation, both HTR8/SVneo and BeWo cell lines showed a significant up-regulation in the protein expression of ALDH3A1 in DOX-treated parental compared to other conditions. In contrast to mRNA expressions, there was no significant difference in the protein expression level of ALDH3A1 in TEV-1 cells, in all conditions. Overall, the protein expression of ALDH3A1 was significantly higher in DOX-treated parental cells and untreated spheroid cells derived from JEG-3 cells. This increased expression of ALDH3A1 in both untreated and DOX-treated spheroids may indicate that spheroidal cells have increased their stem cell-like features. Interestingly, there was a significant up-regulation of

ALDH3A1 protein expression in MCF-7 spheroidal cells compared to parental conditions. This could be because MCF-7 is a breast cancer cell line as stated earlier (Tanei *et al.,* 2009).

- **AURK-A**

As explained in Chapter 3, AURK-A shows a high expression in PE tissue samples. AURK-A plays an important role in cell cycle progression, and has been implicated in tumour formation and progression (Fu *et al.,* 2007). It is highly expressed in several tumour types such as breast, lung, colon, prostate and pancreas (Siggelkow *et al.,* 2012). Furthermore, polymorphisms in the AURK-A gene are associated with increased primary breast cancer risk (Fletcher *et al.,* 2006). Interestingly, the protein expression of AURK-A in MCF-7 cells was significantly higher in untreated spheroids compared with other conditions. A recent study showed that the protein expression of AURK-A was elevated in the MCF-7 cell line (Sun *et al.,* 2014). According to the data presented in this chapter, the protein expression level of AURK-A was increased in HTR8/SVneo untreated spheroids compared to other conditions. A significant increase in protein expression of AURK-A in TEV-1 DOX-treated spheroidal cells was observed, compared to their spheroidal cell counterparts. This suggests that spheroids produced from the transformed trophoblast cell lines may have gained the ability to proliferate. On the other hand, despite their cancerous origins, there were no significant changes in the expressions of AURK-A in spheroids produced from JEG-3 and BeWo, as higher levels of expression were expected.

- **AURK-C**

The expression of AURK-C in trophoblast cells has not been reported yet. As explained in Chapter 3, there was a significant increase in the mRNA and protein expression of AURK-C in NT placental tissues compared to PE. In the cell lines, a significant reduction in protein expression of AURK-C was observed in HTR8/SVneo, TEV-1 and JEG-3, in spheroidal cells (untreated and DOX-treated) compared to other conditions. However, in BeWo cells the protein expression was up-regulated in untreated spheroids compared to DOX-treated spheroids. Since AURK-C is overexpressed in cell transformation and tumour formation (Khan *et al.,* 2011), in fact, this is the first study to show the expression of AURK-C in these cell lines and their spheroids.

- **PDGFRα**

PDGFRα signalling has important functions during embryogenesis, and its overexpression is associated with several pathological conditions such cancer (Carvalho *et al.,* 2005). The expression of PDGFR-α in trophoblast cell lines has not previously been investigated. The current data shows, a significant increase in protein expression of PDGFRα observed in DOX-treated spheroidal cells of HTR8/SVneo. In addition TEV-1 cells showed a significant increase in protein expression of PDGFRα in both spheroidal cells (untreated and DOX-treated) compared to parental conditions. Increased expression of PDGFRα in untreated and DOX-treated spheroids in both transformed cell lines (HTR8/SVneo and TEV-1) may indicate that spheroidal cells have increased their stem-like cell features, [as PDGFRα was expressed by multipotent cardiovascular progenitors in mouse and human embryonic stem cell systems (Tallquist and Soriano, 2002)]. In contrast a significant reduction in protein expression was observed in spheroidal cells (untreated and DOX-treated) of BeWo cells compared to their parental cell counterparts. This was unexpected as PDGFR-α expression has been previously reported in various tumour types such as ovary, prostate, colon and lung (Bronzert *et al.,* 1987). On the other hand, there was a significant difference in protein expression of PDGFRα between untreated spheroidal cells of MCF-7 confirming its expression being correlated with invasive breast carcinomas (Carvalho *et al.,* 2005).

- **TWIST1**

TWIST1 plays many roles in promoting tumour metastasis (Kang and Massagué, 2004). Furthermore, studies showed TWIST1 plays a role in promoting trophoblast invasion in mice (Abell *et al.,* 2009). However, the role of TWIST in human trophoblast invasion is still not clear. The current data shows that the protein expression of TWIST1 was significantly increased in the case of HTR8/SVneo spheroids (both DOX-treated and untreated) compared to their parental cells counterparts. This actually confirms the finding of Ng *et al.* (2012) that the mRNA and protein expressions of TWIST1 was substantially increased in HTR8/SVneo (more than both choriocarcinoma cell lines JEG-3 and BeWo). Regardless of the differences in the aims of the present study and the study by Ng *et al*. (2012), the findings of both studies agree that TWIST1 could play important role in spheroidal transformation and/or trophoblast invasion.

- **JAG1 (Jagged1)**

Interestingly, the result from Chapter 3 showed that JAG1 mRNA and protein expression were high in human placental tissues. However, the result from this chapter showed that there was no significant change in the mRNA and protein expression levels of JAG1 observed in trophoblast cells (HTR8/SVneo, TEV-1 and BeWo). On the other hand, the protein expression level was up-regulated in JEG3 DOX-treated parental cells compared to both (a) untreated parental, and (b) DOX-treated spheroidal cells. The MCF-7 cell line showed similar results to the trophoblast cell lines, (i.e. there was no significant change in mRNA and protein expression level of JAG1). According to Herr *et al.,* (2011) NOTCH receptors 1-4 and their ligands JAG1, -2 are expressed in first and third trimester human placental tissue. Also many studies have identified NOTCH1 receptors in the endometrium, and blastocyst. Moreover, JAG1 was detected in placental endothelial cells (Zhao *et al.*, 2013). It has also been demonstrated that NOTCH3 up-regulates its own ligand Jagged1 in human primary mammospheres (Zhang *et al.,* 2010), and in human breast cancer cell lines, such as MCF-7 and MDA-MB-231 (Shao *et al.,* 2015). NOTCH signalling plays important roles in implantation/placentation by the regulation of EVT invasion and spiral artery remodelling in the decidua and angiogenesis in the placenta (Cuman *et al.*, 2013). However, the data obtained here did not show any changes with spheroidal transformation.

6.3.2 Proteomics on global expressions of protein in transformed trophoblast cell lines

Proteomics technology can provide valuable information on the dynamic changes of proteins (Yang *et al.,* 2015). In this study, using SWATH-MS the up-regulated proteins between the following comparisons were identified: (a) untreated parental Vs. untreated spheroids; (b) untreated parental Vs. DOX-treated parental; (c) untreated spheroids Vs. DOX-treated spheroids; and (D) DOX treated parental Vs. DOX-treated spheroids. SWATH-MS analysis has identified up-/down-regulations of several proteins in different comparisons in transformed trophoblast (HTR8/SVneo and TEV-1) and choriocarcinoma (BeWo and JEG-3) cell lines. However, due to the high volume of data only the proteins that have shown up-regulation in fold changes in HTR8/SVneo and TEV-1 are discussed below. Interestingly, many of those proteins are found to be involved in cell proliferation, invasion, and differentiation. Others are involved in embryonic development and inflammation. These were up-regulated mainly in both un-/DOX-treated spheroids. As seen in Table 6.1 (A) and (C), in HTR8/SVneo both untreated and DOX-treated spheroids have shown up-regulation of many proteins. These include plasminogen and vitronectin. On the other hand, in TEV-1 cells only the untreated spheroids have shown up-regulation of these proteins.

Plasminogen is a precursor of plasmin during the blood clotting cascade (Stoppelli, 2013). Plasmin is one of the most important and reactive serine protease enzymes, present in blood that degrades many blood plasma proteins, including fibrin clots (Deryugina and Quigley, 2012). It plays a role in different physiological processes such as embryo development, wound healing (thrombolysis), and cancer development (Andreasen *et al.*, 2000). The plasminogen system is composed of two types includes the urokinase-type (uPA) and the tissue-type (tPA) (Alfano *et al.*, 2005) uPA is generally agreed to be the enzyme of most relevance to tumour biology, whereas tPA has a role in the generation of plasmin for fibrinolysis. As plasminogen activation plays an important role in vascular and tissue remodelling, tumour growth, and cancer progression (Andreasen *et al.*, 2000) and the fact that is up-regulated mainly in untreated spheroids (in TEV-1) and DOX-treated spheroids (in HTR8/SVneo cells) compared to parental cells indicate that these cells might have gained stemness features.

In contrast, vitronectin (VNTC) showed up-regulation mainly in DOX-treated spheroidal cells followed by un-treated spheroids in HTR8/SVneo cells. On the other hand, TEV-1 cells showed the highest fold change only in un-treated spheroids. Vitronectin is an abundant adhesion glycoprotein in blood plasma associated with different extracellular matrix sites and tumour cells (Preissner and Reuning, 2011). Vitronectin is produced in the liver, however, its mRNA has been detected in various tissues, including the brain and heart, and this suggests its production by other cells (Seiffert *et al.*, 1994). It plays an important role in cell migration, tissue repair and, tissue remodelling (Seiffert *et al.*, 1994). Moreover, it has many physiological functions such as cell adhesion, regulation of fibrinolysis, coagulation and immune defence, which could be key in the incidence and progression of severe PE, mainly in early-onset severe PE (Shen *et al.*, 2012). Different studies have reported that vitronectin protein expression has been found in breast cancer (Aaboe *et al.*, 2003). In addition, a significant increase in expression level of VTNC protein was found in the maternal-foetal interface of early-onset severe preeclampsia (Shen *et al.*, 2012). Here, the up-regulation of VNTC in spheroidal cells might be linked to their transformation and gaining invasiveness.

The other protein that showed high fold changes in the up-regulation in spheroidal cells was cysteine-rich protein 2 (CRIP2). This protein was up-regulated in untreated spheroids and DOX-treated parental of HTR8/SVneo cells. It is also worth noting, ALDH1A3 was observed to be up-regulated in untreated spheroids in both HTR8/SVneo and TEV-1 cells as identified by SWATH-MS. However, the qRT-PCR (mRNA) and western blotting (protein) results of ALDH3A1 did not completely agree with this. This may be mainly due to

ALDH1A3 is a different gene to ALDH3A1, which there are from same grup (ALD), but under different family and member. Overall the SWATH-MS data have identified several proteins that are up-regulated in untreated and DOX-treated spheroids. Some of the changes in proteins are consistent between HTR8/SVneo and TEV-1 cells (See Table 6.3). These proteins are linked with either cell proliferation, invasion or cell cycle control. For example, vitronectin has been identified as a component of serum which drives the differentiation of both breast and prostate CSCs (Hurt *et al.,* 2010). It is also used as a substrate substitute in matrigel to study the maintenance and differentiation of human pluripotent stem cells (hPSCs) (Braam *et al.,* 2008). This suggest the spheroidal cells expressing these proteins have gained "stem-like" behaviour; confirming the data obtained in Chapter 4.

6.4 Conclusion

According to the data from this study, the mRNA and protein expression of ALDH1A3, AURK-(A and C), PDGFRα, TWIST1, and JAG1 were differentially expressed in spheroidal and parental cells. Also, SWATH-MS analysis highlighted up-regulation of some proteins that are associated with proliferation, invasion and cell cycle control. This suggests that spheroidal (untreated and DOX-treated) generated from both transformed trophoblast cell lines, HTR8/SVneo and TEV-1, may have gained the "stemness" features.

Chapter 7
General Discussion

7.0 Discussion

The aims of this study were firstly, to compare the expression patterns of common factors related to invasion, such as ALDH3A1, AURK-A and C, PDGFRα, TWIST1, and JAG1 between normotensive (NT) and pre-eclamptic (PE) placentae. Secondly, to generate spheroidal cells from transformed trophoblast cells (HTR8/SVneo, TEV-1), and choriocarcinoma (JEG-3, BeWo) (using breast cancer cell line MCF-7 as non-placental tumour control). In addition, to check the effects of a chemotherapeutic agent (Doxorubicin) in producing drug resistant spheroids from all four trophoblast cell lines. This was followed by a characterisation of "stemness" feature by studying the expressions of stem cell markers, such as OCT4, SOX-2, NANOG, CDX2 and NOTCH1. Thirdly, to compare the migration and invasive potentials amongst non-resistant/drug-resistant spheroids and their original (parental) cells. Next linking with the first aim, the expression patterns of the common factors such as ALDH3A1, AURK- (A and C), PDGFRα, TWIST1, and JAG1 in spheroidal cells and their parental controls (both untreated and DOX-treated) were looked at. Finally, the study aimed to investigate the changes in the global protein (peptide) expression profiles in parental and spheroidal cells (untreated and DOX-treated) using SWATH-MS technique.

7.1 Expression analysis factors of interest in NT and PE

Differential gene expression techniques, such as microarray, have identified several candidate genes/factors involved in PE. As explained in chapter 3, these include growth factors, transcription factors, extracellular matrix proteins, and proteins involved in signalling pathways (Hansson *et al.,* 2006; Sood *et al.,* 2006; Louwen *et al.,* 2012). Using murine microarrays established by Dr Ali (Nottingham Trent University), some common molecules that might be hypothetically involved in trophoblast invasion were identified (eg. ALDH3A1, AURK-A, AURK-C, PDGFRα, TWIST1 and JAG1). To begin with, the mRNA and protein expression of these factors were compared in NT and PE placentae.

Although, pathophysiology of PE is still unclear, it is associated with abnormal vascular remodelling of the spiral arterioles and shallow invasion (Goldman-Wohl and Yagel, 2002). The abnormal remodelling reduces the oxygen supply to the placenta and decidua, creating a hypoxic condition which leads to the production of reactive oxygen species (ROS) and ultimately to oxidative stress **(www[23])**. Oxidative stress plays an important role in the pathophysiology of PE **(www[23])**. The data explained in chapter 3 suggest that the expression of these factors are definitely altered in PE. Since many of these factors are involved in cell proliferation and/or invasion, their altered expressions in PE placentae confirms previous

findings/hypothesis of trophoblast dysfunctions being responsible for PE (Burton and Jauniaux, 2004; Pennington *et al.,* 2012; Vaiman *et al.,* 2013). The changes in the individual proteins are discussed below.

Interestingly, the enzyme ALDH3 family has an important role during cell proliferation, differentiation, and also plays an important physiological role against cellular oxidative stress by detoxifying aldehydes derived from oxidative processes, such as ethanol metabolism (Marchitti *et al.,* 2010). The present study showed that both mRNA and protein levels of ALDH3A1 are significantly increased in PE placentae compared to NT. ALDH3A1 was recognized as an oxidative stress response protein as oxidative stress leads to increased ALDH3A1 expression (Moreb *et al.,* 2008; Kim *et al.,* 2014). ALDH3A1 is presumed to have a protective role against oxidative stress-induced apoptosis. This result is consistent with the hypothesis that oxidative stress is a significant factor in the pathogenesis of PE. Therefore, the higher levels of ALDH3A1 in PE could be a mechanism to overcome the oxidative stress induced apoptosis.

Likewise, AURK-A plays an important role in the regulation of mitosis and cytokinesis (Kimura *et al.,* 1999). Dysregulated Aurora-A expression leads to mitotic faults and results in pathological conditions (Mortlock *et al.,* 2007). To date no studies on AURK-A expression in human placental tissues have been reported. A study carried out by Cho *et al* (2014), illustrated that oxidative DNA damage can be related to the expression of AURK-A protein. Significant up-regulation of mRNA and protein expression of AURK-A in PE was observed in present study. Interestingly, results from IHC illustrated that AURK-A also showed higher staining for PE than NT placentae. It can be assumed that the AURK-A expression increasing in PE due to the high oxidative stress. However, both mRNA and protein expression levels of AURK-C were increased in NT compared to PE. The data was also confirmed by IHC which illustrated higher staining for NT than PE. AURK-C has a role in the regulation of mitosis and cytokinesis (Kimura *et al.,* 1999). It is expressed in many types of cancer, however the function of AURK-C in normal cellular processes is not fully understood (Quartuccio and Schindler, 2015). Therefore, it is difficult to predict the biological significance of this expression on the disease. Interestingly, it can be predicted that AURK-C might be expressed during first trimester trophoblast cells to enhance proliferation and invasion of EVT cells, which are important for successful pregnancy. Additionally, AURK-C could play a role during implantation by regulating cytokinesis (Mortlock *et al.,* 2007). The biological effects of PDGFs are exerted by activation of two

tyrosine kinases platelet-derived growth factor receptor PDGFRα and β. PDGFRα is instrumental during embryonic organogenesis and development by directing the cell proliferation, differentiation, migration, and function of specialised mesenchymal cells (Karlsson *et al.*, 1999).

The present study showed the mRNA and protein expression levels of PDGFRα are increased significantly in PE compared to NT. PDGFRα was studied only in early placenta but not near-term placental tissues. Therefore, a high expression in term PE samples could be an indication of malformation of the placenta.

TWIST1 plays a role in cell proliferation, migration and differentiation in embryonic progenitor cell populations and transformed tumour cells (Ansieau *et al.,* 2008). The current study shows a statistically significant increase of TWIST1 mRNA and protein expression in PE. Interestingly, these results were also validated with IHC and intense staining for TWIST1 was detected in the STB layer of PE placentae rather than NT placentae. Ng *et al* (2012) demonstrated that TWIST1 and N-cadherin are abundantly expressed in highly invasive EVT propagated from first-trimester human placenta. It could be suggested that TWIST1 over-expression in placental tissues might only has advantages in the early stage. A high expression of TWIST1 in PE placental samples could be a compensatory change to counteract the defective trophoblast invasion in PE.

JAG1 is one of the five cell surface proteins (ligands) that interact with four receptors in the mammalian NOTCH signalling pathway (Zhao and Lin, 2012). Overall they play an important role in normal development of human placenta. Therefore, the defect of NOTCH signalling pathway could contribute to the pregnancy complications, such as PE (Zhao and Lin, 2012). Sahin *et al*. (2011), detected a significant decrease in the immunoreactivity of NOTCH proteins in PE compared to normal placentae. This was consistent with the present data where both mRNA and protein expression levels of JAG-1 were decreased in PE compared to NT placentae. A study by Hunkapiller *et al.* (2011) speculated that there was a correlation between reduced JAG-1 expression and failed vascular remodelling in PE. The low expression of JAG1 in PE in this study could be associated with incomplete remodelling of human spiral arterioles.

These factors of interest were also investigated in trophoblast cell lines to confirm their expression patterns in these cells. The data showed that mRNA and protein expression of ALDH1A3, AURK-(A and C), PDGFRα, TWIST1, and JAG1 are expressed in these

trophoblast derived cell lines. However their expression levels in each trophoblast cell line were found to be different. The disparities in mRNA and protein expression could be due to their origins and differences in immortalization method used to develop these cells. In summary the factors that were identified from murine microarrays as potential markers for defective trophoblast invasion have all showed changes in PE placentae.

7.2 Generation of spheroids from trophoblast and tumour cell lines

In this study, both transformed trophoblast cells (HTR8/SVneo, TEV-1) and choriocarcinoma cells (JEG-3, BeWo) and also MCF-7 cells have shown the ability to produce non-resistant (normal) spheroids under non-adherent conditions. Moreover, they were able to revert back to normal growth under adherent conditions. Due to the nature of the MCF-7 cells, they produced a larger sized spheroid when compared to the spheroids produced from trophoblast cell lines. In 2013, Webber *et al.* illustrated that HTR8/SVneo cells have a high ability to form spheroidal bodies. Likewise multicellular spheroids were established from JEG-3 and BeWo in culture by Grummer *et al.* (1994). In the case of MCF-7 cells, several studies have shown that the cell line can be used as a model of 3-D cellular organization, which has ability to grow as multicellular spheroids (Villalobos *et al.*, 1995; Guttilla *et al.*, 2011). Based on these findings the spheroid body-forming cells have several features, which include self-renewal, differentiation into specialized cell types and proliferation (Cheng *et al.*, 2012; Liu *et al.*, 2013). The current findings suggest that all four investigated trophoblast cell lines have stem cell features; that is they are more than just aggregates of cells. Although previous studies have shown this spheroidal transformation abilities in HTR8/Svneo, JEG-3 and BoWo cell lines, to the best of the author's knowledge, this was the first study to produce and characterise the spheroidal cells from TEV-1 cells. Since TEV-1 cells are also derived from first trimester trophoblast cells, this finding proves that most of the transformed EVT cells have the ability to produce spheroidal cells. Moreover, DOX was used in this study to select drug resistant spheroids generated from four trophoblast cell lines and also to check their aggressive profile.

After producing spheroids, the expression of transcription factors (OCT4, SOX2 and NANOG), trophoblast transcription factor (CDX2), and NOTCH1 were checked. OCT4 plays a key regulatory role in self-renewal and differentiation of pluripotency of mouse and human embryonic stem cells (Pan *et al.*, 2002). Thus, the expression of OCT4 in trophoblast spheroids may be linked to "stem-like cells" properties, such as self-renewal, of these cells.

From current data, compared to parental cells, the mRNA and protein expression of OCT4 showed a significant increase in spheroidal cells (both DOX-treated and untreated) produced

from JEG-3, BeWo and MCF-7cell lines. Likewise, SOX2 and NANOG play regulatory roles along with other transcriptional factors (OCT4 and NANOG) maintain pluripotancy and self-renewal features in human and mouse ESCs (Boyer *et al.*, 2005). Interestingly, both, immunofluorescence staining and western blot, results suggested that SOX2 expression increased in spheroidal cells. In contrast, the mRNA expression of SOX2 was up-regulated only under untreated spheroid conditions compared to the parental conditions in TEV-1, JEG-3 and MCF-7 cells. The difference in expression patterns between mRNA and protein in this study, may be due to the half-life of mRNA, as protein cannot be translated from mRNA with very short or long half-life (Wang *et al.*, 2002; Yang *et al.*, 2003).

The fact that the "stemness" markers OCT4, SOX2 and NANOG have increased especially in spheroidal cells from all four trophoblast cell lines suggests that these cells have transformed themselves into "stem-like" cells. According to Desoizet *et al.* (1998) the spheroids were used in oncology for studying the multi-drug resistant types of cancer. Moreover, it was also useful in studying the resistance to chemo- or radiotherapy. By using a spheroid model, it is possible to investigate cell to cell and extracellular matrix (ECM) to cell interactions *in vitro* (Nederman *et al.*, 1984; Oudar, 2000; Mehta *et al.*, 2013). The data explained in chapter 5 have clearly shown that DOX treated trophoblast cells produced spheroids that not only displaying "stemness" features, such as self-renewal by reverting back into a monolayer when re-grown under normal conditions, but also showed resistance against DOX treatment. Therefore, these cells may be used as a model to study the toxicological effects of other chemotherapeutic effects on "physiologically rapidly dividing" cells.

7.3 Migration capacities of spheroidal from trophoblast cell lines

The ability for the cells to migrate is an important characteristics of all stem-like cells. However, as spheroidal cells grow in aggregate, they were transformed into the normal adherent flasks to study their capacities of migration. The current data showed that the migration rate of HTR8/SVneo and TEV-1 untreated spheroids was faster than the parental cells at 48 hours. This was expected since spheroids act like solid tumours *in vivo* with deregulated proliferation and an uncontrolled speed of migration (Ferretti *et al.*, 2007). However, DOX-treated spheroidal cells showed low rate of migration at 48 hours. Spheroid monolayers are different from normal cell monolayers and they still have 'stem like cells' features and should show the ability to resist drug treatment. However the low rate of migration showed by the monolayers formed by the spheroidal cells may be due to the enhanced penetration by DOX. That is the penetration of DOX into the spheroidal cell clusters will be difficult; and therefore its effects will be limited in cells that are growing in

3-D culture. However, the DOX exposure would have been greater when these cells were re-transformed into monolayers. Thus, DOX could have been absorbed rapidly. In fact, the 3-D structures provide a multicellular resistance model that mimics the chemotherapy resistance often found in solid tumours *in vivo* (Oudar, 2000). This might have affected the migration of spheroidal, especially DOX-treated cells. Unfortunately due to the growth patterns of choriocarcinoma cells (BeWO and JEG-3), it was impossible to carry out a wound healing assay even with parental cells. These cells do not produce cell monolayers and it was extremely difficult to produce a uniform wound (or scratch) as such attempts disrupted cell attachments.

7.4 Invasion capacities of spheroidal cells from trophoblast cell lines

The analysis of growth, proliferation and invasion of trophoblast cells in culture is essential, to understand the functions of the placenta by using different trophoblast cell lines (Zuo *et al.*, 2014). Moreover, study of trophoblast cell invasion will lead to a better understanding of trophoblast invasion mechanisms and this will be essential for the treatment of pathological conditions which are involved in placental over-invasion (e.g., choriocarcinoma) or under-invasion (e.g., pre-eclampsia). Moreover, it is also important to develop therapies for cancer (Graham and Lala, 1992). However, comparing the invasion of parental and spheroidal cells is difficult. Therefore, two different approaches were made (a) A 2-D invasion assay to compare the invasive potentials between parental and spheroidal cells. For this the spheroidal cells were manually disrupted into single cells. This was essential as the BD Bio-coat invasion assay kit has a membrane that would only allow single cells with the optimum diameter of 8 μm. Also by breaking spheroids into single cells, it would be interesting to see whether they have gained true transformation into "stem-like cells" and (b) A 3-D invasion assay to see and compare the invasive potential of un-treated and DOX-treated spheroidal clusters that were made from trophoblast cells. In fact monolyer spheroidal cells are not entirely appropriate to study the interactions between the invasive spheroid and the basement membranes. Thus, 3-D invasion was used to compare the invasive behaviour of spheroidal cells.

The current data strongly suggest that in 2-D invasion assay all trophoblast cell lines (HTR8/SVneo, TEV-1, JEG-3, and BeWo) showed a higher invasion in untreated spheroids compared to other conditions with different capacity in each cell lines. This shows that untreated spheroidal cells have truly transformed into "stem-like cells". In addition the 3-D invasion assay using a BME-3D kit, have shown, with time the invasion of untreated spheroidal cells of all trophoblast cell lines (HTR8/Svneo, TEV-1, JEG-3 and BeWo) was higher than that of DOX-treated spheroids. Moreover the data suggested that spheroids of

choriocarcinoma can potentially invade faster than that of transformed trophoblast cells. It may be due to the nature of these cells, as they are malignant trophoblastic tumour cells. However, DOX-treated spheroids in both JEG-3 and BeWo showed a strange behaviour, where the distorted shape of spheroid did not show any invasion in both cell lines. This may be due to the persisting effect of the DOX treatment in these small spheroids. According to Gong *et al.* (2015), the penetration capability of DOX can be influenced by spheroid size. Their study reported that stronger DOX penetration was observed within the smaller spheroids compared to larger spheroids which showed higher chemo-resistance. Likewise the study by Gong *et al.* (2015), suggested that 3-D spheroids drug sensitivity depended on the spheroids size. Unfortunately, both untreated and DOX-treated spheroid of non-invasive cells (MCF-7) remained as cell aggregates and did not show any ability to invade into the surrounding invasion matrix in 3-D assay. That is despite the ability of MCF-7 producing spheroids under non-adherent conditions with serum-free medium contained growth factors (See Chapter4), they did not show any invasion in 3-D cell invasion assay. This was not expected as MCF-7 was used as a non-placental tumour positive control to detect/compare invasions with trophoblast cell lines.

According to studies supplementary growth factors, such as bFGF, FGF, EGF and insulin (IGF), are necessary to maintain and influence cell proliferation, motility, survival and morphogenesis (Rodrigues *et al.,* 2010). However the effect of each growth factor is different. For example, bFGF has a role in forming tumour spheres and in maintaining the characteristics of sphere-forming cells (Min *et al.,* 2015). FGF plays an important role in creating tumour spheroids and increasing the internal population (Kondo *et al.*, 2004). It has been reported that EGF promoted sphere formation and enhanced the self-renewal capacities of human glioma-derived cancer stem cells CSCs (Soeda *et al.,* 2008). Insulin has an essential role in proliferation of normal stem cell (Ziegler *et al.,* 2014). Arsenijevic *et al.* (2001) reported that in the absence of IGF, EGF or FGF embryonic cells were unable to stimulate sphere formation. Furthermore, study of Min *et al.* (2015) reported that the spheroids from MCF-7 cells maintained in media containing growth factors showed greater cell proliferation than spheroids in media with FBS. Therefore, it can be assumed that the growth factors might play a role in MCF-7 spheroid formation under 3-D culture.

7.5 Global expressions of protein in transformed trophoblast cell line

Comparative SWATH-MS analysis amongst spheroid and parental cells (untreated and DOX-treated) have identified up-regulation of 14 novel proteins generated from HTR8/SVneo cell lines. Likewise 8 novel proteins have been identified to be up-regulated in TEV-1. Interestingly, most of these proteins were associated with cell adhesion, proliferation, differentiation, invasion and embryo implantation. The most interesting proteins that were found in both HTR8/SVneo and TEV-1 cell lines under different conditions are plasminogen, vitronectin and ALDH1A3. Due to time restrictions it was not possible to further analyse the real time expression profiles of all the new/novel peptides that were identified by the SWATH-MS analysis as up-/down-regulated in different spheroid cells (See Section 7.7)

7.6 Conclusion

The data from this study suggest that

- The mRNA and protein expression of ALDH1A3, AURK-(A and C), PDGFRα, TWIST1, and JAG1 were differentially expressed in NT, and PE placenta. Interestingly their expression was also found to be different in untreated and DOX-treated spheroidal cells compared to their parental counterparts.
- This study has successfully generated and characterised "stem-like" spheroidal cells from four different trophoblast cell lines (namely HTR8/SVneo, TEV1, JEG-3 and BeWo) using non-adherent 3-D culture.
- These spheroids showed increased protein expression of stem cells markers, such as OCT4, SOX2 and NANOG. On the other hand, both trophoblast CDX2 and the cell fate determining transcription factor, NOTCH1, are reduced in spheroidal cells.
- Spheroids generated from different trophoblast cell lines may also be used as an *in vitro* model to study the toxicological effects of chemotherapeutic agents on physiologically rapidly dividing cells.
- SWATH-MS analysis highlighted up-regulation of novel proteins that are associated with proliferation, invasion and cell cycle control in both transformed trophoblast cell lines (See the synopsis of the PhD thesis).

SYNOPSIS OF THE PhD THESIS

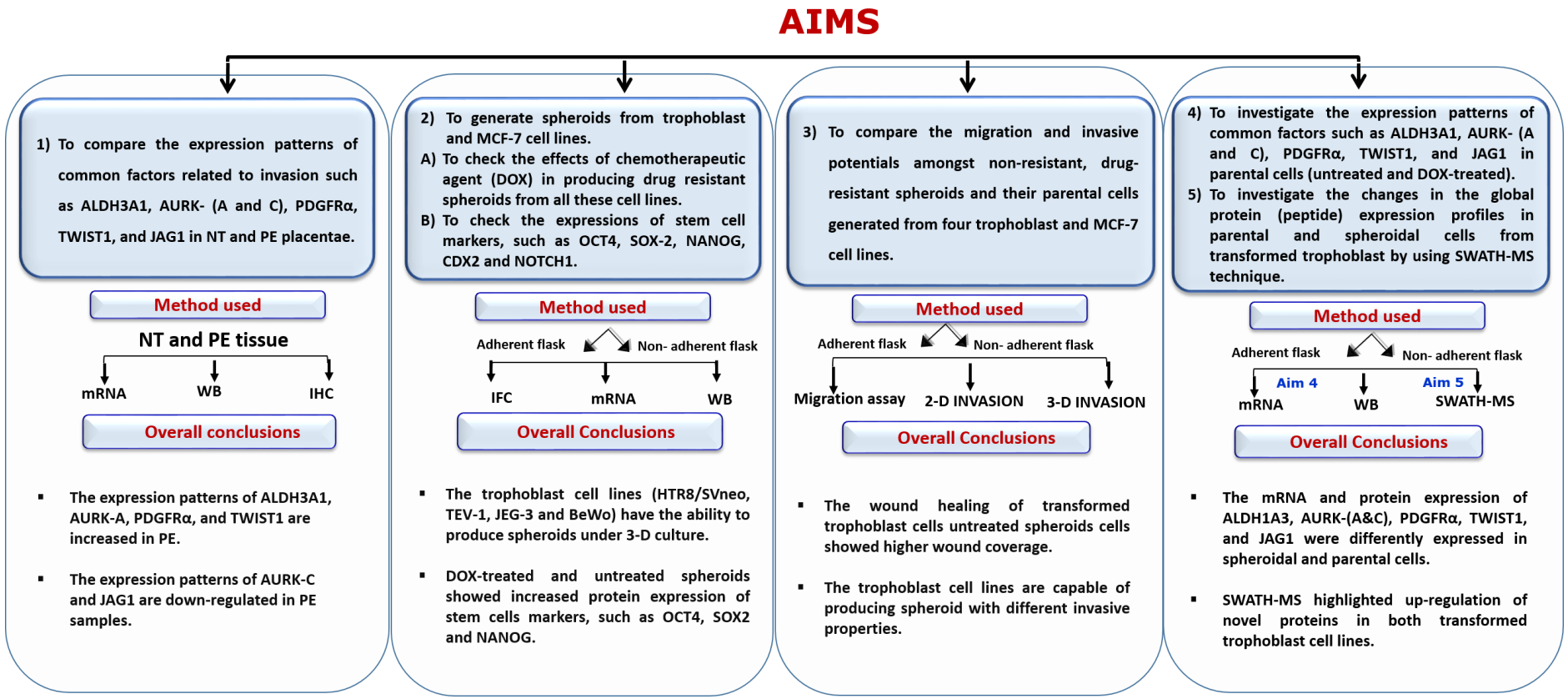

7.8 Future work

Firstly the comparative expression analysis between NT and PE samples need to be extended to check the status of the molecules/proteins that were using SWATH-MS with a larger number of placental samples to identify the changes in global protein expression profiles in PE samples. The status of these identified proteins would then be checked in real time using qRT-PCR and immunoblots. Also by using primary culture, such as CTBs, and EVTs, the role of these newly identified factors during first trimester can be investigated using *in vitro* invasion studies. This will be shed some light on functional relationships of these proteins during placental invasion. The cellular expression of these proteins can also be identified using cellular fractionation techniques such as micro-dissection and coupled with mRNA/protein expression studies in particular cellular groups, such as CTB, STB and deciduas.

Interestingly, this study has successfully showed the potentials of producing "stem-like" spheroid cells. Further studies may also be appropriate to check the status of other "stemness" markers such as CD44, CD34, CD90 and CD133 in spheroids produced from trophoblast cells lines, especially HTR8/Svneo and TEV-1 to confirm the stem-like transformation during 3-D culture. Upon confirmation, the effects of oxidative stress, a contributing factor for PE, on the invasion of spheroid cells can be compared with their respective parental cells. The results would show whether there are any differences in the responses to oxidative stress by spheroids.

Furthermore exploration studies using these cells as *in vitro* models of physiologically rapidly dividing cells are essential. Using 3-D spheroids of transformed trophoblast cell lines HTR8/Svneo and TEV-1, the effects of current chemotherapeutic agents on physiologically rapidly dividing cells can be studied in relation to other non-trophoblast tumour cell lines. Depending on the results, it may be possible also to investigate the ability of primary trophoblast cells such as CTBs, ST and EVTs to produce spheroid under the same conditions.

Also as explained in section 7.6 (and in chapter 5), the MCF-7 clone used in this study was found to be non-invasive; therefore it is essential to repeat the invasion assays with spheroids obtained from invasive clones of MCF-7 or other non-placental tumour cell lines. This would not only confirm the invasive capacities of drug-resistant spheroids from non-placental tumours, but also compare the differences between the drug-resistant spheroids that are produced from trophoblast (physiologically rapidly dividing cells) and tumour cells.

Most importantly it is essential to explore all the proteins that have been identified by SWATH-MS to have several fold (of either increase or reduced) changes during spheroids transformation. This was not possible during this study due to time restrictions. Using bioinformatics, the cellular functions of these proteins/peptides can be identified. Following this the real time status of these proteins can be investigated using qRT-PCR and western blotting.

Appendix

A.1 :Clinical data of patients

Table A 1: Clinical Data

Serial No.	Normotensive:	Maternal age (Years)	Gestational age (Weeks)	Systolic BP (mmHg)	Diastolic BP (mmHg)	Placental Weight (Grams)	Mode of Delivery	Gestational weight (Kg)	Gestational Sex	BMI	Protein in urine (g/L)
N1	**V6**	34	38.4	122	60	855	Vaginal	4.24	male	21.6	N/D
N2	**V7**	32	38.9	120	90	700	Vaginal	3.3	female	24.5	N/D
N3	**V8**	29	40.1	140	68	520	Vaginal	3.8	male	23	N/D
N4	**V9**	36	39.2	128	68	579	Vaginal	3.12	male	24.2	N/D
N5	**V10**	39	39.2	130	70	636	Vaginal	3.03	male	23.5	N/D
N6	**V11**	35	38.1	120	70	654	Vaginal	3	male	23	N/D
N7	**V12**	34	38.3	120	72	725	Vaginal	3.33	female	23	N/D
N8	**V13**	40	38.4	123	70	852	Vaginal	4.24	male	24.2	N/D
N9	**V15**	29	39.2	122	66	625	Vaginal	3.21	male	23.5	N/D
N10	**V23**	36	39.1	110	70	579	Vaginal	3.01	male	24	N/D
N11	**V24**	35	39.2	125	71	560	Vaginal	3.01	female	24.7	N/D
N12	**SITE-1**	35	38.5	109	78	698	Vaginal	3.5	female	23.5	N/D
N13	**ALISON**	34	39.3	122	67	524	Vaginal	3.51	male	24.5	N/D
	Average	34.46	38.92	122.38	70.77	654.38		3.41		23.63	
	STD	3.20	0.55	7.94	7.04	109.85		0.44		0.86	

Serial no.	Pre-eclamptic:	Maternal age (Years)	Gestational age (Weeks)	Systolic BP (mmHg)	Diastolic BP (mmHg)	Placental Weight (Grams)	Mode of Delivery	Gestational weight (Kg)	Gestational Sex	BMI	Protein in urine (g/L)
P1	**Kirsty**	28	33	150	92	360	Vaginal	1.66	male	23.5	2.5
P2	**PE3**	27	36	168	95	470	Cesearean	2.3	male	22.8	1.5
P3	**PE5**	29	37	152	110	505	Cesearean	1.87	male	22.5	1.14
P4	**V14**	29	38	150	111	420	Vaginal	1.82	female	24.4	1.01
P5	**V16**	27	36	160	92	545	Cesearean	2.6	male	24.6	1
P6	**V17**	28	39	160	90	480	Cesearean	1.76	male	22.8	0.9
P7	**V18**	32	37	150	90	510	Cesearean	2.98	male	22.5	0.98
P8	**V19**	28	38	150	90	529	Cesearean	3.1	female	21	1
P9	**V22**	28	39.5	155	95	510	Cesearean	2.8	male	23.5	0.91
P10	**V25**	28	38	155	112	517	Cesearean	2.9	male	22.8	0.875
P11	**V26**	29	39	140	108	620	Vaginal	3.59	female	23	0.88
P12	**Angela**	29	39.4	156	98	610	Cesearean	3.12	male	22	1.1
	Average	28.5	37.5	153.3	98.5	506.3		2.54		22.95	1.14
	STD	1.31	1.86	6.99	8.98	71.79		0.64		0.98	0.46

A.2: The extraction of RNA from NT (Panel A) and PE (panel B) placental tissues.

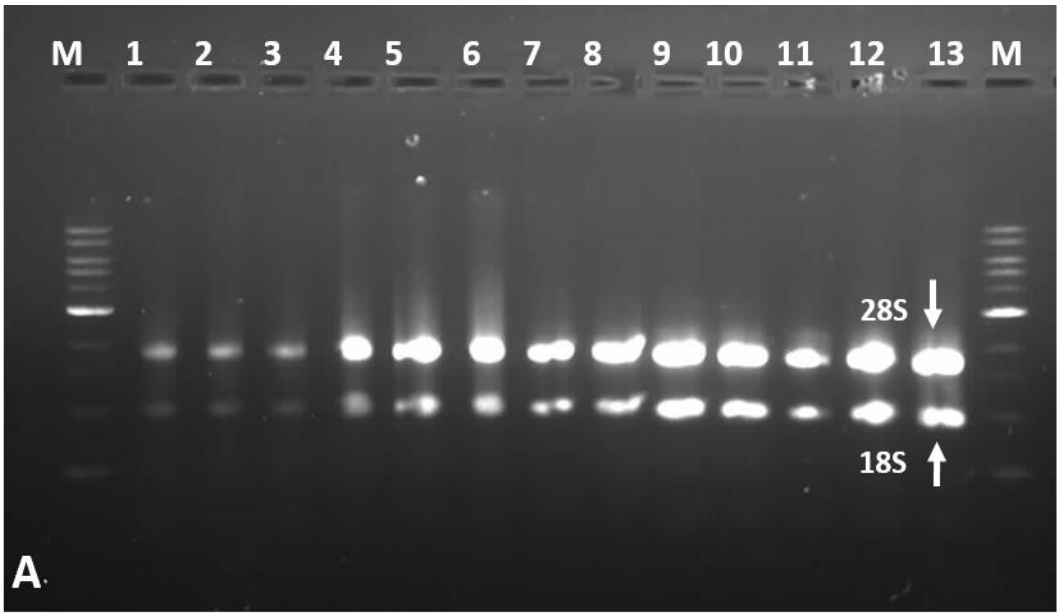

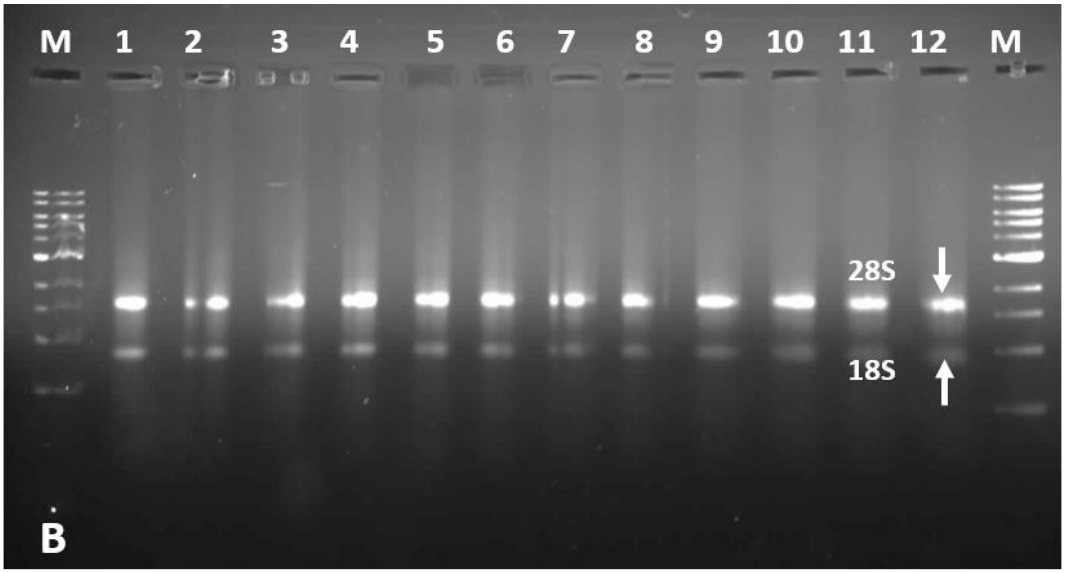

Figure A 1 The purity of extracted RNA from NT and PE placental tissues.

[M= 1Kb Molecular marker; Panel A = RNA extracted from 13 ***NT*** *samples; Panel B = RNA extracted from 12* ***PE*** *samples]*

A.3:Temperature optimisation for factors of interest

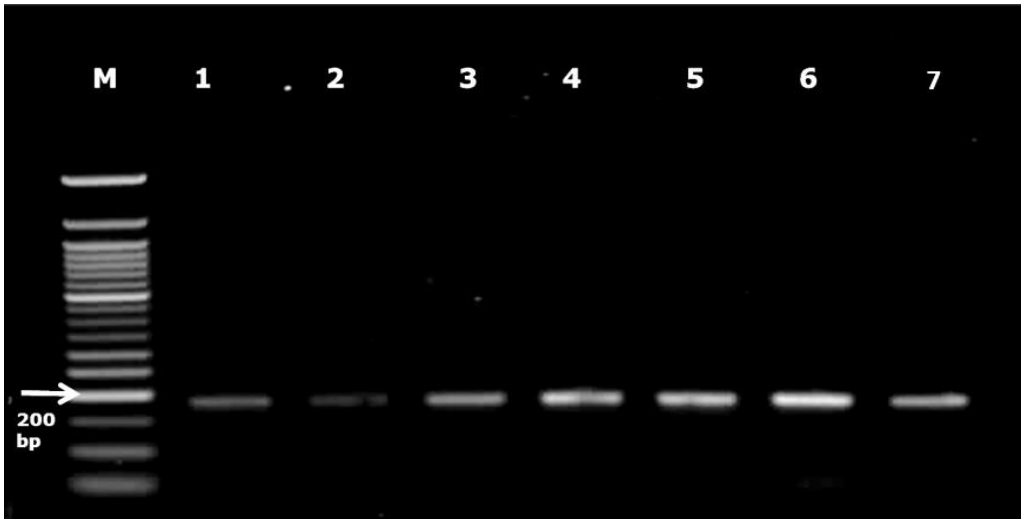

Figure A 2: Confirmation of PCR products in agarose gel.

*[Amplified factor products with placental sample. M-Molecular marker (ladder) 50bp, lane1- **ALDH3A1**, lane2- **AURK-A**, lane3- **AURK C**, lane4- **PDGFR-α,** lane5- **TWIST1,** lane6- **JAG1** and lane7- **MCF-7** (used as positive control).*

A.4: Accession numbers for target factors used for primer designing

Table A 2: NCBI accession numbers for factors.

Factor	NCBI accession number
ALDH3A1	NM_001135168.1; NM_001135167.1
AURK- A	NM_198433.1; NM_003600.2
AURK-C	NM_001015878.1;NM_001015879.1;NM_003160.2
PDGFR-α	NM_006206.4
TWIST-1	NM_000474.3
JAG1	NM_000214.2

A.5: Example of sequencing

Figure A 3 : The DNA sequencing data for AURK-A PCR product.

The bases represented by N were replaced by the specific bases identified by their coloured peaks (**A- Green**, **T- Red**, **G- Black** and **C- Blue**).

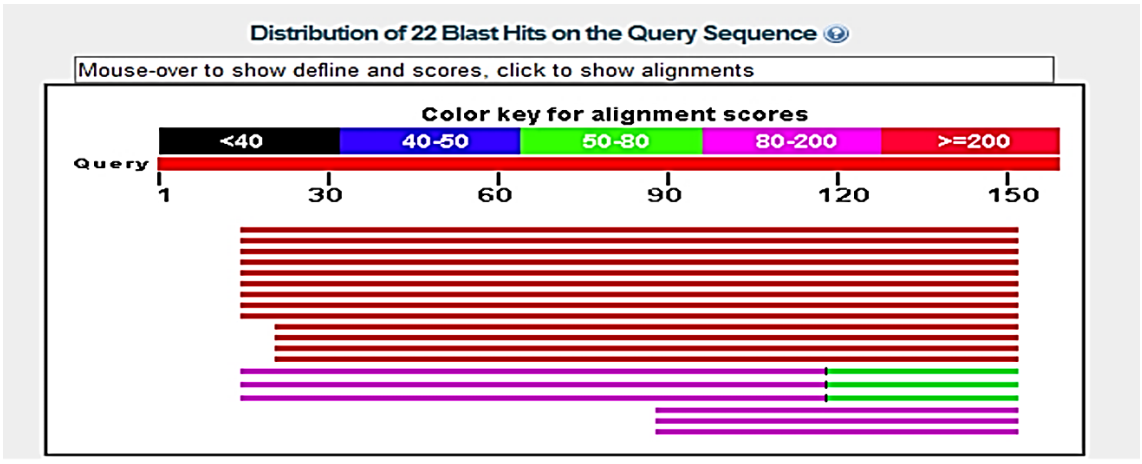

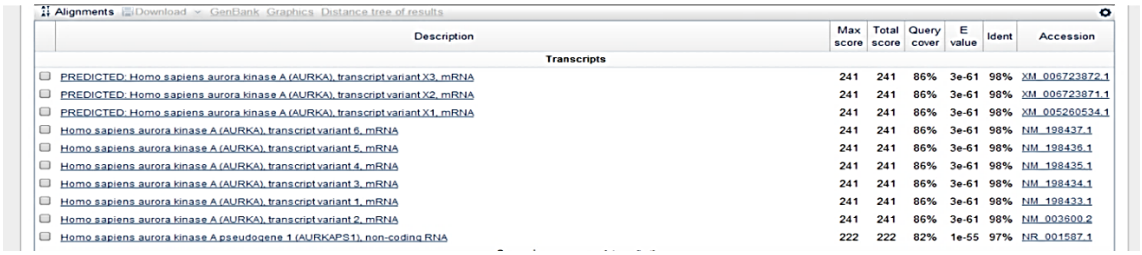

Figure A 4: Example of BLAST matching data for AURK-A sequence obtained from sequencing.

The red bands shows >=200 alignment score for the DNA sequence received from the company and the gene of interest PASD1 (with 99% maximum identity).

A.6: The extraction of RNA from trophoblast cell lines

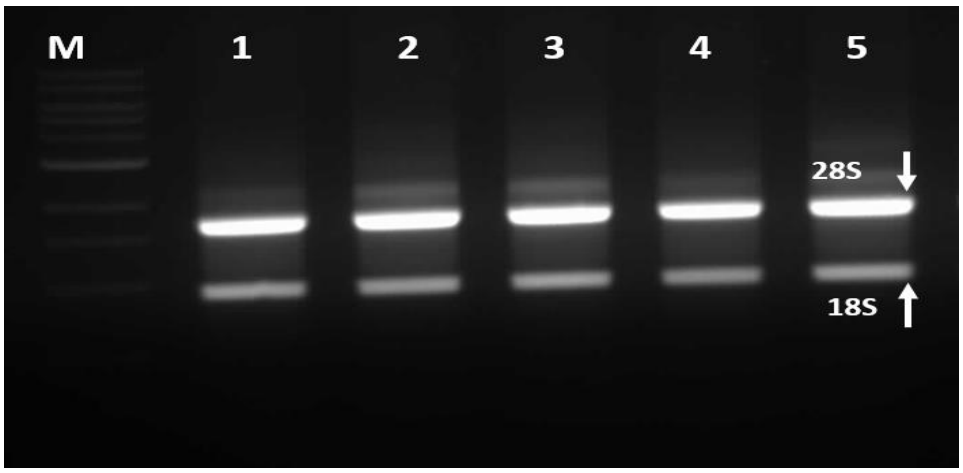

Figure A 5: The purity of extracted RNA from trophoblast cell lines in parental conditions.

*[M= 1Kb Molecular marker; lane1- **HTR8/SVneo,** lane2- **TEV-1**, lane3- **JEG-3**, lane4- **BeWo,** lane5- **MCF-7** (used as positive control).*

A.7: Temperature optimisation for markers of interest

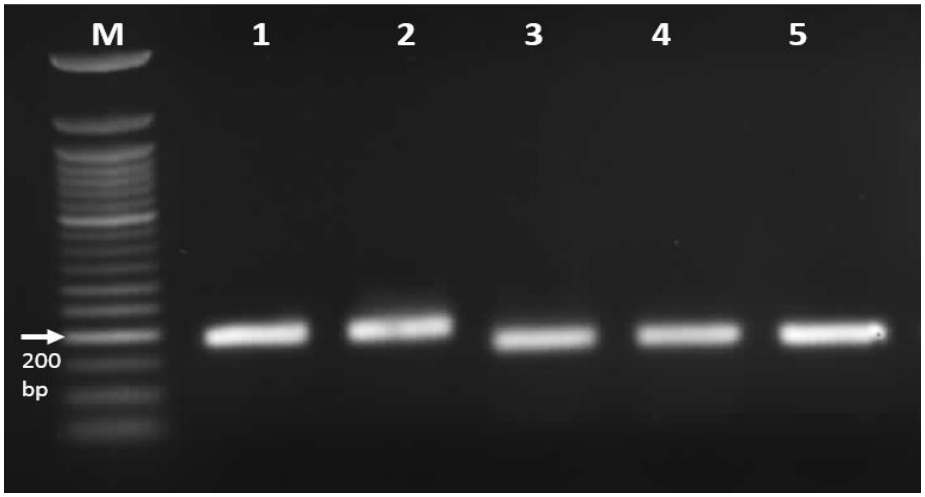

Figure A 6: Example of PCR product confirmation in Agarose gel.

*[Amplified marker (OCT4) products with trophoblast cell line (parental conditions). M- Molecular marker (ladder) 50bp, lane1- **HTR8/SVneo,** lane2- **TEV-1**, lane3- **JEG-3**, lane4- **BeWo,** lane5- **MCF-7** (used as positive control).*

A.8: Accession numbers for target factors used for primer designing

Table A 3: NCBI accession numbers for markers.

Marker	NCBI accession number
OCT4	NM_001173531.2; NM_001285986.1; NM_001285987.1
SOX2	NM_003106.3
NANOG1	NM_001297698.1
CDX2	NM_001265.4
NOTCH	NM_017617.3

References

Aaboe, M., Offersen, B.V., Christensen, A. and Andreasen, P.A. (2003) 'Vitronectin in human breast carcinomas', *Biochimica et Biophysica Acta (BBA) - Molecular Basis of Disease*, **1638**(1), pp. 72–82.

Abell, A.N., Granger, D.A., Johnson, N.L., Vincent-Jordan, N., Dibble, C.F. and Johnson, G.L. (2009) 'Trophoblast stem cell maintenance by Fibroblast growth factor 4 requires MEKK4 activation of Jun n-terminal Kinase', *Molecular and Cellular Biology*, **29**(10), pp. 2748–2761.

Achilli, T.-M., Meyer, J. and Morgan, J.R. (2012) 'Advances in the formation, use and understanding of multi-cellular spheroids', *Expert Opinion on Biological Therapy*, **12**(10), pp. 1347–1360.

Albelda, S., Mette, S., Elder, D., Stewart, R., Damjanovich, L., Herlyn, M. and Buck, C. (1990) 'Integrin distribution in malignant melanoma: Association of the beta 3 subunit with tumor progression', *Cancer research*, **50**(20), pp. 6757–64.

Alfano, D., Franco, P., Vocca, I., Gambi, N., Pisa, V., Mancini, A., Caputi, M., Carriero, M.V., Iaccarino, I. and Stoppelli, M.P. (2005) 'The urokinase plasminogen activator and its receptor. Role in cell growth and apoptosis', *Thrombosis and Haemostasis*.

Al-Hajj, M., Wicha, M.S., Benito-Hernandez, A., Morrison, S.J. and Clarke, M.F. (2003) 'Prospective identification of tumorigenic breast cancer cells', *Proceedings of the National Academy of Sciences*, **100**(7), pp. 3983–3988.

Alnouti, Y. and Klaassen, C.D. (2007) 'Tissue distribution, Ontogeny, and regulation of Aldehyde Dehydrogenase (Aldh) enzymes mRNA by prototypical microsomal enzyme Inducers in mice', *Toxicological Sciences*, **101**(1), pp. 51–64.

Alvarez, R.H., Kantarjian, H.M. and Cortes, J.E. (2006) 'Biology of Platelet-Derived growth factor and its involvement in disease', *Mayo Clinic Proceedings*, **81**(9), pp. 1241–1257.

Andrae, J., Gallini, R. and Betsholtz, C. (2008) 'Role of platelet-derived growth factors in physiology and medicine', *Genes & Development*, **22**(10), pp. 1276–1312.

Andreasen, P.A., Egelund, R. and Petersen, H.H. (2000) 'The plasminogen activation system in tumor growth, invasion, and metastasis', *Cellular and Molecular Life Sciences (CMLS)*, **57**(1), pp. 25–40.

Anin, S., Vince, G. and Quenby, S. (2004) 'Trophoblast invasion', *Human Fertility*, **7**(3), pp. 169–174.

Ansieau, S., Bastid, J., Doreau, A., Morel, A.-P., Bouchet, B.P., Thomas, C., Fauvet, F., Puisieux, I., Doglioni, C., Piccinin, S., Maestro, R., Voeltzel, T., Selmi, A., Valsesia-Wittmann, S., Caron de Fromentel, C. and Puisieux, A. (2008) 'Induction of EMT by twist proteins as a collateral effect of tumor-promoting inactivation of premature Senescence', *Cancer Cell*, **14**(1), pp. 79–89.

Aplin, J. (1991) 'Implantation, trophoblast differentiation and haemochorial placentation: Mechanistic evidence in vivo and in vitro', *Journal of cell science.*, **99**, pp. 681–92.

Aplin, J., Sattar, A. and Mould, A. (1992) 'Variant choriocarcinoma (BeWo) cells that differ in adhesion and migration on fibronectin display conserved patterns of integrin expression', *Journal of cell science.*, **103**, pp. 435–44.

Arai, K.Y., Nishiyama, T. and kojiarai (2007) 'Developmental changes in Extracellular matrix messenger RNAs in the mouse Placenta during the Second Half of pregnancy: Possible factors involved in the regulation of Placental Extracellular matrix expression', *Biology of Reproduction*, **77**(6), pp. 923–933

Arsenijevic, Y., Weiss, S., Schneider, B. and Aebischer, P. (2001) 'Insulin-like growth factor-i is necessary for neural stem cell proliferation and demonstrates distinct actions of epidermal growth factor and fibroblast growth factor-2', *The Journal of neuroscience : the official journal of the Society for Neuroscience.*, **21**(18), pp. 7194–7202.

Ashton, S.V., St J Whitley, G., Dash, P.R., Wareing, M., Crocker, I.P., Baker, P.N. and Cartwright, J.E. (2005) 'Uterine spiral artery remodeling involves endothelial Apoptosis induced by Extra villous Trophoblasts through Fas/FasL interactions', *Arteriosclerosis, Thrombosis, and Vascular Biology*, **25**(1), pp. 102–108.

Avasthi, S., Srivastava, R.N. and Singh, A. (2008) 'Stem cell: Past, present and future- A review article', *Internet Journal of Medical Update - E-journal*, **3**(1).

Avo Santos, M., van de Werken, C., de Vries, M., Jahr, H., Vromans, M.J.M., Laven, J.S.E., Fauser, B.C., Kops, G.J., Lens, S.M. and Baart, E.B. (2011) 'A role for Aurora C in the chromosomal passenger complex during human preimplantation embryo development', *Human Reproduction*, **26**(7), pp. 1868–1881.

Balber, A.E. (2011) 'Concise review: Aldehyde Dehydrogenase bright stem and Progenitor cell populations from normal tissues: Characteristics, activities, and emerging uses in Regenerative medicine', *Stem Cells*, **29**(4), pp. 570–575.

Balboula, A.Z. and Schindler, K. (2014) 'Selective disruption of Aurora C Kinase reveals distinct functions from Aurora B Kinase during Meiosis in mouse Oocytes', *PLOS Genetics*, **10**(2), pp. e1004194.

Bartholoma, P. (2005) 'A more aggressive breast cancer Spheroid model coupled to an electronic capillary sensor system for a high-content screening of Cytotoxic agents in cancer therapy: 3-Dimensional in vitro tumor Spheroids as a screening model', *Journal of Biomolecular Screening*, **10**(7), pp. 705–714.

Beard, J. (1911) 'The Enzyme Treatment of Cancer and its Scientific Basis', *New York: New Spring Press,2010. (Original work published in 1911)*.

Behrens, J. (1993) 'Loss of epithelial differentiation and gain of invasiveness correlates with tyrosine phosphorylation of the E-cadherin/beta-catenin complex in cells transformed with a temperature-sensitive v-sRC gene', *The Journal of Cell Biology*, **120**(3), pp. 757–766.

Benedito, R., Roca, C., Sörensen, I., Adams, S., Gossler, A., Fruttiger, M. and Adams, R.H. (2009) 'The notch ligands Dll4 and jagged1 have opposing effects on Angiogenesis', **137**(6), pp. 1124–1135.

Berdnik, D. and Knoblich, J.A. (2002) 'Drosophila Aurora-A is required for Centrosome maturation and Actin-Dependent asymmetric protein localization during Mitosis', *Current Biology*, **12**(8), pp. 640–647.

Betsholtz, C., Karlsson, L. and Lindahl, P. (2001) 'Developmental roles of platelet-derived growth factors', *Bioessays*, **23**(6), pp. 494–507.

Bhat, M., Philp, A., Glover, D. and Bellen, H. (1996) 'Chromatid segregation at anaphase requires the barren product, a novel chromosome-associated protein that interacts with Topoisomerase II', *Cell.*, **87**(6), pp. 1103–1114.

Bilban, M., Haslinger, P., Prast, J., Klinglmüller, F., Woelfel, T., Haider, S., Sachs, A., Otterbein, L.E., Desoye, G., Hiden, U., Wagner, O. and Knöfler, M. (2009) 'Identification of novel Trophoblast invasion-related genes: Heme Oxygenase-1 controls Motility via Peroxisome Proliferator-Activated receptor γ', *Endocrinology*, **150**(2), pp. 1000–1013.

Bilban, M., Tauber, S., Haslinger, P., Pollheimer, J., Saleh, L., Pehamberger, H., Wagner, O. and Knöfler, M. (2010) 'Trophoblast invasion: Assessment of cellular models using gene expression signatures', *Placenta*, **31**(11), pp. 989–996.

Boer, B., Cox, J.L., Claassen, D., Mallanna, S.K., Desler, M. and Rizzino, A. (2009) 'Regulation of the Nanog gene by both positive and negative cis -regulatory elements in embryonal carcinoma cells and embryonic stem cells', *Molecular Reproduction and Development*, **76**(2), pp. 173–182.

Bolos, V., Mira, E., Martínez-Poveda, B., Luxán, G., Cañamero, M., Martínez-A, C., Mañes, S., de Biotecnología, C.N., CSIC, Unit, C.P. and Program, B. (2013) 'Breast cancer research', *Breast Cancer Research*, **15**(4), pp. 1.

Bourassa, S., Fournier, F., Nehmé, B., Kelly, I., Tremblay, A., Lemelin, V., Lamarche, B., Couture, P. and Droit, A. (2015) 'Evaluation of iTRAQ and SWATH-MS for the quantification of proteins associated with insulin resistance in human duodenal biopsy samples', *PLOS ONE*, **10**(5), pp. e0125934.

Boyer, L.A., Lee, T.I., Cole, M.F., Johnstone, S.E., Levine, S.S., Zucker, J.P., Guenther, M.G., Kumar, R.M., Murray, H.L., Jenner, R.G., Gifford, D.K., Melton, D.A., Jaenisch, R. and Young, R.A. (2005) 'Core Transcriptional regulatory circuitry in human embryonic stem cells', *Cell*, **122**(6), pp. 947–956

Braam, S.R., Zeinstra, L., Litjens, S., Ward-van Oostwaard, D., van den Brink, S., van Laake, L., Lebrin, F., Kats, P., Hochstenbach, R., Passier, R., Sonnenberg, A. and Mummery, C.L. (2008) 'Recombinant Vitronectin is a functionally defined substrate that supports human embryonic stem cell self-renewal via αVβ5 Integrin', *Stem Cells*, **26**(9), pp. 2257–2265.

Bravo-Cordero, J.J., Hodgson, L. and Condeelis, J. (2012) 'Directed cell invasion and migration during metastasis', *Current Opinion in Cell Biology*, **24**(2), pp. 277–283.

Bronzert, D.A., Pantazis, P., Antoniades, H.N., Kasid, A., Davidson, N., Dickson, R.B. and Lippman, M.E. (1987) 'Synthesis and secretion of platelet-derived growth factor by human breast cancer cell lines', *Proceedings of the National Academy of Sciences*, **84**(16), pp. 5763–5767.

Bubeník, J. (2003) 'Tumour MHC class I downregulation and immunotherapy (review)', *Oncology reports.*, **10**(6), pp. 2005–8.

Buck, V.U., Gellersen, B., Leube, R.E. and Classen-Linke, I. (2015) 'Interaction of human trophoblast cells with gland-like endometrial spheroids: A model system for trophoblast invasion', *Human Reproduction*, **30**(4), pp. 906–916.

Burleigh, D.W., Kendziorski, C.M., Choi, Y.J., Grindle, K.M., Grendell, R.L., Magness, R.R. and Golos, T.G. (2007) 'Microarray analysis of BeWo and JEG3 Trophoblast cell lines: Identification of Differentially expressed transcripts', *Placenta*, **28**(5-6), pp. 383–389.

Burleson, K., Casey, R., Skubitz, K., Pambuccian, S., Oegema, T. and Skubitz, A. (2004) 'Ovarian carcinoma ascites spheroids adhere to extracellular matrix components and mesothelial cell monolayers', *Gynecologic oncology.*, **93**(1), pp. 170–81.

Burton, G. and Jauniaux, E. (2006) 'Placental oxidative stress: From miscarriage to preeclampsia', *Journal of the Society for Gynecologic Investigation*, **11**(6), pp. 342–352.

Butt, A.J., Firth, S.M. and Baxter, R.C. (1999) 'The IGF axis and programmed cell death', *Immunology and Cell Biology*, **77**(3), pp. 256–262.

Cabrera Je, E. (2013) 'The role of transcription factor TWIST in cancer cells', *Journal of Genetic Syndromes & Gene Therapy*, **04**(01).

Carlson, B.M. and Mosby, S.L. (1994) 'Human embryology and developmental biology

Carvalho, I., Milanezi, F., Martins, A., Reis, R.M. and Schmitt, F. (2005) *Breast Cancer Research*, **7**(5), pp. R788.

Castellucci, M., Kosanke, G., Verdenelli, F., Huppertz, B. and Kaufmann, P. (2000) 'Villous sprouting: Fundamental mechanisms of human placental development', *Human reproduction update*, **6**(5), pp. 485–494.

Chaddha, V., Viero, S., Huppertz, B. and Kingdom, J. (2004) 'Developmental biology of the placenta and the origins of placental insufficiency', *Seminars in fetal & neonatal medicine*, **9**(5), pp. 357–69.

Chang, C., Shieh, G., Wu, P., Lin, C., Shiau, A. and Wu, C. (2008) 'Oct-3/4 expression reflects tumor progression and regulates Motility of bladder cancer cells', *Cancer Research*, **68**(15), pp. 6281–6291.

Chang, S.-D., Chao, A.-S., Peng, H.-H., Chang, Y.-L., Wang, C.-N., Cheng, P.-J., Lee, Y.-S. and Wang, T.-H. (2011) 'Analyses of placental gene expression in pregnancy-related hypertensive disorders', *Taiwanese Journal of Obstetrics and Gynecology*, **50**(3), pp. 283–291.

Chen, H.-F., Huang, C.-H., Liu, C.-J., Hung, J.-J., Hsu, C.-C., Teng, S.-C. and Wu, K.-J. (2014) 'Twist1 induces endothelial differentiation of tumour cells through the jagged1-KLF4 axis', *Nature Communications*, 225, pp. 4697.

Chen, Y., Shi, L., Zhang, L., Li, R., Liang, J., Yu, W., Sun, L., Yang, X., Wang, Y., Zhang, Y. and Shang, Y. (2008) 'The molecular mechanism governing the Oncogenic potential of SOX2 in breast cancer', *Journal of Biological Chemistry*, **283**(26), pp. 17969–17978.

Chen, Z.F. and Behringer, R.R. (1995) 'Twist is required in head mesenchyme for cranial neural tube morphogenesis', *Genes & Development*, **9**(6), pp. 686–699.

Ciftci, K., Su, J. and Trovitch, P.B. (2003) 'Growth factors and chemotherapeutic modulation of breast cancer cells', *Journal of Pharmacy and Pharmacology*, **55**(8), pp. 1135–1141.

Cobb, L. (2013) 'Cell based assays: The cell cycle, cell proliferation and cell death', *Materials and Methods*, **3**.

Cohen, M. and Bischof, P. (2007) 'Factors regulating Trophoblast invasion', *Gynecologic and Obstetric Investigation*, **64**(3), pp. 126–130.

Coskun, M., Troelsen, J.T. and Nielsen, O.H. (2011) 'The role of CDX2 in intestinal homeostasis and inflammation', *Biochimica et Biophysica Acta (BBA) - Molecular Basis of Disease*, **1812**(3), pp. 283–289.

Crocker, I.P., Cooper, S., Ong, S.C. and Baker, P.N. (2003) 'Differences in Apoptotic susceptibility of Cytotrophoblasts and Syncytiotrophoblasts in normal pregnancy to those complicated with Preeclampsia and intrauterine growth restriction', *The American Journal of Pathology*, **162**(2), pp. 637–643.

Cuman, C., Menkhorst, E., Winship, A., Van Sinderen, M., Osianlis, T., Rombauts, L.J. and Dimitriadis, E. (2013) 'Fetal-maternal communication: The role of notch signalling in embryo implantation', *Reproduction*, **147**(3), pp. R75–R86.

Curran, S. and Murray, G. (2000) 'Matrix metalloproteinases: Molecular aspects of their roles in tumour invasion and metastasis', *European journal of cancer (Oxford, England : 1990).*, **36**, pp. 1621–1630.

Czeczuga-Semeniuk, E., Lemancewicz, D. and Wołczyński, S. (2004) 'Estradiol and tamoxifen differently affects the inhibitory effects of vitamin A and their metabolites on the proliferation and expression of α2β1 integrins in MCF-7 breast cancer cells', *Advances in Medical Sciences*, **54**(1).

Dar, A.A., Goff, L.W., Majid, S., Berlin, J. and El-Rifai, W. (2010) 'Aurora Kinase inhibitors - rising stars in cancer Therapeutics?', *Molecular Cancer Therapeutics*, **9**(2), pp. 268–278.

Das, R., Gregory, P., Hollier, B., Tilley, W. and Selth, L. (2014) 'Epithelial plasticity in prostate cancer: Principles and clinical perspectives', *Trends in molecular medicine*. **20**(11), pp. 643–651.

De Falco, M., Cobellis, L., Giraldi, D., Mastrogiacomo, A., Perna, A., Colacurci, N., Miele, L. and De Luca, A. (2007b) 'Expression and distribution of notch protein members in human Placenta throughout pregnancy', *Placenta*, **28**(2-3), pp. 118–126.

DeBerardinis, R.J., Lum, J.J., Hatzivassiliou, G. and Thompson, C.B. (2008) 'The biology of cancer: Metabolic Reprogramming fuels cell growth and proliferation', *Cell Metabolism*, **7**(1), pp. 11–20.

Den van, der, van, Cheung, H., Buijs, J., Lippitt, J., Guzmán-Ramírez, N., Hamdy, F., Eaton, C., Thalmann, G., Cecchini, M. and Pelger, R. (2010) 'High aldehyde dehydrogenase activity identifies tumor-initiating and metastasis-initiating cells in human prostate cancer', *Cancer research.*, **70**(12), pp. 5163–5173.

Denard, B., Lee, C. and Ye, J. (2012) 'Doxorubicin blocks proliferation of cancer cells through proteolytic activation of CREB3L1', *eLife*, **1**.

DeNardo, D.G., Andreu, P. and Coussens, L.M. (2010) 'Interactions between lymphocytes and myeloid cells regulate pro- versus anti-tumor immunity', Cancer and Metastasis Reviews, **29**(2), pp. 309–316.

Deryugina, E.I., Quigley, J.P. and Corporation, H.P. (2012) 'Cell surface remodeling by Plasmin: A new function for an old enzyme', *BioMed Research International*, 2012.

Dickson, B.C., Mulligan, A.M., Zhang, H., Lockwood, G., O'Malley, F.P., Egan, S.E. and Reedijk, M. (2007) 'High-level JAG1 mRNA and protein predict poor outcome in breast cancer', *Modern Pathology*, **20**(6), pp. 685–693.

Dieterich, K., Soto Rifo, R., Karen Faure, A., Hennebicq, S., Amar, B.B., Zahi, M., Perrin, J., Martinez, D., Sèle, B., Jouk, P.-S., Ohlmann, T., Rousseaux, S., Lunardi, J. and Ray, P.F. (2007) 'Homozygous mutation of AURKC yields large-headed polyploid spermatozoa and causes male infertility', *Nature Genetics*, **39**(5), pp. 661–665.

Dimova, I., Popivanov, G. and Djonov, V. (2014) 'Angiogenesis in cancer - general pathways and their therapeutic implications', *Journal of B.U.ON. : official journal of the Balkan Union of Oncology.*, **19**(1), pp. 15–21.

Djamgoz, M.B.A., Coombes, R.C. and Schwab, A. (2014) 'Ion transport and cancer: From initiation to metastasis', *Philosophical Transactions of the Royal Society B: Biological Sciences*, **369**(1638), pp. 20130092–20130092.

Doillon, C., Gagnon, E., Paradis, R. and Koutsilieris, M. (2004) 'Three-dimensional culture system as a model for studying cancer cell invasion capacity and anticancer drug sensitivity', *Anticancer research.* **24**(4), pp. 2169–2177.

Donnelly, L. and Campling, G. (2014) 'Functions of the placenta', *Anaesthesia & Intensive Care Medicin*e, **15**(3), pp. 136–139.

Doroshow, J.H. (1986) 'Role of hydrogen peroxide and hydroxyl radical formation in the killing of Ehrlich tumor cells by anticancer quinones', *Proceedings of the National Academy of Sciences*, **83**(12), pp. 4514–4518.

Douville, J., Beaulieu, R. and Balicki, D. (2009) 'ALDH1 as a functional marker of cancer stem and Progenitor cells', *Stem Cells and Development*, **18**(1), pp. 17–26.

Duong, H.S., Le, A.D., Zhang, Q. and Messadi, D.V. (2004) 'A novel 3-dimensional culture system as an in vitro model for studying oral cancer cell invasion', *International Journal of Experimental Pathology*, **86**(6), pp. 365–374.

Eckert, M.A., Lwin, T.M., Chang, A.T., Kim, J., Danis, E., Ohno-Machado, L. and Yang, J. (2011) 'Twist1-Induced Invadopodia formation promotes tumor Metastasis', *Cancer Cell*, **19**(3), pp. 372–386.

Edmondson, R., Broglie, J.J., Adcock, A.F. and Yang, L. (2014) 'Three-Dimensional cell culture systems and their applications in drug discovery and cell-based Biosensors', *ASSAY and Drug Development Technologies*, **12**(4), pp. 207–218.

Elmore, S. (2007) 'Apoptosis: A review of programmed cell death', **35**(4).

Enquobahrie, D.A., Meller, M., Rice, K., Psaty, B.M., Siscovick, D.S. and Williams, M.A. (2008) 'Differential placental gene expression in preeclampsia', *American Journal of Obstetrics and Gynecology*, **199**(5), pp. 566.e1–566.e11.

Falco, D., Cobellis, L., Giraldi, D., Mastrogiacomo, A., Perna, A., Colacurci, N., Miele, L. and Luca, D. (2006) 'Expression and distribution of notch protein members in human placenta throughout pregnancy', *Placenta.*, **28**, pp. 118–126.

Fang, B., Kovačević, Ž., Park, K., Kalinowski, D., Jansson, P., Lane, D., Sahni, S. and Richardson (2013) 'Molecular functions of the iron-regulated metastasis suppressor, NDRG1, and its potential as a molecular target for cancer therapy', *Biochimica et biophysica acta.*, **1845**(1), pp. 1–19.

Fellmeth, J.E., Gordon, D., Robins, C.E., Scott, R.T., Treff, N.R. and Schindler, K. (2015) 'Expression and characterization of three Aurora kinase C splice variants found in human oocytes', *Molecular Human Reproduction*, **21**(8), pp. 633–644.

Feng, H., Choy, M., Deng, W., Wong, H., Lau, W., Cheung, A., Ngan, H. and Tsao, S. (2005) 'Establishment and characterization of a human First-Trimester Extravillous Trophoblast cell line (TEV-1)', *Journal of the Society for Gynecologic Investigation*, **12**(4), pp. e21–e32.

Ferretti, C., Bruni, L., Dangles-Marie, V., Pecking, A.P. and Bellet, D. (2007) 'Molecular circuits shared by placental and cancer cells, and their implications in the proliferative, invasive and migratory capacities of trophoblasts', *Human Reproduction Update*, **13**(2), pp. 121–141.

Findeklee, S. and Costa, S.D. (2015) 'Placenta Accreta and total Placenta Previa in the 19th week of pregnancy', *Geburtshilfe Frauenheilkd*, **75**(8).

Fitzgerald, J., Busch, S., Wengenmayer, T., Foerster, K., de, la, Poehlmann, T. and Markert, U. (2005) 'Signal transduction in trophoblast invasion', *Chemical immunology and allergy.*, **88**, pp. 181–99.

Fletcher, O., Johnson, N., Palles, C., dos Santos Silva, I., McCormack, V., Whittaker, J., Ashworth, A. and Peto, J. (2006) 'Inconsistent association between the STK15 F31I genetic Polymorphism and breast cancer risk', *JNCI Journal of the National Cancer Institute*, **98**(14), pp. 1014–1018.

Fogh, J. and Orfeo, T. (1997) 'one hundred and twenty -seven cultured human tumor cell lines producing tumors in nude mice', *J.Nati.Cancer inst.*, **59**, pp. 221–226.

Folkman, J. (1971) 'Tumor angiogenesis: Therapeutic implications', *The New England journal of medicine.*, **285**(21), pp. 1182–1186.

Fong, H., Hohenstein, K.A. and Donovan, P.J. (2008) 'Regulation of self-renewal and Pluripotency by Sox2 in human embryonic stem cells', *Stem Cells*, **26**(8), pp. 1931–1938.

Forbes, K. and Westwood, M. (2010) 'Maternal growth factor regulation of human placental development and fetal growth', *Journal of Endocrinology*, **207**(1), pp. 1–16.

Fotakis, G. and Timbrell, J.A. (2006) 'In vitro cytotoxicity assays: Comparison of LDH, neutral red, MTT and protein assay in hepatoma cell lines following exposure to cadmium chloride', *Toxicology Letters*, **160**(2), pp. 171–177.

Frank, H.-G., Funayama, H., Gaus, G. and Schmitz, U. (1999) 'Choriocarcinoma-trophoblast hybrid cells: Reconstructing the pathway from normal to malignant trophoblast — concept and perspectives', *Placenta*, **20**, pp. 11–24.

Fu, J., Bian, M., Jiang, Q. and Zhang, C. (2007) 'Roles of Aurora Kinases in Mitosis and Tumorigenesis', *Molecular Cancer Research*, **5**(1), pp. 1–10.

Funahashi, Y., Shawber, C.J., Sharma, A., Kanamaru, E., Choi, Y.K. and Kitajewski, J. (2011) 'Notch modulates VEGF action in endothelial cells by inducing matrix Metalloprotease activity', *Vascular Cell*, **3**(1), pp. 2.

Gabrilovich, D., Chen, H., Girgis, K., Cunningham, H., Meny, G., Nadaf, S., Kavanaugh, D. and Carbone, D. (1996) 'Production of vascular endothelial growth factor by human tumors inhibits the functional maturation of dendritic cells', *Nature medicine.*, **2**(10), pp. 1096–1103.

Gajewski, E., Gaur, S., Akman, S.A., Matsumoto, L., van Balgooy, J.N.A. and Doroshow, J.H. (2007) 'Oxidative DNA base damage in MCF-10A breast epithelial cells at clinically achievable concentrations of doxorubicin', *Biochemical Pharmacology*, **73**(12), pp. 1947–1956.

Gao, J.-X. (2007) 'Stem cells review series: Cancer stem cells: The lessons from pre-cancerous stem cells', *Journal of Cellular and Molecular Medicine*, **12**(1), pp. 67–96.

Gewirtz, D. (1999) 'A critical evaluation of the mechanisms of action proposed for the antitumor effects of the anthracycline antibiotics adriamycin and daunorubicin', *Biochemical Pharmacology*, **57**(7), pp. 727–741.

Gilmore, A.P. (2005) 'Anoikis', *Cell Death and Differentiation*, **12**, pp. 1473–1477.

Ginestier, C., Hur, M.H., Charafe-Jauffret, E., Monville, F., Dutcher, J., Brown, M., Jacquemier, J., Viens, P., Kleer, C.G., Liu, S., Schott, A., Hayes, D., Birnbaum, D., Wicha, M.S. and Dontu, G. (2007) 'ALDH1 is a marker of normal and malignant human mammary stem cells and a predictor of poor clinical outcome', *Cell Stem Cell*, **1**(5), pp. 555–567.

Goldman-Wohl, D. and Yagel, S. (2002) 'Regulation of trophoblast invasion: From normal implantation to pre-eclampsia', *Molecular and Cellular Endocrinology*, **187**(1-2), pp. 233–238.

Gong, X., Lin, C., Cheng, J., Su, J., Zhao, H., Liu, T., Wen, X. and Zhao, P. (2015) 'Generation of Multicellular tumor Spheroids with Microwell-Based Agarose Scaffolds for drug testing', *PLOS ONE*, **10**(6), pp. e0130348.

Graham, C. (1993) 'Establishment and characterization of First trimester human Trophoblast cells with extended Lifespan', *Experimental Cell Research*, **206**(2), pp. 204–211.

Graham, C.H. and Lala, P.K. (1992) 'Mechanisms of placental invasion of the uterus and their control', *Biochemistry and Cell Biology*, **70**(10-11), pp. 867–874.

Grill, S., Rusterholz, C., Zanetti-Dällenbach, R., Tercanli, S., Holzgreve, W., Hahn, S. and Lapaire, O. (2009) 'Potential markers of preeclampsia – a review', *Reproductive Biology and Endocrinology*, **7**(1), pp. 70.

Grizzi, F., Di Ieva, A., Russo, C., Frezza, E.E., Cobos, E., Muzzio, P. and Chiriva-Internati, M. (2006) *Theoretical Biology and Medical Modelling*, **3**(1), pp. 37. Grümmer, R., Hohn, H.., Mareel, M.M. and Denker, H.. (1994) 'Adhesion and invasion of three human choriocarcinoma cell lines into human endometrium in a three-dimensional organ culture system', *Placenta*, **15**(4), pp. 411–429.

Grümmer, R., Hohn, H.. and Denker, H.. (1989) 'Choriocarcinoma cell Spheroids: An in vitro model for the human Trophoblast', *Trophoblast Invasion and Endometrial Receptivity*, , pp. 97–111.

Gude, N., Roberts, C., Kalionis, B. and King, R. (2004) 'Growth and function of the normal human placenta', *Thrombosis research.*, **114**, pp. 397–407.

Guibourdenche, J., Fournier, T., Malassinas, A. and Evain-Brion, D. (2009) 'Development and hormonal functions of the human placenta', *Polish Histochemical and Cytochemical Society.*, **47**(5).

Guttilla, I., Phoenix, K., Hong, X., Tirnauer, J., Claffey, K. and White, B. (2011) 'Prolonged mammosphere culture of MCF-7 cells induces an EMT and repression of the estrogen receptor by microRNAs', *Breast cancer research and treatment.*, **132**(1), pp. 75–85.

Guttmacher, A.E., Maddox, Y.T. and Spong, C.Y. (2014) 'The human Placenta project: Placental structure, development, and function in real time', *Placenta*, **35**(5), pp. 303–304.

Haider, S. and Knöfler, M. (2009) 'Human Tumour necrosis factor: Physiological and pathological roles in Placenta and Endometrium', *Placenta*, **30**(2), pp. 111–123.

Haider, S., Meinhardt, G., Velicky, P., Otti, G., Whitley, G., Fiala, C., Pollheimer, J. and Knöfler, M. (2014) 'Notch signaling plays a critical role in motility and differentiation of human first-trimester cytotrophoblasts', *Endocrinology.*, **155**(1), pp. 263–274.

Hamilton, W.J. and Boyd, J.D. (1960) 'Development of the human placenta in the first three months of gestation', **94**(Pt 3).

Hammer, A. (2011) 'Immunological regulation of trophoblast invasion', *Journal of reproductive immunology.*, **90**(1), pp. 21–28.

Han, G., Wang, H. and Hao, J. (2013) 'Pluripotent stem cells'.

Hanahan, D. and Weinberg, R.A. (2000) 'The hallmarks of cancer', *Cell*, **100**(1), pp. 57–70.

Hanahan, D. and Weinberg, R.A. (2011) 'Hallmarks of cancer: The next generation', *Cell*, **144**(5), pp. 646–674.

Hannan, N.J., Paiva, P., Dimitriadis, E. and Salamonsen, L.A. (2009) 'Models for study of human embryo implantation: Choice of cell lines', *Biology of Reproduction*, **82**(2), pp. 235–245.

Hansson, S., Chen, Y., Brodszki, J., Hernandez-Andrade, E., Inman, J., Kozhich, O., Larsson, I., Marsál, K., Medstrand, P., Xiang, C. and Brownstein, M. (2006) 'Gene expression profiling of human placentas from preeclamptic and normotensive pregnancies', *Molecular human reproduction.*, **12**(3), pp. 169–179.

Harrington, E.A., Bebbington, D., Moore, J., Rasmussen, R.K., Ajose-Adeogun, A.O., Nakayama, T., Graham, J.A., Demur, C., Hercend, T., Diu-Hercend, A., Su, M., Golec, J.M.C. and Miller, K.M. (2004) 'VX-680, a potent and selective small-molecule inhibitor of the Aurora kinases, suppresses tumor growth in vivo', *Nature Medicine*, **10**(3), pp. 262–267.

Harris, L.K. (2010) 'Review: Trophoblast-Vascular cell interactions in early pregnancy: How to Remodel a vessel', *Placenta*, **31**, pp. S93–S98.

Heerboth, S., Housman, G., Leary, M., Longacre, M., Byler, S., Lapinska, K., Willbanks, A. and Sarkar, S. (2015) 'EMT and tumor metastasis', *Clinical and Translational Medicine*, **4**(1).

Hendrix, M.J.C., Seftor, E.A., Hess, A.R. and Seftor, R.E.B. (2003) 'Angiogenesis: Vasculogenic mimicry and tumour-cell plasticity: Lessons from melanoma', *Nature Reviews Cancer*, **3**(6), pp. 411–421.

Herr, F., Schreiner, I., Baal, N., Pfarrer, C. and Zygmunt, M. (2011) 'Expression patterns of notch receptors and their ligands jagged and delta in human placenta', *Placenta*, **32**(8), pp. 554–563.

Herreros-Villanueva, M., Zhang, J.-S., Koenig, A., Abel, E.V., Smyrk, T.C., Bamlet, W.R., de Narvajas, A.A.-M., Gomez, T.S., Simeone, D.M., Bujanda, L. and Billadeau, D.D. (2013) 'SOX2 promotes dedifferentiation and imparts stem cell-like features to pancreatic cancer cells', *Oncogenesis*, **2**(8), p. e61.

Hiden, U., Wadsack, C., Prutsch, N., Gauster, M., Weiss, U., Frank, H.-G., Schmitz, U., Fast-Hirsch, C., Hengstschläger, M., Pötgens, A., Rüben, A., Knöfler, M., Haslinger, P., Huppertz, B., Bilban, M., Kaufmann, P. and Desoye, G. (2007) 'The first trimester human trophoblast cell line ACH-3P: A novel tool to study autocrine/paracrine regulatory loops of human trophoblast subpopulations – TNF-α stimulates MMP15 expression', *BMC Developmental Biology*, **7**(1), p. 137.

Hilton, M.J., Tu, X., Wu, X., Bai, S., Zhao, H., Kobayashi, T., Kronenberg, H.M., Teitelbaum, S.L., Ross, F.P., Kopan, R. and Long, F. (2008) 'Notch signaling maintains bone marrow mesenchymal progenitors by suppressing osteoblast differentiation', *Nature Medicine*, **14**(3), pp. 306–314.

Ho, K.K., Mukhopadhyay, A., Li, Y.F., Mukhopadhyay, S. and Weiner, H. (2008) 'A point mutation produced a class 3 aldehyde dehydrogenase with increased protective ability against the killing effect of cyclophosphamide', *Biochemical Pharmacology*, **76**(5), pp. 690–696.

Holmgren, L., O'Reilly, M.S. and Folkman, J. (1995) 'Dormancy of micrometastases: Balanced proliferation and apoptosis in the presence of angiogenesis suppression', *Nature Medicine*, **1**(2), pp. 149–153.

Holtan, S.G., Creedon, D.J., Haluska, P. and Markovic, S.N. (2009) 'Cancer and pregnancy: Parallels in growth, invasion, and immune modulation and implications for cancer therapeutic agents', *Mayo Clinic Proceedings*, **84**(11), pp. 985–1000.

Hsu, P.P. and Sabatini, D.M. (2008) 'Cancer cell metabolism: Warburg and beyond', *Cell*, **134**(5), pp. 703–707.

Huang, E.H., Hynes, M.J., Zhang, T., Ginestier, C., Dontu, G., Appelman, H., Fields, J.Z., Wicha, M.S. and Boman, B.M. (2009) 'Aldehyde Dehydrogenase 1 is a marker for normal and malignant human colonic stem cells (SC) and tracks SC overpopulation during colon Tumorigenesis', *Cancer Research*, **69**(8), pp. 3382–3389.

Hunkapiller, N.M., Gasperowicz, M., Kapidzic, M., Plaks, V., Maltepe, E., Kitajewski, J., Cross, J.C. and Fisher, S.J. (2011) 'A role for notch signaling in trophoblast endovascular invasion and in the pathogenesis of pre-eclampsia', *Development*, **138**(14), pp. 2987–2998.

Hunter, K.W., Crawford, N.P. and Alsarraj, J. (2008) 'Mechanisms of metastasis', *Breast Cancer Research*, **10**(Suppl 1), pp. S2.

Huppertz, B. (2008) 'The anatomy of the normal placenta', *Journal of Clinical Pathology*, **61**(12), pp. 1296–1302.

Hurt, E.M., Chan, K., Serrat, M.A.D., Thomas, S.B., Veenstra, T.D. and Farrar, W.L. (2010) 'Identification of Vitronectin as an Extrinsic Inducer of cancer stem cell differentiation and tumor formation', **28**(3).

Igakura, T., Kadomatsu, K., Kaname, T., Muramatsu, H., Fan, Q., Miyauchi, T., Toyama, Y., Kuno, N., Yuasa, S., Takahashi, M., Senda, T., Taguchi, O., Yamamura, K. and Arimura, K. (1998) 'A null mutation in basigin, an immunoglobulin superfamily member, indicates its important roles in peri-implantation development and spermatogenesis', *Developmental biology.*, **194**(2), pp. 152–65.

Igney, F.H. and Krammer, P.H. (2002) 'Death and anti-death: Tumour resistance to apoptosis', *Nature Reviews Cancer*, **2**(4), pp. 277–288.

Ishihara, N., Matsuo, H., Murakoshi, H., Laoag-Fernandez, J.B., Samoto, T. and Maruo, T. (2002) 'Increased apoptosis in the syncytiotrophoblast in human term placentas complicated by either preeclampsia or intrauterine growth retardation', *American Journal of Obstetrics and Gynecology*, **186**(1), pp. 158–166.

Jain, P., Worthylake, R.A. and Alahari, S.K. (2012) 'Quantitative analysis of random migration of cells using time-lapse video microscopy', *Journal of Visualized Experiments*, (63).

James, J.L., Carter, A.M. and Chamley, L.W. (2012) 'Human placentation from nidation to 5 weeks of gestation. Part I: What do we know about formative placental development following implantation *Placenta*, **33**(5), pp. 327–334.

Januchowski, R., Wojtowicz, K. and Zabel, M. (2013) 'The role of aldehyde dehydrogenase (ALDH) in cancer drug resistance', *Biomedicine & Pharmacotherapy*, **67**(7), pp. 669–680.

Jarvenpaa, J., Vuoristo, J., Savolainen, E., Ukkola, O., Vaskivuo, T. and Ryynanen, M. (2007) 'Altered expression of angiogenesis-related placental genes in pre-eclampsia associated with intrauterine growth restriction', Gynecological endocrinology: the official journal of the *International Society of Gynecological Endocrinology.*, **23**(6), pp. 351–5.

Ji, L., Brkić, J., Liu, M., Fu, G., Peng, C. and Wang, Y.-L. (2013) 'Placental trophoblast cell differentiation: Physiological regulation and pathological relevance to preeclampsia', *Molecular Aspects of Medicine*, **34**(5), pp. 981–1023.

Jia, R.-Z., Ding, G.-C., Gu, C.-M., Huang, T., Rui, C., Wang, Y.-X. and Lu, Q. (2014) 'CDX2 enhances HTR-8/SVneo Trophoblast cell invasion by altering the expression of matrix Metalloproteinases', *Cellular Physiology and Biochemistry*, **34**(3), pp. 628–636.

Jiang, F., Qiu, Q., Khanna, A., Todd, N.W., Deepak, J., Xing, L., Wang, H., Liu, Z., Su, Y., Stass, S.A. and Katz, R.L. (2009) 'Aldehyde Dehydrogenase 1 is a tumor stem cell-associated marker in lung cancer', *Molecular Cancer Research*, **7**(3), pp. 330–338.

Jin, T., Branch, D.R., Zhang, X., Qi, S., Youngson, B. and Goss, P.E. (1999) 'Examination ofPOU homeobox gene expression in human breast cancer cells', *International Journal of Cancer*, **81**(1), pp. 104–112.

Jones, R.G. and Thompson, C.B. (2009) 'Tumor suppressors and cell metabolism: A recipe for cancer growth', *Genes & Development*, **23**(5), pp. 537–548.

Jurcovicova, J., Krueger, K.S., Nandy, I., Lewis, D.F., Brooks, G.G. and Brown, E.G. (1998) 'Expression of platelet-derived growth factor-a mRNA in human placenta: Effect of magnesium infusion in pre-eclampsia', *Placenta*, **19**(5-6), pp. 423–427.

Kam, E.P.Y. (1999) 'The role of trophoblast in the physiological change in decidual spiral arteries', *Human Reproduction*, **14**(8), pp. 2131–2138.

Kang, Y. and Massagué, J. (2004) 'Epithelial-Mesenchymal transitions', *Cell*, **118**(3), pp. 277–279.

Karanu, F.N., Murdoch, B., Gallacher, L., Wu, D.M., Koremoto, M., Sakano, S. and Bhatia, M. (2000) 'The notch ligand jagged-1 represents a novel growth factor of human Hematopoietic stem cells', *The Journal of Experimental Medicine*, **192**(9), pp. 1365–1372.

Karlsson, L., Bondjers, C. and Betsholtz, C. (1999) 'Roles for PDGF-A and sonic hedgehog in development of mesenchymal components of the hair follicle', Development (Cambridge, England), **126**(12), pp. 2611–21.

Kaufman, H.L. and Disis, M.L. (2004) 'Immune system versus tumor: Shifting the balance in favor of DCs and effective immunity', **113**(5).

Kaur, S., Kumar, T., Uruno, A., Sugawara, A., Jayakumar, K. and Kartha, C. (2009) 'Genetic engineering with endothelial nitric oxide synthase improves functional properties of endothelial progenitor cells from patients with coronary artery disease: An in vitro study', *Basic research in cardiology*, **104**(6), pp. 739–749.

Kay, H., Nelson, M.D. and Wang, Y. (2011) *The Placenta: From development to disease*. John Wiley.

Kenyon, G., DeMarini, D., Fuchs, E., Galas, D., Kirsch, J., Leyh, T., Moos, W., Petsko, G., Ringe, D., Rubin, G., Sheahan, L. and Research, N. (2002) 'Defining the mandate of proteomics in the post-genomics era: Workshop report', *Molecular & cellular proteomics: MCP*, **1**(10), pp. 763–780.

Khan, J., Ezan, F., Crémet, J.-Y., Fautrel, A., Gilot, D., Lambert, M., Benaud, C., Troadec, M.-B. and Prigent, C. (2011) 'Overexpression of active Aurora-C Kinase results in cell transformation and Tumour formation', *PLoS ONE*, **6**(10), p. e26512.

Kim, N., Piatyszek, M., Prowse, K., Harley, C., West, M., Ho, P., Coviello, G., Wright, W., Weinrich, S. and Shay, J. (1994) 'Specific association of human telomerase activity with immortal cells and cancer', *Science (New York, N.Y.)*, **266**(5193), pp. 2011–2015.

Kim, S.W., Lee, J., Lee, B. and Rhim, T. (2014) 'Proteomic analysis in pterygium; upregulated protein expression of ALDH3A1, PDIA3, and PRDX2', 20.

Kimura, M., Matsuda, Y., Yoshioka, T. and Okano, Y. (1999) 'Cell cycle-dependent expression and Centrosome localization of a Third human Aurora/Ipl1-related protein Kinase, AIK3', *Journal of Biological Chemistry*, **274**(11), pp. 7334–7340.

King, A., Thomas, L. and Bischof, P. (2000) 'Cell culture models of Trophoblast II: Trophoblast cell Lines— A workshop report', *Placenta*, **21**, pp. S113–S119.

Kinder JM, Jiang TT, Ertelt JM, Xin L, Strong BS, Shaaban AF, Way SS. Cross-Generational Reproductive Fitness Enforced by Microchimeric Maternal Cells. Cell. 2015; **162**(3):505-15.

Kita, N., Mitsushita, J., Ohira, S., Takagi, Y., Ashida, T., Kanai, M., Nikaido, T. and Konishi, I. (2003) 'Expression and activation of MAP Kinases, ERK1/2, in the human Villous Trophoblasts', *Placenta*, **24**(2-3), pp. 164–172.

Kleinrouweler, E.C., van Uitert, M., Moerland, P.D., Ris-Stalpers, C. and Afink, G.B. (2013) 'Differentially expressed genes in the Pre-Eclamptic Placenta: A systematic review and Meta-Analysis', *PLoS ONE*, **8**(7).

Knöfler, M. and Pollheimer, J. (2005) 'Human placental trophoblast invasion and differentiation: A particular focus on Wnt signaling', *Frontiers in Genetics*, **4**.

Kollareddy, M., Dzubak, P., Zheleva, D. and Hajduch, M. (2008) 'Aurora kinases: Structure, functions and their association with cancer', *Biomedical papers of the Medical Faculty of the University Palacký, Olomouc, Czechoslovakia.*, **152**(1), pp. 27–33.

Kondo, T., Setoguchi, T. and Taga, T. (2004) 'Persistence of a small subpopulation of cancer stem-like cells in the C6 glioma cell line', *Proceedings of the National Academy of Sciences*, **101**(3), pp. 781–786.

Kong, D., Li, Y., Wang, Z. and Sarkar, F. (2011) 'Cancer stem cells and Epithelial-to-Mesenchymal transition (EMT)-Phenotypic cells: Are they cousins or twins?', *Cancers*, **3**(4), pp. 716–729.

Kramer, N., Walzl, A., Unger, C., Rosner, M., Krupitza, G., Hengstschläger, M. and Dolznig, H. (2013) 'In vitro cell migration and invasion assays', *Mutation Research/Reviews in Mutation Research*, **752**(1), pp. 10–24.

Krebs, L.T., Xue, Y., Norton, C.R., Shutter, J.R., Maguire, M., Sundberg, J.P., Gallahan, D., Closson, V., Kitajewski, J., Callahan, R., Smith, G.H., Stark, K.L. and Gridley, T. (2000) 'Notch signaling is essential for vascular morphogenesis in mice', **14**(11).

Laga, A.C., Lai, C.-Y., Zhan, Q., Huang, S.J., Velazquez, E.F., Yang, Q., Hsu, M.-Y. and Murphy, G.F. (2010) 'Expression of the embryonic stem cell transcription factor SOX2 in human skin', *The American Journal of Pathology*, **176**(2), pp. 903–913.

Lala, P., Lee, B., Xu, G. and Chakraborty, C. (2002) 'Human placental trophoblast as an in vitro model for tumor progression', *Canadian journal of physiology and pharmacology.*, **80**(2), pp. 142–149.

Lam, C., Lim, K.. and Karumanchi, S.A. (2005) 'Circulating Angiogenic factors in the pathogenesis and prediction of Preeclampsia', *Hypertension*, **46**(5), pp. 1077–1085.

Landskron, G., De la fuente, M., Thuwajit, Peti, Thuwajit, Chanitra and Hermoso, M.A. (2014b) 'Chronic inflammation and Cytokines in the tumor Microenvironment', *Journal of Immunology Research*, 2014, pp. 1–19.

Lash, G.E., Hornbuckle, J., Brunt, A., Kirkley, M., Searle, R.F., Robson, S.C. and Bulmer, J.N. (2007) 'Effect of low oxygen concentrations on Trophoblast-Like cell line invasion', *Placenta*, **28**(5-6), pp. 390–398.

Lengner, C.J., Camargo, F.D., Hochedlinger, K., Welstead, G.G., Zaidi, S., Gokhale, S., Scholer, H.R., Tomilin, A. and Jaenisch, R. (2007) 'Oct4 expression is not required for mouse somatic stem cell self-renewal', *Cell Stem Cell*, **1**(4), pp. 403–415.

Leptin, M. (1991) 'Twist and snail as positive and negative regulators during Drosophila mesoderm development', *Genes & Development*, **5**(9), pp. 1568–1576.

Li, S., Du, L., Zhang, L., Hu, Y., Xia, W., Wu, J., Zhu, J., Chen, L. and Yang, S. (2013) 'Cathepsin B contributes to autophagy-related 7 (Atg7)-induced nod-like receptor 3 (NLRP3)-dependent proinflammatory response and aggravates lipotoxicity in rat insulinoma cell line', *The Journal of biological chemistry.*, **288**(42), pp. 30094–104.

Li, X., Wang, J., Xu, Z., Ahmad, A., Li, E., Wang, Y., Qin, S. and Wang, Q. (2012) 'Expression of Sox2 and Oct4 and their clinical significance in human non-small-cell lung cancer', *International Journal of Molecular Sciences*, **13**(12), pp. 7663–7675.

Liang, C., Park, A. and Guan, J. (2007) 'In vitro scratch assay: A convenient and inexpensive method for analysis of cell migration in vitro', *Nature Protocols*, **2**(2), pp. 329–333.

Librach, C.L. (1991) '92-kD type IV collagenase mediates invasion of human cytotrophoblasts', *The Journal of Cell Biology*, 113(2), pp. 437–449.

Ling, G.-Q. (2012) 'Expression of the pluripotency markers Oct3/4, Nanog and Sox2 in human breast cancer cell lines', *Oncology Letters*, .

Liotta, L.A., Nageswara Rao, C. and Wewer, U.M. (1986) 'Biochemical interactions of tumor cells with the basement membrane', *Annual Review of Biochemistry*, 55(1).

Liu, K., Lin, B., Zhao, M., Yang, X., Chen, M., Gao, A., Liu, F., Que, J. and Lan, X. (2013) 'The multiple roles for Sox2 in stem cell maintenance and tumorigenesis', *Cellular Signalling*, **25**(5), pp. 1264–1271.

Liu, Y., Peterson, DA, Kimura, H. and Schubert, D. (1997) 'Mechanism of cellular 3-(4, 5-dimethylthiazol-2-yl)-2, 5-diphenyltetrazolium bromide (MTT) reduction', *Journal of Neurochemistry.*, **69**(2), pp. 581–593.

Livak, K. and Schmittgen, T. (2001) 'Analysis of relative gene expression data using real-time quantitative PCR and the 2(-delta delta C(T)) method', *Methods (San Diego, Calif.).*, **25**(4), pp. 402–408.

Looman, C., Sun, T., Yu, Y., Zieba, A., Ahgren, A., Feinstein, R., Forsberg, H., Hellberg, C., Heldin, C., Zhang, X., Forsberg-Nilsson, K., Khoo, N., Fundele, R. and Heuchel, R. (2007) 'An activating mutation in the PDGF receptor-beta causes abnormal morphology in the mouse placenta', *The International journal of developmental biology.*, **51**(5), pp. 361–70.

López-Lázaro, M. (2007) 'Why do tumors metastasize', *Cancer Biology & Therapy*, **6**(2), pp. 141–144.

Louwen, F., Muschol-Steinmetz, C., Reinhard, J., Reitter, A. and Yuan, J. (2012) 'A lesson for cancer research: Placental microarray gene analysis in preeclampsia', *Oncotarget*, **3**(8), p. 759.

Lu, J., Ye, X., Fan, F., Xia, L., Bhattacharya, R., Bellister, S., Tozzi, F., Sceusi, E., Zhou, Y., Tachibana, I., Maru, D.M., Hawke, D.H., Rak, J., Mani, S.A., Zweidler-McKay, P. and Ellis, L.M. (2013) 'Endothelial cells promote the Colorectal cancer stem cell Phenotype through a soluble form of jagged-1', *Cancer Cell*, **23**(2), pp. 171–185.

Lund, L., Romer, J., Bugge, T., Nielsen, B., Frandsen, T., Degen, J., Stephens, R. and Danø, K. (1999) 'Functional overlap between two classes of matrix-degrading proteases in wound healing', *The EMBO Journal.*, **18**(17), pp. 4645–56.

Lunghi, L., Ferretti, M.E., Medici, S., Biondi, C. and Vesce, F. (2007b) *Reproductive Biology and Endocrinology*, **5**(1), p. 6.

Lyall, F. (2006) 'Mechanisms regulating cytotrophoblast invasion in normal pregnancy and pre-eclampsia', *The Australian & New Zealand journal of obstetrics & gynaecology.*, **46**(4), pp. 266–73.

Ma, C., Cummings, C. and Liu, X.J. (2003) 'Biphasic activation of Aurora-A Kinase during the Meiosis I- Meiosis II transition in Xenopus Oocytes', *Molecular and Cellular Biology*, **23**(5), pp. 1703–1716.

Maestro, R., Tos, D., Hamamori, Y., Krasnokutsky, S., Sartorelli, V., Kedes, L., Doglioni, C., Beach, D. and Hannon, G. (1999) 'Twist is a potential oncogene that inhibits apoptosis', *Genes & development.*, **13**(17), pp. 2207–17.

Majumdar, K., Radotra, B.D., Vasishta, R.K. and Pathak, A. (2009) 'Platelet-derived growth factor expression correlates with tumor grade and proliferative activity in human oligodendrogliomas', *Surgical Neurology*, **72**(1), pp. 54–60.

Mani, S., Guo, W., Liao, M., Eaton, E., Ayyanan, A., Zhou, A., Brooks, M., Reinhard, F., Zhang, C., Shipitsin, M., Campbell, L., Polyak, K., Brisken, C., Yang, J. and Weinberg, R. (2008) 'The epithelial-mesenchymal transition generates cells with properties of stem cells', *Cell.*, **133**(4), pp. 704–15.

Manuel Iglesias, J., Beloqui, I., Garcia-Garcia, F., Leis, O., Vazquez-Martin, A., Eguiara, A., Cufi, S., Pavon, A., Menendez, J.A., Dopazo, J. and Martin, A.G. (2013) 'Mammosphere formation in breast carcinoma cell lines depends upon expression of E-cadherin', *PLoS ONE*, 8(10), pp. e77281.

Marchand, M., Horcajadas, J.A., Esteban, F.J., McElroy, S.L., Fisher, S.J. and Giudice, L.C. (2011) 'Transcriptomic signature of Trophoblast differentiation in a human embryonic stem cell model', *Biology of Reproduction*, **84**(6), pp. 1258–1271.

Marchitti, S.A., Brocker, C., Stagos, D. and Vasiliou, V. (2008) 'Non-p450 aldehyde oxidizing enzymes: The aldehyde dehydrogenase superfamily', *Expert Opinion on Drug Metabolism & Toxicology*, **4**(6), pp. 697–720.

Marzusch, K. (1995) 'Expression of the p53 tumour suppressor gene in human placenta: An immunohistochemical study', *Placenta*, **16**(1), pp. 101–104.

Matsuo, H., Strauss, J.F. and Mochizuki, M. (1994) 'Peroxisome proliferator and retinoid regulate JEG-3 choriocarcinoma cell function', *Placenta*, **15**(7), p. A47.

Mehta, G., Hsiao, A.Y., Ingram, M., Luker, G.D. and Takayama, S. (2013) 'Opportunities and challenges for use of tumor spheroids as models to test drug delivery and efficacy', *Journal of Controlled Release*, **164**(2), pp. 192–204.

Miki, T. and Strom, S.C. (2006) 'Amnion-derived pluripotent/multipotent stem cells', *Stem Cell Reviews*, **2**(2), pp. 133–141.

Min, S., Lee, S., Bak, S. and Kim, K. (2015) 'Ideal sphere-forming culture conditions to maintain pluripotency in a hepatocellular carcinoma cell lines', *Cancer cell international*, ***15***.

Mironchik, Y. (2005) 'Twist Overexpression induces in vivo Angiogenesis and Correlates with Chromosomal instability in breast cancer', *Cancer Research*, **65**(23), pp. 10801–10809.

Miyazawa, K., Tanaka, T., Nakai, D., Morita, N. and Suzuki, K. (2014) 'Immunohistochemical expression of four different stem cell markers in prostate cancer: High expression of NANOG in conjunction with hypoxia-inducible factor-1α expression is involved in prostate epithelial malignancy', *Oncology Letters*.

Moreb, J.S., Baker, H.V., Chang, L.-J., Amaya, M., Lopez, M.C., Ostmark, B. and Chou, W. (2008) 'ALDH isozymes downregulation affects cell growth, cell motility and gene expression in lung cancer cells', *Molecular Cancer*, **7**(1), pp. 87.

Morey, J.S., Ryan, J.C. and Dolah, F.M. (2006) 'Microarray validation: Factors influencing correlation between oligonucleotide microarrays and real-time PCR', *Biological Procedures Online*, **8**(1), pp. 175–193.

Mortlock, A., Foote, K., Heron, N., Jung, F., Pasquet, G., Lohmann, J., Warin, N., Renaud, F., Savi, D., Roberts, N., Johnson, T., Dousson, C., Hill, G., Perkins, D., Hatter, G., Wilkinson, R., Wedge, S., Heaton, S., Odedra, R., Keen, N., Crafter, C., Brown, E., Thompson, K., Brightwell, S., Khatri, L., Brady, M., Kearney, S., McKillop, D., Rhead, S., Parry, T. and Green, S. (2007) 'Discovery, synthesis, and in vivo activity of a new class of pyrazoloquinazolines as selective inhibitors of aurora B kinase', *Journal of medicinal chemistry.*, **50**(9), pp. 2213–2224.

Moser, G., Gauster, M., Orendi, K., Glasner, A., Theuerkauf, R. and Huppertz, B. (2010) 'Endoglandular trophoblast, an alternative route of trophoblast invasion? Analysis with novel confrontation co-culture models', *Human reproduction (Oxford, England).*, **25**(5), pp. 1127–1136.

Mousa, N.A., Bedaiwy, M.A. and Casper, R.F. (2006) 'Bioline international official site (site up-dated regularly)', *Middle East Fertility Society Journal*, **11**(3), pp. 152–168.

Murre, C., McCaw, P. and Baltimore, D. (1989) 'A new DNA binding and dimerization motif in immunoglobulin enhancer binding, daughterless, MyoD, and myc proteins', *Cell.*, **56**(5), pp. 777–783.

Murthi, P., Rajaraman, G., Brennecke, S.P. and Kalionis, B. (2011) 'The role of Placental Homeobox genes in human fetal growth restriction', *Journal of Pregnancy*, 2011, pp. 1–11.

Muzio, G., Maggiora, M., Paiuzzi, E., Oraldi, M. and Canuto, R.A. (2012) 'Aldehyde dehydrogenases and cell proliferation', *Free Radical Biology and Medicine*, **52**(4), pp. 735–746.

Nagaraja, G.M., Othman, M., Fox, B.P., Alsaber, R., Pellegrino, C.M., Zeng, Y., Khanna, R., Tamburini, P., Swaroop, A. and Kandpal, R.P. (2006) 'Gene expression signatures and biomarkers of noninvasive and invasive breast cancer cells: Comprehensive profiles by representational difference analysis, microarrays and proteomics', *Oncogene*, **25**(16), pp. 2328–2338.

Negi, R., Pande, D., Karki, K., Khanna, R.S., Khanna, H.D., Scientific and Publishing, A. (2011) 'Oxidative stress and Preeclampsia', *Advances in Life Sciences*, **1**(1), pp. 20–23.

Negrini, S., Gorgoulis, V.G. and Halazonetis, T.D. (2010) 'Genomic instability [mdash] an evolving hallmark of cancer: Abstract: Nature reviews molecular cell biology', *Nature Reviews Molecular Cell Biology*, **11**(3), pp. 220–228.

Ng, Y.H., Zhu, H. and Leung, P.C.K. (2012) 'Twist Modulates human Trophoblastic cell invasion via regulation of N-Cadherin', *Endocrinology*, **153**(2), pp. 925–936.

Nishida, N., Yano, H., Nishida, T., Kamura, T. and Kojiro, M. (2006) 'Angiogenesis in cancer', *Vascular Health and Risk Management*, **2**(3), pp. 213–219.

Norwitz, E.R., Schust, D.J. and Fisher, S.J. (2001) 'Implantation and the survival of early pregnancy', *New England Journal of Medicine*, **345**(19), pp. 1400–1408.

Novakovic, B., Gordon, L., Wong, N.C., Moffett, A., Manuelpillai, U., Craig, J.M., Sharkey, A. and Saffery, R. (2011) 'Wide-ranging DNA methylation differences of primary trophoblast cell populations and derived cell lines: Implications and opportunities for understanding trophoblast function', *Molecular Human Reproduction*, **17**(6), pp. 344–353.

O'Rourke, M. and Tam, P. (2002) 'Twist functions in mouse development', *The International journal of developmental biology.*, **46**(4), pp. 401–13.

Ochsenbein, A., Sierro, S., Odermatt, B., Pericin, M., Karrer, U., Hermans, J., Hemmi, S., Hengartner, H. and Zinkernagel, R. (2001) 'Roles of tumour localization, second signals and cross priming in cytotoxic t-cell induction', *Nature.*, **411**(6841), pp. 1058–1064.

Oka, H., Shiozaki, H., Kobayashi, K., Tahara, H., Tamura, S., Miyata, M., Doki, Y., Iihara, K., Matsuyoshi, N., Hirano, S., Takeichi, M. and Mori, T. (1993) 'Immunohistochemical evaluation of E-cadherin adhesion molecule expression in human gastric cancer', *Virchows Archiv A Pathological Anatomy and Histopathology*, **421**(2), pp. 149–156.

Oklu, R., Walker, T.G., Wicky, S. and Hesketh, R. (2010) 'Angiogenesis and current Antiangiogenic strategies for the treatment of cancer', *Journal of Vascular and Interventional Radiology*, **21**(12), pp. 1791–1805.

Orendi, K., Kivity, V., Sammar, M., Grimpel, Y., Gonen, R., Meiri, H., Lubzens, E. and Huppertz, B. (2011) 'Placental and trophoblastic in vitro models to study preventive and therapeutic agents for preeclampsia', *Placenta*, **32**, pp. S49–S54.

Osborne, C., Hobbs, K. and Trent, J. (1987) 'Biological differences among MCF-7 human breast cancer cell lines from different laboratories', *Breast cancer research and treatment.*, **9**(2), pp. 111–121.

Osterlund, C., Wramsby, H. and Pousette, A. (1996) 'Temporal expression of platelet-derived growth factor (PDGF)-A and its receptor in human preimplantation embryos', *Molecular human reproduction*, **2**(7), pp. 507–512.

Oudar, O. (2000) 'Spheroids: Relation between tumour and endothelial cells', *Critical Reviews in Oncology/Hematology*, **36**(2-3), pp. 99–106.

Pan, G.J., Chang, Z.Y., Scholer, H.R. and Pei, D. (2002) 'Cell research - abstract of article: Stem cell pluripotency and transcription factor Oct4', *Cell Research*, **12**(5), pp. 321–329.

Pattillo, R.A. and Gey, G.O. (1968) 'The establishment of a cell line of human Hormone-synthesizing Trophoblastic cells in vitro', *Cancer Research*, 28(7), pp. 1231–1236.

Peng, C. (2003) 'The TGF-beta superfamily and its roles in the human ovary and placenta', *Journal of obstetrics and gynaecology Canada: JOGC*, **25**(10), pp. 834–844.

Pennington, K.A., Schlitt, J.M., Jackson, D.L., Schulz, L.C. and Schust, D.J. (2011) 'Preeclampsia: Multiple approaches for a multifactorial disease', *Disease Models & Mechanisms*, **5**(1), pp. 9–18.

Phung, Y., Barbone, D., Broaddus, V. and Ho, M. (2011) 'Rapid generation of in vitro multicellular spheroids for the study of monoclonal antibody therapy', *Journal of Cancer*, **2**, pp. 507–14.

Pichot, C.S., Hartig, S.M., Xia, L., Arvanitis, C., Monisvais, D., Lee, F.Y., Frost, J.A. and Corey, S.J. (2009) 'Dasatinib synergizes with doxorubicin to block growth, migration, and invasion of breast cancer cells', *British Journal of Cancer*, **101**(1), pp. 38–47.

Pollheimer, J., Husslein, P. and Knöfler, M. (2005) 'Invasive trophoblasts generate regulatory collagen XVIII cleavage products', *Placenta*, **26**, pp. S42–S45.

Prasad, S.M., Czepiel, M., Cetinkaya, C., Smigielska, K., Weli, S.C., Lysdahl, H., Gabrielsen, A., Petersen, K., Ehlers, N., Fink, T., Minger, S.L. and Zachar, V. (2009) 'Continuous hypoxic culturing maintains activation of notch and allows long-term propagation of human embryonic stem cells without spontaneous differentiation', *Cell Proliferation*, **42**(1), pp. 63–74.

Preissner, K. and Reuning, U. (2011) 'Vitronectin in vascular context: Facets of a multitalented matricellular protein', *Seminars in thrombosis and hemostasis*, **37**(4), pp. 408–24.

Purow, B., Haque, R., Noel, M., Su, Q., Burdick, M., Lee, J., Sundaresan, T., Pastorino, S., Park, J., Mikolaenko, I., Maric, D., Eberhart, C. and Fine, H. (2005) 'Expression of notch-1 and its ligands, delta-like-1 and jagged-1, is critical for glioma cell survival and proliferation', *Cancer research*, **65**(6), pp. 2353–63.

Purow, B.W. (2013) 'Expression of notch-1 and its ligands, delta-like-1 and jagged-1, is critical for Glioma cell survival and proliferation', *Cancer Research*, **65**(6), pp. 2353–2363.

Qin, Q., Xu, Y., He, T., Qin, C. and Xu, J. (2012) 'Cell research - normal and disease-related biological functions of twist1 and underlying molecular mechanisms', *Cell Research*, **22**(1), pp. 106–190.

Quartuccio, S.M. and Schindler, K. (2015) 'Functions of Aurora kinase C in meiosis and cancer', *Frontiers in Cell and Developmental Biology*, **3**.

Raica, M. and Cimpean, A.M. (2010) 'Platelet-Derived growth factor (PDGF)/PDGF receptors (PDGFR) axis as target for Antitumor and Antiangiogenic therapy', *Pharmaceuticals*, **3**(3), pp. 572–599.

Red-Horse, K., Zhou, Y., Genbacev, O., Prakobphol, A., Foulk, R., McMaster, M. and Fisher, S.J. (2004) 'Trophoblast differentiation during embryo implantation and formation of the maternal-fetal interface', *Journal of Clinical Investigation*, **114**(6), pp. 744–754.

Redman, C.W. (2005) 'Latest advances in understanding Preeclampsia', *Science*, **308**(5728), pp. 1592–1594.

Reya, T., Morrison, S., Clarke, M. and Weissman, I. (2001) 'Stem cells, cancer, and cancer stem cells', *Nature*, **414**(6859), pp. 105–111.

Rizzino, A. (2013) 'Concise review: The Sox2-Oct4 connection: Critical players in a much larger interdependent network integrated at multiple levels', *Stem Cells*, **31**(6), pp. 1033–1039.

Roberts, J. and Cooper, D. (2001) 'Pathogenesis and genetics of pre-eclampsia', *Lancet (London, England)*, **357**(9249), pp. 53–56.

Roberts, J.M. and Hubel, C.A. (2009) 'The Two stage model of Preeclampsia: Variations on the theme', *Placenta*, **30**, pp. 32–37.

Rodrigues, M., Griffith, L.G. and Wells, A. (2010) 'Growth factor regulation of proliferation and survival of multipotential stromal cells', *Stem Cell Research & Therapy*, **1**(4), p. 32.

Rosario, F.J., Sadovsky, Y. and Jansson, T. (2012) 'Gene targeting in primary human trophoblasts', *Placenta*, **33**(10), pp. 754–762.

Rudbeck, L. (2016) 'Adding quality to your qualitative IHC', MLO: medical laboratory observer., **47**(12), pp. 18–9.

Ryan, K.M., Phillips, A.C. and Vousden, K.H. (2001) 'Regulation and function of the p53 tumor suppressor protein', *Current Opinion in Cell Biology*, **13**(3), pp. 332–337.

Saad, R.S. (2011) 'CDX2 as a marker for intestinal differentiation: Its utility and limitations', *World Journal of Gastrointestinal Surgery*, **3**(11), pp. 159.

Saftlas AF, Levine RJ, Klebanoff MA, Martz KL, Ewell MG, Morris CD, Sibai BM. Abortion, changed paternity, and risk of preeclampsia in nulliparous women. Am J Epidemiol. 2003; **157**(12):1108-14.

Sahin, Z., Acar, N., Ozbey, O., Ustunel, I. and Demir, R. (2011) 'Distribution of notch family proteins in intrauterine growth restriction and hypertension complicated human term placentas', *Acta Histochemica*, **113**(3), pp. 270–276.

Salk, J.J., Fox, E.J. and Loeb, L.A. (2010) 'Mutational heterogeneity in human cancers: Origin and consequences', *Annual Review of Pathology: Mechanisms of Disease*, **5**(1), pp. 51–75.

Samatov, T.R., Tonevitsky, A.G. and Schumacher, U. (2013) 'Epithelial-mesenchymal transition: Focus on metastatic cascade, alternative splicing, non-coding RNAs and modulating compounds', *Molecular Cancer*, **12**, pp. 107.

Sankaralingam, S., Arenas, I.A., Lalu, M.M. and Davidge, S.T. (2006) 'Preeclampsia: Current understanding of the molecular basis of vascular dysfunction', *Expert Reviews in Molecular Medicine*, **8**(03).

Sarikaya, D.P. and Jerome-Majewska LA (2011) 'Notch1 and the activated NOTCH1 intracellular domain are expressed in differentiated trophoblast cells', *Cell Biology International*, **35**(5), pp. 443–447.

Schindler, K., Davydenko, O., Fram, B., Lampson, M.A. and Schultz, R.M. (2012) 'Maternally recruited Aurora C kinase is more stable than Aurora B to support mouse oocyte maturation and early development', *Proceedings of the National Academy of Sciences*, **109**(33), pp. E2215–E2222.

Scholer, H., Ruppert, S., Suzuki, N., Chowdhury, K. and Gruss, P. (1990) 'New type of POU domain in germ line-specific protein Oct-4', *Nature*, **344**(6265), pp. 435–439.

Schwanhausser, B., Busse, D., Li, N., Dittmar, G., Schuchhardt, J., Wolf, J., Chen, W. and Selbach, M. (2013) 'Corrigendum: Global quantification of mammalian gene expression control', *Nature*, **495**(7439), pp. 126–127.

Seiffert, D., Crain, K., Wagner, N.V. and Loskutoff, D.J. (1994) 'Vitronectin gene expression in vivo: Evidence for extrahepatic synthesis and acute phase regulation', *Fibrinolysis*, **8**, pp. 121.

Sethi, N., Dai, X., Winter, C.G. and Kang, Y. (2011) 'Tumor-derived jagged1 promotes Osteolytic bone Metastasis of breast cancer by engaging notch signaling in bone cells', *Cancer Cell*, **19**(2), pp. 192–205.

Shao, S., Zhao, X., Zhang, X., Luo, M., Zuo, X., Huang, S., Wang, Y. and Gu, S. (2015) 'Notch1 signaling regulates the epithelial–mesenchymal transition and invasion of breast cancer in a slug-dependent manner', *Molecular Cancer*, **14**(1), pp. 28.

Sharma, G., Tyagi, A., Singh, R., Chan, D. and Agarwal, R. (2004) 'Synergistic anti-cancer effects of grape seed extract and conventional cytotoxic agent doxorubicin against human breast carcinoma cells', *Breast cancer research and treatment.*, **85**(1), pp. 1–12.

Shen, J., X, Yi, F., Rasul, A. and Cui, M. (2012) 'Increased expression levels of vitronectin in the maternal-fetal interface of placenta in early-onset severe preeclampsia', *Molecular medicine reports*, **7**(1), pp. 53–58.

Shen, L.-C., Chen, Y.-K., Lin, L.-M. and Shaw, S.-Y. (2010) 'Anti-invasion and anti-tumor growth effect of doxycycline treatment for human oral squamous-cell carcinoma – in vitro and in vivo studies', *Oral Oncology*, **46**(3), pp. 178–184.

Shi, G. and Jin, Y. (2010) 'Role of Oct4 in maintaining and regaining stem cell pluripotency', Stem cell research & therapy, 1(5).

Shuda, K., Schindler, K., Ma, J., Schultz, R.M. and Donovan, P.J. (2009) 'Aurora kinase B modulates chromosome alignment in mouse oocytes', *Molecular Reproduction and Development*, **76**(11), pp. 1094–1105.

Siggelkow, W., Boehm, D., Gebhard, S., Battista, M., Sicking, I., Lebrecht, A., Solbach, C., Hellwig, B., Rahnenführer, J., Koelbl, H., Gehrmann, M., Marchan, R., Cadenas, C., Hengstler, J.G. and Schmidt, M. (2012) 'Expression of aurora kinase A is associated with metastasis-free survival in node-negative breast cancer patients', *BMC Cancer*, **12**(1), p. 562.

Singh, S., Brocker, C., Koppaka, V., Chen, Y., Jackson, B.C., Matsumoto, A., Thompson, D.C. and Vasiliou, V. (2013) 'Aldehyde dehydrogenases in cellular responses to oxidative/electrophilicstress', *Free Radical Biology and Medicine*, **56**, pp. 89–101.

Siu, M.K.Y., Wong, E.S.Y., Chan, H.Y., Ngan, H.Y.S., Chan, K.Y.K. and Cheung, A.N.Y. (2008) 'Overexpression of NANOG in gestational Trophoblastic diseases', *The American Journal of Pathology*, **173**(4), pp. 1165–1172.

Sivasubramaiyan, K., Totey, S., Bhat, V. and Deb, K. (2009) 'Y-27632 enhances differentiation of blastocyst like cystic human embryoid bodies to endocrinologically active trophoblast cells on a biomimetic platform', *Journal of Biomedical Science*, **16**(1), pp. 88.

Soeda, A., Inagaki, A., Oka, N., Ikegame, Y., Aoki, H., Yoshimura, S., Nakashima, S., Kunisada, T. and Iwama, T. (2008) 'Epidermal growth factor plays a crucial role in mitogenic regulation of human brain tumor stem cells', *The Journal of biological chemistry.*, **283**(16), pp. 10958–66.

Sood, R., Zehnder, J.L., Druzin, M.L. and Brown, P.O. (2006) 'Gene expression patterns in human placenta', *Proceedings of the National Academy of Sciences*, **103**(14), pp. 5478–5483.

Soundararajan, R. and Rao, A.J. (2004) 'Trophoblast 'pseudo-tumorigenesis': Significance and contributory factors' *Reproductive Biology and Endocrinology*, **2**(1), pp. 15.

Staff, S., Isola, J., Jumppanen, M. and Tanner, M. (2010) 'Aurora-A gene is frequently amplified in basal-like breast cancer', *Oncology Reports.*, 23(2), pp. 307–12.
Staun-Ram, E. and Shalev, E. (2005) *Reproductive Biology and Endocrinology*, **3**(1), pp. 56.

Stoppelli, P.M. (2013) 'The Plasminogen activation system in cell invasion', *Madame Curie Bioscience Database.*

Sun, H., Wang, Y., Wang, Z., Meng, J., Qi, Z. and Yang, G. (2014) 'Corrigendum to "Aurora-A controls cancer cell radio- and chemoresistance via ATM/Chk2-mediated DNA repair networks" [Biochim. Biophys. Acta 1843 (2014) 934–944]', *Biochimica et Biophysica Acta (BBA) - Molecular Cell Research*, 1843(7), pp. 1308.

Suzuki, F., Hashimoto, K., Kikuchi, H., Nishikawa, H., Matsumoto, H., Shimada, J., Kawase, M., Sunaga, K., Tsuda, T., Satoh, K. and Sakagami, H. (2005) 'Induction of tumor-specific cytotoxicity and apoptosis by doxorubicin', *Anticancer research.*, **25**, pp. 887

Tallquist, M. and Soriano, P. (2002) 'Cell autonomous requirement for PDGFRalpha in populations of cranial and cardiac neural crest cells', *Development (Cambridge, England).*, **130**(3), pp. 507–18.

Tanei, T., Morimoto, K., Shimazu, K., Kim, S.J., Tanji, Y., Taguchi, T., Tamaki, Y. and Noguchi, S. (2009) 'Association of breast cancer stem cells identified by Aldehyde Dehydrogenase 1 expression with resistance to Sequential Paclitaxel and Epirubicin-Based chemotherapy for breast cancers', *Clinical Cancer Research*, **15**(12), pp. 4234–4241.

Thijssen, V.L.J.L., Poirier, F., Baum, L.G. and Griffioen, A.W. (2007) 'Galectins in the tumor endothelium: Opportunities for combined cancer therapy', *Blood*, **110**(8), pp. 2819–2827.

Tolkunova, E., Cavaleri, F., Eckardt, S., Reinbold, R., Christenson, L.K., Schöler, H.R. and Tomilin, A. (2006) 'The Caudal -related protein Cdx2 promotes Trophoblast differentiation of mouse embryonic stem cells', *Stem Cells*, **24**(1), pp. 139–144.

Töpfer, K., Kempe, S., Müller, N., Schmitz, M., Bachmann, M., Cartellieri, M., Schackert, G. and Temme, A. (2011) 'Tumor evasion from T cell surveillance', *Journal of Biomedicine and Biotechnology*, 2011, pp. 1–19.

Tuch, B. (2006) 'Stem cells--a clinical update', *Australian family physician*, **35**(9), pp. 719–21.

Uzan, J., Carbonnel, M., Piconne, O., Asmar, R. and Ayoubi, J. (2011) 'Pre-eclampsia: Pathophysiology, diagnosis, and management', *Vascular health and risk management.* 7, pp. 467–474.

Vader, G. and Lens, S.M.A. (2008) 'The Aurora kinase family in cell division and cancer', *Biochimica Biophysica Acta (BBA) - Reviews on Cancer*, **1786**(1), pp. 60–72.

Van Mourik, M.S.M., Macklon, N.S. and Heijnen, C.J. (2008) 'Embryonic implantation: Cytokines, adhesion molecules, and immune cells in establishing an implantation environment', *Journal of Leukocyte Biology*, **85**(1), pp. 4–19.

Van Zijl, F., Krupitza, G. and Mikulits, W. (2011) 'Initial steps of metastasis: Cell invasion and endothelial transmigration', *Mutation Research/Reviews in Mutation Research*, **728**(1-2), pp. 23–34.

Villalobos, M., Aranda, M., Nunez, M.I., Becerra, D., Olea, N., de Almodovar, M.R. and Pedraza, V. (1995) 'Interaction between ionizing radiation, Estrogens and Antiestrogens in the modification of tumor Microenvironment in estrogen dependent Multicellular Spheroids', *Acta Oncologica*, **34**(3), pp. 413–417.

Wang, B., David, M.D. and Schrader, J.W. (2005) 'Absence of Caprin-1 results in defects in cellular proliferation', *The Journal of Immunology*, **175**(7), pp. 4274–4282.

Wang, J., Sheng, Q. and Shyr, Y. (2015) 'SWATH-MS in proteomics: Current status', *International Journal of Computational Biology and Drug Design*, **8**(3), pp. 192.

Wang, M., Chiou, S., and Wu, C. (2013) 'Targeting cancer stem cells: Emerging role of Nanog transcription factor', *OncoTargets and therapy*, **6**, pp. 1207.

Wang, S., Konorev, E.A., Kotamraju, S., Joseph, J., Kalivendi, S. and Kalyanaraman, B. (2004) 'Doxorubicin induces Apoptosis in normal and tumor cells via distinctly different mechanisms: intermediacy of H_2O_2 and p53-dependent pathways', *Journal of Biological Chemistry*, **279**(24), pp. 25535–25543.

Weber, M., Knoefler, I., Schleußner, E., Markert, U. and Fitzgerald, J. (2013) 'HTR8/SVneo, but not JEG3, cells display trophoblast progenitor cell-like characteristics indicative of self-renewal, repopulation activity and expression of "stemness"- associated transcription factors', *Zeitschrift für Geburtshilfe und Neonatologie*, **217**(S 01).

Whiteside, T.L. (2008) 'The tumor microenvironment and its role in promoting tumor growth', *Oncogene*, **27**(45), pp. 5904–5912.

Wong, R.S. (2011) 'Apoptosis in cancer: From pathogenesis to treatment', *Journal of Experimental and Clinical Cancer Research*, **30**(1), pp. 87.

Wu, F., Ye, X., Wang, P., Jung, K., Wu, C., Douglas, D., Kneteman, N., Bigras, G., Ma, Y. and Lai, R. (2013) 'Sox2 suppresses the invasiveness of breast cancer cells via a mechanism that is dependent on twist1 and the status of Sox2 transcription activity', *BMC Cancer*, **13**(1), pp. 317.

Xiang, R., Liao, D., Cheng, T., Zhou, H., Shi, Q., Chuang, T.S., Markowitz, D., Reisfeld, R.A. and Luo, Y. (2011) 'Downregulation of transcription factor SOX2 in cancer stem cells suppresses growth and metastasis of lung cancer', *British Journal of Cancer*, **104**(9), pp. 1410–1417.

Yagel, S., Casper, R.F., Powell, W., Parhar, R.S. and Lala, P.K. (1989) 'Characterization of pure human first-trimester cytotrophoblast cells in long-term culture: Growth pattern, markers, and hormone production', *American Journal of Obstetrics and Gynecology*, **160**(4), pp. 938–945.

Yang, J.I., Kong, T.W. and Kim, H.S. (2015) 'The Proteomic analysis of human Placenta with Pre-eclampsia and normal pregnancy', *Journal of Korean Medical Science*, **30**(6), pp. 770.

Yang, M.-H., Wu, M.-Z., Chiou, S.-H., Chen, P.-M., Chang, S.-Y., Liu, C.-J., Teng, S.-C. and Wu, K.-J. (2008) 'Direct regulation of TWIST by HIF-1α promotes metastasis', *Nature Cell Biology*, **10**(3), pp. 295–305.

Yoon, Y., Cowley, D.O., Gallant, J., Jones, S.N., Van Dyke, T. and Rivera-Perez, J.A. (2012) 'Conditional Aurora A deficiency differentially affects early mouse embryo patterning', *Developmental Biology*, **371**(1), pp. 77–85.

Zawacka-Pankau, J., Kostecka, A., Sznarkowska, A., Hedström, E. and Kawiak, A. (2010) 'P73 tumor suppressor protein: A close relative of p53 not only in structure but also in anti-cancer approach', *Cell Cycle*, **9**(4), pp. 720–728.

Zhang, S. (2015) 'Sox2, a key factor in the regulation of pluripotency and neural differentiation', *World Journal of Stem Cells*, **6**(3), pp. 305.

Zhang, X., Zhang, F., Guo, L., Wang, Y., Zhang, P., Wang, R., Zhang, N. and Chen, R. (2013) 'Interactome analysis reveals that C1QBP (complement component 1, q subcomponent binding protein) is associated with cancer cell Chemotaxis and Metastasis', *Molecular & Cellular Proteomics*, **12**(11), pp. 3199–3209.

Zhang, Z., Wang, H., Ikeda, S., Fahey, F., Bielenberg, D., Smits, P. and Hauschka, P.V. (2010) 'Notch3 in human breast cancer cell lines regulates Osteoblast-Cancer cell interactions and Osteolytic bone Metastasis', *The American Journal of Pathology*, **177**(3), pp. 1459–1469.

Zhao, W., Ji, X., Zhang, F., Li, L. and Ma, L. (2012) 'Embryonic stem cell markers', *Molecules*, **17**(12), pp. 6196–6236.

Zhou, Y., Fisher, S.J., Janatpour, M., Genbacev, O., Dejana, E., Wheelock, M. and Damsky, C.H. (1997) 'Human cytotrophoblasts adopt a vascular phenotype as they differentiate. A strategy for successful endovascular invasion', *Journal of Clinical Investigation*, **99**(9), pp. 2139–2151.

Ziegler, A.N., Chidambaram, S., Forbes, B.E., Wood, T.L. and Levison, S.W. (2014) 'Insulin-like growth Factor-II (IGF-II) and IGF-II Analogs with enhanced insulin receptor-a binding affinity promote neural stem cell expansion', *Journal of Biological Chemistry*, **289**(8), pp. 4626–4633.

Zuo, Y., Fu, Z., Hu, Y., Li, Y., Xu, Q., Sun, D. and Tan, Y. (2014) 'Effects of transforming growth factor-β1 on the proliferation and invasion of the HTR-8/SVneo cell line', *Oncology Letters*,

Website links:

www[1]: http://www.etymonline.com/index.php?term=placenta

www[2]: Quizlet.com

www[3]: http://www.pathologyoutlines.com/topic/placentanormalanatomy.html

www[4]: http://www.mhhe.com

www[5]: http://www.embryology.ch/anglais/gnidation/etape02.html

www[6]:https://www.researchgate.net/publication/6515520_Control_of_human_trophoblast_function/figures

www[7]: http://womensandinfantshealth.ca/fetal-medicine/placenta/placental-complications-of-pregnancy/

www[8]: http://www.who.int/en/

www[9]: http://www.ncbi.nlm.nih.gov/gene/182

www[10]: http://www.google.co.uk/patents/US8551775

www[11]: http://stemcells.nih.gov/info/basics/pages/basics1.aspx

www[12]: http://www.ncbi.nlm.nih.gov/gene/6657

www[13]: http://www.ncbi.nlm.nih.gov/gene/1045

www[14]: http://www.ncbi.nlm.nih.gov/

www[15]: http://primer3.ut.ee/

www[16]: https://www.idtdna.com/calc/analyzer

www[17]: http://www.ebi.ac.uk/Tools/msa/clustalw2/

www[18]: http://blast.ncbi.nlm.nih.gov/Blast.cgi

www[19]: http://www.wimasis.com

www[20]: http://stemcells.nih.gov/info/basics/pages/basics4.aspx

www[21]:http://www.genengnews.com/gen-articles/advertorial-3-d-tumor-spheroids-in-extracellular-matrix-old-hat-new-trick/4812/

www[22]: http://www.pubfacts.com/detail/25602070/The-placenta-a-multifaceted-transient-organ

www[23]: https://minerva-access.unimelb.edu.au/handle/11343/5250